DOCTORAL (PhD) DISSERTATION

JUAN PABLO AGUINAGA BÓSQUEZ

Budapest
2025

Hungarian University of Agriculture and Life Sciences

MONITORING FOOD QUALITY ALTERATIONS INDUCED BY STRESS FACTORS USING NEAR INFRARED SPECTROSCOPY, ELECTRONIC TONGUE, AND ELECTRONIC NOSE

JUAN PABLO AGUINAGA BÓSQUEZ

Budapest

2025

PhD School/ Program

Name: Doctoral School of Food Science

Field   Food Science

Head: **Livia Simon Sarkadi, DSc**

Department of Nutrition

Institute of Food Science and Technology

Hungarian University of Agriculture and Life Sciences

Supervisors: **Zoltan Kovacs, PhD**

Department of Food Measurements and Process Control

Institute of Food Science and Technology

Hungarian University of Agriculture and Life Sciences

Zoltan Gillay, PhD

Department of Food Measurements and Process Control

Institute of Food Science and Technology

Hungarian University of Agriculture and Life Sciences

The applicant met the requirement of the PhD regulations of the Hungarian University of Agriculture and Life Sciences and the thesis is accepted for the defense process.

....
Head of Doctoral School   Supervisor   Supervisor

TABLE OF CONTENTS

LIST OF ABREVIATIONS

ANOVA	Analysis of variance
DeTr	Detrend
E-nose	Electronic nose
E-tongue	Electronic tongue
LDA	Linear discriminant analysis
MSC	Multiplicative scatter correction
NIRS	Near infrared spectroscopy
PCA	Principal component analysis
PC	Principal component
PCA-LDA	Linear discriminant analysis based on principal component analysis
PLSR	Partial least square regression
RMSEC	Root mean square error of calibration
RMSECV	Root mean square error of cross-validation
RMSEP	Root mean square error of prediction
R^2C	Determination coefficient of calibration
R^2CV	Determination coefficient of cross-validation
R^2pred	Determination coefficient of prediction
SG	Savitzky–Golay smoothing filter
SNV	Standard normal variate

1. INTRODUCTION

Food quality defines the characteristics of food that are acceptable to the consumer, for that quality assurance is a fundamental topic of study. Quality encompasses many intrinsic and extrinsic features or attributes. These attributes are given in accordance with consumer expectations, including color, shape, size, freedom from defects as well as texture, sweetness, acidity, aroma, flavor, shelf life and nutritional value (Margeta *et al.*, 2019; Petrescu, Vermeir and Petrescu-Mag, 2020).

Quality assurance plays a critical role throughout various stages of the agriculture and food chain, from producing crops of high value until their transformation into final food products. Effective quality control at the raw material stage is essential, as it directly influences subsequent transformation processes within the agroindustry sector (Zugarramurdi *et al.*, 2004; Pokharel, 2023). The perishable nature of many agricultural products and their variable quality introduce uncertainty, necessitating careful planning of transformation processes, as well as active involvement in primary production to ensure food security (Tadesse, 2024). Once raw materials are transformed into food products, their quality can undergo further changes. Such variations are commonly attributed to factors such as storage conditions, transportation, shelf life, or food treatments prior to consumption (Sousa Gallagher, Mahajan and Yan, 2011; Dunno *et al.*, 2016). This highlights the need for quality assessments at different stages, capturing the food journey from field to table.

Different methods are used to determine the quality of food. The most traditional methods comprise sensory evaluation, chemical and microbiological analyses (Ramos, 2012; Mian K. *et al.*, 2017; Chauhan and Jindal, 2020). However, more advanced and less conventional techniques, such as spectroscopic methods, electronic nose and tongue systems, among others, have gained attention in recent years due to their speed, non-destructive nature, and potential for automation (Aouadi *et al.*, 2020).

This research focuses on the study of three important food matrices (eggs from hens, probiotic food supplements and pea microgreens), in which factors such as the diet of laying hens in the case of egg production can affect their organoleptic profile; temperature of water and concentration of probiotic powder during drink preparation may influence the viability of the probiotics; or environmental factors in the case of microgreens can affect their development and biochemical properties.

In the field of egg analysis, sensory evaluation has traditionally been carried out by human panels assessing gustatory and olfactory characteristics. While valuable, this approach has limitations due to the inherent subjectivity and variability of human perception.

1

Given the growing interest in egg enrichment through feed modification, in the first part of this research, advanced sensory technologies including electronic tongue (e-tongue) and electronic nose (e-nose) were used to evaluate the effects of an industrial by-product in the diet of hens. The e-tongue, which detects soluble compounds in liquids, and the e-nose, which identifies volatile compounds in gases and aromas, offer an objective and reproducible alternative to traditional sensory analysis (Aouadi *et al.*, 2020; Cho and Moazzem, 2022). These technologies have the potential to reveal subtle sensory differences in eggs resulting from specific feed fortification and storage conditions. By reducing the variability associated with human judgement, these tools could provide a more reliable and comprehensive understanding of egg quality.

Moreover, new methods, based on optical techniques, have been developed to overcome the limitations of previous traditional methods. As a result, NIRS (near infrared spectroscopy) with a non-destructive, economic, environmentally friendly, fast, real time, and online monitoring approach has gained more popularity in recent years.

NIRS enables the determination of quality features by optical spectral measurements, allowing for non-contact, real time monitoring of food samples. The prominence of this method in quality and features determination lies in the nature of NIR spectrum that is closely linked to overtones and combinations of chemical bonds between carbon, hydrogen, and nitrogen (C-H, O-H, N-H). All of which have an impact on several food properties (Burns and Ciurczak, 2008; Workman and Weyer, 2012; Ozaki, Genkawa and Futami, 2017).

In this context, the second part of this research will explore the applicability of NIRS for characterizing and predicting the viability of commercial probiotic powders when exposed to different concentration and temperature conditions of water for beverage preparation prior to ingestion. These stressors, such as temperature and concentration, mimic real-life conditions that probiotics may encounter during preparation and storage. The primary target is to assess how these stressors affect the stability, viability and efficacy of the probiotics, ensuring that NIRS can provide a rapid, reliable and non-destructive method for monitoring product quality.

The third part of this research will explore the potential of NIRS to characterize pea microgreens exposed to different temperature and photoperiod conditions and evaluate the ability of NIRS to predict important agronomic and physicochemical properties. These environmental stressors, such as extreme temperatures or altered light cycles, are known to affect plant growth and the accumulation of key compounds such as pigments and antioxidants, etc. The study aims to demonstrate the ability of NIRS to provide a real-time, non-invasive approach to monitoring plant responses to stressors and to develop more

efficient and accurate models for predicting the nutritional and physical quality of microgreens under different growing conditions, thus supporting more sustainable and optimized agricultural practices.

Although the multiple advantages of these technologies (e-nose, e-tongue and NIRS) are well established, they require certain level of expertise to properly analyze their measurements and to adjust mathematical and statistical developed models to new conditions and products (Siesler *et al.*, 2002; Baldwin *et al.*, 2011). In this dissertation, these techniques, combined with chemometric methods, are employed to create robust models for the characterization of food matrices (eggs, probiotics and microgreens) and the prediction of parameters. Exploratory methods like principal component analysis (PCA) are used to identify patterns and relationships in the data, while supervised techniques, such as discriminant analysis and partial least squares regression (PLSR), are applied to classify and predict the properties of the samples. These advanced approaches ensure that the developed models are both accurate and adaptable to different food products and conditions, highlighting the potential of these technologies for comprehensive food quality analysis.

2. OBJECTIVES

The primary objective of this thesis is to determine the applicability and effectiveness of rapid correlative methods: near infrared spectroscopy (NIRS), electronic tongue (e-tongue), and electronic nose (e-nose), for assessing changes or alterations in food quality caused by significant stress factors, offering potential advantages over conventional quality evaluation techniques.

The first research aim was to evaluate the applicability of e-tongue and e-nose to detect the possible alteration of the organoleptic properties of eggs produced by hens, with diets containing different levels of an organic zinc-enriched by-product.

1. Develop models for e-tongue to discriminate, classify, and predict eggs based on the level of zinc-enriched by-product in the diet.
2. Develop models for e-nose to discriminate, classify, and predict eggs based on the level of zinc-enriched by-product in the diet and storage time.

The second aim of our study was to determine the applicability of NIRS to detect changes in probiotic drinks prepared with varying concentrations of probiotic powder and different water temperatures prior to consumption.

1. Develop models for characterization of three commercial probiotic food supplement powders containing lactic acid bacteria (LAB) subjected to probiotic concentration and water temperature conditioning factors.
2. Develop models for viability prediction of lactic acid bacteria (LAB) from three commercial probiotic food supplement powders subjected to probiotic concentration and water temperature conditioning factors.

The third research aim was to determine the applicability of NIRS for detecting changes induced by different environmental conditions during the growth of pea microgreens.

1. Develop models to characterize pea microgreens and predict key agronomical and physicochemical properties under varying temperature and photoperiod conditions.
2. Develop and assess models for two different sample types: microgreens fresh-cut samples and aqueous microgreens extracts samples.

3. LITERATURE REVIEW

In this section, a comprehensive exploration of quality assessment methods for food materials (eggs, probiotics and pea microgreens) is conducted. The first section examines the quality assessment of eggs from hens, addressing their nutritional composition, the influence of various factors on their sensory and nutritional profiles, and sensory evaluation methods, including both conventional and emerging techniques which emphasis in e-tongue and e-nose. The review then shifts to quality evaluation of probiotics, highlighting their significance for human health, the factors impacting probiotic viability, and microbiological assessment methods. The quality assessment of pea microgreens follows, covering their importance and factors influencing plant quality. The review also insights on near infrared spectroscopy as a novel innovative tool for food quality analysis with emphasis in its application for microbiological assessment and for evaluating plant parameters. Finally, the role of chemometrics in preprocessing, analyzing and interpreting complex data from these advanced techniques is addressed, underscoring its importance in modern food quality assessment.

3.1. Quality evaluation of eggs from hens

3.1.1. Importance of eggs in human nutrition

Hen eggs are recognized as important for their contribution to human nutrition. The nutritional profile of eggs is notably rich in a diversity of elements, encompassing in first place essential macronutrients such as proteins of high quality and bioavailability, a balanced fatty acid composition, and a relatively low content of carbohydrates (IEH, 2009; Chasapis *et al.*, 2020; Hailemariam *et al.*, 2022). The richness of eggs in high quality protein content makes them particularly important as they contain essential amino acids vital for human health (Réhault-Godbert, Guyot and Nys, 2019).

Eggs are appreciated for possessing a large number of essential micronutrients, including vitamins (such as A, B2, B12 and D, E, etc) and minerals (such as phosphorus, selenium, iron, choline, and zinc, etc) (IEH, 2009). In particular, the inclusion of zinc is relevant for the diets of both animals and humans which influences a greater variety of essential life functions than any other individual micronutrient (Lowe *et al.*, 2024). Turan (2019) and Chasapis *et al.* (2020) mentioned the essential role of zinc in various physiological processes. This element compromise immune system function, wound healing, DNA synthesis, cells differentiation, normal growth and development, and enzyme activation or inhibition, marking vital to include it in the diet for the human body. When the diet is unbalanced, it can lead to a rapid zinc deficiency, given the body's

5

inability to store zinc reserves. While severe zinc deficiency is uncommon, mild deficiencies are frequently reported globally. Zinc is primarily linked to antioxidant properties, and numerous studies also have explored its association with the risk of cancer (Skrajnowska and Bobrowska-Korczak, 2019; Mukherjee, Chakraborty and Chakraborty, 2020). According to the 2001 dietary reference intake (DRI) guidelines, released by the National Academies of Sciences, the recommended daily dietary intake of zinc is 8 mg for children aged 9–12 years and females (excluding those aged 14–18 years, who require 9 mg/day); meanwhile, for males, a daily intake of 11 mg is advised (Trumbo et al., 2001). Zinc from the diet is absorbed in the small intestine and distributed throughout the body. The major zinc reservoirs are bones and skeletal muscles, storing 30% and 60%, respectively. Other organs like the brain, liver, kidney, pancreas, spleen, etc., collectively account for only 10% (Hara *et al.*, 2017). Adding zinc, an essential trace element, contributes to the rich nutritional profile of eggs (Miranda *et al.*, 2015; Réhault-Godbert, Guyot and Nys, 2019).

Most researchers suggest that moderate egg consumption improves health nutrition and does not pose a significant risk of cardiovascular diseases attributed to dietary cholesterol. However, the debate persists regarding whether high egg intake could elevate the risk, particularly in individuals with preexisting risk factors such as type 2 diabetes (Blesso and Fernandez, 2018; Réhault-Godbert, Guyot and Nys, 2019; Drouin-Chartier *et al.*, 2020).

3.1.2. Factors affecting the quality of eggs

Various factors, genetic and non-genetic, determine the characteristics of eggs, which are related not only to their physical attributes but also the nutritional and sensory characteristics of eggs (Berkhoff *et al.*, 2020; Hailemariam *et al.*, 2022). The inherent traits of a hen, which are largely determined by its genetics, play a role in influencing the composition of its eggs. The genetic factors are the ones that set the productive potential of animals and have influence on the levels of essential nutrients, such as proteins, vitamins, and minerals, as well as impact the overall sensory perception of the end product (Goto *et al.*, 2019; Hejdysz *et al.*, 2024). On the other hand, non-genetic factors encompass different elements, from the hen's diet and living conditions to environmental stressors. The diet, for instance, is one of the most important factors that directly affects the nutritional richness of the egg and also is related to variations in the sensory attributes (Leeson, Caston and Maclaurin, 1998; Hammershøj and Johansen, 2016; Kaewsutas, Nararatwanchai and Sittiprapaporn, 2016; Fatogoma *et al.*, 2023).

The careful selection and breeding of hens with desirable genetic characteristics, coupled with an effective nutrition, are fundamental and determine the nutritional composition of eggs. Different dietary strategies for egg enrichment have proven effective in elevating the levels of

omega-3 fatty acids (Betancourt and Díaz, 2009), essential vitamins such as B12 and D (Betancourt and Díaz, 2009; Kaewsutas, Nararatwanchai and Sittiprapaporn, 2016; Lima and Souza, 2018) and essential microelements, including iron (fe), zinc (zn), copper (cu), between others (Inal *et al.*, 2001; Ramadan *et al.*, 2010; Yu *et al.*, 2020).

A proper selection and formulation of diets for laying hens is also relevant because it can affect the sensory properties of the eggs they produce. Various ingredients incorporated into the diet, such as herbs, specific grains, and particular sources of fatty acids, have the potential to directly influence the organoleptic characteristics of the eggs (Leeson, Caston and Maclaurin, 1998; Hammershøj and Johansen, 2016; Brelaz *et al.*, 2019). Moreover, the use of by-products that incorporate different nutrients and that are used as feed for animals have become of interest, as they typically exhibit characteristics that are beneficial in comparison to conventional synthetic chemical products (Świątkiewicz and Koreleski, 2008; Moon and Jung, 2010; Fontinele *et al.*, 2017). They are considered more sustainable, often possessing a reduced environmental footprint that are in alignment with eco-friendly agricultural practices (Nunes *et al.*, 2024). By-products originating from industrial processes can retain essential nutrients such as protein, fats, between other macro and microelements; as well as bioactive compounds such us: polyphenols, carotenoids, vitamins, organic acids, nucleotides, and phytosterols. Consequently, these by-products are frequently utilized for animal feed or as fertilizer, or they are discarded in landfills or incinerated (de Castro *et al.*, 2020). As mentioned through this section, despite the benefits that different formulas can exhibit, it is relevant to recognize that, while modifying the diet can enhance the nutritional properties of eggs, there exists a potential to alter their sensory characteristics.

3.1.3. Eggs sensory evaluation methods

Traditional sensory evaluation methods, encompassing visual inspection, taste testing, and aroma assessment, have long been employed to gauge the organoleptic qualities of eggs. Several studies have evaluated changes in the sensory characteristics of eggs induced by storage time (Adamiec *et al.*, 2002; Sati *et al.*, 2020; Nwamo *et al.*, 2021). Furthermore, these analyses also evaluate the influence of different housing or production systems, such as conventional and organic methods. Not to mention, assessing overall egg quality and characteristics, especially after enriching them with various bioactive components. Enriching eggs with bioactive compounds that positively affect consumer health can enhance the properties of egg products. However, it is crucial for the eggs to maintain compositional stability and meet sensory expectations for consumer satisfaction (Margeta *et al.*, 2019).

The methods for sensory evaluation of eggs involve a systematic process carried out by a trained or an untrained sensory panel. A trained panel typically comprises individuals with expertise in food science and sensory analysis. The selection of sensory methods for evaluating egg sensory attributes is contingent upon the test objective and test type, where the selection of right assessors, proper area for testing, and appropriate preparation of samples must be achieved (Margeta *et al.*, 2019). The sensory panel, often consisting of 8 to 12 trained individuals, participates in blind taste testing, where they evaluate characteristics such as flavor, texture, and overall palatability. A carefully selected number of egg samples are presented to the panel members, who systematically assess various sensory attributes. The presentation of samples follows a randomized order to prevent bias, and panelists may cleanse their palates between samples using water or unsalted crackers. Attributes such as egg color, yolk consistency, and overall appearance are also scrutinized visually (Hayat *et al.*, 2010; Kalus *et al.*, 2020). A controlled environment (illumination and air conditioning, noise level, available space) is maintained to eliminate external influences that may affect the evaluators' perceptions. Each panelist is provided with multiple samples of eggs, to ensure a comprehensive assessment (Margeta *et al.*, 2019).

Complementary, novel methods have emerged to enhance the precision and comprehensiveness of sensory evaluations. Advanced techniques, developed in the late 20th century, include electronic nose (e-nose) and electronic tongue (e-tongue), that utilize sophisticated sensors to detect and analyze specific odor and taste profiles that may be suitable for evaluating the quality of eggs.

3.2. Electronic tongue and electronic nose

The food industry has recently implemented high-performing systems across the production chain, particularly with the arrival of electronic tongue and electronic nose technologies, also known as e-senses (Modesti *et al.*, 2022). These innovative methods have gathered significant attention from researchers and industries as viable alternatives to human sensory testing (Aouadi *et al.*, 2020; Cho and Moazzem, 2022). When combined with advanced chemometric tools, e-senses provide a high-throughput and cost-effective approach that reduces reliance on traditional, labor-intensive methods (Aouadi *et al.*, 2020). They address common challenges associated with sensory evaluations conducted by human panels, such as subjectivity, sensory fatigue among panelists, high costs, and time-consuming procedures (Cho and Moazzem, 2022).

The electronic nose (e-nose) try to mimic human and animal olfaction by using sensors that interact with odor molecules to produce electronic signals analyzed by a computer employing

multivariate statistics to extract the corresponding pattern (Baldwin *et al.*, 2011; Aouadi *et al.*, 2020). E-noses can utilize various sensors, including organic polymers, metal oxides, quartz crystal microbalances, and can also incorporate gas chromatography (GC) with mass spectrometry (MS) to enhance their non-selective detection capabilities (Baldwin *et al.*, 2011).

For instance, an advanced type of e-nose, like The Heracles II electronic nose (Alpha MOS), features a rapid gas chromatograph designed for odor separation, an ion flame detector for identifying volatile compounds, and robust data processing software that correlates with sensory panel results. Once calibrated, the device can substitute sensory panels for routine quality control (AlphaM.O.S., 2018; Cho and Moazzem, 2022).

This device employs a dual-column gas chromatograph with two detectors to achieve enhanced compound separation and detection. The system uses Kovats retention index (RI) to standardize the retention times of volatile compounds, enabling more accurate identification and comparison across different chromatographic instruments and conditions (AlphaM.O.S., 2018).

The index is calculated by interpolating the retention times of a target compound between two n-alkanes with known carbon chain lengths. Each n-alkane is assigned an index based on its carbon number multiplied by 100, meaning that hexane (C6) has an index of 600, heptane (C7) is 700, and so on. (Babushok, 2015; AlphaM.O.S., 2018)

This approach is particularly useful in aroma profiling because it allows the comparison of chromatograms across different instruments and experimental setups. The Kovats index improves compound identification accuracy when coupled with mass spectrometry or other databases (Babushok, 2015). In the context of food analysis, Kovats index values are frequently employed to identify relevant volatile compounds responsible for sensory attributes, such as flavor and aroma (Umano *et al.*, 1990; Bianchi *et al.*, 2007).

The use of Kovats retention indices in electronic nose systems, such as the Heracles NEO, is central to the identification of volatile compounds. The system relies on this index to map volatile fingerprints against the AroChemBase library, allowing for rapid identification of unknown substances in food products (AlphaM.O.S., 2018).

Electronic tongue (e-tongue) devices function by employing artificial sensors that try to mimic the human tongues, with cross-sensitivity and partial selectivity to analyze substances in liquids. Cross-sensitivity allows the sensors to respond to multiple compounds rather than being specific to a single analyte, improving their ability to detect complex mixtures. Partial selectivity ensures that while the sensors are not entirely specific, they exhibit a degree of preference for certain compounds or classes of substances. This combination allows e-tongues to capture subtle differences in chemical compositions, producing a unique chemical pattern, commonly known as a "fingerprint" which characterizes each sample. This fingerprinting technology serves as the core

9

principle for artificial taste sensing instruments (Kovacs *et al.*, 2020). The non-selective sensors of the e-tongue generate unique signal combinations or fingerprints. E-tongues use various sensors responsive to salts and sugars, transmitting signals to a computer for analysis, this in certain sense is compatible with human tongue, although the later has around 10,000 taste buds with 50 to 100 taste cells each that detect five primary flavors: sweet, sour, bitter, salty, and umami. The common e-tongue sensor types include potentiometry, voltammetry, and impedance spectroscopy (Baldwin *et al.*, 2011). For instance, Alpha MOS manufacturer, specializes in producing potentiometric electronic tongues with array of electrodes, a reference sensor and autosampler system (Cho and Moazzem, 2022).

The e-tongue, e-nose, or a combination of both can serve as an efficient and robust tool for evaluating sensory profiles and detecting quality, showing substantial correlations with human sensory evaluations. These instruments are frequently acknowledged for their heightened sensitivity in detecting subtle changes or differences that may go unnoticed by a human panel (Cho and Moazzem, 2022). Regarding studies involving egg quality assessment, electronic sensory evaluations have been most commonly applied to estimate the freshness status of eggs throughout storage (Yimenu, Kim and Kim, 2017), and to evaluate differences of sensory qualities of eggs from different laying breeder strains (Dong *et al.*, 2021; Gao *et al.*, 2022).

The combination of traditional and novel sensory evaluation methods allows for a comprehensive understanding of the egg's sensory profile. This combined approach allows for the evaluation of traditional sensory characteristics while also incorporating modern technologies to detect subtle differences that might be missed in traditional assessments.

3.3. Quality evaluation of probiotics

3.3.1. Importance of probiotics for human health

The conventional description of probiotics involves live microorganisms that, when supplied in sufficient amounts, offer health advantages to the host by promoting a positive balance of microbiota and their functions in the gastrointestinal (GI) tract (FAO/WHO, 2002; Parker *et al.*, 2018). Probiotics have emerged as necessary elements in the domain of food supplements. These microbial organisms, predominantly sourced from bacterial groups such as *Lactobacillus, Bifidobacterium*, and *Enterococcus*, as well as yeast strains like *Saccharomyces boulardii*, play a vital role in shaping the delicate balance of the human microbiota (Menezes *et al.*, 2018; Sanders *et al.*, 2018).   Their significance extends beyond the realms of traditional fermented foods, such as yogurt and sauerkraut, into the front line of dietary supplements, where they're principally employed in a freeze-dried powder format and generally encapsulated, formed into tablets, or

presented as powder in stick packaging or sachet formats to preserve the unique microbial properties for convenient and targeted consumption (Nagashima *et al.*, 2013; Hill *et al.*, 2014; Fenster *et al.*, 2019; Gómez-Gaete *et al.*, 2024). Probiotics act as helpers of digestive health, harmonizing multiple benefits that encompass optimal nutrient absorption, safeguarding of harmful microbial overgrowth, and the conservation of a harmonious microbial community. A disturbance in the balance of the microbiota has been linked to over 25 diseases affecting the gastrointestinal system, autoimmune responses, and emotional well- being, among others (De Vos and De Vos, 2012). Probiotics are commonly employed for the prevention and regulation of conditions such as inflammatory bowel diseases, diarrhea, and liver disorders; and reducing the risk of cardiovascular conditions, hypertension, obesity, arteriosclerosis, cancer, and slowing down the aging process (Sanders *et al.*, 2018; Eslami *et al.*, 2019; Oniszczuk *et al.*, 2021; Choudhary *et al.*, 2023).

When presented in the form of powder, granules, or capsules, probiotics offer a unique versatility in their composition (Li *et al.*, 2017; Baral *et al.*, 2021; G. Wang *et al.*, 2022). These supplements may host a single strain of beneficial microorganisms, ideal for addressing specific health concerns or leveraging the benefits associated with a particular strain. Alternatively, some products are strategically formulated with multiple strains, creating a diverse cast of beneficial microorganisms that can collaboratively provide a broader range of health benefits (Kwoji *et al.*, 2021). It is crucial to thoroughly review the label of each product to understand the specific strains present and ensure they align with desired health goals. Additionally, some formulations may integrate prebiotics, substances that nourish and promote the growth of probiotics in the digestive system, adding an additional level of complexity and holistic benefits to these probiotic supplements (Peng *et al.*, 2020; Kwoji *et al.*, 2021). This combination highlights the multifaceted nature of probiotics, emphasizing their adaptability and broad spectrum of potential advantages for overall health.

3.3.2. Factors affecting the viability of probiotics

The effectiveness of probiotics for human health can be influenced not only by the composition of these probiotic supplements but also by external factors that may affect their characteristics or properties. Biopolymers with specific biocompatible and biodegradable properties such as chitosan, pectin, starch, alginate, maltodextrin, cellulose and other polymeric compounds, play a pivotal role as carriers frequently used to encapsulate and ensure the viability of live probiotic microorganisms (Asgari *et al.*, 2020; G. Wang *et al.*, 2022; Xie *et al.*, 2023). Maltodextrin, derived from starch through partial hydrolysis, serves as a soluble and easily digestible carrier. Its high solubility makes it suitable for various probiotic formulations, including

powders and capsules. Additionally, maltodextrin can act as a source of energy for microorganisms. On the other hand, cellulose, a complex carbohydrate found in plant cell walls, serves as an inert carrier due to its resistance to digestion by human enzymes. This property allows cellulose to protect probiotics from environmental factors and stomach acids until they reach the intestines.

Several critical factors during the manufacturing, packaging, and storage processes need to be considered to ensure the viability and potency of probiotics (Baral *et al.*, 2021; G. Wang *et al.*, 2022). Temperature control is vital, as probiotics are sensitive to high temperatures that can compromise their viability. Moisture levels must be carefully managed, as excessive humidity can activate probiotic microorganisms prematurely, reducing their shelf life. Acidity, particularly in the stomach environment, poses a challenge to probiotic survival, necessitating the use of enteric coatings or acid-resistant capsules. Oxygen exposure during manufacturing and packaging can lead to oxidation, potentially impacting probiotic viability. The temperature and pH conditions required for certain probiotics can exhibit variability. For instance, the optimal temperature for many probiotics is typically between 35-39°C, which is near to the 37 °C of the human body temperature. Regarding pH, most probiotics thrive within a pH range of 2.5 to 8.0, allowing them to withstand stomach acidity and colonize the intestine (Asgari *et al.*, 2020; Xie *et al.*, 2023).

Temperature is one of the most important factors and a vast amount of research was carried out employing various methods to assess the thermal resistance of probiotics, such as simulating probiotic growth under diverse fermentation temperatures and evaluating the thermal stability of probiotics during manufacturing, storage, and transportation. For example, in probiotic manufacturing, examining spray-dried lactic acid bacteria (LAB) exposed to elevated growth temperatures demonstrated that following heat treatment at 60°C, the survival of heat-adapted *Lactobacillus cremoris* and *Lactobacillus rhamnosus* GG increased by 0.7-1.5 and 0.3 log, respectively (Hao *et al.*, 2021). In an assessment of the preservation of LAB probiotics through three double-microencapsulation techniques, microencapsulated LAB exposed to the three methods exhibited enhanced tolerance to elevated temperatures in comparison to free cells, they were exposed for 60 min at 60 °C, for 30 min at 70 °C, and for 30 s at 80 and 100 °C (Pupa *et al.*, 2021). Concerning fermentation and storage conditions, an assessment of lactic acid beverages containing probiotics (stored for 21 days at 7 °C) indicated a preference for fermentation temperatures of 37°C over 45 °C, attributing this choice to improved storage stability (Fiorentini *et al.*, 2011).

While most probiotics are designed to withstand a range of temperatures, however, extreme heat may negatively affect the live microorganisms. Exposing probiotics to elevated temperatures, as encountered in processes like blanching, canning, or high-temperature cooking methods, is not

feasible as it exceeds 80°C, leading to cell death (Liu *et al.*, 2014). Hot water may lead to a reduction in viability, as heat can compromise the structural integrity and metabolic activity of the beneficial bacteria and yeast strains. Manufacturers play a vital role in ensuring probiotics' viability by addressing factors like temperature, moisture, and packaging. However, consumers also contribute by storing supplements properly and when preparing probiotic drinks following dosage and water temperature instructions. Proper adherence to these guidelines maximizes the potential health benefits of probiotics, promoting digestive health and overall well-being. Several products available in the market incorporate probiotic bacteria; nevertheless, the quantity of bacteria present in the product might not consistently align with the manufacturer's stated declaration (Zawistowska-Rojek, Zaręba and Tyski, 2022).

3.3.3. Microbiological assessment methods

Traditional microbiological techniques have long been employed to assess the quality and viability of probiotics. These methods typically involve cultivating microorganisms under specific conditions and observing their growth and characteristics. The most common technique for assessment is plate counting. This classic method involves spreading a known volume of a probiotic sample on a solid growth medium, allowing viable microorganisms to form visible colonies. The plate count method, while straightforward, necessitates extended incubation periods and the careful choice of suitable culture media. The assessment of probiotic microbe counts in medicinal products, dietary supplements, or specialized medical foods is primarily contingent on the product's composition (featuring one, two, or multiple microorganism types) and its format (capsules, powder, drops, tablets) (Zawistowska-Rojek, Zaręba and Tyski, 2022). Microscopic examination is another technique where direct observation under a microscope allows for the assessment of microbial morphology, motility, and cellular structure (Schmolze *et al.*, 2011; Pasulka *et al.*, 2021). Most probable number (MPN) method is also currently employed. This statistical method estimates the number of viable microorganisms based on the presence or absence of growth in a series of liquid media tubes (Weenk, 2003). While these methods are well-established, they often require time, skilled personnel, and may not capture the full complexity of the probiotic community.

In recent years, new methods like flow cytometry, PCR (Polymerase chain reaction), and near infrared spectroscopy (NIRS) have emerged to overcome some of the challenges posed by traditional microbiological techniques in assessing probiotics. Of these, NIRS is particularly notable for its speed and non-destructive nature, requiring minimal sample preparation while handling large numbers of samples efficiently. By capturing detailed spectral data that reflect the

chemical and physical traits of probiotic samples, NIRS enables a more thorough evaluation of microbial viability and quality.

3.4. Quality evaluation of pea microgreens

3.4.1. Importance of microgreens in human nutrition

The cultivation of microgreens has attracted increasing attention in the fields of functional foods and modern gastronomy (Paraschivu *et al.*, 2022; Singh *et al.*, 2024). Microgreens represent an early stage of growth for edible plants. They are cultivated in different substrates and are characterized by their small leaves and intense flavors. The harvesting of microgreens is done when they have reached only a few inches in height and have developed their first true leaves (Lone, Pandey and Gayacharan, 2024). This occurs typically within one to two weeks after seedling. They are particularly suitable for vertical farming for short cultivation cycle, high seeding density, compact height, and high market value (Balázs *et al.*, 2023). The cultivation and consumption of microgreens is attributed to the their freshness and the high concentration of nutrients and bioactive compounds (Gunjal *et al.*, 2024).

Plants that have been traditionally cultivated for their seeds, such as peas, beans, cereals, and sunflowers, are now harvested as microgreens (Balázs *et al.*, 2023). A wide range of species can be consumed as microgreens, with *Brassicaceae* varieties, particularly broccoli, dominating the global market at 15%, followed closely by arugula at 9%. Paraschivu et al. (2022) has also mentioned a variety of plants that can be cultivated as microgreens, including amaranth, mustard, parsley, celery, cilantro, kale, beets, and basil; various cereals, such as rice, oats, wheat, corn, and barley; as well as legumes such as chickpeas, beans, and lentils.

Microgreens are rich in phytonutrients such as vitamins, minerals, carotenoids, polyphenols, and organic acids. In fact, their concentration can be up to forty times higher than those found in mature leaves. It has been mentioned that a regular consumption of fruits and vegetables with high levels of these compounds can reduce the risk of chronic conditions such as cardiovascular conditions, diabetes, cancer, and degenerative disorders (Xiao *et al.*, 2016; Zhang *et al.*, 2021; Gunjal *et al.*, 2024).

A number of phenolic compounds have antioxidant capacity such as phenolic acids, flavonoids and tannins. They are common secondary metabolites that can repair the damage caused by free radicals (Dai and Mumper, 2010). Antioxidants are a type of phytonutrient that helps to mitigate the damage caused by oxidative stress. This category includes vitamin C, carotenoids, phenolics, and minerals such as copper, zinc, and selenium, among others. Several studies have reported higher levels of antioxidants in microgreens compared to their mature

counterparts, meanwhile others, have indicated the opposite by showing higher levels of antioxidants in mature plants (Pinto *et al.*, 2015; Choe, Yu and Wang, 2018; Yadav *et al.*, 2019; Di Bella *et al.*, 2020). Evaluating microgreens from five Brassica species researchers identified 164 polyphenols; showing that microgreens possess a richer polyphenol composition and higher concentrations than mature Brassica plants, making them valuable sources of antioxidants (Cartea *et al.*, 2011; Sun *et al.*, 2013).

In another comparative study, the ascorbic acid, total phenolics (expressed in gallic acid equivalent - GAE), and total flavonoids (expressed in Catechin equivalents – CE) in microgreens ranged from 6.00 to 46.50 mg/100 g, 25.00 to 152.10 mg GAE/100 g, and 9.58 to 142.39 mg CE/100 g, respectively. In contrast, these same compounds in mature leafy greens presented ranges of 10.00 to 199.99 mg/100 g, 69.01 to 313.92 mg GAE/100 g, and 43.00 to 292.53 mg CE/100 g.

Carotenoids and phenolics are present in significant amounts in microgreens. Carotenoids, which include pigments such as β-carotene and lutein, possess antioxidant properties (Rodriguez-Amaya, 2015). In a study analyzing microgreens of wheat and barley, it was observed that carotenoid content increased significantly during the microgreen phase, surpassing that of the seed phase (Niroula *et al.*, 2019).

Several researchers have compared concentrations of microelements, which have shown that antioxidant levels in microgreens vary among species. For instance, Lenzi et al. (2019) found that small burnet presents higher concentrations of zinc and selenium compared to dandelion. Xiao et al. (2016), showed that rapini microgreens had the highest zinc content among 30 varieties of *Brassicaceae*. Kyriacou et al. (2019), evaluating 13 microgreen species, noted that pak choi and tatsoi had higher total chlorophyll content, while mustard had the highest concentration of anthocyanins. Marchioni et al. (2021), evaluating five microgreens of *Brassicaceae* family, indicated that anthocyanins were more abundant in mustard, while broccoli had the highest total polyphenol content compared to other microgreens. According to Xiao et al. (2012) red sorrel, cilantro, and red cabbage stand out for their high β-carotene content, with cilantro and red sorrel also showing elevated concentrations of lutein and zeaxanthin. Such compositional differences among microgreens are often related to the specific genetic characteristics of each specie and differences in their photosynthetic efficiency and metabolic regulation (Niroula *et al.*, 2019).

A study evaluated ten species for seed germination, growth, and consumer acceptance. Among these, lettuce, carrot, and green peas were the most favored. For antioxidant activity, green pea microgreens showed a higher total phenolic content (1871 mg/100 g dry weight) compared to their seeds and sprouts, indicating enhanced nutritional value at this stage (Senevirathne, Gama-Arachchige and Karunaratne, 2019).

3.4.2. Factors affecting the quality of microgreens

The cultivation of microgreens involves the management of biotic and abiotic conditions to ensure their proper development and an optimal yield. Some of the most important factors include the selection of suitable species, proper growing techniques, substrate selection, using seed of quality, implementing proper irrigation and fertilization, maintaining phytosanitary standards, and employing effective postharvest storage practices (Di Gioia, Renna and Santamaria, 2017; Ebert, 2022). Environmental factors, such as temperature, humidity, and photoperiod, are also determinant for proper microgreen growth.

Temperature is a factor that significantly impacts the growth and development of plants, with various species having specific temperature requirements (Wheeler *et al.*, 2000). The ideal conditions for producing microgreens may vary depending on the plant species or variety. However, it is considered as a mild temperature for growth between 18 to 25 °C. When the temperatures is above this range, it can increase the microbial growth (Li, Lalk and Bi, 2021). In case of extreme temperatures the germination can be delayed and the plant can suffer from heat stress which negatively affects its development (Wheeler *et al.*, 2000). Additionally, high ambient temperatures can disrupt stomatal production which in consequence increase the risk of thermal damage and dehydration (Driesen *et al.*, 2020). Another important consideration regarding temperature is its influence in the nutrient content and absorption of sprouts, as well as the accumulation of phytochemicals. Studies involving sprouts show that when they are germinated at lower temperatures, they tend to exhibit improved phytochemical properties and higher levels of antioxidant activity (Calderon Flores *et al.*, 2021; Kim *et al.*, 2022). For instance, by maintaining temperatures below 4 °C for approximately four days, it is enhanced antioxidant content accumulation (Kim *et al.*, 2022). Thus, it is necessary to maintain optimal temperature ranges during cultivation to promote metabolic processes and facilitate the conversion of stored nutrients into energy.

Regarding to relative humidity (RH), microgreens generally grow adequately in environments with RH levels between 30% and 70%, although research on the precise humidity requirements is still limited (Li, Lalk and Bi, 2021). An effective air circulation is very important for promoting healthy growth and reducing the risk of diseases, as it helps regulate both temperature and humidity within the growing area (Chakraborty *et al.*, 2014; Sharma *et al.*, 2016). This can be achieved by using horizontal airflow fans or natural air vents to facilitate air exchange. Adequate air movement is also important for preventing mold, particularly in species prone to mildew. For optimal growth, microgreens should be grown at a pH of 6.56 to 7.54, with an electrical conductivity of 0.41 mS cm^{-1} of nutrient solution in fertigation (Kyriacou *et al.*, 2020).

However, the electrical conductivity in agricultural irrigation water commonly ranges from 0 to 3 mS cm^{-1}, depending on the source and water quality standards (Moliner and Masaguer, 1996).

Light is fundamental for the cultivation of microgreens, as it directly influences their growth and development. To achieve optimal growth, the use of light emitting diodes (LED) lights is recommended, as they are efficient and capable of emitting specific spectrums, primarily red and blue light, that plants absorb, which favor photosynthesis. The ideal light intensity ranges from 120 to 220 µmol m^{-2} s^{-1}, and a photoperiod of 12 to 16 hours is common. It is essential to allow adequate periods of darkness for processes like respiration. Moreover, photoperiod influence the antioxidant content of microgreens. In red beet microgreens a 16-hour light cycle increased phenolic compounds, total betalains, and antioxidant capacity compared to the 12-hour light cycle by 32%, 49%, and 25%, respectively, but decreased overall yield by 23%. In contrast, a 12-hour photoperiod yielded more microgreens and improved resource efficiency. Thus, while the longer photoperiod enhanced antioxidant properties, the shorter cycle was more beneficial for growth and resource management (Hernández-Adasme, Palma-Dias and Escalona, 2023). Historically, growers enhanced natural lighting with gas-discharge lamps (GDL), but now LEDs are becoming increasingly important in the horticultural sector as advancements in artificial lighting technologies continue (Ajdanian, Babaei and Aroiee, 2019). The light quality significantly influences various facets of plant growth and their phytochemical properties (Brazaitytė *et al.*, 2018; Ajdanian, Babaei and Aroiee, 2019). Researches indicate that red and blue light can positively impact certain crops; for instance, (Ajdanian, Babaei and Aroiee, 2019) observed that cress plants exposed to red and blue light produced greater yields than those grown under natural light. Additionally, it has been noted that red and blue light can promote elongation in crops like cabbage, kale, arugula, and mustard without compromising their yield or quality (Kong and Zheng, 2019). Furthermore, other studies investigated how different light intensity levels affect the growth of pea microgreens in hydroponic setups. After a 12-day growth period under both consistent and inconsistent lighting conditions, measurements were taken for the plants' fresh weight and shoot height. Although the overall yield was comparable for trays with the same average photosynthetic photon flux density (PPFD), variations in local light intensity accounted for 31% of the differences in fresh weight. These findings highlight the importance of light distribution in enhancing microgreen cultivation within vertical farming systems (Balázs *et al.*, 2023).

3.4.3. Microgreens status assessment methods

Understanding how environmental and agronomic factors influence microgreens requires accurate methods to assess their growth, composition, and quality. By evaluating both individual

traits and their combined effects, we can gain comprehension on how these plants respond to varying conditions.

Key growth parameters, such as height and weight (both fresh and dry), are crucial indicators of the agronomic performance of microgreens. Tools such as rulers or digital calipers, precision scales and drying ovens are used to measure these parameters (Lenzi *et al.*, 2019; Balázs *et al.*, 2023).

Chemical and optical measurements play a crucial role in understanding the quality and composition of microgreens. For visual appearance, the Lab color system is often employed, where lightness L*, redness a*, and yellowness b* are measured using tools like colorimeters or spectrophotometers. On the chemical level, parameters such as pH, conductivity, and °Brix are assessed with portable instruments, providing insight into acidity, mineral content, and sugar content (Araméndiz, Cardona-Ayala and Alzate, 2017; Li *et al.*, 2017).

The nutritional properties of microgreens are linked to their pigment and bioactive compound content. Pigments such as chlorophyll A, chlorophyll B, and carotenoids, are evaluated for their impact in photosynthesis and visual appearance. Total polyphenols and antioxidant capacity are analyzed to gauge the health benefits these plants offer. These assessments are commonly performed using spectrophotometric methods with advanced techniques such as high-performance liquid chromatography (HPLC) (Kyriacou *et al.*, 2019; Niroula *et al.*, 2019; Di Bella *et al.*, 2020).

Given the influence of environmental factors on microgreen quality, near infrared spectroscopy could offer a promising approach to assessing how these conditions affect microgreen characteristics. NIRS has the potential for rapid, non-destructive analysis of the chemical and physical properties of plant materials, which may provide insights into changes in nutritional content, phytochemical composition, and overall quality under various environmental influences.

3.5. Near infrared spectroscopy

Near infrared spectroscopy (NIRS) is a non-destructive analytical technique that utilizes the near infrared region of the electromagnetic spectrum (wavelengths between 800 and 2500 nm) (Burns and Ciurczak, 2008; Workman and Weyer, 2012; Ozaki, Genkawa and Futami, 2017). It is widely employed for qualitative and quantitative analysis in various fields, including chemistry, agriculture, pharmaceuticals, and food science. Significant recognition is due to researchers in the field of agricultural science, particularly K. H. Norris (Burns and Ciurczak, 2008).

NIRS detects molecular vibration responses within the near infrared region of the electromagnetic spectrum. This analytical technique relies on the interaction of near infrared light

with the overtones and combinations of fundamental vibrations of molecular bonds, such as C-H, N-H, and O-H bonds. As near infrared light is absorbed by these molecular vibrations, characteristic absorption bands are generated, providing valuable information about the chemical composition of the sample (Siesler *et al.*, 2002; Burns and Ciurczak, 2008; Ozaki, Genkawa and Futami, 2017). NIRS excels in quantitative analysis, enabling the simultaneous measurement of multiple components within a sample. The technique is non-destructive, allowing for real-time analysis without the need for complex sample preparation (Siesler *et al.*, 2002; Ozaki, Genkawa and Futami, 2017). Calibration models, established with reference values, permit NIRS to predict concentrations of specific constituents in unknown samples, while also facilitating the characterization of complex matrices by identifying important spectral features and chemical properties (Siesler *et al.*, 2002).

In its basic configuration, NIRS equipment typically consists of a light source, a sample interface, a spectrometer and a detector. After passing through the sample, light is broken down into different wavelengths by a prism or a grating (although other mechanisms may also be used) and is sensed by the detector. The collected data is used to construct the absorption spectrum of the sample (Siesler *et al.*, 2002; Aouadi *et al.*, 2020). Numerous studies that aimed at improving the reliability of NIR techniques have led to the creation of diverse instruments, such as interference filter spectrometers, scanning grating spectrometers, LED-based spectrometers, Acousto-Optic Tunable Filters (AOTF) devices, diode array grating polychromators, and portable or miniaturized spectrometers to keep up with the expectations of the evolving industry (Aouadi *et al.*, 2020). There are three major arrangement types in NIR spectroscopy, depending on the manner with which the light from the spectrometer interacts with the sample. In transmission, light passes through the sample; in reflectance, the light reflected from the sample's surface is measured; and in transflectance, both reflected and transmitted light are evaluated (Burns and Ciurczak, 2008).

3.5.1. NIRS for plants parameters assessment

Initially, NIRS served as a rapid, non-destructive method for real-time monitoring of crop nutrients, aiding in the optimization of nutrient application timing. In research on plant leaves, NIRS is capable of accurately predicting levels of macronutrients (N, P, K, S, Ca, Mg) and micronutrients (Fe, Zn, Mn, Cu), with macronutrient predictions generally being more precise. It directly detects significant macronutrients like N, P, and S due to their presence in organic compounds that respond to NIR, while some inorganic micronutrients and macronutrients (e.g., Ca, Mg, K) are identified through their association with these organic compounds. Total nitrogen content in leaf tissues is the most reliably predicted nutrient, with median R^2 values of 0.98 for

19

NIR and 0.90 for Vis-NIR. Other macronutrients, including P, K, Ca, and Mg, also exhibit accuracy (median $R^2 > 0.64$ for Vis-NIR and > 0.62 for NIR). Among micronutrients, Fe shows acceptable median R^2 values of 0.72 for NIR and 0.74 for Vis-NIR, while Zn meets acceptable standards with NIRS. In contrast, predictive accuracy for other micronutrients is comparatively low for both methods, likely due to their lower concentrations in plant tissues and the fact that they are not directly involved in NIR-active organic bonds. Their weak or indirect spectral features may be masked by stronger signals from water, carbohydrates, or structural proteins, making accurate prediction more challenging (Prananto, Minasny and Weaver, 2020).

Moreover, in other studies NIRS have been used to evaluate the status of plants. Chemometrics was applied to evaluate *Brassica carinata* under different abiotic growing conditions. The analysis showed a moderate correlation between NIR spectra and aboveground biomass, indicating that NIRS can be a useful tool for predicting biomass yield. This suggests potential for using NIRS in monitoring the growth and health of *B. carinata* in both indoor and outdoor environments (Huynh, 2023).

Researchers also have investigated non-destructive methods for detecting cold stress in soybean plants using near infrared spectroscopy and aquaphotomics. Spectra from five genetically engineered cultivars were collected at optimal (27 °C) and reduced (22 °C) temperatures. Analysis revealed significant differences in spectral profiles, with soft independent modeling of class analogy (SIMCA) achieving 100% accuracy in distinguishing between stressed and unstressed plants. The results indicated changes in water molecular structure and metabolism, highlighting cultivar variations in cold stress responses (Muncan *et al.*, 2022).

Vis-NIR spectroscopy (380–1000 nm) was explored by Marín-Ortiz et al. (2020) to detect biochemical changes in asymptomatic tomato plants infected with vascular wilt disease. The standard normal variate (SNV) pretreatment method proved most effective for high accuracy classification. Early infection signs included discoloration from green to yellow, while leaf turgidity remained stable, complicating visual detection. Significant reflectance differences between healthy and infected plants were observed mainly in the 380 to 750 nm range. Five key spectral bands related to the disease were identified: two in the visible range (448–523 nm and 624–696 nm) and three in the near infrared range (740–960 nm, 973–976 nm, and 992–995 nm), enabling successful classification of infected plants with 100% accuracy, 12 days prior to visible symptoms. Moreover, Vis-NIR spectroscopy is effective in classifying disease severity in plants. Liaghat et al. (2014) demonstrated this belief by using a k-nearest neighbors (kNN) model to differentiate mildly infected oil palm plants from healthy ones, achieving 97% accuracy before symptoms appeared. The visible and near infrared regions are equally crucial for assessing stress responses. Key absorbance bands at 550 nm and 720 nm indicate chlorophyll content, while bands

at 740 nm, 840 nm, 970 nm, 1200 nm, 1460 nm, and 1850 nm relate to water content. Each pigment absorbs light at specific wavelengths, chlorophyll in the red and blue regions, carotenoids in the violet and blue-green regions; enabling early detection of stress and infection through changes in spectral reflectance (Zahir *et al.*, 2022).

Furthermore, NIRS have been used to evaluate physiological and biochemical characteristics of plants. A study compared short-wavelength (SW) and long-wavelength (LW) near infrared spectroscopy with color compensation to predict soluble solids content in apples. The independent component analysis-support vector machine models (ICA-SVM) showed the best performance. SWNIR achieved an R^2p of 0.9398 and an RMSEP of 0.3870%, while LWNIR reached an R^2p of 0.9455 and an RMSEP of 0.3691%. The results showed that color compensation significantly improved showing its potential for real-time apple quality monitoring (Guo *et al.*, 2016). Furthermore, Hărmănescu et al. (2008), determined the total polyphenols content in seventeen Romanian medicinal plants using NIR spectroscopy. Correlations were established between polyphenols content (mM/g) measured by the Folin-Ciocalteu method and NIR reflectance values. The PLS-Leverage method yielded a strong correlation coefficient ($R^2 = 0.994752$) and low deviation values (6% to 8%), indicating high predictive quality for the regression model. By using a Micro-NIRS device connected to a smartphone, Y. J. Wang et al. (2020), analyzed pigments in tea plants. The variable combination population analysis (VCPA) and genetic algorithm (GA) denoted as VCPA-GA-PLSR models demonstrated strong performance in predicting chlorophyll a, chlorophyll b, and carotenoids, with correlation coefficients of 0.9226, 0.9006, and 0.8313, respectively, and low prediction errors.

3.6. Chemometric analysis

Chemometrics, also denoted as multivariate data analysis, utilizes mathematical and statistical techniques to analyze complex datasets produced by analytical instruments. This field encompasses both experimental design and data evaluation to obtain meaningful insights. While a comprehensive grasp of mathematics and statistics is recommended, having a solid understanding of the specific application and exercising good judgment are crucial for accurately interpreting the results (Gemperline, 2006; Roussel *et al.*, 2014).

3.6.1. NIRS preprocessing techniques

Preprocessing NIR spectral data is essential in chemometrics modeling to eliminate physical interferences in the spectra, thereby enhancing the performance of multivariate regression, classification, or exploratory analysis. The most common preprocessing methods

encompass techniques for scatter correction and spectral derivatives (Rinnan, Berg and Engelsen, 2009).

The Savitzky-Golay (SG) method is a numerical approach used for smoothing and differentiating data (Savitzky and Golay, 1964), and is widely applied in spectral analysis. It works by fitting a low-degree polynomial to a symmetric set of data points around a central point, mainly to reduce noise while retaining important spectral characteristics. Besides smoothing, it can also be adapted to calculate derivatives of different orders, which helps in improving spectral resolution.

Derivatives are used to address peak overlap and remove constant and linear baseline shifts among samples. In practice, first and second derivatives are more commonly utilized than higher-order derivatives, as they effectively enhance spectral features and correct baseline variations without excessively amplifying noise, which is a common drawback of higher-order derivatives (H. P. Wang *et al.*, 2022). Key factors in applying the SG method include selecting the appropriate window size and polynomial degree, which affect the method's sensitivity and effectiveness in capturing data characteristics (Rinnan, Berg and Engelsen, 2009).

Multiplicative scatter correction (MSC) first introduced by Martens et al. in 1983 and standard normal variate (SNV) introduced by Barnes et al. 1989 are the most frequently employed preprocessing methods for near infrared spectroscopy. Additionally, detrending applies linear or polynomial regression to adjust for baseline shifts and curvilinearity in reflectance spectra (Barnes, Dhanoa and Lister, 1989). These techniques help by dealing with challenges in diffuse reflectance spectrometry arising from particle size, scattering, and multicollinearity. The interaction of these factors significantly complicates the interpretation of near infrared diffuse reflectance spectra, with most variance attributed to sample particle size and minimal variance linked to chemical composition (Rinnan, Berg and Engelsen, 2009). To address these issues, these scatter correction techniques effectively eliminate interferences from scattering and particle size. As a result, this processing produces NIR diffuse reflectance spectra that are free from multicollinearity and the intricacies associated with the use of derivatives in spectroscopy (Barnes, Dhanoa and Lister, 1989; Liu *et al.*, 2019). MSC involves selecting a reference spectrum, typically the average from a calibration dataset, and aligning individual sample spectra with this reference. This technique aims to correct for variations in baseline and scaling among different spectra. On the other hand, SNV standardizes each spectrum by calculating its mean and standard deviation, transforming the data to have a mean of zero and a standard deviation of one. Both MSC and SNV enhance the reliability of spectral data, making subsequent interpretation and analysis more effective (Ozaki, Genkawa and Futami, 2017; Liu *et al.*, 2019).

3.6.2. Multivariate data analysis methods

Principal component analysis (PCA) is a widely used exploratory technique in spectroscopy for building linear multivariate models from complex datasets. It utilizes principal components (orthogonal basis vectors) to capture significant variations and reduce measurement errors, thereby minimizing noise and simplifying analysis. PCA aims to identify relationships among samples by creating new variables, with results visualized in scores plots that display spectra as scores in a transformed space and loadings plots that illustrate the contributions of original variables, such as wavelengths (Gemperline, 2006; Tsenkova *et al.*, 2018).

As mentioned by Qu and Pei, (2024), linear discriminant analysis (LDA) was first proposed by R.A. Fisher in 1936. LDA is a classification technique that utilizes orthogonal transformations to streamline and improve the efficiency of data processing and analysis. It is often used for multiclass classification of different samples. It is a supervised method so the class membership has to be known for the analysis (Granato *et al.*, 2018).

Moreover, discriminant analysis based on principal component analysis (PCA-LDA) is a method that combines aspects from both PCA and LDA. In PCA-LDA, the principal components obtained from PCA are then used as input features for the subsequent LDA. This integrated approach combines the dimensionality reduction capability of PCA with the discriminatory power of LDA. PCA-LDA is often used for spectroscopic data, where there are multiple correlated dependent variables and where LDA alone is not effective, and the goal is to classify or discriminate between different groups or classes based on the underlying structure of the data. This integrating technique offers a powerful tool for pattern recognition, classification, and discrimination tasks in various fields, including food quality assessment and chemometrics.

Partial least square (PLS) regression, introduced by H. Wold in the 1960s, is widely used in industrial applications for multivariate calibration due to its speed and accuracy advantages over other methods (Gemperline, 2006). In PLS, determining the number of basis vectors, also known latent variables (LV), is crucial for building the model. This parameter serves to reduce the dimensionality of the regression space and refine the regression vector (Gemperline, 2006). PLS regression aims to enhance the relationship between the X and Y datasets by creating latent variables that capture the variance in X and maintain a strong correlation with Y (Granato *et al.*, 2018). PLS consists of two key steps: reducing dimensionality via score projections and integrating a weight vector (w) that optimizes the covariance between X and Y scores (Roussel *et al.*, 2014). The performance of the PLSR model is assessed through the coefficient of determination (R^2) and the root mean square error (RMSE) typically obtained from calibration and cross-validation (Tsenkova *et al.*, 2018).

Figure 1, outlines the systematic approach to achieving reliable results through the integration of sample preparation, NIRS data collection, chemometric analysis, quantitative analysis, and informed decision making. The process begins with the careful selection of representative samples, followed by their homogenization to ensure consistency. NIRS is employed for spectral data acquisition, with rigorous preprocessing techniques applied to enhance data quality. Chemometric methods, including multivariate data analysis (MVDA), PCA, LDA and PLS regression, are utilized for data exploration and model building. Calibration models are validated and optimized to ensure accuracy in qualitative and quantitative analysis. Finally, the interpretation of results leads to effective reporting and decision making based on quality parameters and established acceptance criteria. This comprehensive workflow emphasizes the importance of each step in producing reliable findings from spectral data.

| **Sample Preparation**	**NIR Data Collection**	**Chemometric Analysis**	**Reporting and Decision Making**
• Selection of representative samples • Homogenization of samples	• Spectral data acquisition using NIRS • Pre-processing sing of spectral data	• Data exploration (PCA) • Qualitative analysis (Discriminant analysis) • Quantitative analysis (PLSR)	• Interpretation of results • Decision based on quality parameters and acceptance criteria

Figure 1. Integrated workflow: NIRS-based chemometric analysis for quality food assessment

4. MATERIALS AND METHODS

This section outlines the materials and methods adopted for the execution of various experiments. Studies have been conducted to assess the sensory profile of hen eggs using human sensory analysis, electronic tongue, and electronic nose; evaluation of probiotic characteristics and viability using NIRS; and the evaluation of microgreens growing under stress conditions using NIRS.

4.1. Materials and methods for egg sensory evaluation

4.1.1. Hens' dietary intervention and initial quality evaluation

The feeding trial with laying hens adhered to the European Commission Council Directives (86/609/EEC) (COUNCIL OF THE EUROPEAN COMMUNITIES, 1986) and the Hungarian Act for the Protection of Animals in Research (The Parliament, 2021). A total of 900 Lohmann Brown Classic hens, aged 56 weeks and weighing an average of 1.88 kg ($\pm$ 0.12), were housed in environmentally controlled cages (EV 2240-EU, Big-Dutchman, HAT-AGRO Baromfitechnológia Kft., Győr, Hungary). The hens were divided into three groups (300 hens each): Control (0% Zincoppyeast), ZP 2.5% (2.5% Zincoppyeast), and ZP 5.0% (5.0% Zincoppyeast). Zincoppyeast, a yeast biomass in dried form, was produced by SC AGSIRA SRL, Romania, using spent brewing yeast mixed with organic zinc-enriched yeast from S.C. PHARMACORP INNOVATION SRL, Romania. The birds were fed isonitrogenous and isoenergetic corn-extracted soybean meal– distiller's dried grains with solubles (DDGS)–wheat-based diets, formulated according to National Research Council (NRC) guidelines (National Research Council, 1994) and the Lohmann Brown Classic Management Guide. Proximate analysis was conducted to determine the chemical composition of the feeds, ensuring they met the same category requirements (Aurand, Woods and Wells, 1987). The calculated diet values are presented in Appendix-A2_Table 1, additionally, the quantified chemical composition and energy content is shown in Appendix-A2_Table 2, confirming the diets' uniform energy content for evaluating the effects of varying Zincoppyeast levels. Feeds were assessed for moisture, crude protein, fat, fiber, calcium, phosphorus, and sodium content according to AOAC standards (AOAC, 2006). Fresh water was provided ad libitum daily. In the ZP 2.5% and ZP 5.0% groups, part of the extracted soybean meal was replaced with Zincoppyeast. After a two-week adaptation period to the diets, the three-month experimental period commenced. Eggs were collected daily (during which average daily egg production exceeded 91% in all groups); however, only eggs collected on day-30 and day-60 were considered for sensory analysis. The remaining time until day-90 was a safety

period in case we needed to repeat the sampling due to any failures of any analysis done on day-30 or day-60 samples.

Eggs from the three groups collected for evaluation on day 30 (batch 1) and day 60 (batch 2) of the experimental period, totaling 90 samples per batch for human sensory analysis, 18 for e-tongue analysis, and 90 for e-nose analysis. The number of eggs used for human sensory analysis was higher because multiple samples were needed per the number of testers within the panel. For the e-nose, the large number of available slots on the tray permitted to analyze more samples, improving the reliability of statistical tests, and repeatability and stability of the system. For the e-tongue, only a limited number of samples could be analyzed due to the small capacity of the autosampler and the long duration of each measurement, so additional samples were not required.

Evaluating both batches aims to finding a more comprehensive understanding of potential temporal variations in the quality of eggs, which may influence both nutritional and sensory qualities of eggs. Differences may arise, due to egg laying time, in different egg parameters regarding egg weight, shell, albumin, and yolk characteristics (Şekeroğlu *et al.*, 2024). Samples of batch1 were disinfected with ozone and stored (in cold, 4–8 °C) until the analysis, the same procedure was done for samples belonging to the 2nd batch. Batch 1 and batch 2 samples were not analyzed at the same time, but with 30 days difference. Laboratories performing the sensory analysis were not informed that batch 2 was a repetition of batch 1. Those were considered to be a separate test with three feeding groups on both occasions. Fresh samples were used for human sensory and e-tongue analyses; while for e-nose analysis, samples were stored for 0 (corresponding to fresh samples), 30, and 60 days in the fridge (10–14 °C). Chemical assays were performed on 12 eggs per batch, and microbiological assays on 30 eggs per batch.

The data presented in Appendix-A2_Tables 1 to 4 were obtained from experimental measurements and analyses conducted in collaboration with accredited laboratory (MTKI Mosomagyarovar, Hungary) as part of this study, following AOAC standards (AOAC, 2006).

4.1.2. Sample preparation and analysis of eggs

Human sensory evaluation

To assess sensory attributes, the human organoleptic evaluation of the egg samples followed the guidelines outlined in MSZ ISO 6658: 2018, serving as a reference test method (MSZT, 2003). Five trained reviewers participated in the evaluation process, employing an experimental design known as Williams Latin Squares, with each sample from the three feeding groups (Control, ZP 2.5%, and ZP 5.0%) evaluated in two replicates. The eggs underwent assessment in three different presentations: raw, boiled, and fried.

Sample Preparation Details:

- Boiled eggs were kept in boiling water for 10 min.
- For fried eggs, oil was poured into a pan and heated, then the previously beaten eggs were poured in and agitated during the cooking time.

The evaluation was conducted using an intensity scale ranging from 0 to 9 points. A comprehensive evaluation encompassed a total of 21 sensory characteristics (Table 1).

Table 1. Sensory characteristics evaluated in raw, boiled, and fried eggs

Egg Type	Evaluated Attributes
Raw eggs	Albumin color, Yolk color, Yolk shape, Albumin density
Boiled eggs	Albumin color, Yolk color, Egg odor, Unusual odor, Albumin flavor, Unusual taste, Albumin flexibility, Yolk creaminess
Fried eggs	Yolk color, Egg odor, Sweet aroma, Unusual odor, Egg taste, Sweet taste, Unusual taste, Texture

Electronic tongue analysis

The taste profile of the egg samples was assessed using an Alpha Astree electronic tongue from AlphaMOS, located in Toulouse, France. Equipped with a 16-position auto-sampler, the measurements were conducted at the Department of Measurements and Process Control within the Institute of Food Science and Technology at the Hungarian University of Agriculture and Life Sciences. This sophisticated device features seven food-grade sensors, according to the manufacturers naming ZZ, JE, BB, CA, GA, HA, JB, designed to detect and identify complex organic and inorganic compounds in liquid samples. Utilizing a methodology based on measuring differences in potential changes against the Ag/AgCl 3M KCl reference electrode, the sensors display cross-sensitivity and partial selectivity, allowing them to detect multiple compounds in complex liquid mixtures while still showing a preferential response to certain substances. Researchers can employ this technology as a state-of-the-art fingerprint-like analysis to discern general patterns among the samples measured on the seven sensors (AlphaM.O.S., 2021).

Sample preparation details:

The eggs underwent initial processing by crushing, followed by transfer of the contents into a porcelain dish, where they were beaten for a duration of 1 minute. Subsequently, 2 grams of the homogenized egg mixture were carefully transferred into individual 100 mL volumetric flasks and then filled up to the mark with distilled water. From each of the three experimental groups, six parallel samples were prepared, totaling N = 18 eggs for both tested batches. These samples

were then subjected to analysis using e-tongue. Due to constraints posed by the limited positions of the auto-sampler, the samples were organized into three separate sequences. Each sequence included one technical replicate from each of the three groups and underwent analysis four times, resulting in a total of 24 measurement points per sample group. The acquisition time for each sample was standardized at 120 seconds with a steering velocity of 3, while the sensors were cleansed with distilled water for 20 seconds at a steering velocity of 6.

Electronic nose analysis

The assessment of aroma profiles in the samples was carried out utilizing the Alpha MOS Heracles NEO electronic nose (Alpha MOS, Toulouse, France) within the facilities of ADEXGO Ltd. Correltech® laboratory (Balatonfüred, Hungary). This advanced e-nose, specialized in volatile compound analysis, functions as a high-speed chromatograph analyzer featuring dual columns. The analysis process initiates with the concentration of odors within a cold trap, followed by trap flushing, heating, and subsequent injection of the concentrated odor into the columns. Within these columns, volatile compounds undergo separation and detection via two flame ionization detectors (FID). Evaluation of the acquired chromatograms was facilitated by AlphaSoft v17 software (Alpha MOS, Toulouse, France), which systematically records retention time and delineates peak positions. This software automatically calculates the Kovats-index for each detected peak. These indexes can be matched against the AroChemBase database for identification of volatile substances associated with the odor (AlphaM.O.S., 2018).

Sample preparation and Analysis Procedure:

In alignment with the methodologies employed for human sensory evaluation and e-tongue analysis, e-nose assessments were conducted on freshly collected egg samples (0 days of storage). However, to comprehensively assess potential variations, additional examinations were performed on egg samples subjected to refrigeration for 30 and 60 days, respectively. This approach aimed to elucidate any differential outcomes influenced by storage duration and feeding-mode group.
In the e-nose, the egg samples are injected in a trap or odor concentrator which is heated to allow volatilization of liquids. The selected preheating, before the subsequent phases of the gas chromatography analysis, consisted in employing temperatures of 50 °C and 80 °C. Two preheating temperatures (50°C and 80°C) were selected to improve volatile compound recovery. 50°C is often optimal for capturing a broad range of volatile organic compounds. Raising the temperature to 80°C enables the detection of those requiring more thermal energy to volatilize. 80°C can increase the extraction of certain compounds but with the risk of degradation. Measurements were carried out across two columns of the e-nose equipment, namely column

MXT-5 and MXT-1701. Each column separates volatile compounds, which are then detected by two Flame Ionization Detectors (FIDs) and recorded using AlphaSoft. The data reported in this study correspond to the MXT-5 column.

Compounds identification:

The analysis facilitated the identification of characteristic compounds through reference to the AroChemBase v8 database integrated into AlphaSoft (AlphaM.O.S., 2018). This database encompasses domains such as "Food, Flavors, and Fragrances". Furthermore, compound determination was associated with the most relevant sensors from the egg discriminant analysis. These sensors were linked to the closest Kovats indexes, with very close magnitudes, listed in the AroChemBase v8 database. In the database, Kovacs index are associated with specific volatile compounds and sensory characteristics. This meticulous approach significantly enhanced the accuracy of volatile compound association, contributing to a more robust interpretation of the results.

4.1.3. Statistical methods for eggs samples evaluation

Human sensory evaluation results underwent statistical evaluation using one-way analysis of variance (ANOVA), with each parameter assessed individually. Upon detecting significant differences ($p < 0.05$) among the three groups, Tukey's Honestly Significant Difference (HSD) post hoc tests ($p < 0.05$) were executed for comprehensive inter-group comparisons (Madsen, 2011).

For e-tongue assessments, statistical analysis involved computing Euclidean distances within a space of seven dimensions (that are corresponding to seven sensors) across the feeding groups on a scale from 0 to 30. As the differences between groups become more pronounced, the Euclidean distance increases. The Euclidean distances were calculated for the samples of the two batches (separately).

Furthermore, principal component analysis was used as exploratory data analysis to uncover nuanced multidimensional patterns. Linear discriminant analysis facilitated group classification, with model robustness assessed through three-fold cross-validation to ensure reliable performance. This process divided the data, ensuring that repeated measurements of the same sample were not included at the same time in both training and validation sets. Two-thirds of the data were used for model training, while the remaining one third served as the validation set. The data was iteratively split into training and validation sets three times to ensure each sample's participation in both calibration and validation sets.

Data from the e-nose were subjected to PCA-LDA to discern significant sensors contributing to group differentiation based on the Kovats index. Model evaluation embraced thorough three-fold cross-validation to ascertain the optimal number of principal components (PC) for discriminant analysis models, where the chosen number of PCs was the one that achieved the highest correct classification accuracies while maintaining the smallest decrease from training to validation, therefore mitigating the risk of overfitting while looking for robust performance.

To further assess the discriminant models for the e-tongue and e-nose using real data, additional models were developed with simulated data (Defernez and Kemsley, 1997). Given the large gap between calibration and cross-validation results, this approach helped determine whether the real models retained some predictive power despite overfitting. If the simulated models performed worse, it suggested that the real models still captured relevant patterns in the data (A2_Table 5, A2_Table 6).

The "aquap2" package (Kovacs and Pollner, 2016) was employed for multivariate analysis in the R-project environment.

The comprehensive evaluation integrated diverse factors, including batch variations and feeding group compositions across varying storage times, enhancing the interpretability of the findings. Figure 2, summarizes the methodological approach employed in the enriched eggs experiment, detailing the pre-establishment of the trial and the subsequent sensory and instrumental analyses.
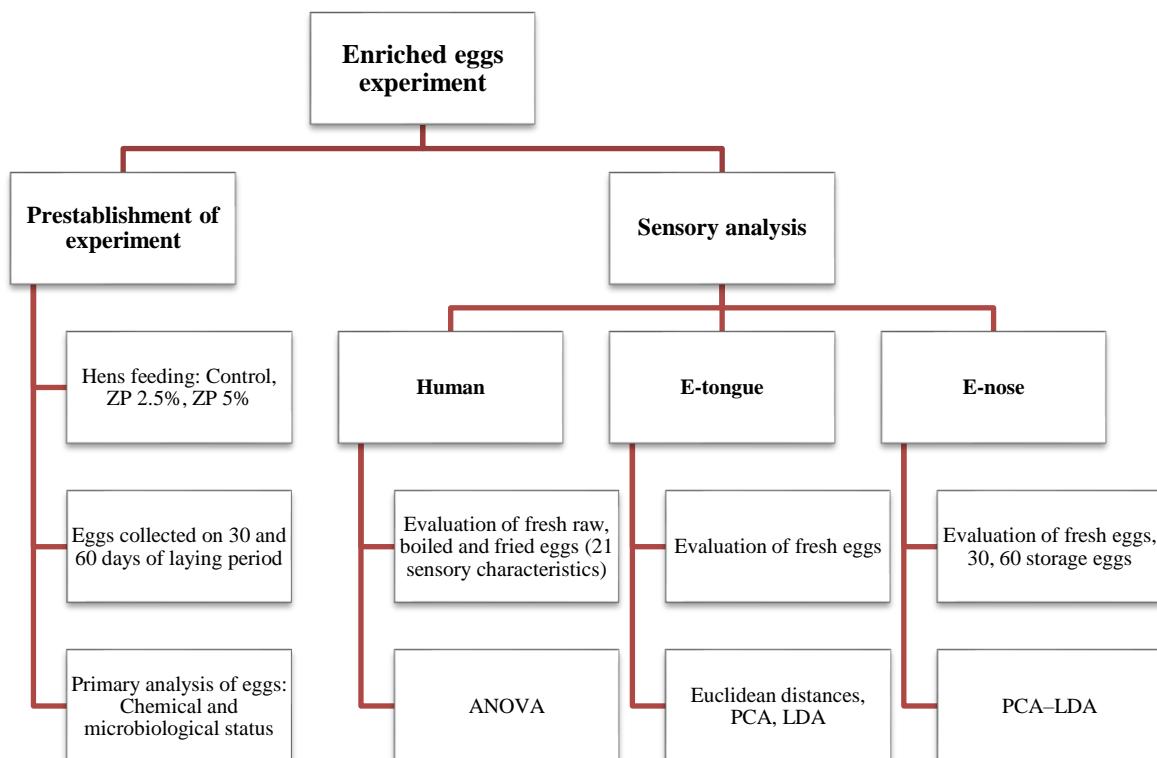

Figure 2. Methodological scheme for sensory and analytical assessment of enriched eggs

4.2. Materials and methods for probiotics evaluation

4.2.1. Sample preparation and analysis of probiotics

This study utilized three commercial probiotic food supplements in powder form, which their specific names are not included to maintain confidentiality and avoid potential commercial bias. Instead, they are identified as probiotic N (Istanbul, Turkey) and probiotics P and A (Budapest, Hungary). Probiotics P and A are from the same commercial brand, while probiotic N is from a different brand. As shown in Appendix- A2_Table 7, the probiotic P, A and N show a CFU content per dose in the same range and different composition of bacterial strains according to the labels.

To prepare the drinks for each probiotic product, three concentration levels were considered: C1 (3 g/125 mL), C2 (2.5 g/125 mL), and C3 (2 g/125 mL). These concentrations reflect the daily doses stated on the product labels: 2 g for probiotic P and 3 g for probiotics A and N. Additionally, three temperature levels were tested to simulate typical consumer practices: T1 (25 °C), T2 (60 °C), and T3 (90 °C). The preparation involved accurately weighing the probiotic powder and mixing it with distilled water at the specified temperatures. Samples were allowed to cool to near room temperature before analysis, with cooling times of 35 minutes for 60 °C and 44 minutes for 90 °C. Each preparation was repeated three times, yielding 81 samples (3 probiotics × 3 concentrations × 3 temperatures × 3 repetitions).

Microbiological analysis

The cultivation of *Lactobacillus* spp. was conducted using Man, Rogosa, and Sharp (MRS) agar (Biolab, Hungary), a low-selectivity medium, employing the pour plating method. To facilitate dilutions, maximum recovery diluent (MRD) consisting of 1 g bacteriological peptone and 8.5 g NaCl per liter of distilled water was prepared and subsequently autoclaved at 121 °C for 15 minutes. Each sample, prepared according to the probiotic-concentration-temperature combinations, was subjected to serial dilution in MRD, followed by plating on MRS agar. Plates were then incubated at 37 °C for 72 hours to facilitate bacterial growth, after which colony-forming units (CFU/g) were enumerated to quantify bacterial concentrations.

Near infrared spectroscopic analysis

The near-infrared spectral data were gathered using a benchtop MetriNIR spectrophotometer (MetriNIR Research, Development and Service Co., Budapest, Hungary). It was used a custom-designed circular cuvette, thermally regulated at 25 °C, that is made up of: a metallic wall (inner diameter: 5 cm; outer diameter: 8.5 cm) and a crystal layer (thickness: 0.4

mm). After the sample is placed in the cuvette, it is covered with a lid equipped with a white reflector. The acquisition of transflectance spectra is across the 900-1700 nm wavelength range with 0.5 nm resolution. A comprehensive analysis encompassed 81 prepared samples, three replicates for each sample was scanned and three consecutive scans, thereby yielding 27 spectra for every probiotic product and treatment. This protocol resulted in a dataset comprising 729 scans, with an even distribution across the three probiotic products. Prior to NIR scanning, sample sequences were randomized to mitigate any potential bias.

4.2.2. Statistical methods for probiotic samples evaluation

Statistical analysis of viable counts (Log CFU/g) was conducted using ANOVA and Tukey's test ($p < 0.05$) to evaluate group differences, considering the different combinations of probiotics and temperatures (with concentrations treated as replicates).

The NIRS spectra were analyzed in the 950–1630 nm wavelength range. PCA was used for patter recognition in the spectra. The classification of samples was performed according to probiotic type, concentration and temperature by using PCA-LDA analysis and using three-fold cross-validation to obtain the different models. Additionally, to obtain the most possible accurate PCA-LDA models, a total of 41 spectral pretreatments (single and combined) were evaluated: The individual spectrum pretreatments encompassed a Savitzky–Golay smoothing filter (SG) using a 2nd-order polynomial (13, 17, or 21 points), first and second derivatives, multiplicative scatter correction (MSC), standard normal variate (SNV), and detrending (DeTr). Meanwhile the combined pretreatment is comprised for 2 or more single pretreatments simultaneously (Appendix-A2_Table 8). Prediction models for the viability of probiotic drinks according to log CFU/g were built by using PLSR by correlating the NIR spectra with the counting colony forming units from microbiological analysis results. The repetitions R2 and R3 were utilized for constructing the PLSR models, which correspond the two-thirds of the data. Cross-validation was conducted by excluding the spectra of one treatment (probiotic-concentration-temperature) in each step. Subsequently, the remaining one-third of the data (R1) was employed for prediction to assess the robustness of the final model.

The "aquap2" package (Kovacs and Pollner, 2016) was employed for multivariate analysis in the R-project environment.

Figure 3, summarizes the experimental approach used to evaluate the viability of probiotic drinks under varying conditions of concentration and temperature. The integration of microbiological reference analyses and NIRS-based chemometric methods provided a comprehensive framework

for assessing the impact of these factors, enabling the prediction of probiotic viability and the characterization of relevant spectral data.
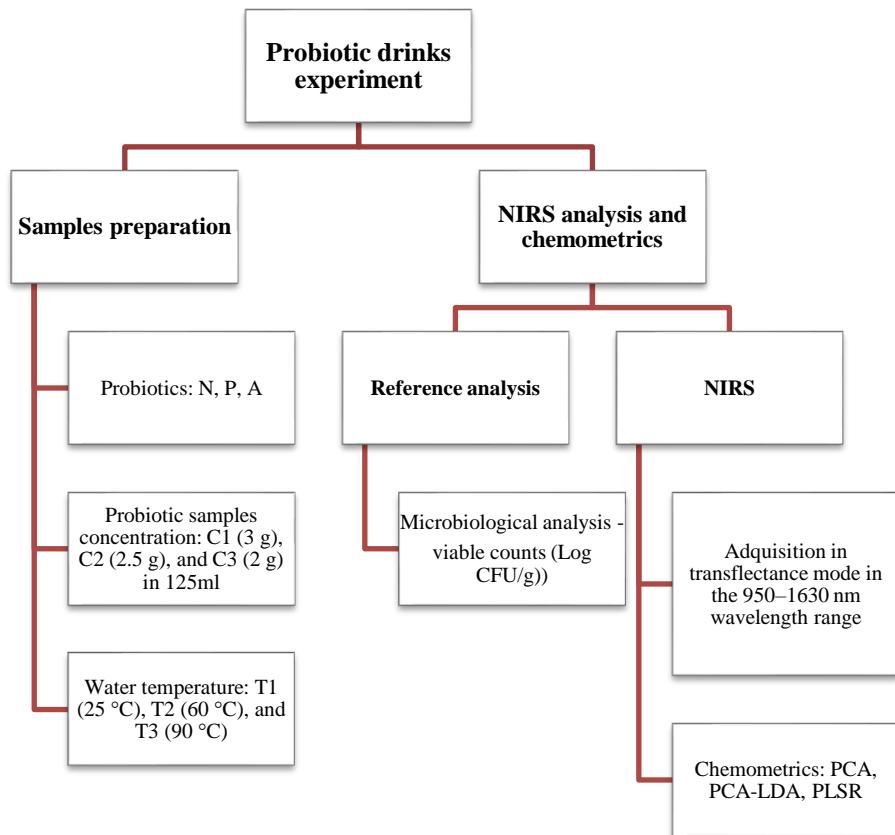
Figure 3. Methodological scheme for probiotic drinks assessment

4.3. Materials and methods for microgreens evaluation

4.3.1. Development of climate chambers and cultivation of pea microgreens

A critical phase of the project involved the development of custom-designed climate chambers, achieved through a stepwise approach. Initially, individual control components were developed separately and subsequently integrated into a unified system.

(a) Control systems

Photoperiod Control

Temperature Control

Humidity Control-
ventilation control

(b) Single chamber set up

Components
- Led strips
- Fan
- Humidity sensor

(c) Single refrigerator set up

Components
- Cooling system
- Heating plaques

(d) Complete setup

Components
- 3 refrigerators
- 12 chambers
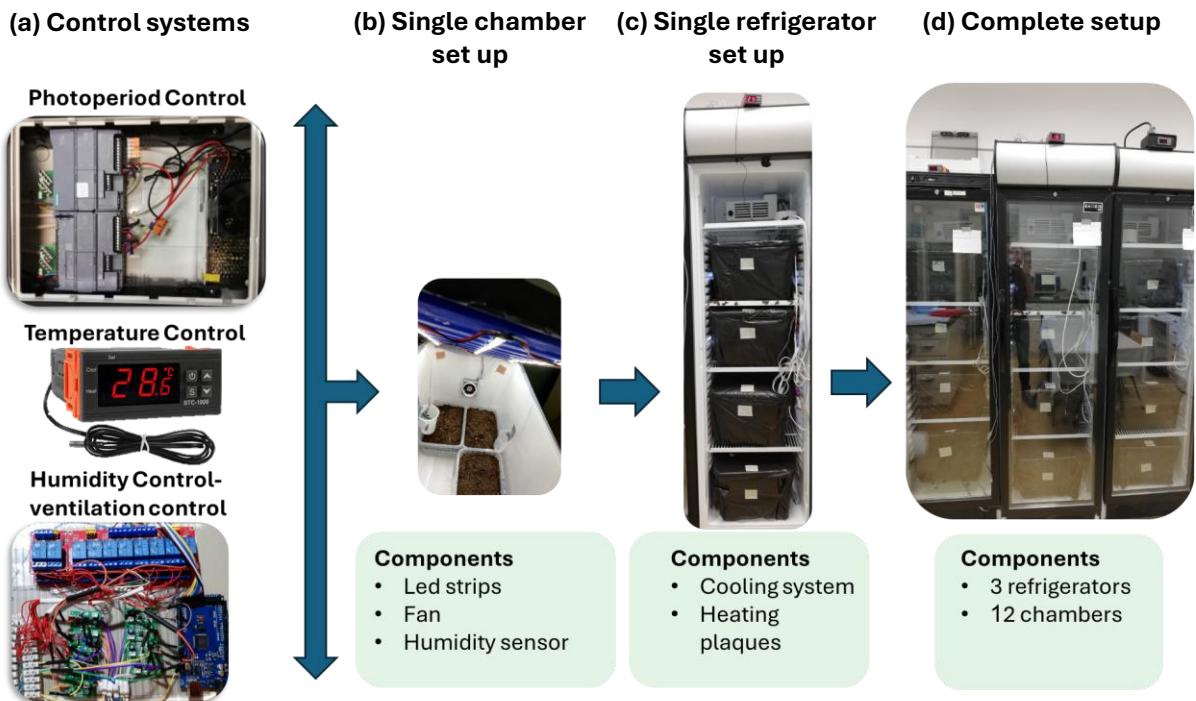
Figure 4. Set up for pea microgreens growth under different temperature and photoperiod

Figure 4, shows an overlook of the developed set up for pea microgreens growth under different temperatures and photoperiods. The first step implemented an ON-OFF temperature control system (Figure 4a) using three STC controllers (equipped with temperature sensors) connected to commercial refrigerators. These refrigerators facilitated temperature reduction, while heating plates installed inside enabled temperature elevation (Figure 4c). For photoperiod control, smaller individual chambers were constructed from plastic boxes featuring a white interior, black exterior, and lids fitted with white LED strips that covered the full visible spectrum (Figure 4b).

A light distribution test was conducted in these chambers by measuring photosynthetic photon flux density (PPFD) at five points at the base level using the Mavospec Base spectrometer (Gossen, Germany). The measurements yielded a mean of 75.7 µmol/m²/s and a low standard deviation of 4.96, confirming uniform illumination and ensuring homogeneous conditions for plant and microgreen experiments. These photoperiod-controlled chambers were subsequently placed inside the temperature-controlled refrigerators (Figure 4c and d).

Photoperiod control (Figure 4a) relied on Siemens S7 1200 AC/DC/RLY PLC controllers (Siemens AG, Munich, Germany) programmed via TIA Portal software (Totally Integrated Automation Portal, Siemens AG, Munich, Germany), implementing an ON-OFF system to regulate light and dark hours per day for each treatment (Appendix-A2_Figure 1). A total of 12 chambers were created: 9 equipped with lighting systems and 3 without, the latter reserved for control treatments (Figure 4d). Additionally, HDC1080 temperature and humidity sensors were installed in each chamber for real-time humidity monitoring. A ventilation system was installed in

each chamber to manage air flow (Figure 4b), programmed using an Arduino MEGA controller (Figure 4a) with Arduino IDE software (Arduino S.r.l., Monza, Italy).

Cultivation of plants

In this study, pea microgreens were grown under different environment stress conditions, which included both mild (normal) conditions and others that, while allowing growth, were less than optimal, thus classifying them as stress conditions. These were maintained in self-developed climate chambers, using soil as the growth medium (Figure 5).
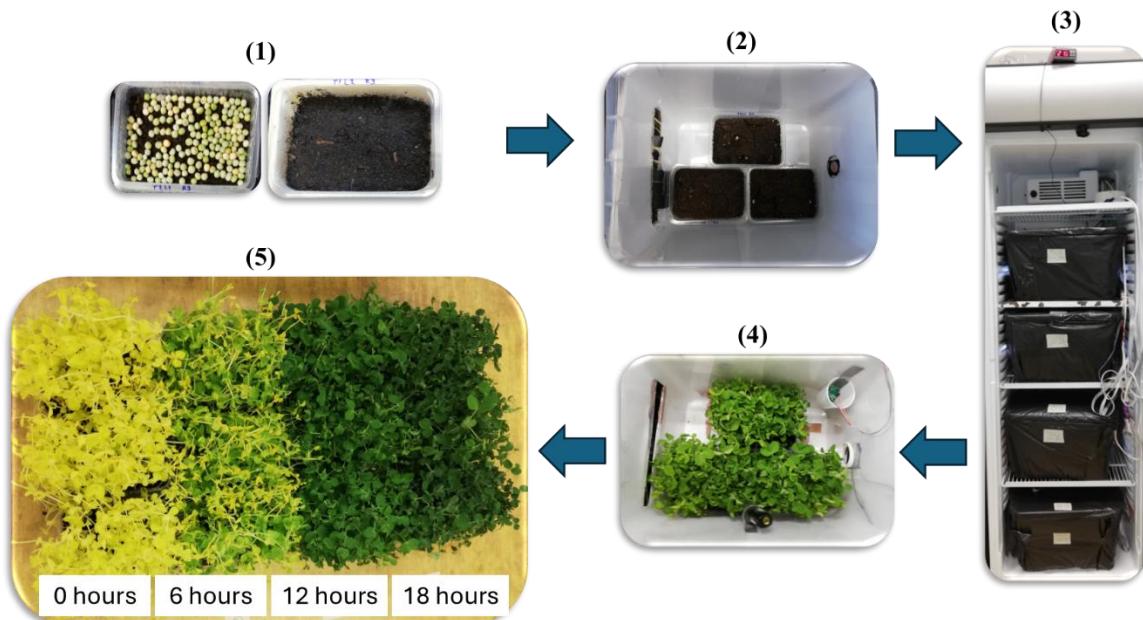
Figure 5. Growth and cultivation process of pea microgreens under controlled conditions. 1) Microgreens sowing, 2) Preparation of growth trays in individual climate chambers, 3) Environmental control setup, 4) Growth and monitoring in controlled conditions, 5) Harvesting at different photoperiods/temperature

First, pee seeds (Debrecen sötétzöld, from Hermes brand and comercialized by hermes kertészbolt) were soaked for 8 hours. Subsequently, seeds were planted in containers with wet soil. The soil was an organic horticultural substrate from the Florimo brand, commercially available from Hermes Kertészbolt. It contained a minimum of 40% organic matter, with nutrient contents of 0.3% nitrogen (N), 0.1% phosphorus pentoxide (P_2O_5), and 0.1% potassium oxide (K_2O), and a pH of 6.53 ± 0.5. Containers were placed in climate chambers with controlled environmental conditions (Table 2): temperature (15, 20, 25 ºC), photoperiod (0 hours of light, 6 hours of light, 12 hours of light, 18 hours of light), relative humidity around 70-80%. Three repeats were considered for each treatment consisting of a temperature-photoperiod condition. The microgreens were harvested on three different days (for each temperature). For temperatures of 20 and 25 ºC, higher temperatures promoted faster emergency and growth, plants were harvested at 7, 11 and 14 days after sowing. For the temperature of 15 ºC, the emergency and growth were slower, therefore

plants were harvested on 11th, 14th and 18th day. Under this consideration the three temperatures had 2 days of harvesting in common (11 and 14 days after sowing).

Table 2. Pea microgreen set up according to different treatments (temperature-photoperiod)

	Temperature of 15 ºC	Temperature of 20 ºC	Temperature of 25 ºC
0 hours of light (00L)	15ºC_00L (R1, R2, R3)	20ºC_00L (R1, R2, R3)	25ºC_00L (R1, R2, R3)
6 hours of light (06L)	15ºC_06L (R1, R2, R3)	20ºC_06L (R1, R2, R3)	25ºC_06L (R1, R2, R3)
12 hours of light (12L)	15ºC_12L (R1, R2, R3)	20ºC_12L (R1, R2, R3)	25ºC_12L (R1, R2, R3)
18 hours of light (18L)	15ºC_18L (R1, R2, R3)	20ºC_18L (R1, R2, R3)	25ºC_18L (R1, R2, R3)

4.3.2. Sample preparation and analysis of pea microgreens

Measurement of variables

Several agronomical and physicochemical variables were measured during the experiment, including height and weight (physical parameters); Lab color components (optical parameters), pH, conductivity and °Brix (chemical properties) and pigments and bioactive compounds (chlorophyll A, B, total carotene, total water-soluble phenolic compounds (TPC) and antioxidant capacity (TAC).

Weight and height of plants

On each harvesting day, plants were cut from the base (without roots). For each treatment, a number of plants was counted in 6 grams, which was dependent on the rate of growth of the plants of each treatment. The weight results are presented in g/plant. Height of plants were measured by taking ten plants per treatment.

Color measurement

For color measurement plants were cut in homogeneous pieces (around 2.5 cm) and placed in a circular holder. The samples were photographed, and the images were then analyzed to extract the color components in the CIELab space using *Image Color Summarizer 0.82* software (Krzywinski, 2025). L* is a definitive measure of lightness, ranging from black (0) to white (100). a* describes the red–green colour range (a* > 0 indicates redness, a* < 0 indicates greenness),

while b* describes the yellow–blue colour range (b* > 0 indicates yellowness, b* < 0 indicates blueness). It is important to note that, due to technical limitations, it was not possible to establish a fully controlled camera setup with strict calibration of imaging parameters and illumination conditions. As such, the extracted color data is considered for informational purposes only, acknowledging that the methodology does not meet the standards required for reproducible and accurate color measurements. Following the image analysis, the sample was transferred to NIRS benchtop device for scanning.

After scanning, the plants (already cut into homogeneous pieces) were divided into two portions to prepare liquid extracts with different solvents. A portion of 5 g was used for the preparation of pea microgreens-distilled water extracts, while a portion of 1 g was destined for the preparation of pea microgreens-acetone extracts. The distilled water extracts were analyzed for pH, conductivity, °Brix, total water-soluble phenolic compounds (TPC), and total antioxidant capacity (TAC). Meanwhile, the acetone extracts were utilized for determining the levels of chlorophyll A, chlorophyll B, and total carotenoids.

pH, conductivity, °Brix, TPC and TAC determination.

For aqueous microgreens extracts samples preparation, a proportion of 1:5 plant-distilled water (5g plant- homogeneous cut pieces per 25 ml DW) was blended for 30 seconds and filtered. The aliquots of the aqueous microgreens extracts samples were used for measuring pH, conductivity, °Brix, TPC, TAC (and additionally for NIRs scanning). °Brix was determined using a MA871 digital sucrose refractometer (Milwaukee Instruments, Inc., Rocky Mount, NC, USA), which was calibrated with a standard liquid solution provided by the manufacturer prior to sample measurements. For TPC and TAC measurement, color development-absorbance measurement was determined spectrophotometrically using a Helios Alpha spectrophotometer (Thermo Spectronic, Cambridge, England). It should be noted that, since distilled water was used as the extraction solvent, the results for both TPC and TAC reflect only the water-soluble antioxidant compounds, rather than the total content typically obtained using hydroalcoholic mixtures.

The total water-soluble phenolic content (TPC) was assessed using the Folin-Ciocalteu reagent (Singleton and Rossi, 1965), with gallic acid serving as the reference standard. TPC values were reported as milligrams of gallic acid equivalents (GAE) per gram of plant material (mg GAE/g of plant). To evaluate antioxidant capacity, the cupric ion reducing antioxidant capacity (CUPRAC) method was applied (Apak *et al.*, 2004), with trolox used as the reference standard. The results were expressed in micromoles of trolox equivalents (TE) per gram of plant (µmol TE/g). The reagents used for TPC and TAC analysis came from different suppliers: Neocuproine (Sigma-Aldrich, product no. N1501), gallic acid (Sigma-Aldrich, product no. G7384), and (+)-catechin

hydrate (Sigma-Aldrich, product no. 22110) were purchased from Merck Life Science Kft. (Budapest, Hungary). Ethanol, methanol, glacial acetic acid, Folin–Ciocalteu's reagent, anhydrous sodium carbonate, boric acid, and methyl red were purchased from VWR International Kft. (Debrecen, Hungary). Copper (II) chloride dihydrate, trolox (Acros Organics, product no. 218940050).

Chlorophyll A, B and total carotene determination

For pigments determination, a proportion 1:20 plant-acetone (1g plant-homogeneous cut pieces per 20 ml of acetone) was blended for 30 seconds and filtered with cellulose filter paper MN 612 (Macherey-Nagel, Germany; 4-12 µm pore size, Ø125 mm). Absorbance was measured in XDS RLA spectrometer device (Metrohm, Herisau, Switzerland) at 470 nm, 645 nm and 662 nm, for chlorophyll A, chlorophyll B and total carotene, respectively. Pigments content expressed in µg/g of plant were calculated according the equations proposed by Lichtentaler and Wellburn (1985), as cited by Dere et al. (1998) as shown in Equations (1)–(3):

$$Chlorophyll\ A\ =\ 11.75 \times A_{662} - 2.350 \times A_{645}$$

(1)

$$Chlorophyll\ B\ =\ 18.61 \times A_{645} - 3.960 \times A_{662}$$

(2)

$$T.carotene\ =\ 1000 \times A_{470} - 2.270 \times Chl.A - 81.4 \times Chl.B/227$$

(3)

Near infrared spectroscopic analysis of Microgreens fresh-cut samples and aqueous microgreens extracts samples

Samples were scanned using a benchtop NIR XDS spectrometer (Metrohm, Herisau, Switzerland), with two modules: Rapid Solid Analyzer (RCA) and Rapid Liquid Analyzer (RLA). Microgreens fresh-cut samples were placed in a circular crystal cuvette (inner diameter of 43.20 mm), covered with the 0.50 MM lid (0.50 mm thickness) and scanned with an XDS-RCA operating in reflectance mode. Microgreens aqueous microgreens extracts samples were placed in a cuvette (1 mm pathlength) in XDS-RLA operating in transmission.

NIR XDS operates over the 400 to 2500 nm range, with a spectral data interval of 0.5 nm and a wavelength accuracy of 0.05 nm. A total of 32 successive scans for each recorded spectrum were collected then averaged for each sample. This was performed three times to obtain three consecutive scans per sample.

4.3.3. Statistical methods for pea microgreen samples evaluation

It is necessary to denote that although the same kind of spectral pretreatments, PCA, PCA-LDA and PLSR regression modeling were applied to microgreen fresh-cut samples and aqueous microgreens extracts samples, the analyses were conducted independently for each sample type. However, once the models were established, further discussion can be considered for their comparative insights.

NIRS analysis of pea microgreens was performed in the 1150 to 1850 nm spectral range. The spectral range for NIRS analysis was limited to 1150-1850 nm due to two primary reasons. Firstly, a sensor transition occurs around 1150 nm, which is visually identifiable as a discontinuity in the spectra. This transition can introduce noise and distortions, potentially leading to errors and inaccurate classification and prediction models if the entire range is used without careful preprocessing. Secondly, different spectral intervals were tested during preliminary analyses, including 1150-1850 nm, 1150-2200 nm, and 1300-1600 nm (the latter two are not included in the thesis). It was determined that the 1150-1850 nm range provided the most accurate and reliable results, with higher predictive performance in the evaluated models. Therefore, this range was selected to ensure the robustness and reliability of the developed models.

SG (p=2, n=45, m=0) and SNV spectral pretreatments were applied after outlier detection and elimination. Outlier detection was carried out through visual inspection of raw and preprocessed spectral data, as well as through the evaluation of sample distribution in PCA score plots. Spectra exhibiting atypical patterns or extreme positioning in the multivariate space were excluded prior to further analysis. PCA data exploration according to harvesting day, temperature and photoperiod coloring was performed on the full data for pattern recognition.

PCA-LDA analysis was performed according to harvesting day, temperature, photoperiod and treatment (temperature-photoperiod) for the full data. Moreover, sub datasets comprising of a specific harvesting day were clustered according to treatment, temperature and photoperiod. Furthermore, sub-selecting a single treatment discrimination was realized according to harvesting day. A supervised three-fold cross-validation according to repeat (in each iteration one repeat is left out) was performed. The term *supervised* refers to the manual definition of the cross-validation units (biological replicates or hereafter referred to as *repetitions*) rather than allowing the algorithm to randomly select individual scans, which could result in overfitting since multiple scans from the same replicate share spectral similarity.

To select the optimal number of latent variables (LVs) in the PCA-DA models, the highest %CV value was considered. The maximum number of LVs, while avoiding overfitting, was determined as described by Defernez and Kemsley (1997), as shown in Equation (4):

$$LV=n-g/3 \qquad\qquad (4)$$

where:

n = total number of samples,

g = number of groups or classes in the dataset, and

3 = serves as a regularization factor to prevent overfitting by limiting the number of LVs.

Some PCA-DA models used a relatively high number of LVs compared to the number of PCs. To assess their predictive performance, models were built using randomly generated (simulated) data (Defernez and Kemsley, 1997). This approach helped determine whether the real data models had better predictive power than the simulated ones, ensuring that the observed classification patterns were not merely a result of overfitting (Appendix-A2_Table 12).

PLSR was performed for the variables: height, weight, Lab color components, pH, conductivity, °Brix, chlorophyll A, B, total carotene. Repetitions R1 and R2, comprising two-thirds of the dataset, were used to build the PLSR models. Cross-validation involved leaving out the spectra from one sample at each iteration. The remaining one-third of the data (R3) was then utilized for predictions to assess the model's robustness.

Additional PLSR models were conducted for total water-soluble polyphenolic compounds (TPC) and antioxidant capacity (TAC). Due to constraints where repeats 1, 2, and 3 were mixed before TPC and TAC determination, it was also necessary to average the spectra of the three repeats for correct variable measurement and NIRS spectral matching. In this case, leave-one-out cross-validation was applied for the PLSR models.

The PLSR models assessment was determined according to the highest R^2 and lowest RMSE. Additionally, the optimal number of latent variables (LVs) in the PLSR model was determined based on the following criteria:

- The difference between calibration (R^2C) and cross-validation (R^2CV) should be ≤ 0.15 (in most cases) to ensure good predictive performance and reduce the risk of overfitting.

- The calibration (RMSEC), cross-validation (RMSECV), and adjusted cross-validation (RMSECV_adj) errors were analyzed. The optimal LV number was chosen where RMSECV stopped decreasing or started increasing.

- RMSECV and RMSECV_adj reach their lowest values around a certain number of LVs. Beyond this point, additional LVs do not significantly improve prediction and may lead to overfitting (Appendix A2_Figure 2).

The "aquap2" package (Kovacs and Pollner, 2016) was employed for multivariate analysis in the R-project environment.

Figure 6, encompasses the experimental approach used to evaluate pea microgreens growth under different controlled cultivation conditions, showing reference analyses of agronomic and physicochemical parameters, and NIRS evaluation using advanced chemometric methods.
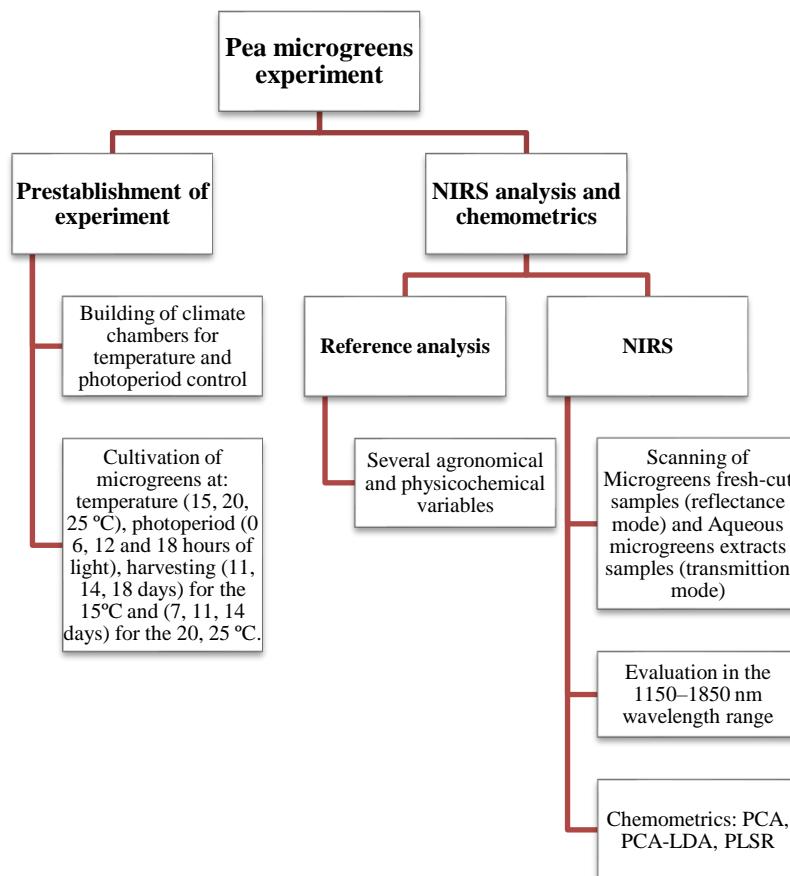
Figure 6. Methodological scheme for pea microgreens assessment

5. RESULTS AND DISCUSSION

5.1. Results of eggs sensory evaluation

The figures and tables presented in this section are based on previously published results (Aguinaga Bósquez et al., 2021).

As a food safety precondition, no significant differences were found in the microbiological statuses of the groups, indicating their suitability for consumption (Appendix-A2_Table 3). However, significant differences in fat and protein content were observed, where control group showed lower protein content and higher fat content compared to ZP 2.5% and ZP 5% groups (Appendix-A2_Table 4)

5.1.1. Eggs sensory evaluation by human panel

The results of the human sensory analysis, presented in Figure 7, Figure 8 and Figure 9, were obtained through the application of ANOVA and Tukey tests, according to the feeding groups: Control, ZP 2.5%, ZP 5.0%; batches: 1 and 2; egg presentation: raw, boiled, and fried. Overall, the majority of sensory attributes did not show significant differences between the various egg groups, especially in case of the boiled and fried eggs. The panellists characterized the twenty-three analysed parameters as representative of fresh eggs.
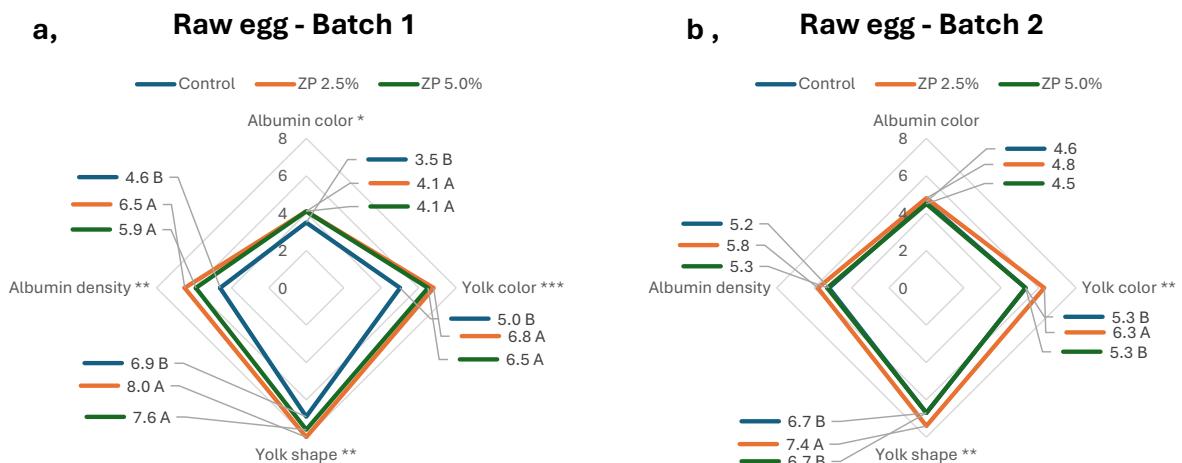
Figure 7. ANOVA and Tukey HSD post-hoc test of human sensory analysis of eggs. Feeding groups: Control, ZP 2.5%, ZP 5.0%. (a) boiled eggs from Batch 1 (b) boiled eggs from Batch 2. Significant difference: $p > 0.05$ (ns), $p < 0.05$ (*), $p < 0.01$ (**), and $p < 0.001$ (***). Reproduced with permission from Aguinaga Bósquez et al. (2021)

A comparison of sensory characteristics between batches suggests a decrease in sensory intensity for some attributes in batch 2. It is possible that, by the time eggs from batch 2 were collected, the hens had already adapted more fully to the supplemented diet, reaching a more

balanced physiological state. The effect is more evident in raw eggs, particularly in terms of visual and textural traits (Figure 7). However, for boiled and fried eggs, differences in gustatory and olfactory parameters were not consistent between batches (Figure 8 and Figure 9). T. Xie et al. (2019) found that dietary supplementation with *Lonicera confusa* and *Astragali Radix* extracts caused changes in sensory characteristics and other quality parameters throughout the laying period. Changes in egg traits across different laying stages were also noted by Şekeroğlu et al (2024), suggesting that the physiological condition in hens can influence how dietary components affect the egg quality.
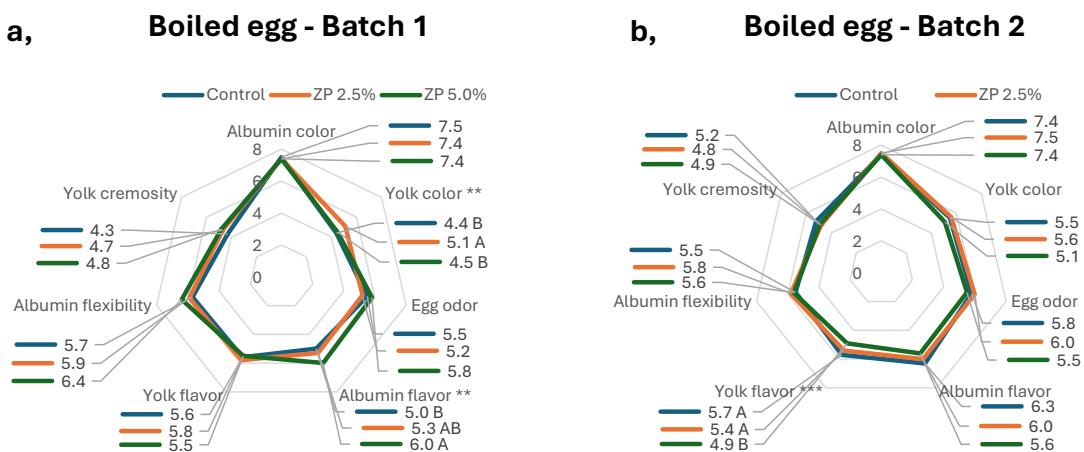
Figure 8. ANOVA and Tukey HSD post-hoc test of human sensory analysis of eggs. Feeding groups: Control, ZP 2.5%, ZP 5.0%. (a) boiled eggs from Batch 1 (b) boiled eggs from Batch 2. Reproduced with permission from Aguinaga Bósquez et al. (2021)
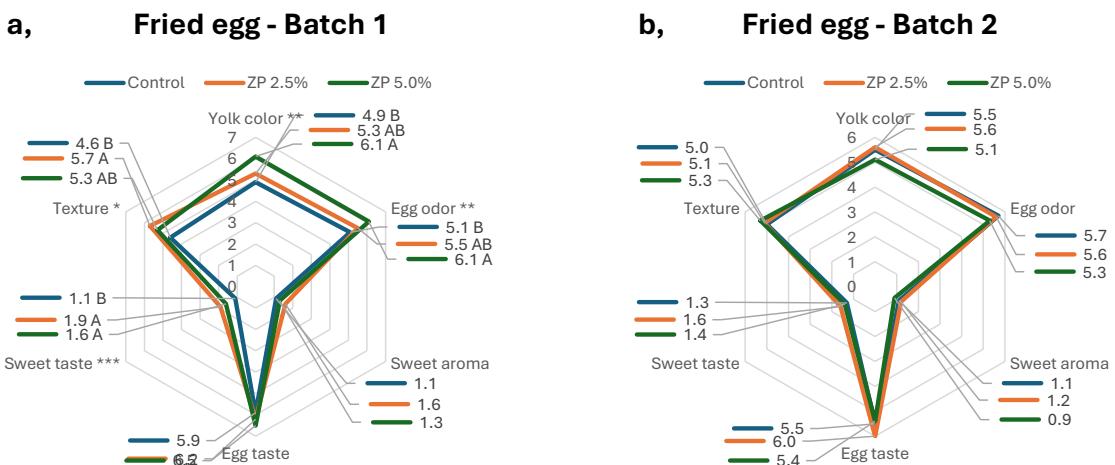
Figure 9. ANOVA and Tukey HSD post-hoc test of human sensory analysis of eggs. Feeding groups: Control, ZP 2.5%, ZP 5.0%. (a) fried eggs from Batch 1 (b) fried eggs from Batch 2. Reproduced with permission from Aguinaga Bósquez et al. (2021)

Figure 7a illustrates the significant inter-group differences observed in the first experimental batch (batch 1). The control group exhibited lower values for all attributes of raw egg compared to the ZP 2.5% and ZP 5.0% groups. This was evident in the higher intensity of

white colouration, greater intensity of yolk colouration, greater convexity of yolks shape, and higher protein density observed in both ZP groups. Similarly, Figure 9a, analysis of the fried eggs, reveals statistically significant differences for yolk colour intensity, egg odour intensity and sweet flavour intensity. These attributes were observed to be less intense in the control group, with values on the scale being lower in comparison to the ZP 2.5% and ZP 5.0% groups. However, in Figure 8a, significant difference was observed in the colour and flavour of the boiled egg between the three experimental groups. The ZP 2.5% group exhibited a slightly more intense yolk colour and white flavour compared to the Control and ZP 5.0% groups.

The disparate outcomes observed for the two experimental batches (especially for boiled and fried eggs) suggest a low degree of inter-sample variability (indiscernible to the trained panel) or a lack of clear differentiation among samples based on the selected sensory characteristics.

5.1.2. Eggs sensory evaluation by electronic tongue

Computed Euclidean distances on the e-tongue data from egg samples belonging to the two experimental batches are presented in Figure 10, the greatest distance between the groups was found between the Control and ZP 5.0% groups for both series of experiments. The distances between the control group and ZP 5.0% group for batch 1 and batch 2 respectively were 22 and 26. The Euclidean distance is greater when there are more significant differences between groups. Consequently, there was a greater disparity between the control group and the ZP 5.0% treatment group than between either of the Control-ZP 2.5% or ZP 2.5%- ZP 5.0% groups.
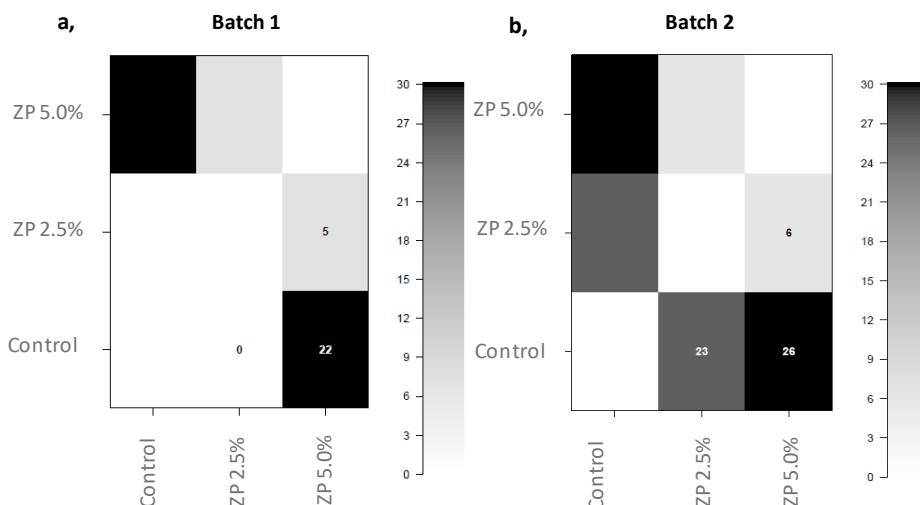
Figure 10. Euclidean distances for the e-tongue analysis of egg samples belonging to the feeding groups: Control, ZP 2.5%, ZP 5.0%. Results presented according to batch 1 (a) and batch 2 (b). Reproduced with permission from Aguinaga Bósquez et al. (2021)

The results of the PCA, as depicted in Figure 11, revealed that the three groups of egg samples exhibited major overlapping. Nevertheless, the analysis of the first three principal

components, in Figure 11a and c between PC1-PC2 and in Figure 11b and d PC1-PC3, reveals a slight differentiation between the data points of the control group and the data points of the other two groups, which is particularly apparent in both batches. As seen in Figure 11b, this differentiation is particularly evident in PC1 and PC3 for batch 1, where a significant proportion of the control group data points do not overlap with those of the ZP 5.0% group. The PCA score plots of batch 2, related to Figure 11c and d, also present a degree of separation of some of the data points from the control group. This is particularly evident in relation to the ZP 5.0% group and is primarily visualized on the PC1 axis. For batch one, the total explained variance between the groups was found to be 66.09% in PC1, 13.22% in PC2 and 9.92% in PC3. In comparison, for batch two, the total variance was found to be 41.65%, 29.35%, and 14.47%, respectively, for PC1, PC2, and PC3.
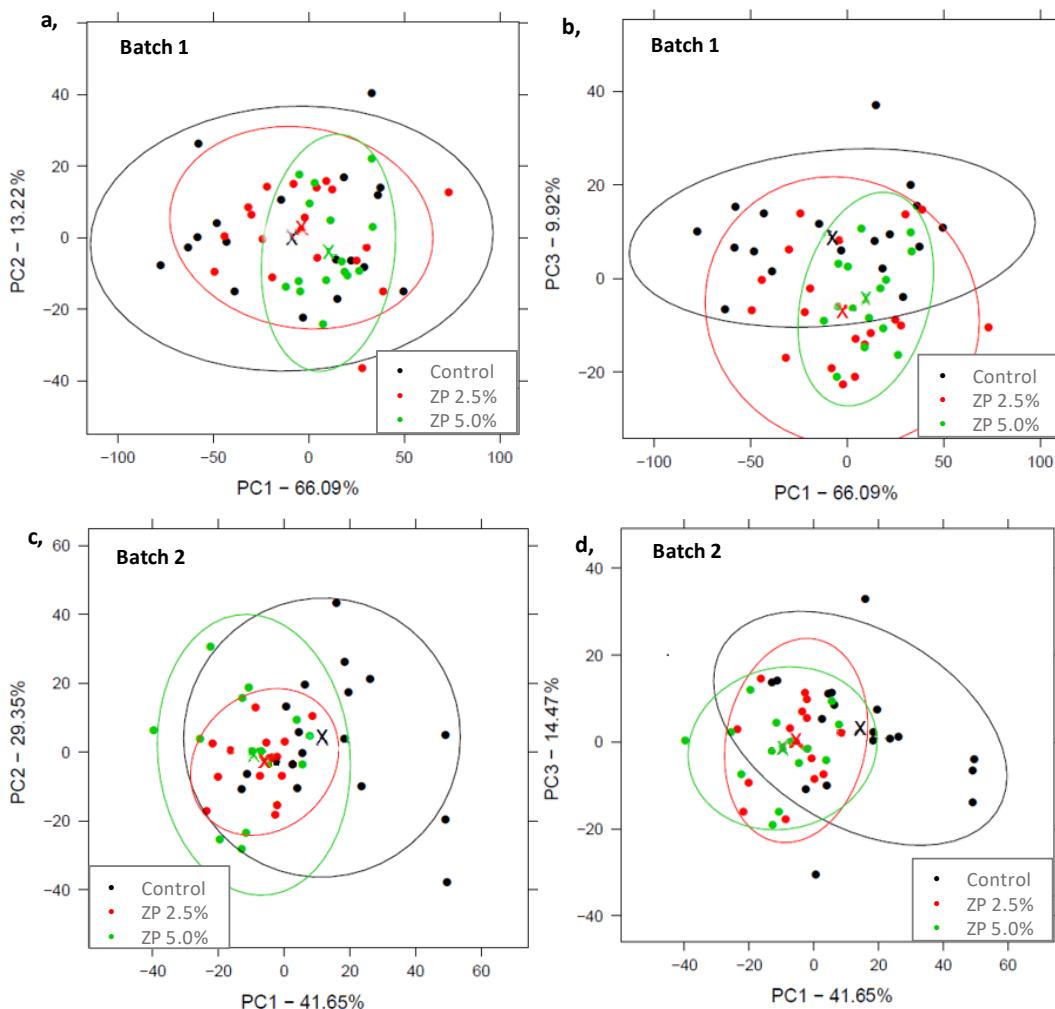
Figure 11. Principal component analysis of the e-tongue data for egg samples belonging to the feeding groups: Control, ZP 2.5%, ZP 5.0%. PCA results are presented according to PC1-PC2 and PC1-PC3, for batch 1 (a, b) and for batch 2 (c, d). 95% confidence intervals of the respective groups are represented by Ellipses, and x-axis represents the group centroids. Reproduced with permission from Aguinaga Bósquez et al. (2021)

The slight group differentiation observed in the PCA score plots can be attributed to the contribution of specific sensors. In batch 1, PC1 was mainly influenced by ZZ, BB and HA, while PC2 and PC3 showed stronger loadings from ZZ, BB, and GA. In batch 2, PC1 was again driven by ZZ and HA. PC2 was shaped by ZZ, GA and HA, and PC3 by ZZ, CA and HA. These sensors are generally associated with sensitivity to metallic, bitter, umami, and acidic compounds, suggesting that differences in formulation may have altered the taste profile. Notably, sensor ZZ consistently contributed across all components, indicating its important role in the overall taste discrimination (Figure 12).

Although the sensors in the ASTREE system show differential sensitivity to certain compound classes, their responses are not specific.
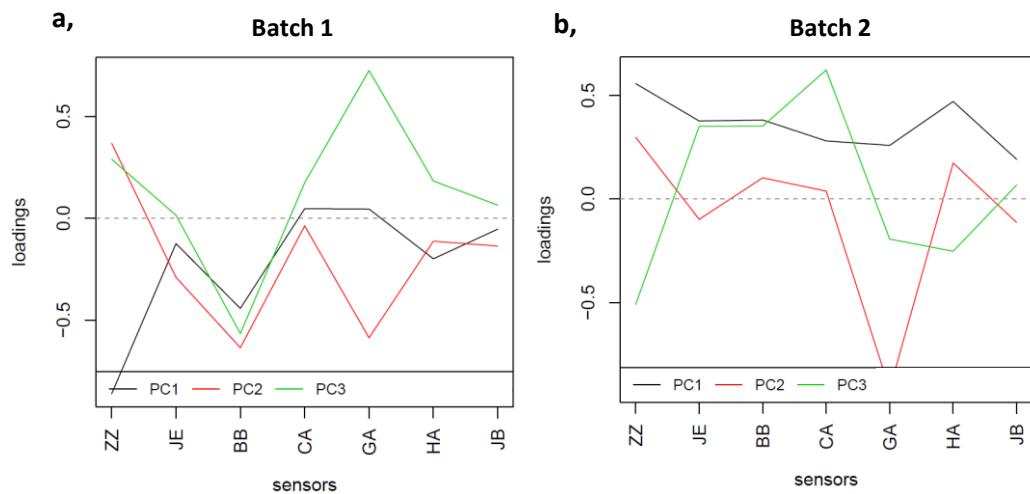
Figure 12. Loadings plots of principal component analysis of the e-tongue data for egg samples belonging to the feeding groups: Control, ZP 2.5%, ZP 5.0%. For batch 1 (a) and for batch 2 (b)

Some degree of separation can be seen within each group of eggs in the discriminant analysis score plots (Figure 13). As the method employed is supervised, the separation of the three treatment groups (Control, ZP 2.5% and ZP 5.0%) is more pronounced in both batches. As illustrated in Figure 13a-batch1, the centroids of each group, marked with a cross, indicate that the Control and ZP 2.5% groups are more closely related, while the ZP 5.0% group is more distinctly separated. The data points from the Control and ZP 5.0% groups exhibit a more pronounced separation. In batch 2 (Figure 13b), the ZP 2.5% and ZP 5.0% groups are more overlapped, and the control group is more separated.

Although in this study the feeding groups are not completely separated in the discriminant analysis (Figure 13), this partial overlap may be attributed to the fact that dietary supplementation with Zincoppyeast does not strongly affect the sensory characteristics of eggs when compared to the control group. Nevertheless, linear discriminant analysis (LDA) was still able to distinguish the groups to a certain extent, highlighting its usefulness in identifying subtle differences between

treatments. In line with this, other studies have reported the effectiveness of LDA in differentiating egg samples subjected to various conditions. For instance, Dong et al. (2021) used LDA to successfully classify eggs from different native hen breeds based on taste profile analyzed with electronic tongue, supporting the method's capacity to reveal underlying patterns even when group separation is not visually striking as they revealed no successful grouping identification by PCA.
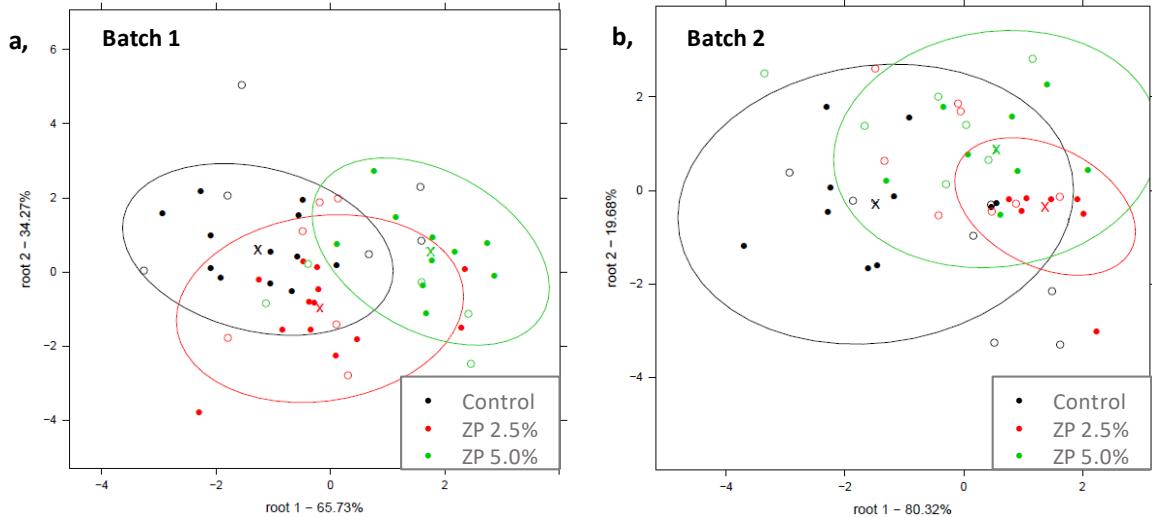

Figure 13. Discriminant analysis of the e-tongue data for egg samples belonging to the feeding groups: Control, ZP 2.5%, ZP 5.0%. Results presented according to batch 1 (a) and batch 2 (b). 95% confidence intervals of the respective groups are represented by Ellipses and x-axis represents the group centroids. Filled dots for calibration, hollow dots for cross-validation. Reproduced with permission from Aguinaga Bósquez et al. (2021)

Table 3 illustrates the confusion table of LDA models with the average percentages of each technical replicate for calibration and cross-validation of egg samples classification (feeding group related) across batch 1 and batch 2, respectively. The outcomes of the three-fold cross-validation demonstrate that the distinction between the three egg groups was not accurate, exhibiting misclassification between neighboring groups. Nevertheless, the differentiation of the Control and ZP 5.0% groups was found to be higher for both experimental batches.

The average calibration accuracy for batch 1 was 95.92%, with a cross-validation accuracy of 64.81%. Additionally, batch 2 exhibited an average calibration accuracy of 100% and a cross-validation accuracy of 56.23%. This suggests that the models capture some useful information from the real data, but there is evidence of overfitting (the large gap between calibration and cross-validation). By analyzing a matrix consisting of random numbers (LDA results presented in Appendix-A2_Table 5) the calibration accuracy was 80.07% and cross-validation accuracy was 29.95%. The difference between 64.81% (real data) and 29.95% (random data) demonstrates that the real data contains relevant information for classification.

Table 3. Confusion table of egg samples classification from e-tongue data. Groups according to feeding regime: Control, ZP 2.5%, ZP 5.0%. Results presented for batch 1 and batch 2. Reproduced with permission from Aguinaga Bósquez et al. (2021)

		Batch 1					Batch 2		
Average Accuracies	%	Control	ZP 2.5%	ZP 5.0%	Average Accuracies	%	Control	ZP 2.5%	ZP 5.0%
Calibration 95.92%	Control	**97.64**	0.00	0.00	Calibration 100.0%	Control	**100.00**	0.00	0.00
	ZP 2.5%	0.00	**97.25**	7.14		ZP 2.5%	0.00	**100.00**	0.00
	ZP 5.0%	2.36	2.75	**92.86**		ZP 5.0%	0.00	0.00	**100.00**
	%	Control	ZP 2.5%	ZP 5.0%		%	Control	ZP 2.5%	ZP 5.0%
Cross-validation 64.81%	Control	**46.02**	15.89	4.72	Cross-validation 56.23%	Control	**88.94**	0.00	33.33
	ZP 2.5%	39.74	**72.95**	19.81		ZP 2.5%	5.53	**61.95**	48.87
	ZP 5.0%	14.25	11.17	**75.47**		ZP 5.0%	5.53	38.05	**17.79**

5.1.3. Eggs sensory evaluation by electronic nose
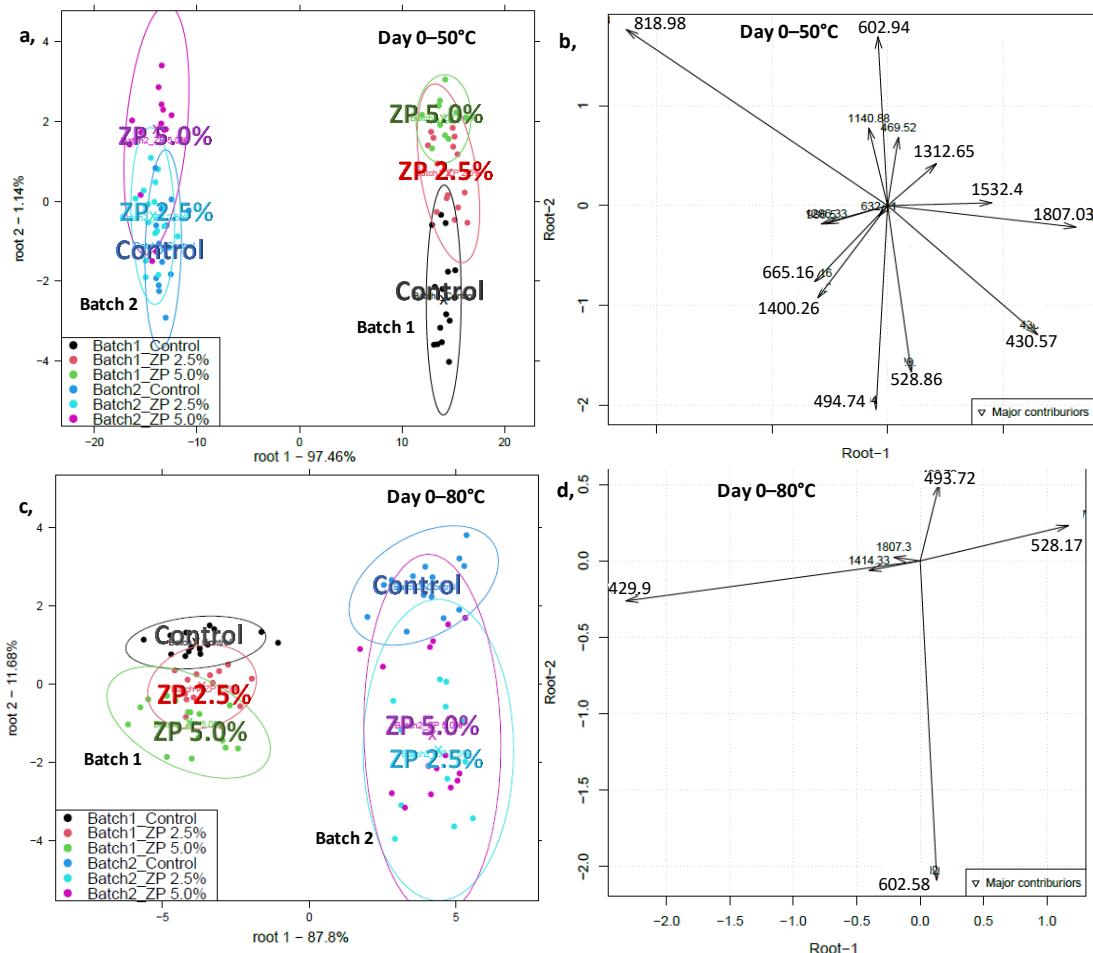
Figure 14. Discriminant analysis on the e-nose data for fresh egg samples belonging to the batches: batch 1, batch 2; and to the feeding groups: Control, ZP 2.5%, ZP 5.0%. PCA–LDA (a,c) and sensor contribution (b,d). E-nose analysis preheating-temperature: (a) 50 °C, LV:23(30), n = 85 and (c) 80 °C, LV:4(30), n = 87. Reproduced with permission from Aguinaga Bósquez et al. (2021)

Upon initial examination of the results for eggs stored for 0, 30, and 60 days, it was observed that the models corresponding to fresh eggs (0 days of storage) demonstrated slightly improved discrimination between the different feeding treatment groups compared to models from longer storage periods. This improved discrimination for fresh eggs (0 days of storage) is illustrated in (Figure 14).

In Figure 14 a and c, it is shown the PCA–LDA score plot results corresponding to the e-nose analysis setting the preheating temperatures for the samples at 50 and 80 degrees Celsius. A clear differentiation in the samples between batches 1 and 2, in both preheating temperatures, is evident. Based on root 1, the explained variance between the two batches accounted for 97.46% for preheating at 50 °C and 87.80% for 80 °C. Moreover, the explained variance in root 2 was 1.14% and 11.68% for the two preheating temperatures, respectively, and indicating a distinct separation tendency of the three feeding groups.

Figure 14 b and d illustrate the sensors that were most effective in differentiating the samples stored at 50 °C and 80 °C for 0 days, respectively. Complementary, the main contributors to the separation between batches, between feeding groups, and between both (batches and feeding groups) are presented in Table 4, Table 5 and

Table *6*, respectively.

Table 4. Main contributing sensors for separation between batches from the discriminant analysis on the e-nose data for fresh egg samples

At 50 °C			At 80 °C		
Sensor	**Compounds**	**Odor Descriptors**	**Sensor**	**Compounds**	**Odor Descriptors**
1807.03	Nootkatone, 2-Hexadecanone	Banana, citrus, grape, sour fruit, spicy, woody	429.9	Acetaldehyde	Ethereal, fresh, fruity, pungent
1532.4	Cadina-1,4-diene, Methyldodecanoate	Fruity, mango, spicy, wood, coconut, creamy, fatty, sweet, waxy	528.17	Methyl acetate, 2-Methylpropanal	Blackcurrant, ethereal, fruity, solvent
1286.33	Isoborneol acetate, Pentyl hexanoate	Balsamic, fruity	1414.3	Linalyl butanoate, (E)-β-Damascone	Floral, pear, sweet, apple
986.5	3-Octanone, 6-Methyl-5-hepten-2-one	Butter, herbaceous, resinous, blackcurrant, boiled fruit, citrus, earthy, mushroom, rubber	1807.3	Nootkatone, 2-Hexadecanone	Banana, citrus, grape, sour fruit, spicy, woody, fruity

Table 5. Main contributing sensors for separation between feeding groups from the discriminant analysis on the e-nose data for fresh egg samples

At 50 °C			At 80 °C		
Sensor	Compounds	Odor Descriptors	Sensor	Compounds	Odor Descriptors
602.94	2-Butanol, n-Butanol	Fusel-alcoholic, oily, winey, cheese, fermented, fruity, medicinal	602.58	2-Butanol, n-Butanol	Fusel-alcoholic, oily, winey, cheese, fermented, fruity, medicinal
1140.88	Homofuraneol, Methyl 3-pyridinecarboxylate	Caramelized, herbaceous, sweet, tobacco	493.72	2-Propanone	Fruity, glue, solvent
528.86	Methyl acetate, 2-Methylpropanal	Blackcurrant, ethereal, fruity, solvent, burnt, green, malty, pungent, spicy, toasted			
494.47	2-Propanone, Propanal	Fruity, glue, solvent, ethereal, plastic, pungent			

Table 6. Main contributing sensors for batch-feeding group separation from the discriminant analysis on the e-nose data for fresh egg samples

At 50 °C		
Sensor	Compounds	Odor Descriptors
818.98	2,4,5-Trimethyl-3-oxazoline, 2-Butanone-3-mercapto	Musty
430.57	Acetaldehyde	Ethereal, fresh, fruity, pungent
1312.65	1-Methylnaphthalene, Cinamyl alcohol	Earthy, green, musty, naphthyl, oily
1400.26	Tetradecane, Diphenyl ether	Alkane, fusel, mild herbaceous, sweet, green
665.16	n-Butanol	Cheese, fermented, fruity

Some common sensors were found for the two preheating temperatures which are close to the 1807, 602, 528, 494 Kovats index. Meanwhile, the sensors that are different were: 1532.40, 1286.33, 986.5, 1140.88, 469.52, 818.98, 430.57, 1312.65, 1400.26, 665.16 Kovats index (50 °C); and 1414.33 Kovats index for 80 °C.

The confusion table of the PCA–LDA models is presented in Table 7, which displays the average values of each of the three technical replicates for both experimental batches at 50 °C and 80 °C preheating temperatures. The average calibration accuracy for fresh eggs belonging to the feeding groups in batches 1 and 2 at 50 °C was 98.00%, while the cross-validation accuracy was 68.49%. At 80 °C, the calibration accuracy was 82.65%, while the cross-validation accuracy was 62.22%. Nevertheless, the outcomes of the three-fold cross-validation indicate that the differentiation between the three groups of eggs was not entirely accurate, presenting misclassification between adjacent groups. Nonetheless, the Control and ZP 5.0% groups displayed an enhanced tendency towards separation.

Similar to the results from e-tongue, the PCA-LDA models developed from e-nose data show a large gap between calibration and cross-validation. By analyzing a matrix consisting of random numbers, LDA results presented in Appendix-A2_Table 6, the calibration accuracy was 98.77% and cross-validation accuracy was 39.64%. The difference between the CV accuracy, 68.49% (real data in Table 7) and 39.64% (random data in Appendix-A2_Table 6), demonstrates that the real data contains relevant information for classification.

Table 7. Confusion table of fresh egg samples from data obtained from e-nose analysis. Groups according to feeding regime: Control, ZP 2.5%, ZP 5.0%. Results presented for batch 1 and batch 2; and e-nose analysis preheating-temperature: 50 °C and 80 °C. Reproduced with permission from Aguinaga Bósquez et al. (2021)

Batch 1, 50 °C					**Batch 2, 50 °C**			
	%	Control	ZP 2.5%	ZP 5.0%	%		Control	ZP 2.5%	ZP 5.0%
Calibration 98.00%	Control	**100.00**	0.00	0.00	Control	**96.04**	0.00	8.03
	ZP 2.5%	0.00	**100.00**	0.00	ZP 2.5%	0.00	**100.00**	0.00
	ZP 5.0%	0.00	0.00	**100.00**	ZP 5.0%	3.96	0.00	**91.97**
	%	Control	ZP 2.5%	ZP 5.0%	%		Control	ZP 2.5%	ZP 5.0%
Cross-validation 68.49%	Control	**38.83**	5.50	0.00	Control	**58.73**	0.00	23.50
	ZP 2.5%	27.83	**83.33**	6.60	ZP 2.5%	11.82	**77.83**	17.67
	ZP 5.0%	33.33	11.17	**93.40**	ZP 5.0%	29.45	22.17	**58.83**

Batch 1, 80 °C					**Batch 2, 80 °C**			
	%	Control	ZP 2.5%	ZP 5.0%	%		Control	ZP 2.5%	ZP 5.0%
Calibration 82.65%	Control	**100.00**	14.78	0.00	Control	**100.00**	0.00	14.78
	ZP 2.5%	0.00	**74.11**	14.78	ZP 2.5%	0.00	**81.00**	29.67
	ZP 5.0%	0.00	11.11	**85.22**	ZP 5.0%	0.00	19.00	**55.56**
	%	Control	ZP 2.5%	ZP 5.0%	%		Control	ZP 2.5%	ZP 5.0%
Cross-validation 62.22%	Control	**77.83**	5.50	0.00	Control	**100.00**	13.40	33.33
	ZP 2.5%	16.67	**77.83**	44.50	ZP 2.5%	0.00	**40.00**	44.50
	ZP 5.0%	5.50	16.67	**55.50**	ZP 5.0%	0.00	46.60	**22.17**

Figure 15 a and c illustrate the results of the PCA-LDA analysis of the e-nose tests conducted at a preheating temperature of 50 °C, wherein the findings of the 0 days and 30, 60 days stored egg samples were evaluated collectively. The data demonstrates a clear distinction between the 0 days-fresh samples, the 30 days, and 60 days samples. However, there was a degree of overlap between the Control, ZP 2.5%, ZP 5.0% treatment groups, in each case.
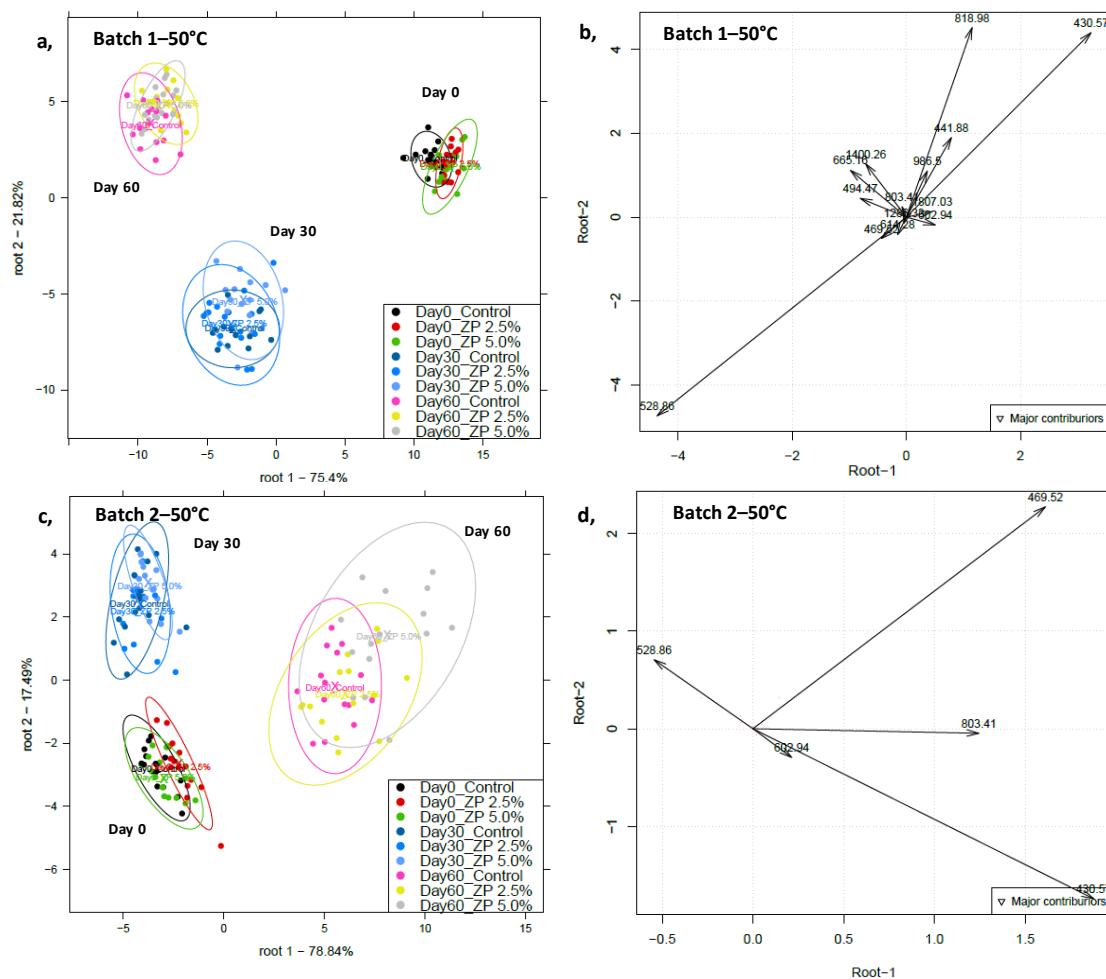
Figure 15. Discriminant analysis on the e-nose data for egg samples belonging to the batches: (a,b) batch 1 (LV: 20 (30), n = 132) , (c,d) batch 2 (LV: 4 (30), n = 133). Grouping according to feeding groups: Control, ZP 2.5%, ZP 5.0%; and storage time: 0, 30, 60 days. PCA–LDA (a,c) and sensor contribution (b,d). E-nose analysis preheating-temperature: 50 °C. Reproduced with permission from Aguinaga Bósquez et al. (2021)

Additionally, in Figure 15 b and d, the main contribution sensors are presented, they are linked to characteristic compounds and related fragrance profile. Complementary, the main contributors to the separation of eggs especially by storage time are presented in Table 8.

Table 8. Main contributing sensors for group separation according to storage time from the discriminant analysis on the e-nose data for fresh egg samples

Batch 1 at 50 °C			Batch 2 at 50 °C		
Sensor	**Compounds**	**Odor Descriptors**	**Sensor**	**Compounds**	**Odor Descriptors**
528.86	Methyl acetate, 2-Methylpropanal	Blackcurrant, ethereal, fruity, solvent	430.57	Acetaldehyde	Ethereal, fresh, fruity, pungent
430.57	Acetaldehyde	Ethereal, fresh, fruity, pungent	602.94	2-Butanol	Fusel-alcoholic, oily, winey (*also reported with alkane, ethereal, kerosene*)
818.98	2,4,5-Trimethyl-3-oxazoline, 2-Butanone, 3-mercapto	Musty, onion, sulfurous	803.41	2-Hexanol, Hexanal	Fatty, fruity, winey, acorn, fishy, grassy, green, herbaceous, leafy, tallowy
Other major contributors with lower loadings: 441.88, 494.47, 803.41, 469.52, 602.94, 665.16, 1400.26, 614.28, 986.50, 1807.03 and 1286.33.			528.86	Methyl acetate, 2-Methylpropanal	Burnt, fruity, green, malty, pungent, spicy, toasted

The principal contributing sensors (with varying loading capacities) appear to be linked to the differentiation between fresh and stored egg samples, with a storage period of either 30 or 60 days. Nevertheless, a minor contribution to the differentiation between feeding groups is also evident.

A comparative analysis of batches 1 and 2 reveals that all the principal contributing sensors identified in batch 2, namely 469.52, 430.57, 602.94, 803.41, 528.86 and 602.94, are shared with batch 1. Conversely, the other significant sensors, namely 818.98, 441.88, 494.47, 665.16, 1400.26, 614.28, 986.50, 1807.03 and 1286.33, are present in batch 1 but absent in batch 2.

The difference in sensor responses between batches may be attributed to the laying day, aging of the hens, feed intake evolution, or other physiological factors, as batch 1 and batch 2 correspond to eggs collected on day 30 and day 60 of the experimental period, respectively. Changes in diet have been shown to affect the gut microbiota, as well as the amino acid, fatty acid, and volatile compound composition of eggs (Yang *et al.*, 2024). These variations are, in turn, influenced by the physiological status of the hens and the stage of the laying period, among other factors (Şekeroğlu *et al.*, 2024). Moreover, volatile compounds in fresh eggs undergo progressive changes and accumulation during storage (Adamiec *et al.*, 2002). Consequently, differences between batches collected at different time points may have influenced the initial volatile composition and its evolution during storage, ultimately resulting in slightly different sensor responses and volatile profiles.

The significance of acetaldehyde, methyl acetate, and 2-methylpropanal as volatile compounds in eggs is evident, in a manner comparable to that depicted in Figure 14. Volatile compounds, including hexanal, 2,4,5-trimethyl-3-oxazoline and 2-butanone, 3-mercapto, were found with greater likelihood to be associated with storage conditions. The concentration of volatile compounds in fresh eggs undergoes a process of change and increase during the storage period (Adamiec *et al.*, 2002). The egg yolks volatile components are particularly prone to alteration, with esters, alkenes, alcohols, and nitrogenous compounds being the most susceptible (Wang *et al.*, 2014). Yanagisawa et al. (2010), as cited in Yimenu et al., (2017) reported an increase of hexanal in yolk during storage via the identification of volatile compounds. In addition, the concentration of other compounds, such as dimethyl sulfide, dimethyl disulfide, dimethyl trisulfide, methyl thioacetate, methanol, ethanol, 1-propanol, acetone, 2-butanone, and ethyl acetate, also undergoes changes during storage.

A similar outcome is observed in the PCA–LDA analysis conducted on samples heated to 80 °C (Figure 16 a and c), where complete separation between days of storage is evident. However, overlap between feeding groups is observed.
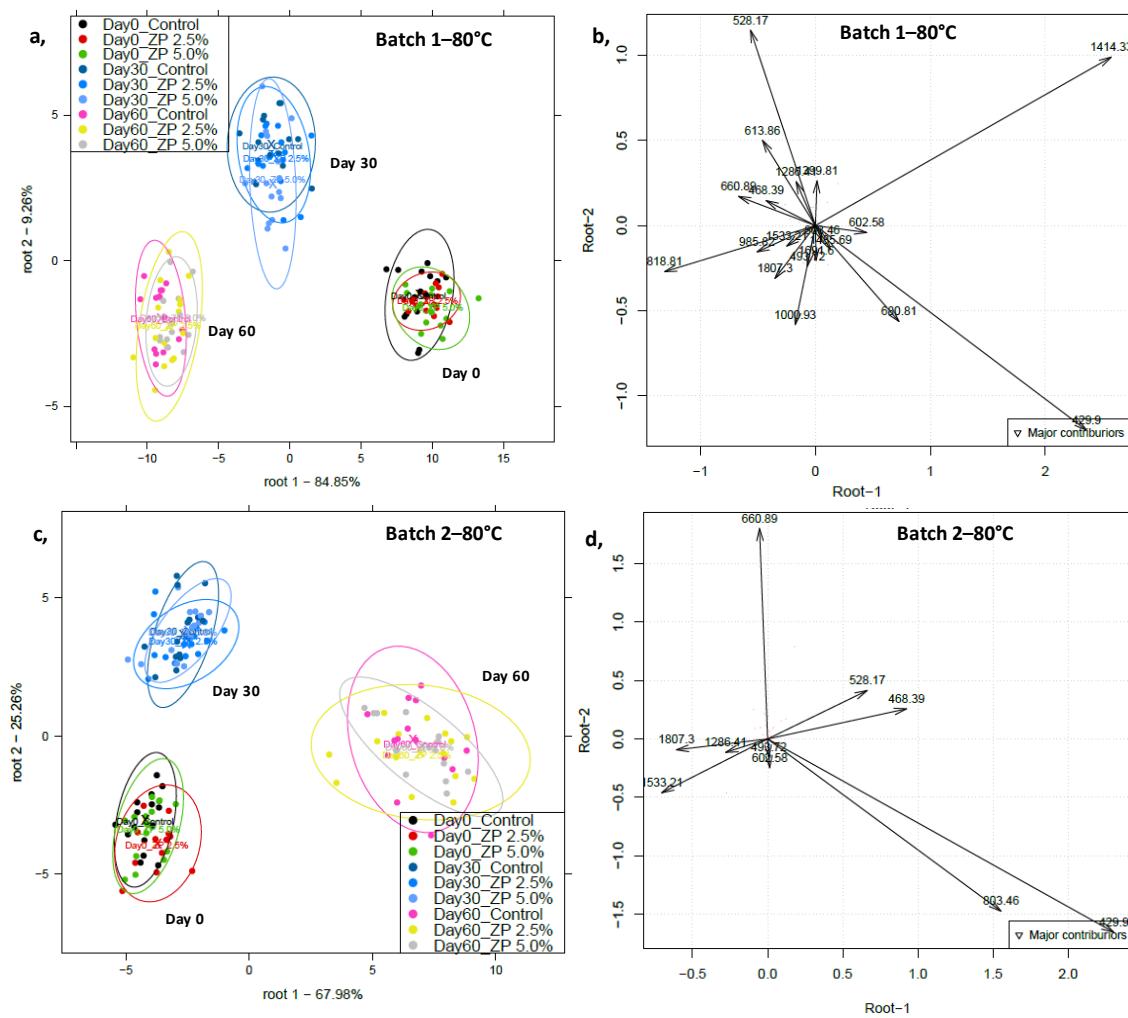
Figure 16. Discriminant analysis on the e-nose data for egg samples belonging to the batches: (a,b) batch 1 (LV: 18 (30), n = 134), (c,d) batch 2 (LV: 11 (30), n = 130). Grouping according to feeding groups: Control, ZP 2.5%, ZP 5.0%; and storage time: 0, 30, 60 days. PCAL–DA (a,c) and sensor contribution (b,d). E-nose analysis preheating-temperature: 80 °C. Reproduced with permission from Aguinaga Bósquez et al. (2021)

Additionally, in Figure 16 b, the main contribution sensors are presented (which are linked to fragrance profile-characteristic compounds). Complementary, the main contributors to the separation of eggs, especially by storage time, are presented in Table 9.

Table 9. Main contributing sensors for group separation according to storage time from the discriminant analysis on the e-nose data for fresh egg samples

Batch 1 at 80 °C			Batch 2 at 80 °C		
Sensor	**Compounds**	**Odor Descriptors**	**Sensor**	**Compounds**	**Odor Descriptors**
1414.3	Linalyl butanoate, (E)-β-damascone	Floral, pear, sweet, apple	803.46	2-Hexanol, Hexanal	Fatty, fruity, winey, solvent, acorn, fishy, grassy, green, herbaceous, leafy, tallowy
429.9	Acetaldehyde	Ethereal, fresh, fruity, pungent	429.9	Acetaldehyde	Ethereal, fresh, fruity, pungent
602.58	2-Butanol	Fusel-alcoholic, oily, winey	468.39 / 660.89	2-Methylbutanal	Almond, cocoa, green, malty, strong burnt
528.17	Methyl acetate, 2-Methylpropanal	Blackcurrant, ethereal, fruity, solvent, burnt, green, malty, pungent, spicy, toasted	1533.21	Cadina-1,4-diene, Methyldodecanoate	Fruity, mango, spicy, wood, coconut, creamy, fatty, sweet, waxy
Other major contributors with lower loadings: 493.72, 803.46, 660.89, 468.39, 818.81, 1807.3, 680.81, 1533.21, 1000.93, 613.86, and 1691.6.			528.17	Methyl acetate, 2-Methylpropanal	Blackcurrant, ethereal, fruity, solvent, burnt, green, malty, pungent, spicy, toasted
			Other major contributors with lower loadings: 602.58, 493.72, 1286.41, 1807.3		

Common sensors for both batch 1 and batch 2 include 429.9, 602.58, 803.46, 468.39, 660.89, 1807.3, 1533.21, and 493.72. In contrast, sensors 818.81, 680.81, 1000.93, 613.86, and 1691.6 were observed exclusively in the first batch, while sensors 528.17 and 1286.41 were only detected in the second batch.

The sensors contribution is primarily associated with the differentiation between fresh and stored egg samples. Nevertheless, a minor contribution to the differentiation between feeding groups was also observed. This is analogous to the analysis of samples conducted at a preheating temperature of 50 °C, as observed in Figure 15.

A summary list of the principal sensors that contribute to the detection of egg volatile compounds, as evidenced by the e-nose data analysis is presented in Appendix-A2_Table 9. In

Table 10, important egg volatile compounds are presented, which have been identified in this study and previously reported by several researchers (Umano *et al.*, 1990; Matiella and Hsieh, 1991; Cherian, Goeger and Ahn, 2002; Yimenu, Kim and Kim, 2017; Xiang *et al.*, 2019):

Table 10. Relevant sensors related to volatile compounds identified in eggs analysis studies

Sensor	Compounds	Odor Descriptors
429.9 / 430.57	Acetaldehyde	Ethereal, fresh, fruity, pungent
528.17 / 528.86	Methyl acetate, 2-Methylpropanal	Blackcurrant, ethereal, fruity, solvent
602.58	2-Butanol	Fusel-alcoholic, oily, winey
818.98	2,4,5-Trimethyl-3-oxazoline, 2-Butanone, 3-mercapto	Musty, onion, sulfurous
1807.03	Nootkatone, 2-Hexadecanone	Banana, citrus, grape, sour fruit, spicy, woody
803.41 / 803.46	2-Hexanol, Hexanal	Fatty, fruity, winey
1414.33	Linalyl butanoate, (E)-β-damascone	Floral, pear, sweet
660.89	2-Methylbutanal	Almond, cocoa, green, malty, strong burnt

A number of studies have identified aldehydes as a significant volatile compound present in eggs. The presence of these compounds has been documented in a number of foodstuffs, including scrambled eggs (Matiella & Hsieh 1991) and cooked eggs (Umano *et al.*, 1990). In addition, volatile aldehydes are present in the greatest quantity in cooked egg yolks, with a significantly lower concentration observed in the case of egg whites (Umano *et al.*, 1990). In their investigation, the authors identified the principal aldehyde present in egg yolk and whole egg volatiles as 2-methylpropanal. The results of this research also demonstrated a significant prevalence of acetaldehyde, methyl acetate, and 2-methylpropanal, which is consistent with the findings of other researchers who have identified aldehydes as volatile flavor components of eggs (Macleod and Cavea, 1975; Cherian, Goeger and Ahn, 2002). In addition, other compounds, such as ketones and 2-propanone (acetone), have been identified in whole eggs and egg whites. Furthermore, this indicates a greater concentration of amino acids in egg white than in egg yolk. Certain amino acids play a pivotal role in the biosynthesis of 2-methylbutanal. Conversely, the whole egg contains alcohol in lower quantities. The majority of alcohols are found in the egg yolk and are associated with lipid oxidation, as evidenced by several studies (Umano *et al.*, 1990; Cherian, Goeger and Ahn, 2002). In the course of our research, we observed that the alcohols present as volatile compounds in eggs exhibited the greatest prevalence in the form of 2-butanol (fusel alcoholic, oily, winey) and 2-hexanol (fatty, fruity, winey).

5.2. Results of probiotics samples evaluation

The figures and tables presented in this section are based on previously published results (Aguinaga Bósquez *et al.*, 2022). The microbiological results, presented in ***Figure 17***, demonstrate the log colony forming unit (CFU) per gram values for each probiotic type according to the water temperature level. This study aimed to investigate the effect of the water temperature applied by consumers prior to consumption of probiotic beverages.
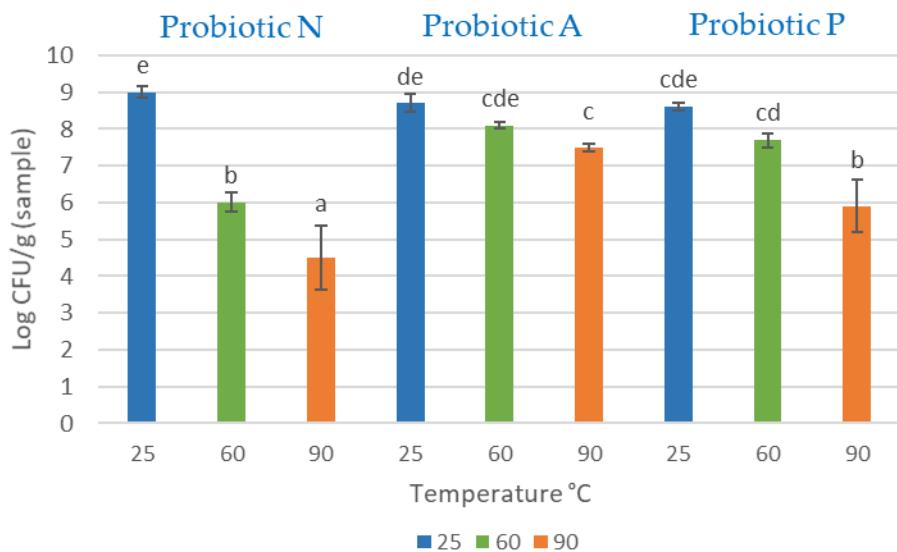
Figure 17. ANOVA and the Tukey HSD post-hoc test of microbiological analysis of probiotics (N, A and P) samples prepared under three different water temperatures (T1: 25°C, T2: 60°C and T3: 90°C). Differences among the groups represented by letters (a–e) at a significance level of α = 0.05. Reproduced with permission from Aguinaga Bósquez et al. (2022).

At 25°C (water at room temperature), the microbial prevalence is higher compared to the log CFU/g values at 60 and 90°C. This trend was observed for all the probiotic types (N, A, and P). Therefore, it is established that probiotic viability is dependent on temperature. Most *Lactobacillus* strains, which are mesophilic, are able to survive at temperatures below 50 °C. In case of thermophilic strains, can grow at temperatures above 50°C (Prasad, Mcjarrow and Gopal, 2003; Desmond *et al.*, 2004; Suokko *et al.*, 2005; Corcoran *et al.*, 2008; Bove *et al.*, 2013).

Probiotic N showed the greatest discrepancy in the microbiological count, exhibiting initially 9.1 log CFU/g at 25 °C. Concomitantly, the value was reduced to 6.0 log CFU/g and 4.5 log CFU/g at higher temperatures of 60 °C and 90 °C, respectively. Probiotics A and P counts exhibited differential responses to temperature, though the observed differences were less pronounced than those observed for probiotic N. The log CFU/g for probiotic A was 8.7 at 25 °C, 8.1 at 60 °C and 7.5 at 90 °C. Meanwhile, the values were 8.6 at 25 °C, 7.7 at 60 °C and 5.9 at 90

°C, for probiotic P. In general, probiotic A exhibited the greatest thermal stability, followed by probiotic P and lastly by probiotic N.

By applying heated water to the probiotics, at 60 and 90°C, and leaving to cool to a temperature of approximately 25°C (room temperature); the results indicated a 3-log reduction in probiotic N, and a 1-log reduction in probiotic A and probiotic P at 60°C. In a comparative study, Franz and Holy (1996) evaluated the heat resistance of three meat spoilage lactic acid bacteria in vitro. Their findings demonstrated that at 60°C, the D-values (time for 90% microbial reduction) ranged from 15 to 40 seconds, indicating a 1-log CFU/g reduction. Conversely, as previously observed by Teoh et al. (2011), a study on probiotics containing *L. acidophilus* and *L. acidophilus* and *B. pseudocatenulatum*, subjected to a 60°C constant temperature for 30 minutes, demonstrated a reduction in probiotic viability from 9 to 4 log CFU/g. The outcome suggests that the methodology employed in this study results in a reduction in viability to a lesser degree than the conventional method. However, this approach offers a more realistic representation from the consumer perspective, particularly when higher temperatures than the recommended are applied.

5.2.1. Near infrared spectra of probiotic samples

Figure 18 illustrates the NIR spectra of probiotic samples, presented in different colours corresponding to the temperature levels (in the 950–1630 nm). A discernible trend emerges within the spectral profiles, distinguished according to temperature especially from 950 to 1400 nm and 1500 to 1630 nm. However, overlapping is noted between consecutive temperatures, it was found to be entirely distinction between T1 (25°C) and T3 (90°C). In addition, the NIR spectra were coloured from one side according to the probiotic types N, A, P and from other side according to the concentration of the probiotics for drinks preparation (not shown), demonstrating that there were higher levels of spectra overlapping, which necessitated the application of further statistical analysis and data treatment to reveal clear trends.
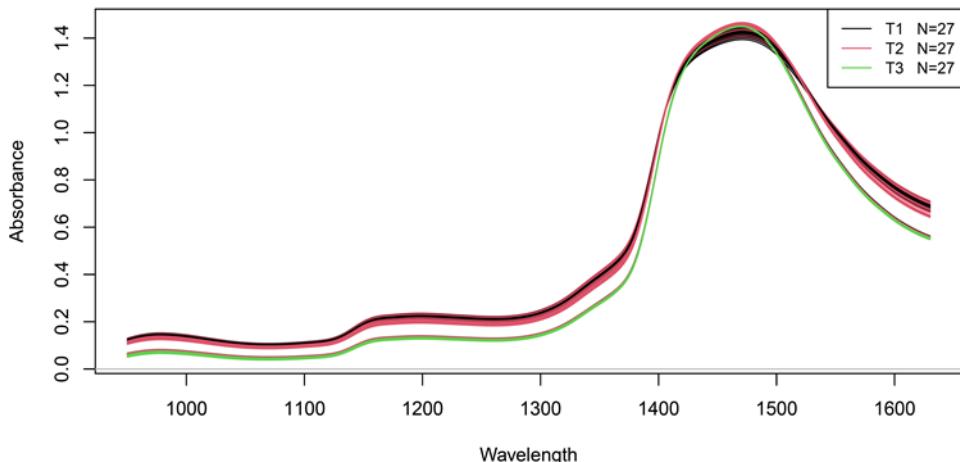
Figure 18. Near infrared raw spectra of probiotic samples analyzed according to varying temperatures (T1: 25 °C; T2: 60 °C; T3: 90 °C). Wavelength range 950-1630 nm. Reproduced with permission from Aguinaga Bósquez et al. (2022).

5.2.2. Classification of probiotic samples

Figure 19 presents the results of the PCA-LDA analysis for the differentiation of the three probiotics (N, A, and P) at 25°C. For this analysis, the entire sample set from the three concentrations was considered as a unified group.
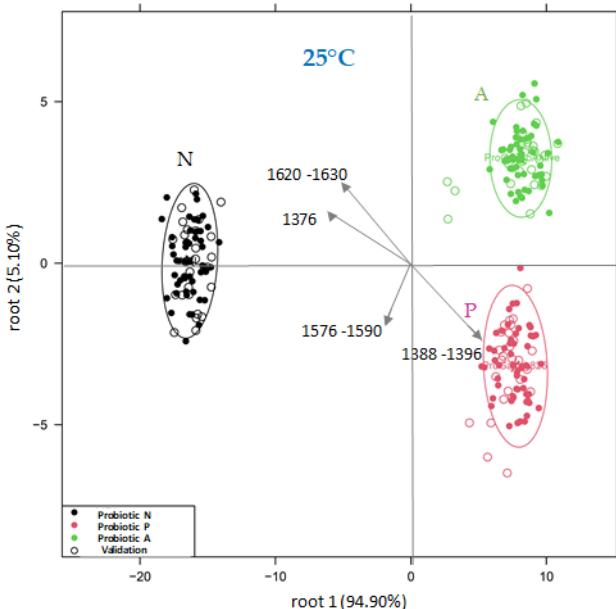
Figure 19. Discriminant analysis on the 25°C prepared-probiotic samples, N scans= 237. Arrows indicate the most important wavelengths for probiotic groups separation. Wavelength range 950-1630 nm. Reproduced with permission from Aguinaga Bósquez et al.(2022).

The probiotics exhibited discrimination on roots 1 (94.90%) and 2 (5.10%), resulting in a clear separation of the sample groups. Probiotics A and P exhibited a closer proximity to each other in comparison to probiotic N, the latter of which exhibited a clear separation from the other groups. It was observed that the liquid matrix from the N samples exhibited distinct visual

60

characteristics when compared to the liquid matrices of the other probiotics. Moreover, probiotics A and P contain a greater number of strains and complementary compounds in common with one another than probiotic N. The optimal classification model was generated through the application of the SG 2-17-0 pretreatment. This approach achieved a 100% and 99.18% correct classification and cross-validation, respectively. Furthermore, at 1376, 1388-1396, and 1576–1590 nm were found important wavelengths that were most influential in the clustering between groups which can be associated with the first overtone region 1300 to 1600 nm of NIRS. This region is characterized by C-H, O-H and N-H intermolecular hydrogen bounds linked to biological aqueous systems and related to primary constituents of the probiotics: water, protein, lipid, sugar, and supplementary organic composites (Ozaki, Genkawa and Futami, 2017; Tsenkova *et al.*, 2018; Muncan and Tsenkova, 2019).

Figure 20 shows the discriminant analysis conducted on a probiotic basis, with each probiotic subjected to a separate concentration-dependent assessment and selecting the dataset from the 90 ℃ (T3) -prepared probiotic beverages which exhibited higher accuracy for discrimination according to concentration compared to 25 ℃ (T1) and 60 ℃ (T2).
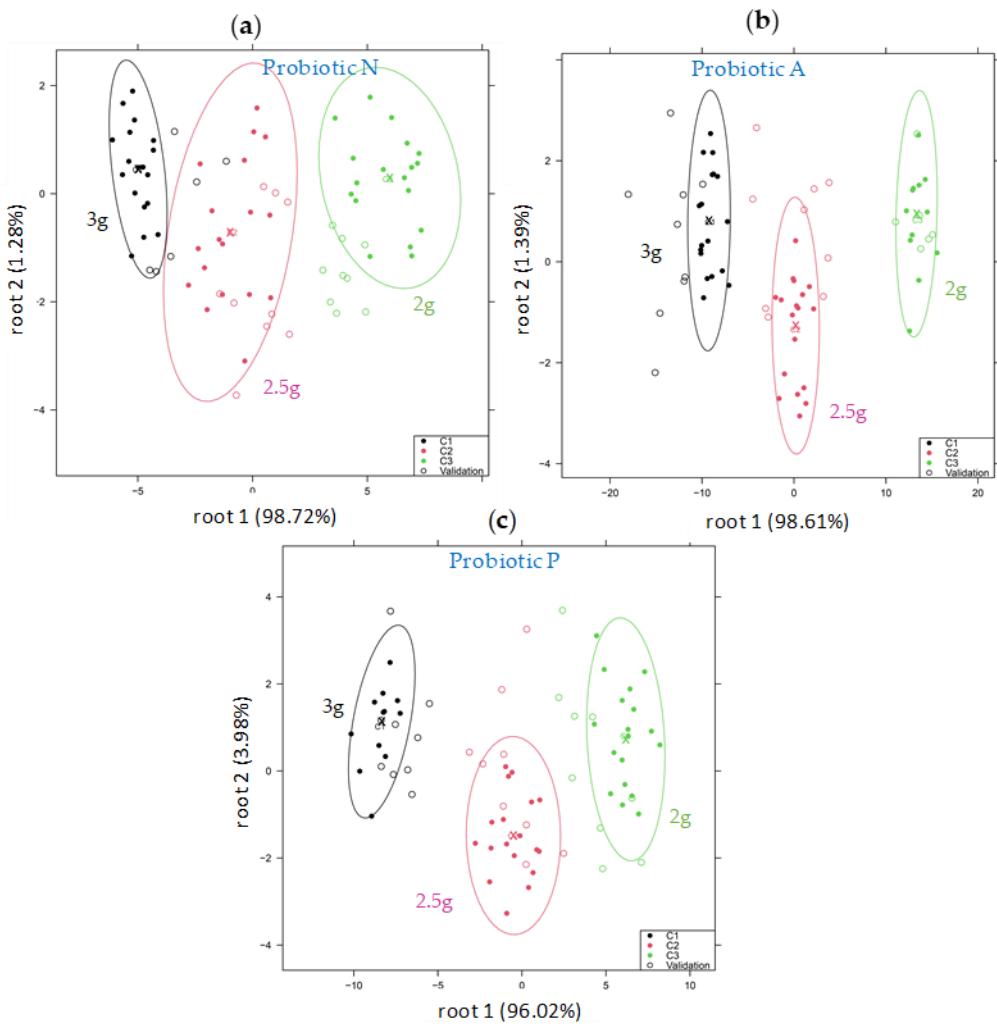
Figure 20. Discriminant analysis on the 90°C prepared-probiotic samples according to varying concentration. Models for the three probiotic types: (a) probiotic N (n=78), (b) probiotic A (n=72) and (c) probiotic P (n=75). Wavelength range 950-1630 nm. Reproduced with permission from Aguinaga Bósquez et al. (2022).

A trend of separation, in all the probiotic-PCA-LDA models, was observed occurring in a specific order according to the according to the following hierarchy: C1, C2, and C3 (from high to low concentration). However, misclassification was exhibited between the different concentrations, with minor overlapping, particularly between consecutive concentrations:C1-C2 and C2-C3.

Complementary, a confusion table of the PCA-LDA models is illustrated in Table 11. For comparison purposes, the table includes the models belonging to the higher and lower water temperature.

Table 11. Discriminant analysis - confusion table of the 25°C and 90°C prepared-probiotic samples. Groups according to the concentration level. Results presented for probiotic N, A and P. Reproduced with permission from Aguinaga Bósquez et al. (2022).

T3 (90°C)	Probiotic N			Probiotic A			Probiotic P		
	Average Calibration (100%)			Average Calibration (100%)			Average Calibration (100%)		
%	C1	C2	C3	C1	C2	C3	C1	C2	C3
C1	**100**	0	0	**100**	0	0	**100**	0	0
C2	0	**100**	0	0	**100**	0	0	**100**	0
C3	0	0	**100**	0	0	**100**	0	0	**100**
	Average Cross-validation (93.52%)			Average Cross-validation (95.06%)			Average Cross-validation (90.12%)		
%	C1	C2	C3	C1	C2	C3	C1	C2	C3
C1	**91.67**	11.11	0	**96.30**	7.41	0	**100**	11.11	11.11
C2	8.33	**88.89**	0	3.70	**88.89**	0	0	**81.48**	0
C3	0	0	**100**	0	3.70	**100**	0	7.41	**88.89**
T1 (25°C)	Probiotic N			Probiotic A			Probiotic P		
	Average Calibration (100%)			Average Calibration (95.68%)			Average Calibration (94.45%)		
%	C1	C2	C3	C1	C2	C3	C1	C2	C3
C1	**100**	0	0	**100**	5.56	0	**96.30**	3.70	0
C2	0	**100**	0	0	**88.89**	1.85	3.70	**92.59**	5.56
C3	0	0	**100**	0	5.56	**98.15**	0	3.70	**94.44**
	Average Cross-validation (93.83%)			Average Cross-validation (60.65%)			Average Cross-validation (60.50%)		
%	C1	C2	C3	C1	C2	C3	C1	C2	C3
C1	**88.89**	7.41	0	**70.83**	37.04	0	**62.96**	14.81	22.22
C2	11.11	**92.59**	0	16.67	**29.63**	18.52	11.11	**51.85**	11.11
C3	0	0	**100**	12.50	33.33	**81.48**	25.93	33.33	**66.67**

The classification of the 90°C (T3)-probiotic samples according to concentration levels is displayed in the upper section of the table. The models for each probiotic showed high correct classification values, with all probiotics approaching 100% correct classification in calibration. Meanwhile, for cross-validation the accuracy was higher than 90% in all cases, exhibiting in decrement order: 95.06%, 93.52% and 90.12% for probiotic A, probiotic P and probiotic N, respectively. C1-C2 and C2-C3 (consecutive concentrations) presented some degree of misclassification. The most optimal models corresponded to the following spectral pre-treatments: DeTr and MSC (for probiotic N), SG 2-21-0 and DeTr (for probiotic A), and SG 2-17-0 and SG 2-17-2 (for probiotic P).

Furthermore, the PCA-LDA results for the probiotic samples subjected to 25°C (T1) are presented in Table 11. However, the models corresponding to probiotic A and probiotic P demonstrated a higher misclassification rate of the concentration levels at this temperature, especially for prediction capacity. Probiotic A exhibited a 96.68% and 60.65% calibration and

cross-validation accuracy, respectively, while probiotic P exhibited a 94.45% and 60.50% calibration and cross-validation accuracy, respectively.

Figure 21 illustrates the PCA-LDA models corresponding to the probiotic strain, with discrimination according to the temperature level. Only samples from concentration 1 (C1) were considered; however, similar results are obtained with other concentrations.
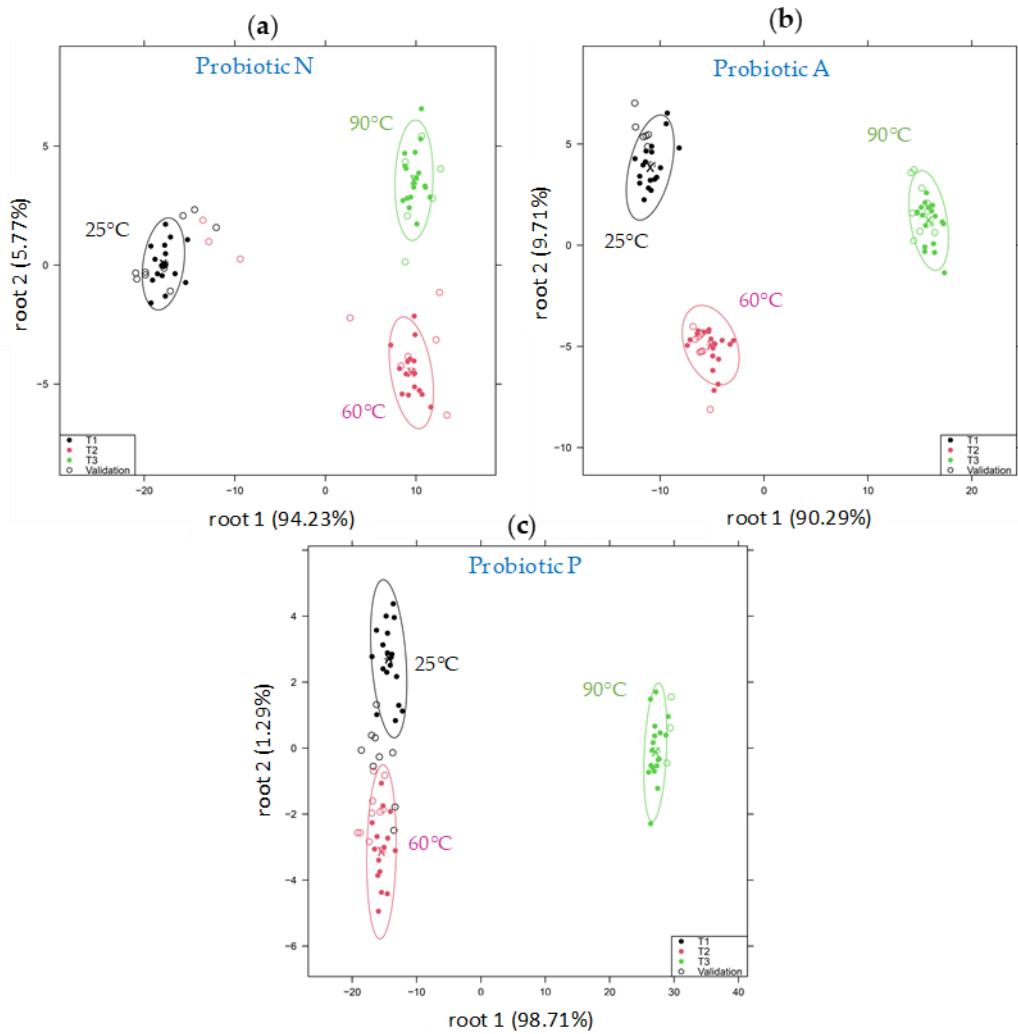
Figure 21. Discriminant analysis on the concentration C1 prepared-probiotic samples according to varying temperature. Models for the three probiotic types: (a) probiotic N (n=75), (b) probiotic A (n=78) and (c) probiotic P (n=72). Wavelength range 1950-1630 nm. Reproduced with permission from Aguinaga Bósquez et al. (2022).

The classification model that exhibited the highest accuracy of 100% in both calibration and cross-validation was the one developed for Probiotic A, which employed the SG 2-17-0 and MSC spectral pretreatment. Similarly, probiotics P and N demonstrated a high degree of accurate differentiation between groups. Probiotic P exhibited 100% and 92.59% accuracy for classification and cross-validation, respectively, upon the application of DeTr spectral pretreatment. Meanwhile,

probiotic N demonstrated 100% and 94.60% accuracy for calibration and cross-validation, respectively, following the application of SG 2-13-0 and SG 2-21-1. Consequently, although greater differentiation of samples based on the temperature of the prepared solutions was observed for all probiotics, the one that stood out was probiotic A (Figure 21b).

Table 12 presents a confusion table, summarizing the PCA-LDA models for the classification of probiotic solutions according to the temperature preparation level. It demonstrates high correct classification for each probiotic, with only minor misclassification (between T1-T2 and T1-T3) observed in the case of probiotic N and (between T1-T2) for probiotic P.

Table 12. Discriminant analysis-confusion table on the concentration C1 prepared-probiotic samples. Groups according to the temperature level. Results presented for probiotic N, A and P. Reproduced with permission from Aguinaga Bósquez et al. (2022).

	Probiotic N			Probiotic A			Probiotic P		
	Average Calibration (100%)			Average Calibration (100%)			Average Calibration (100%)		
%	T1	T2	T3	T1	T2	T3	T1	T2	T3
T1	**100**	0	0	**100**	0	0	**100**	0	0
T2	0	**100**	0	0	**100**	0	0	**100**	0
T3	0	0	**100**	0	0	**100**	0	0	**100**
	Average Cross-validation (94.60%)			Average Cross-validation (100%)			Average Cross-validation (92.59%)		
%	T1	T2	T3	T1	T2	T3	T1	T2	T3
T1	**96.30**	12.50	0	**100**	0	0	**77.78**	0	0
T2	0	**87.50**	0	0	**100**	0	22.22	**100**	0
T3	3.70	0	**100**	0	0	**100**	0	0	**100**

5.2.3. PLSR prediction of probiotic samples viability

A model for predicting CFU counts for all the probiotics (tested in combination according to the concentration and temperature) is presented in Figure 22a and b. Samples from repetitions R2 and R3 were selected for model calibration and cross-validation, while repetition R1 was used for prediction. Additionally, the best model was achieved by applying SG 2-21-0 and SG 2-13-2 pretreatments. The optimal number of components for the model was determined to be seven. The R^2C was 0.87 and RMSEC was 0.54. Meanwhile, the R^2CV was 0.68 and RMSECV was 0.84 (Figure 22a). Furthermore, for the prediction of the samples, the R^2Pr was 0.82 and RMSEP was 0.64 (Figure 22b). Furthermore, the primary wavelengths contributing to the PLSR model are illustrated in Figure 6c. In the 1300–1600 nm wavelength range, a considerable number of contributing wavelengths and the most significant peaks contributing to the prediction of probiotic viability are observed. The prepared probiotic solutions are primarily composed of water and a smaller quantity of organic composites, exhibiting high absorbance in the first overtone region of

water comprised between 1300 and 1600 nm (Siesler *et al.*, 2002; Ozaki, Genkawa and Futami, 2017; Tsenkova *et al.*, 2018; Muncan and Tsenkova, 2019). In this regard, molecular interactions such as OH stretching (Maeda and Ozaki, 1995; Workman, 2000; Izutsu *et al.*, 2006; Slavchev *et al.*, 2015), OH/NH stretching (Wei and Salahub, 1997; Fischer and Tran, 1999; Mizuse and Fujii, 2012; Slavchev *et al.*, 2015) can be associated with specific wavelengths of importance, namely 1458 nm and 1484 nm, respectively. Moreover, In the region of 950-1300 nm, the more prominent wavelength, related to the free water (S0) combination overtone, is assigned to 1140 nm. In a study from Slavchev et al. (2015), this characteristic is described as pertaining to the nearest band at 1155 nm.
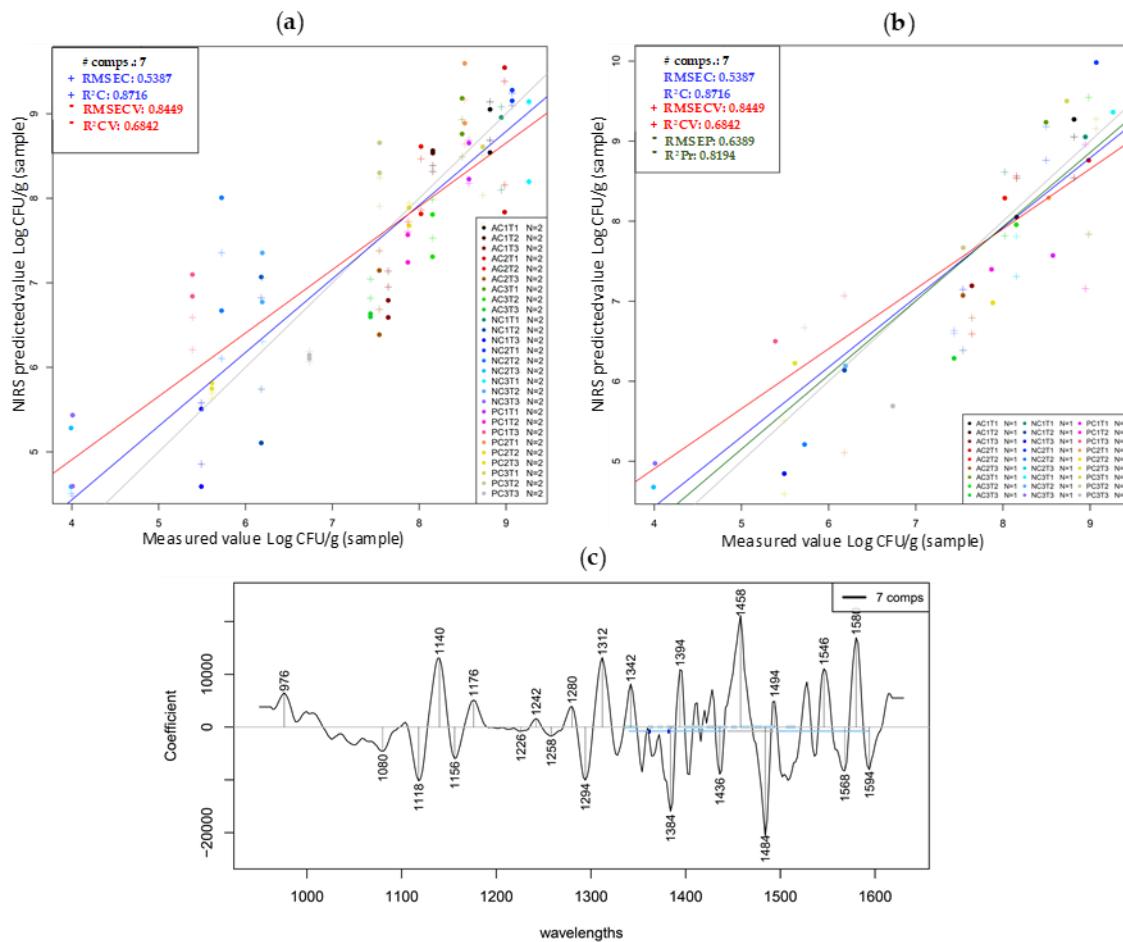
Figure 22. Partial least square regression for viability prediction of probiotic samples. (a) Calibration and cross-validation by selection R2 and R3. (b) Prediction of samples by selecting R1. (c) Calibration coefficients showing important wavelengths for the PLSR model. Wavelength range 1950-1630 nm. Reproduced with permission from Aguinaga Bósquez et al. (2022).

5.3. Results of pea microgreens samples evaluation

To study the growth of pea microgreens under different environmental conditions using NIR spectroscopy, data was first collected on 13 key agronomical and biochemical variables. This approach allowed for a more comprehensive understanding of how these conditions affect the plants, both in terms of individual traits and their overall characteristics.

5.3.1. Results of the agronomic-phytochemical evaluation of pea microgreens

Physical characteristics (weight and height)

In Figure 23, a correspondence between plant height and weight can be observed. As the height of the microgreens increases, their weight also increases, as greater plant development implies more accumulated biomass.
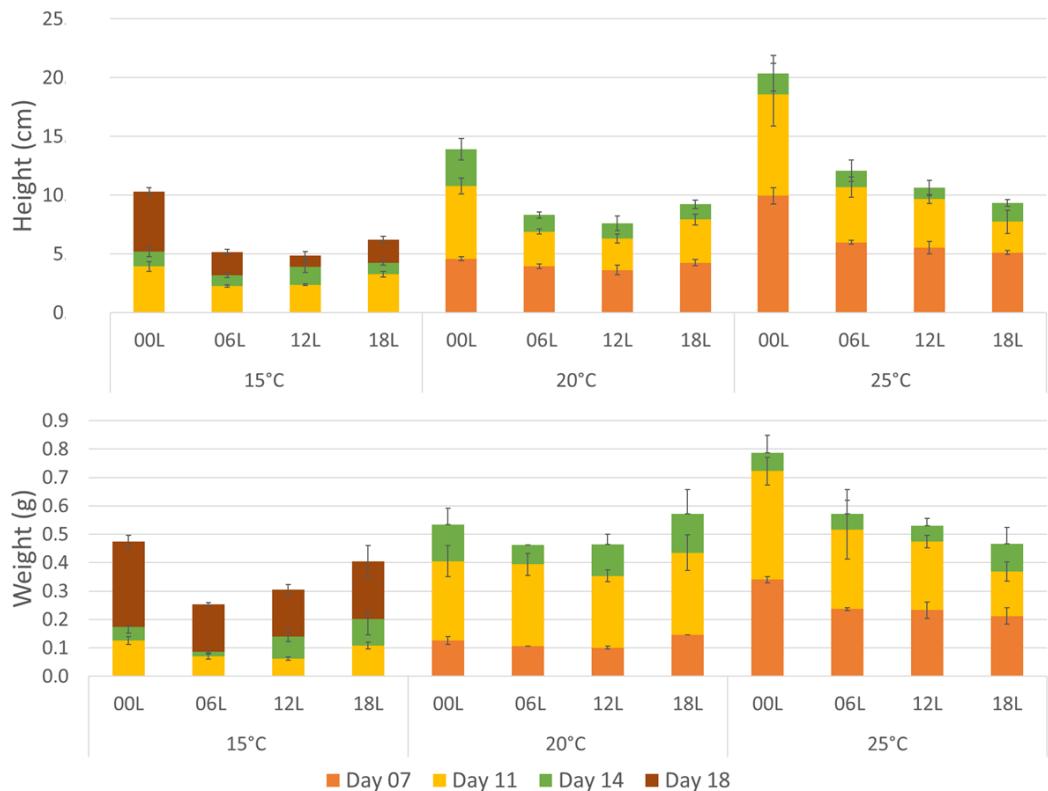
Figure 23. Height and Weight of pea microgreens harvested after 7, 11, 14 and 18 days under different temperatures (15, 20 and 25 °C) and photoperiod (00L, 06L, 12L, 18L) conditions, Standard deviation is represented by whiskers (± SD)

In general, greater plant growth and weight are evident at higher temperatures. Plants grow faster and gain weight as temperature increases because the biochemical reactions that regulate growth, such as photosynthesis and respiration, accelerate with higher temperatures. The enzymes involved in these processes function more efficiently within an optimal temperature range, promoting greater cell development, biomass accumulation, and elongation. The height and weight

of microgreens are important for commercialization. Height influences visual appearance and attractiveness, while weight is related to yield and biomass quantity. Commercially, a height between 5 and 10 cm is preferred (Ajdanian, Babaei and Aroiee, 2019; Niroula *et al.*, 2019; Hernández-Adasme, Palma-Dias and Escalona, 2023). Plants growth at temperatures of 25 °C, 20 °C, and 15 °C reach over 5 cm in height at days 7, 11, and 18, respectively.

The treatment (25C_00L) reached the highest values of height and weight, measuring 18.55 cm and 0.72 g at day 11, and 20.37 cm and 0.79 g at day 14. In contrast, the treatment 15C_06L recorded the lowest values of height and weight, measuring 2.25 cm and 0.07 g at day 11, and 3.21 cm and 0.09 g at day 14. Light and temperature are essential environmental factors that shape how plants grow and develop. Interestingly, they often produce similar effects, both shaded environments and high temperatures can lead to morphological changes such as elongation of the hypocotyl, petioles, and stems (Perrella *et al.*, 2020).

Notably, plants grown in complete darkness (00L) reached greater heights. This can be explained by the phenomenon of etiolation, a process in which plants grow rapidly in the absence of light, characterized by long and thin stems, small leaves, and a lack of chlorophyll, giving them a pale yellow color (Młodzińska, 2009; Seluzicki, Burko and Chory, 2017) . This exaggerated growth is due to the action of hormones such as auxin, which promotes stem elongation as an adaptive response to reach a light source as quickly as possible, allowing the plant to start photosynthesis and survive (Burko *et al.*, 2022). In the presence of light, different behaviors were observed depending on the temperature. For 15 °C and 20 °C, plants with an 18-hour photoperiod (18L) showed greater height compared to 06L and 12L, as the extended light hours allow for more photosynthesis, resulting in faster growth and higher biomass production (Kay and Phinney, 1956; Kong and Zheng, 2019). Conversely, at 25 °C, plants with a 6-hour photoperiod (6L) reached greater heights compared to 12L and 18L. Under high-temperature conditions, a long photoperiod of 18 hours may subject plants to more thermal stress, increase photorespiration, light damage, and water loss, all of which can reduce photosynthetic and energetic efficiency. As a result, plants under a long photoperiod may grow less than those under a short photoperiod of 6 hours, which are less exposed to these stress factors.

Chemical characteristics (°Brix, pH, and conductivity)

In Figure 24, °Brix, pH, and conductivity obtained in this study correspond to a concentration of 0.2 g of plant material per 1 ml of distilled water. The reported results are based on this ratio, allowing for a consistent comparison of the quality parameters of pea microgreens juice under the applied growing conditions.
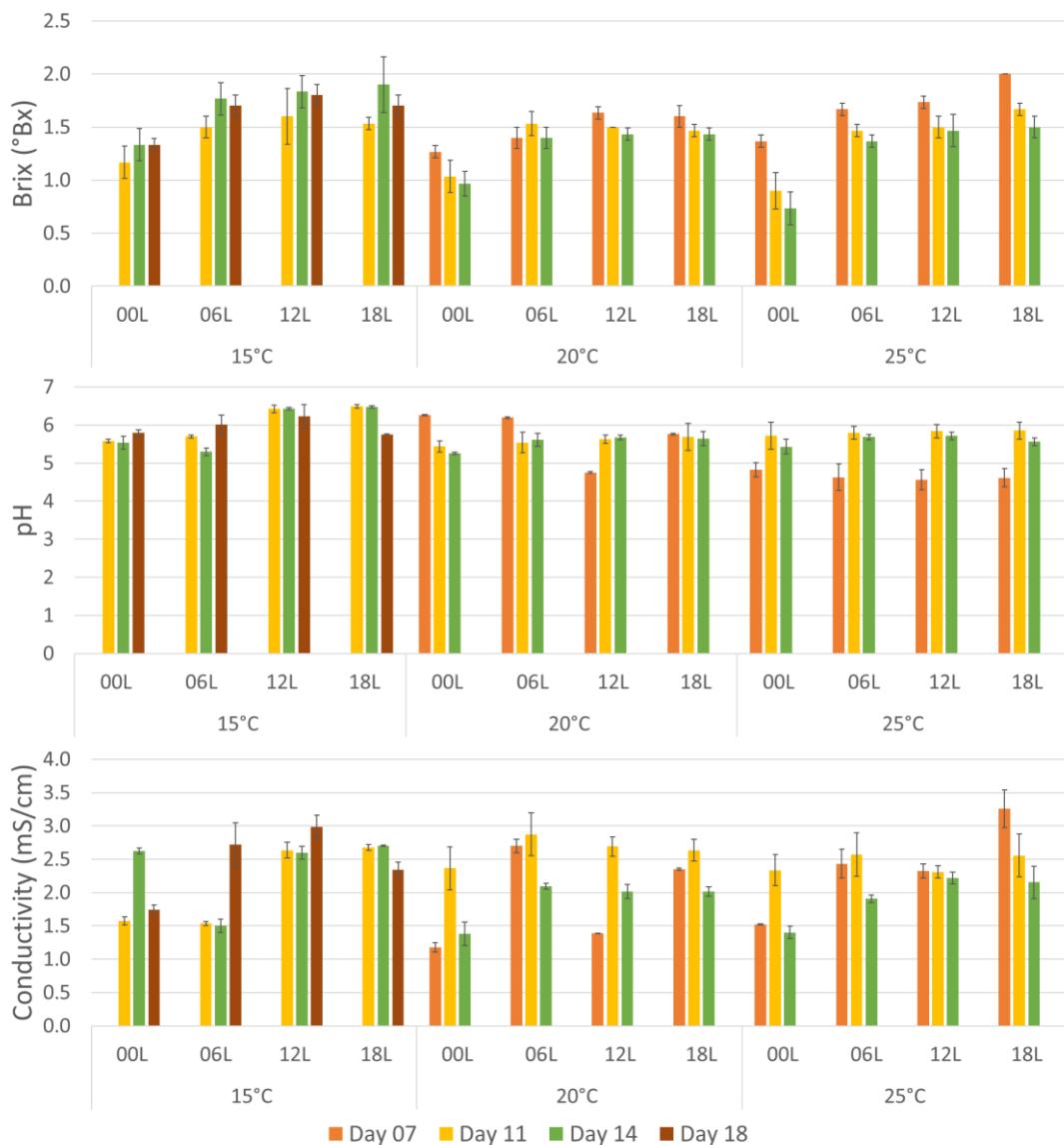
Figure 24. °Brix, pH, and conductivity of pea microgreens harvested after 7, 11, 14 and 18 days under different temperature (15, 20 and 25 °C) and photoperiod (00L, 06L, 12L, 18L). Standard deviation is represented by whiskers (± SD)

°Brix: In the figure, microgreens at 15 °C, the °Brix degrees increase between days 11 and 14, indicating an accumulation of sugars (sucrose) during this growth stage, followed by a decrease on day 18, probably due to the mobilization of these sugars to form new structures. Sucrose, in particular, not only provides energy but also regulates processes related to cell expansion and organ differentiation, this shows the importance of sucrose in the development of plants (Rolland, Baena-Gonzalez and Sheen, 2006). In the treatments at 20 °C and 25 °C, the °Brix degrees

decrease between days 7, 11, and 14, suggesting that at these higher temperatures, sugars are being used more quickly for growth, possibly due to a faster metabolism and higher energy demand. The variability in the °Brix degrees also suggests that temperatures affect the rate of photosynthesis and carbohydrate distribution. Lower temperatures seem to favor sugar accumulation, while higher temperatures promote a rapid use of these resource (Di Bella *et al.*, 2020; Furuyama, Okamoto and Jishi, 2023).

On the 7th day, at 20 and 25 °C, the highest value (2 °Brix) was observed in plants at 25 °C with 18 hours of light (25C_18L); while the lowest value (1.27 °Brix) was at 20 °C with 0 hours of light (20C_00L). At 11 days, at 15, 20, and 25 °C, the highest value (1.67 °Brix) occurred at 25 °C with 18 hours of light (25C_18L), and the lowest value (0.90 °Brix) at 25 °C with 0 hours of light (25C_00L). At 14 days, at 15, 20, and 25 °C, the highest value (1.90 °Brix) was at 15 °C with 18 hours of light (15C_18L), while the lowest (0.73 °Brix) remained at 25 °C with 0 hours of light (25C_00L). At 18 days, at 15 °C, the highest value (1.70 °Brix) was observed with 18 hours of light (15C_18L), and the lowest value (1.33 °Brix) with 0 hours of light (15C_00L). This shows how temperature and photoperiod influence sugar accumulation, with generally higher values in plants with 18 hours of light per day and lower values with 0 hours of light. Exposure to 18 hours of light promotes greater photosynthesis, resulting in increased sugar production. Microgreens that receive light for more hours have more time to convert solar energy into carbohydrates. In contrast, fewer hours of light decrease their photosynthetic rate, which lower sugar levels (Seluzicki, Burko and Chory, 2017). Temperature also affects plant metabolism. At higher temperatures (such as 25 °C), metabolic activity is more intense, enhancing sugar utilization for growth and respiration, the elevated energy demands often lead to reduced sugar accumulation compared to cooler conditions. Thus, microgreens with more light and optimal temperatures have better conditions for photosynthesis, storing sugars, and maintaining vigorous growth. Lack of light drastically reduces sugar production, and temperature also modulates how these sugars are produced and used (Thakulla, Dunn and Hu, 2021; Furuyama, Okamoto and Jishi, 2023).

pH: At 15 °C, treatments without light (15C_00L) or with just 6 hours of light (15C_06L) maintained a relatively stable pH between days 11 and 14, followed by an increase by day 18. In contrast, the 12 and 18 hours light treatments (15C_12L and 15C_18L) showed a steady pH until day 14. Overall, values ranged from 5.5 to 6.5, tending to be slightly higher when more light was available.

At 20 °C, a different trend appeared. In the no-light and 6 hour light treatments (20C_00L and 20C_06L), the pH gradually dropped from day 7 to 14, with values between 5 and 6.5. For the 12 hour light condition (20C_12L), pH increases from day 7 to 11, then stabilizes. The 18 hours light treatment (20C_18L) maintained a steady pH near 5.8.

At 25 °C, all treatments (25C_00L to 25C_18L) followed a similar pattern: pH rose between days 7 and 11, then dipped slightly by day 14. pH values here ranged from 4.5 to 6.

The behavior of pH in general is more stable and some trends that may appear related to photoperiod and temperature are not as clear as those visualized in other studied variables. This might be due to the homeostasis mechanisms in plants that enables the regulation of their internal pH to ensure the optimal functioning of essential metabolic processes (Zhou, Hao and Yang, 2021; Li and Yang, 2023).

Conductivity: At 15 °C, the treatment without light (15C_00L) increased in electrical conductivity (EC) from day 11 to 14, followed by a drop on day 18. Values range between 1.5 and 2.75 mS/cm. For the 6 hours (15C_06L) and 12 hours (15C_12L) light treatments, EC remains fairly stable through days 11 to 14 and increases by day 18. The 18 hours light treatment (15C_18L) behaves similarly through days 11 to 14, but decreases by day 18, the values range between 2.25 and 2.75 mS/cm.

At 20 °C, EC increases from day 7 to day 11 in all treatments, then drops slightly on day 14. The values fall in the 1 to 3 mS/cm range.

At 25 °C, treatments without light (25C_00L) and with 6 hours of light (25C_06L) also show a rise in EC between days 7 and 11, followed by a decrease. EC values range from 1.5 to 2.75 mS/cm. The 12 hours light treatment (25C_12L) shows a slight decline in EC across the same period, staying around 2.25 mS/cm. The 18 hours treatment (25C_18L) also shows a decrease, a bit more pronounced, although values still range between 2.25 and 2.75 mS/cm.

The data overall shows that there is no clear pattern that can be directly linked to harvest day, light exposure, or temperature. The results are quite variable, and it is hard to tell if any of these factors are influencing the changes in conductivity. Moreover, to our knowledge, there are currently no relevant studies addressing this specific aspect in microgreens.

Optical properties (Color Lab components)

In Figure 25, the Lab color coordinates reveal the color's position on the blue-yellow scale through the b* value, while the L* component indicates luminosity. Negative b* values indicate a tendency toward blue, while positive values indicate a lean towards yellow. In the L* component, lighter colors reflect more light (having a higher L* value), while darker colors absorb more light (having a lower L* value). The graph shows that both the b* and the L* values are lower when the plant is subjected to a longer photoperiod. The plant grown in light exhibits a lower b* value, indicating less yellow and more green. This is common in healthy plants, which have high levels of chlorophyll. Chlorophyll primarily absorbs blue and red light, reflecting green, and thus tends

to reduce the b* value toward less positive values (Ajdanian, Babaei and Aroiee, 2019; Kyriacou *et al.*, 2020; Hernández-Adasme, Palma-Dias and Escalona, 2023).
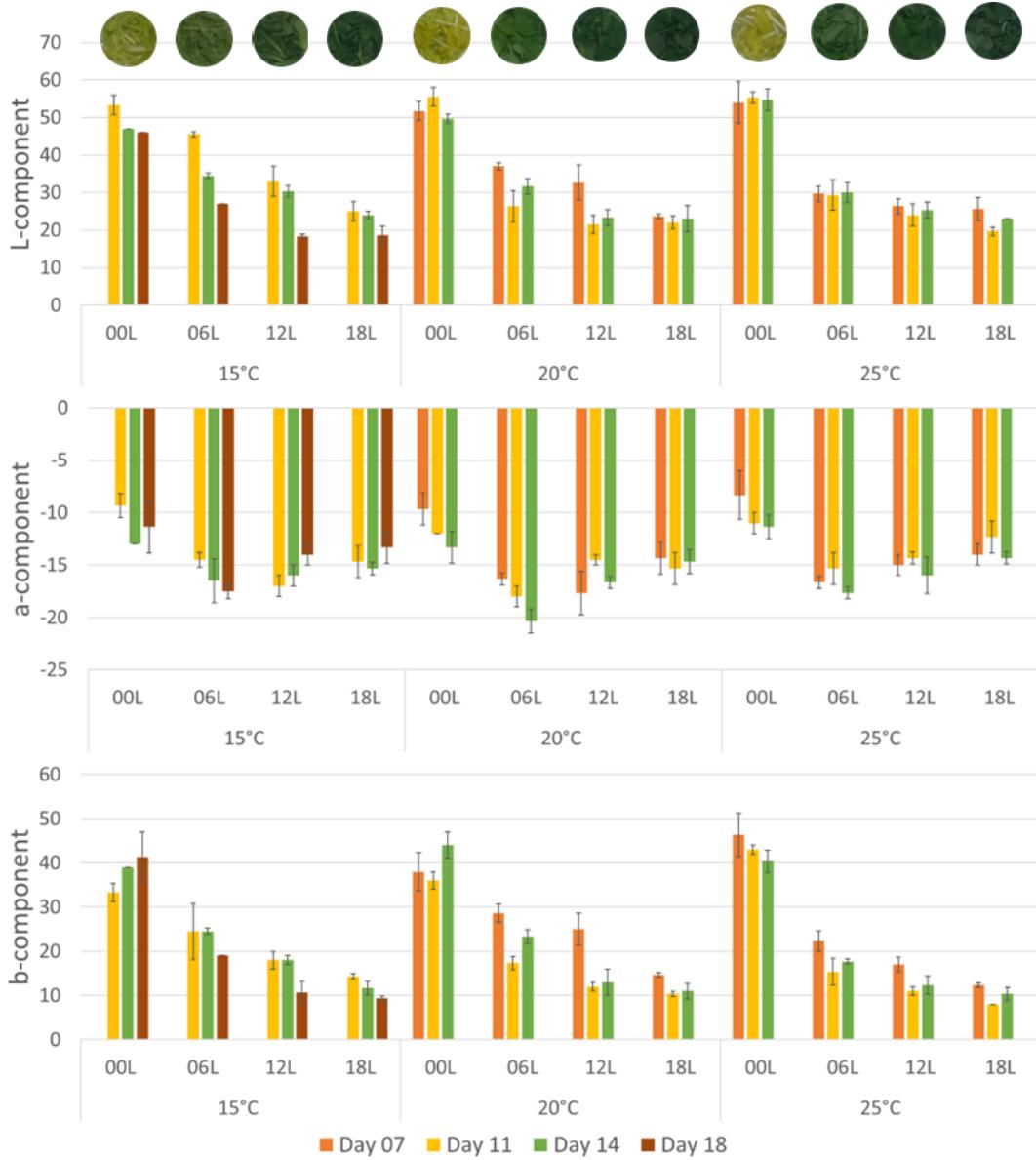
Figure 25. Lab color components of pea microgreens harvested after 7, 11, 14 and 18 days under different temperature (15, 20 and 25 °C) and photoperiod (00L, 06L, 12L, 18L) conditions. Standard deviation is represented by whiskers (± SD)

Temperature affects the growth and development of microgreens, as well as the color components L* (luminosity) and b* (blue-yellow). Optimal temperatures favor chlorophyll production. However, at extreme temperatures, whether high or low, the plants can get stressed, leading to less chlorophyll production and more carotenoids synthesis, which raises L* and b* values, indicating a higher presence of yellow color. As microgreens grow, chlorophyll levels often increase, especially when light is available (Kay and Phinney, 1956; Młodzińska, 2009; Ajdanian, Babaei and Aroiee, 2019), resulting in a decrease in L* and b* values.

The results regarding the 14 days of growth show that the highest L* values were obtained by plants growing at (25C_00L), with the highest values being 54.67 units; for the b* component, the highest values were 15_00L with 44 units. Meanwhile, the lowest L* values were recorded for 20C_18L and 25C_18L with 23 units; the b* component was 25C_18L with 19.33 units.

The a* (green-red) component differs from the L* and b* components. Treatments without light (00L) showed much higher values than those with 6, 12, or 18 hours of light. In the absence of light, less chlorophyll is produced, which reduces the green tone and allows other pigments, such as reddish or yellowish ones, to become more visible (Kay and Phinney, 1956; Młodzińska, 2009; Kong and Zheng, 2019), which is typical in etiolated plants.

Pigments (chlorophyll A, B and total carotene)
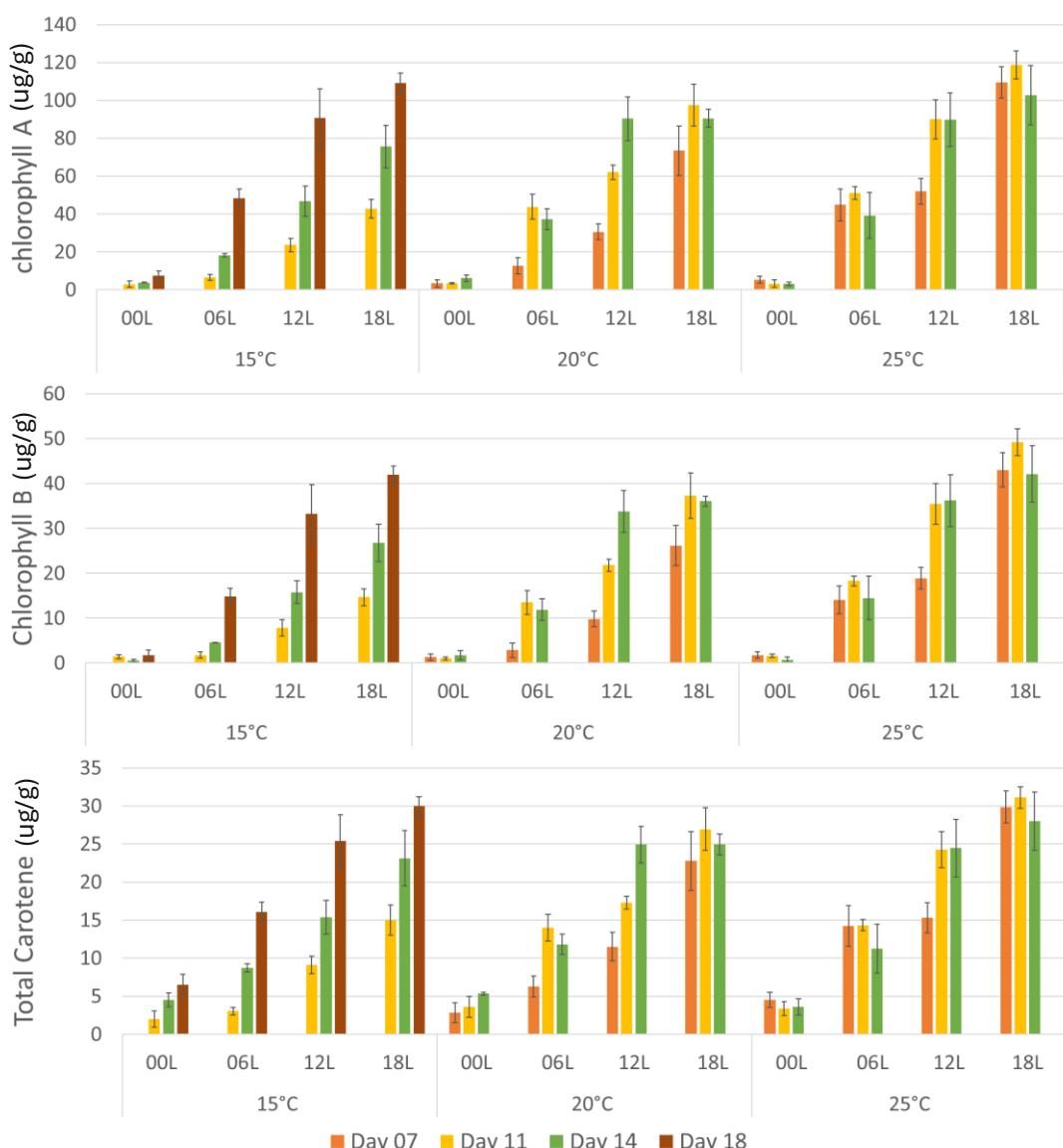
**Figure 26.** Chlorophyll A, B and total carotene content of pea microgreens harvested after 7, 11, 14 and 18 days under different temperature (15, 20 and 25 °C) and photoperiod (00L, 06L, 12L, 18L) conditions. Standard deviation is represented by whiskers (± SD)

In the analysis of pigments in pea microgreens (Figure 26), the levels of chlorophyll A, B, and total carotene consistently increase as the photoperiod lengthens. This is due to the relationship between light and photosynthesis. As light exposure increases, plants have more time to perform photosynthesis, encouraging the production of photosynthetic pigments (Młodzińska, 2009; Ajdanian, Babaei and Aroiee, 2019).

In the present study, the PPFD was 75.7 ± 5 µmol/m²/s, and light treatments ranged from 0 to 18 h·d⁻¹. At 25 °C, the highest values of chlorophyll A, chlorophyll B, and total carotenoids were obtained under the 18 h·d⁻¹ photoperiod (18L), reaching approximately 110, 45, and 30 µg/g, respectively. While 0 h·d⁻¹ photoperiod (00L) shows significantly lower levels close to zero. Comparatively, Liu *et al.* (2022) evaluated the effect of photoperiod duration (12 to 20 h·d⁻¹) on Brassica microgreens and reported that a 16 h·d⁻¹ photoperiod, combined with PPFD levels of 90 µmol·m⁻²·s⁻¹ for cabbage and 70 µmol·m⁻²·s⁻¹ for Chinese kale, was optimal for growth. Under these conditions, cabbage microgreens reached chlorophyll A levels of 77 µg/g, chlorophyll B of 31 µg/g, and carotenoids of 17 µg/g, while Chinese kale microgreens showed chlorophyll A of 68 µg/g, chlorophyll B of 26 µg/g, and carotenoids of 26 µg/g.

Additionally, a progressive increase can be observed in the graph as the cultivation days increase, especially for the lower temperature treatments, however at higher temperature, the variability is higher. The rise in chlorophyll levels tends to correlate with the development of more photosynthetically active tissue, such as leaves. As the leaves expand and increase in area, the number of chloroplasts containing chlorophyll also increases. This increase allows microgreens to capture more light and, therefore, enhances their photosynthetic capacity, which is essential for their development and biomass production. Moreover, the vegetative growth of the plants is closely linked to greater synthesis of photosynthetic pigments to optimize light absorption efficiency (Brazaitytė *et al.*, 2018; Ajdanian, Babaei and Aroiee, 2019). This results in a noticeable increase in pigment content from day 11 to 18 at 15 °C, and from day 7 to 11 at temperatures of 20 °C and 25 °C.

Temperature increase can accelerate the metabolism of microgreens, including the synthesis of pigments such as chlorophyll A, B, and carotene. At higher temperatures within the optimal range for the plant, the enzymatic activity responsible for producing these pigments increases, promoting greater photosynthetic efficiency and adaptation to higher energy demand conditions (Niroula *et al.*, 2019). At 11 days of growth, the highest pigment values correspond to 25C_18L with 118.61, 49.26, and 31.13 µg/g of chlorophyll A, B, and total carotene, respectively.

However, it is important to note that if the temperature exceeds certain limits, it could have negative effects, such as enzyme denaturation or damage to plant tissues, reducing pigment levels (Niroula *et al.*, 2019). For example, the results obtained after 14 days of growth show that the

highest pigment values correspond to 25C_18L with 102.80, 42.14, and 28.01 µg/g of chlorophyll A, B, and total carotene, respectively, although their levels are lower than on day 11.

Bioactive compounds

In this study, chlorophylls and carotene were analyzed separately under the classification of pigments due to their specific roles in photosynthesis and their distinct analytical methods.

In the analysis of bioactive compounds (Figure 27), total water-soluble phenolic compounds (TPC) consistently increase as the photoperiod lengthens, showing a clear difference between 00L and the light treatments (06L, 12L, and 18L), although the difference among the latter is less pronounced or variable. A longer photoperiod may stimulate the accumulation of these phenolics compounds due to increased photosynthetic activity and the need to protect the plant from oxidative stress caused by light (Faraloni, Di Lorenzo and Bonetti, 2021; Kim *et al.*, 2022).
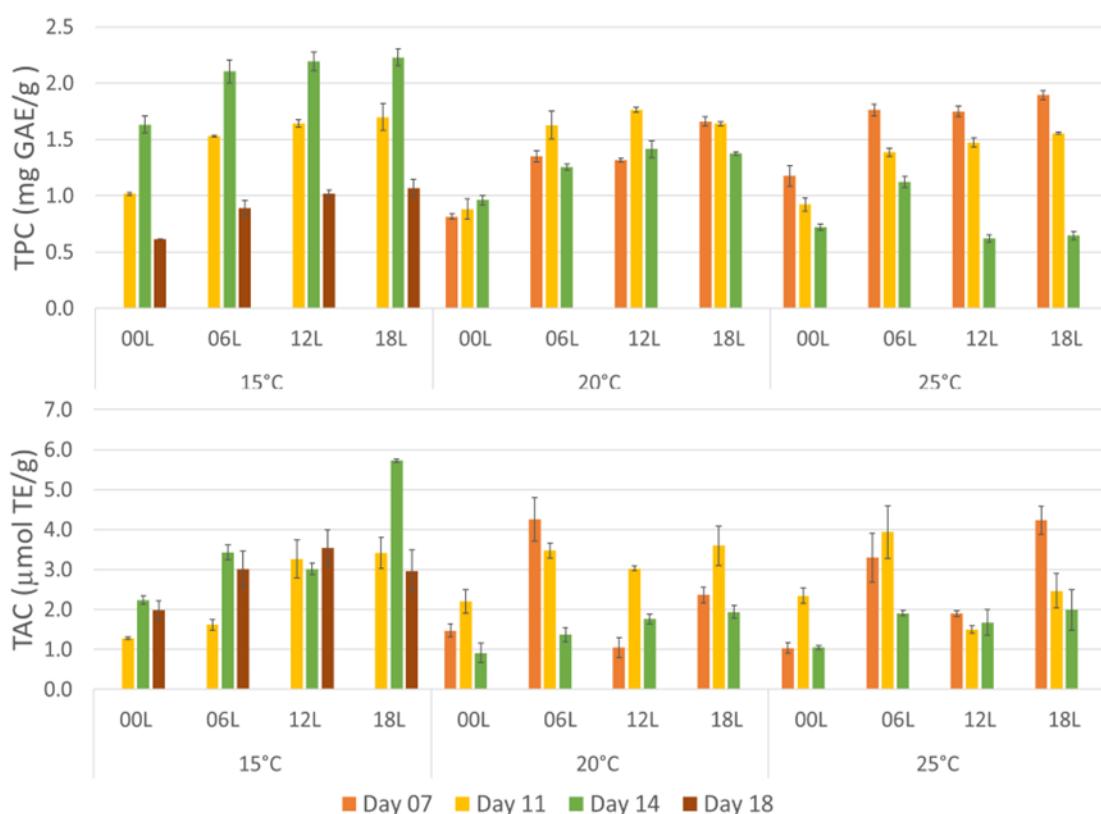
Figure 27. Total water-soluble phenolic compounds (TPC) and Total antioxidant capacity (TAC) of pea microgreens harvested after 7, 11, 14 and 18 days under different temperatures (15, 20 and 25 °C) and photoperiod (00L, 06L, 12L, 18L) conditions

Regarding temperature, a higher concentration of total water-soluble phenolic compounds was observed at the lower temperature of 15 °C compared to 20 °C and 25 °C. The increased accumulation of phenolic compounds at lower temperatures may be related to the stress imposed on the plant. Low temperatures often induce moderate stress that activates defense mechanisms in the plant, including the production of phenolic compounds. These compounds, which have

antioxidant properties, help protect the plant from oxidative damage that can occur under thermal stress conditions. At higher temperatures, the plant's metabolism may focus more on growth and respiration, potentially decreasing the accumulation of phenolics (Kim *et al.*, 2022).

There is a difference in phenolic accumulation linked to temperature and days of growth. At 15 °C, an increase in total water-soluble phenolic compounds is observed between days 11 and 14, followed by a decrease on day 18. This behavior may relate to a shift in the balance between synthesis and degradation of phenolics as the plant matures. At 20 °C, the treatment without light (20C_00L) shows a slight increase in phenolics between days 7 and 14. In the light treatments (20C_06L, 20C_12L, and 20C_18L), phenolics increase from day 7 to 11 but then decrease by day 14. This suggests that light initially induces the production of phenolics, but the effect moderates or even reverses in later stages. At 25 °C, a noticeable decrease in total water-soluble phenolic compounds is observed between days 7 and 11, with a more pronounced decline by day 14. This pattern may be associated with the plant's growth, where, in the initial days, size and weight (including total water-soluble phenolic compounds) increase, while by day 14, respiratory metabolism becomes more pronounced, possibly coupled with sensitivity to high temperatures that promote increased respiratory metabolism and degradation of phenolics (Di Bella *et al.*, 2020; Kim *et al.*, 2022). Although the Folin–Ciocalteu method is commonly used to estimate phenolic content, it should be noted that it can also react with other reducing compounds, which could slightly influence the accuracy of the measured phenolic levels (Singleton, Orthofer and Lamuela-Raventós, 1999).

The total antioxidant capacity (TAC) shows similarities to the behavior of total water-soluble phenolic compounds (TPC). At a temperature of 15 °C, TAC increases as the photoperiod extends, suggesting that light stimulates the synthesis of compounds with antioxidant activity (Hernández-Adasme, Palma-Dias and Escalona, 2023). Furthermore, TAC increases between days 11 and 14 and then decreases by day 18, similar to TPC. This pattern could be related to the plant's metabolic activity, where the accumulation of antioxidants peaks during an active growth phase but later decreases due to degradation or consumption of these compounds (Niroula *et al.*, 2019; Senevirathne, Gama-Arachchige and Karunaratne, 2019). At temperatures of 20 °C and 25 °C, although TAC behavior is more erratic, some correspondence with TPC is noted, as both exhibit a decrease between days 11 and 14. This suggests that higher temperatures, along with prolonged exposure, may affect the stability or synthesis of these antioxidant compounds in later growth stages (Niroula *et al.*, 2019). TAC accumulation appears to follow patterns similar to those of TPC, indicating that both indicators are related and their behavior depends on temperature, photoperiod, and growth stage.

In Table 13, a correlation matrix is presented, considering all the variables in the study, The interpretation of correlation strength was based on the classification of correlation coefficient values proposed by (Evans, 1995). There is a very strong correlation between photoperiod and color components L* and b*, pigments; and a strong correlation with °Brix, conductivity, and TPC. This indicates that longer light exposure may enhance pigment synthesis and sugar accumulation (Młodzińska, 2009; Liu *et al.*, 2022; Johnson, Kumar and Thakur, 2024). Meanwhile, a strong correlation exists between temperature with height, weight, and pH, highlighting its role in growth and metabolic processes (Kim *et al.*, 2022; Johnson, Kumar and Thakur, 2024).

In general, pigments show a negative correlation with the L* (lightness) and b* (yellow-blue axis), which causes microgreens to appear darker and less yellowish as the concentration of pigments such as chlorophyll A, B, and total carotene increases, resulting in a more intense green color. This is linked to the fact that chlorophylls strongly absorb blue light (photosynthetic peak at 440 nm) and red light (photosynthetic peak at 640–670 nm), while reflecting green wavelengths (500–550 nm), which is why plants appear green to the human eye (Ajdanian, Babaei and Aroiee, 2019).

On the other hand, pigments correlate positively with °Brix, conductivity, and TAC, which shows that microgreens rich in these pigments also tend to accumulate more sugars and antioxidant compounds. Additionally, °Brix, pH, conductivity, TPC, and TAC tend to have a negative correlation with height, weight, and Lab color components, while showing a positive correlation with pigments.

There is a very strong correlation between height and weight (|R|= 0.9), as well as a strong correlation with °Brix and conductivity. On the other hand, there is a significant correlation between the color components L*and b*, and the pigments (|R|= between 0.8 and 0.9). °Brix and conductivity also show a strong correlation with these variables.

There is a strong correlation between conductivity, TPC, and TAC (|R| between 0.5 and 0.7). Additionally, there is a strong negative correlation of both conductivity and TAC with color components L* and b*, and TAC with height and weight (|R|= 0.5).
°Brix has a very strong correlation (|R|= 0.7) with various variables: height, color L* and b*; and a strong correlation with chlorophyll A, B, carotene, conductivity, TPC, and TAC. Meanwhile, pH and color component a* show the lowest correlation with other variables, suggesting they are less influenced by the studied conditions.

Table 13. Correlation matrix for measured variables of pea microgreens harvested after 7, 11, 14 and 18 days under different temperatures (15, 20 and 25 °C) and photoperiod (00L, 06L, 12L, 18L) conditions

	Day	Photoperiod	Temperature	Plant_height	Plant_weight	L*	a*	b*	Chlorophyll_A	Chlorophyll_B	Total_carotene	Brix	pH	Conductivity	TPC	TAC
Day	1.0	0.0	-0.5	0.2	0.4	-0.1	-0.1	-0.1	0.2	0.2	0.2	0.0	0.4	0.0	-0.3	0.0
Photoperiod	0.0	1.0	0.0	-0.4	-0.2	-0.8	-0.3	-0.9	0.9	0.8	0.9	0.7	0.2	0.5	0.5	0.4
Temperature	-0.5	0.0	1.0	0.6	0.5	0.0	0.1	0.0	0.2	0.2	0.1	-0.2	-0.5	-0.1	-0.2	-0.3
Plant_height	0.2	-0.4	0.6	1.0	0.9	0.4	0.2	0.4	-0.2	-0.1	-0.2	-0.7	-0.2	-0.3	-0.5	-0.4
Plant_weight	0.4	-0.2	0.5	0.9	1.0	0.1	0.1	0.1	0.1	0.1	0.1	-0.5	-0.1	-0.1	-0.5	-0.3
L*	-0.1	-0.8	0.0	0.4	0.1	1.0	0.5	0.9	-0.8	-0.8	-0.8	-0.7	-0.2	-0.5	-0.4	-0.5
a*	-0.1	-0.3	0.1	0.2	0.1	0.5	1.0	0.5	-0.2	-0.2	-0.3	-0.4	0.0	-0.3	-0.3	-0.3
b*	-0.1	-0.9	0.0	0.4	0.1	0.9	0.5	1.0	-0.8	-0.8	-0.8	-0.7	-0.2	-0.6	-0.4	-0.5
Chlorophyll_A	0.2	0.9	0.2	-0.2	0.1	-0.8	-0.2	-0.8	1.0	1.0	1.0	0.6	0.1	0.5	0.2	0.3
Chlorophyll_B	0.2	0.8	0.2	-0.1	0.1	-0.8	-0.2	-0.8	1.0	1.0	1.0	0.5	0.1	0.4	0.2	0.3
Total_carotene	0.2	0.9	0.1	-0.2	0.1	-0.8	-0.3	-0.8	1.0	1.0	1.0	0.6	0.1	0.5	0.3	0.4
Brix	0.0	0.7	-0.2	-0.7	-0.5	-0.7	-0.4	-0.7	0.6	0.5	0.6	1.0	0.0	0.5	0.6	0.6
pH	0.4	0.2	-0.5	-0.2	-0.1	-0.2	0.0	-0.2	0.1	0.1	0.1	0.0	1.0	0.3	0.0	0.3
Conductivity	0.0	0.5	-0.1	-0.3	-0.1	-0.5	-0.3	-0.6	0.5	0.4	0.5	0.5	0.3	1.0	0.5	0.7
TPC_Avg	-0.3	0.5	-0.2	-0.5	-0.5	-0.4	-0.3	-0.4	0.2	0.2	0.3	0.6	0.0	0.5	1.0	0.6
TAC_Avg	0.0	0.4	-0.3	-0.4	-0.3	-0.5	-0.3	-0.5	0.3	0.3	0.4	0.6	0.3	0.7	0.6	1.0

Correlation according to the ranges 0-0.1 (no correlation), 0.1-0.3 (low correlation), 0.3-0.5 (moderate correlation), 0.5-0.7 (strong correlation), 0.7-1 (very strong correlation).

5.3.2. Near infrared spectra and PCA analysis of pea microgreen samples

The spectral analysis was performed in harvested pea plants, samples prepared under two different methods specified in the materials and methods section, named as microgreens fresh-cut samples scanned in reflectance mode (Figure 28a) and in aqueous microgreens extracts samples scanned in transmittance mode (Figure 28b). It shows the NIR spectra of pea microgreens belonging to 7, 11, 14 and 18 days of growing. In both cases the spectra were pretreated with SG 2-45-0 and SNV in the wavelength rage 1150 to 1850 nm. The spectra are colored by treatment (temperature-photoperiod conditions). At this point, there is no observable trend as most of the spectra is overlapped for the 25 ºC treatments. However, spectra from aqueous microgreens extracts samples look much more compact compared to spectra from microgreens fresh-cut samples. In both cases, it is a clear distinction of the first overtone of water with peak around 1450 nm, which is of great importance in biological systems (Tsenkova, 2009; Tsenkova, Kovacs and Kubota, 2015), aqueous microgreens extracts samples registered higher absorbance values.
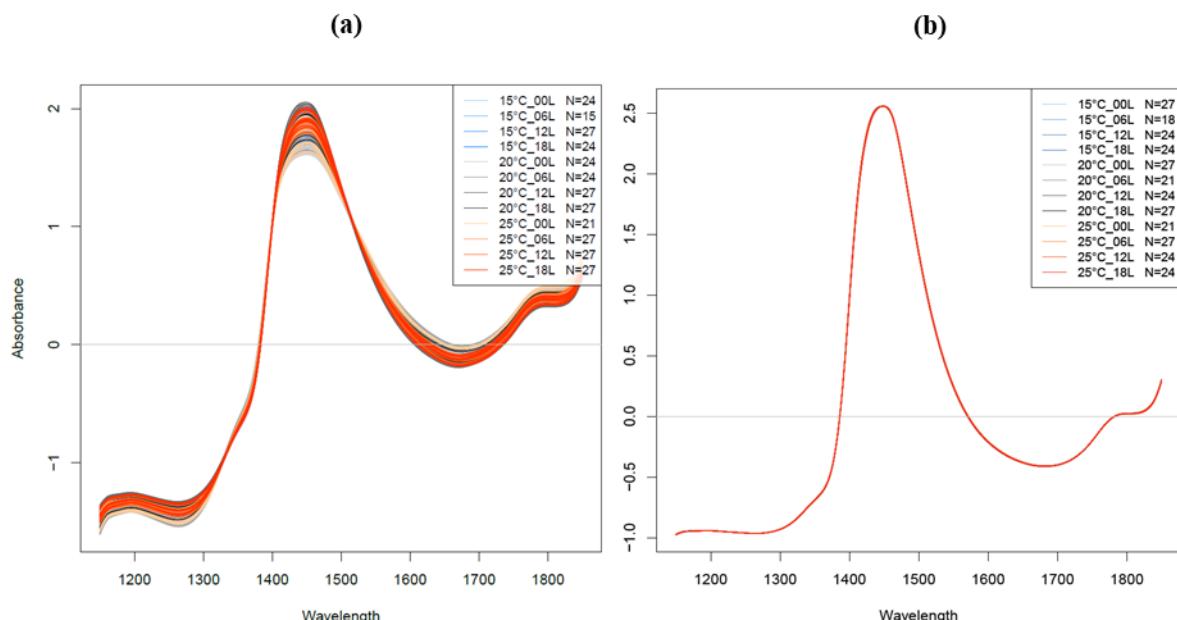
Figure 28. NIRS spectra of pea microgreens (a) fresh-cut samples (n=294) (b) aqueous microgreens extracts samples (n=288), harvested after 7, 11, 14 and 18 days under different temperature (15, 20 and 25 °C) and photoperiod (00L, 06L, 12L, 18L) conditions. Pretreatments SG 2-45-0 and SNV. Wavelength 1150 to 1850nm

PCA results for microgreens fresh-cut samples are presented in Figure 29a. In the PCA plot colored by day, PC1 shows a trend where samples from day 7 and 11 are closer to the axis compared to those from day 14 and 18. Meanwhile, in PC2 there is more distinction between day 11 which is closer to the axis, compared to days 14 and 18. Next, in the PCA plot colored by temperature, there is no clear tendency between the three temperatures, showing major overlapping between them. Moreover, coloring by photoperiod, the most separated group is 00L

which is closer to the PC2 axis, meanwhile, there is major overlapping between the other three photoperiod groups, but some trends are observable where 06L, is closer to PC2 axis and 18L is the farthest. PC1 and PC2 account for 97.17% and 1.11% of the explained variance.

Similarly, PCA results are observable for aqueous microgreens extracts samples in the Figure 29b. The PCA plot colored by temperature shows major overlapping, however, some trends for separation between groups are detected. Furthermore, PCA coloring by photoperiod, the major distinction between groups for aqueous microgreens extracts samples is in PC2 were higher photoperiod levels 18L, 12L, 06L are closer to PC1 axis. PC1 and PC2 account for 97.97% and 1.61% of the explained variance, respectively. Important loadings (Figure 30b) are registered in PC1 at 1412 and 1495 nm.
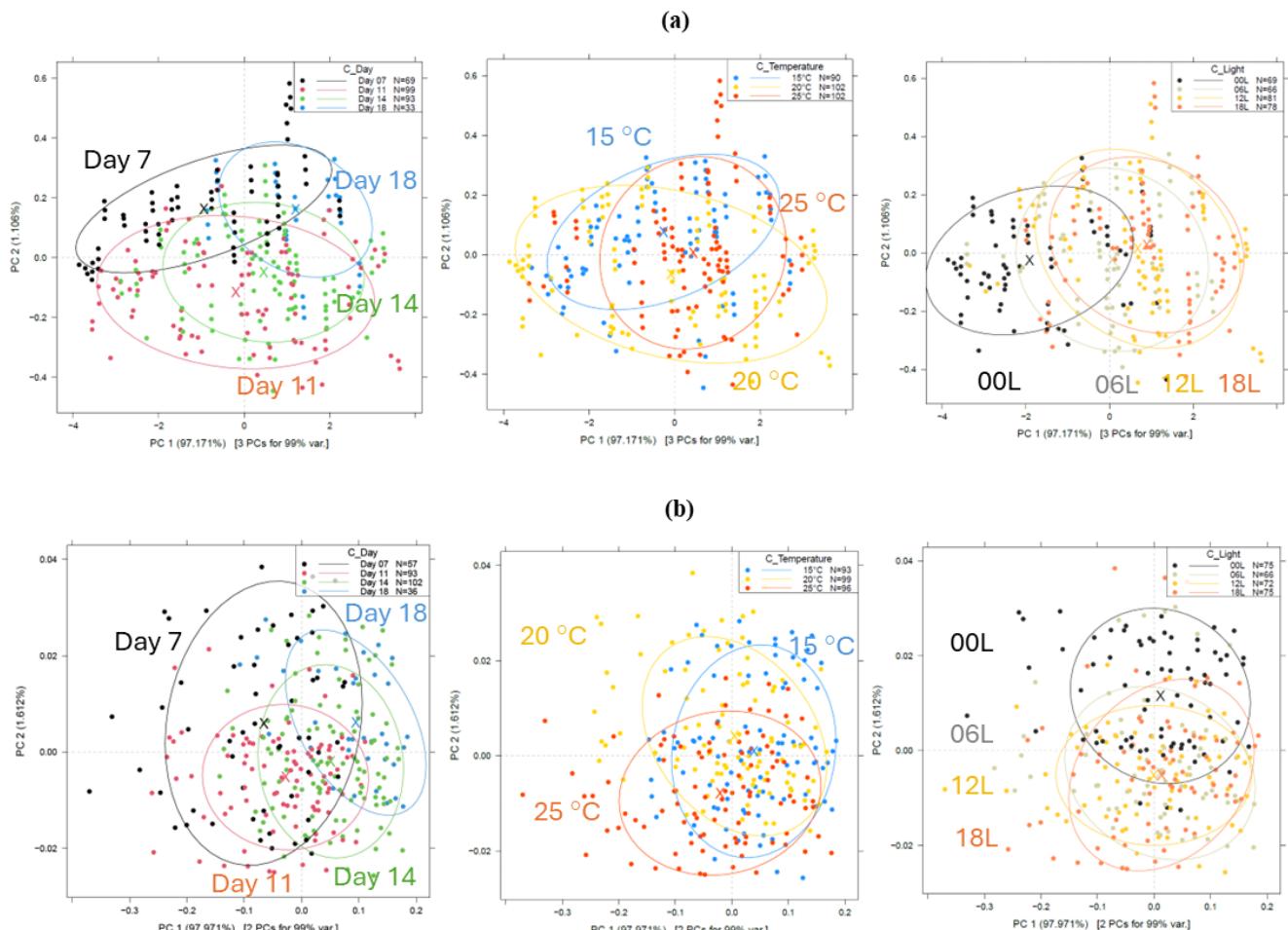
Figure 29. PCA analysis of pea microgreens (a) fresh-cut samples (n=294), (b) aqueous microgreens extracts samples (n=288) harvested after 7, 11, 14 and 18 days under different temperature (15, 20 and 25 °C) and photoperiod (00L, 06L, 12L, 18L) conditions. Coloring by day, temperature and photoperiod. Pretreatments SG 2-45-0 and SNV. Wavelength 1150 to 1850nm. 95% confidence intervals of the respective groups are represented by Ellipses and x-axis represents the group centroids

The wavelengths observed in the NIRS analysis of microgreens reflect the chemical composition of the samples and the impact of their state (fresh-cut samples or aqueous microgreens

extracts samples) on the absorption of infrared radiation. Büning-Pfaue (2003) mentioned how absorption bands and peaks are dependent on the food water content.

In the microgreens fresh-cut samples (Figure 30a), the important loadings in PC1, at 1264nm linked to the 1st overtone of O-H bend deformation vibration, at 1448 and 1380 nm, are associated with O-H bond vibrations in water (Curran, 1989; Slavchev *et al.*, 2015) and C-H bonds in organic compounds (da Costa Filho, 2009; Workman and Weyer, 2012) like carbohydrates and proteins, which are common in plant tissues. Moreover, the range between 1450 to 1850 nm which is highly important in PC1 is also linked to O-H, N-H and C-H valence vibrations (Curran, 1989; Workman and Weyer, 2012).

In the aqueous microgreens extracts samples (Figure 30b), the wavelengths 1412 nm can be associated to O-H bend and C-H stretch which relates with water and carbohydrates (Curran, 1989), and 1495 nm are linked to O-H and N-H stretching bonds associate to carbohydrates, lipids and proteins (Curran, 1989; Slavchev *et al.*, 2015).
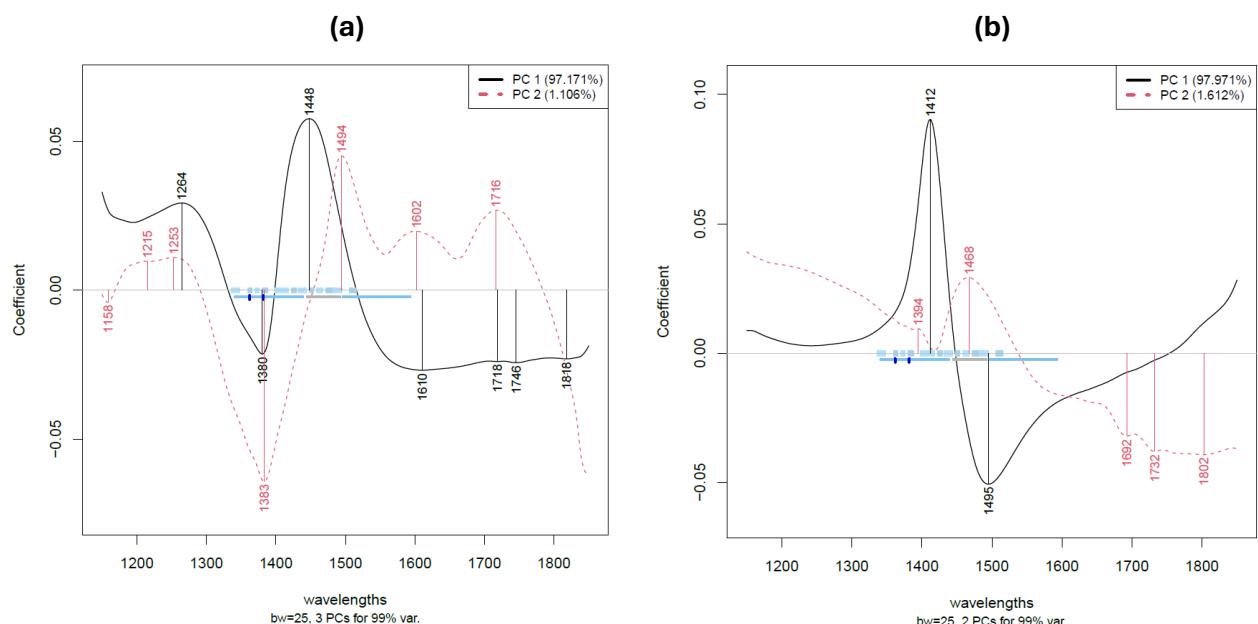

Figure 30. PCA loadings of pea microgreens (a) fresh-cut samples (n=294) (b) aqueous microgreens extracts samples (n=288) harvested after 7, 11, 14 and 18 days under different temperature (15, 20 and 25 °C) and photoperiod (00L, 06L, 12L, 18L) conditions. Pretreatments SG 2-45-0 and SNV. Wavelength 1150 to 1850nm

5.3.3. Classification of pea microgreen samples

The PCA-LDA analysis for the discrimination of microgreens fresh-cut samples from day 11 is shown in Figure 31. Day 11 was selected for this analysis because it is a common time point across all samples grown under different light and temperature conditions. Additionally, it provides a clearer and more reliable assessment of the microgreens' characteristics, allowing for better comparison and interpretation of the data.
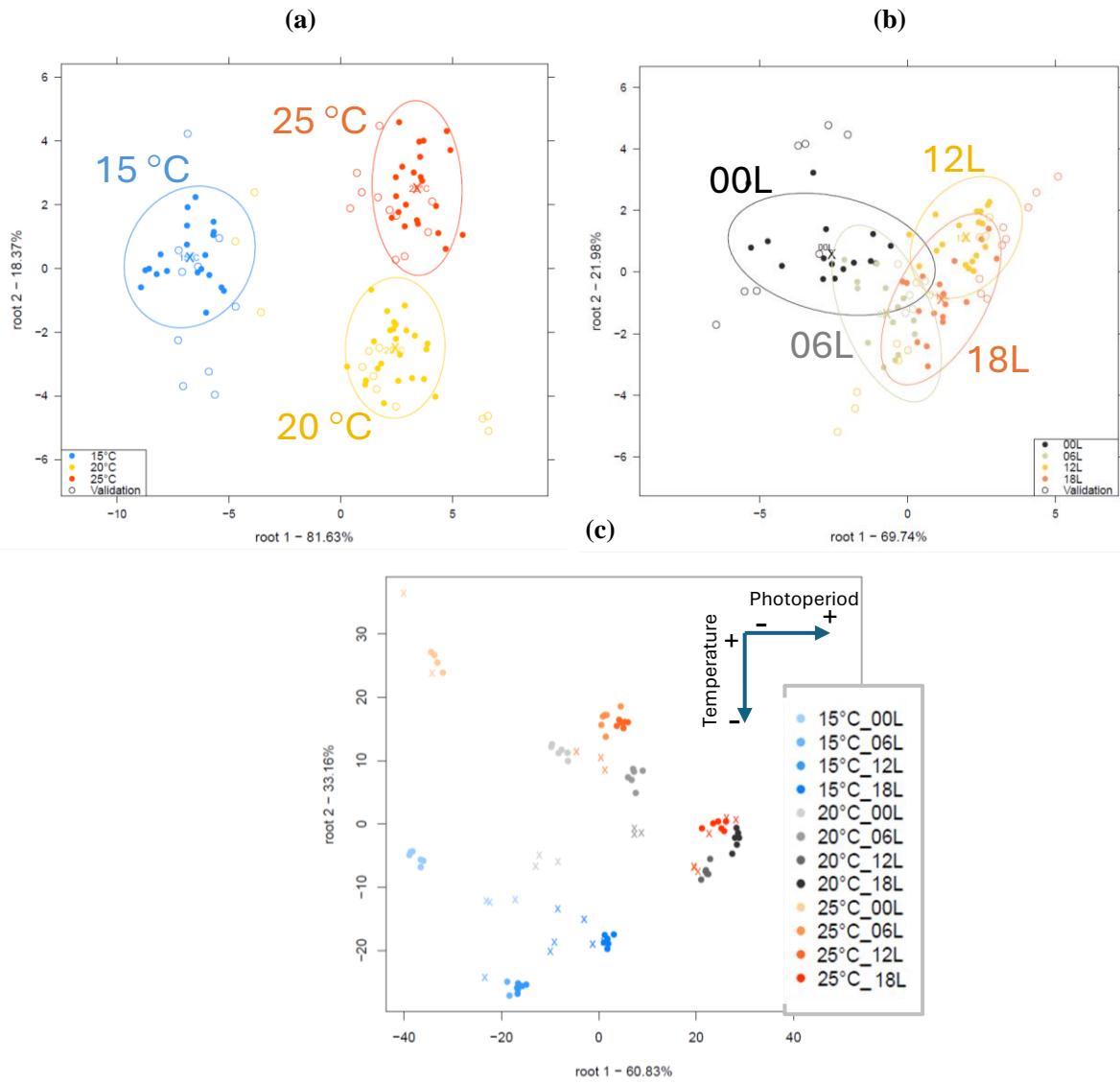
Figure 31. Discriminant analysis (PCA-LDA) of NIRS pea microgreens spectra (fresh-cut samples) harvested after 11 days under different temperature (15, 20 and 25 °C) and photoperiod (00L, 06L, 12L, 18L) conditions. Clustering by (a) temperature, (b) photoperiod and (c) treatment (temperature-photoperiod). Pretreatments SG 2-45-0 and SNV. Wavelength 1150 to 1850nm. In (a) and (b), 95% confidence intervals of the respective groups are represented by Ellipses, and x-axis represents the group centroids. In (c) dots indicate calibration data, and x marks indicate cross-validation data

When grouped by temperature, a slight overlap of samples corresponding to 15 °C, 20 °C, and 25 °C is observed (Figure 31a). The average correct recognition rate is 100%, while the prediction rate is 81.8% (Appendix-A2_Table 10a). Most misclassifications occurred among samples from the consecutive groups 15 °C-20 °C and 20 °C-25 °C. In the case of grouping by photoperiod (Figure 31b), a greater overlap is seen among samples belonging to the 06L, 12L, and 18L groups. The average correct recognition rate is 86.66%, while the prediction rate is 52.4% (Appendix-A2_Table 10b). Most misclassifications occurred between samples from the consecutive groups 00L-06L, 06L-12L, and 12L-18L. On the other hand, grouping by treatment

(Figure 31c) shows varying degrees of overlap among the groups, with 25 °C_00L and 15 °C_00L having the least overlap. Additionally, there is a trend where treatments with a lower photoperiod tend to be closer to the root 2 axis, and treatments with lower temperatures are closer to the root 1 axis. The average correct recognition rate in this case is 100%, and the prediction rate is 48.39% (Appendix-A2_Table 10c).

Figure 32 shows the PCA-LDA analysis results for the discrimination of pea aqueous microgreens extracts samples from day 11.
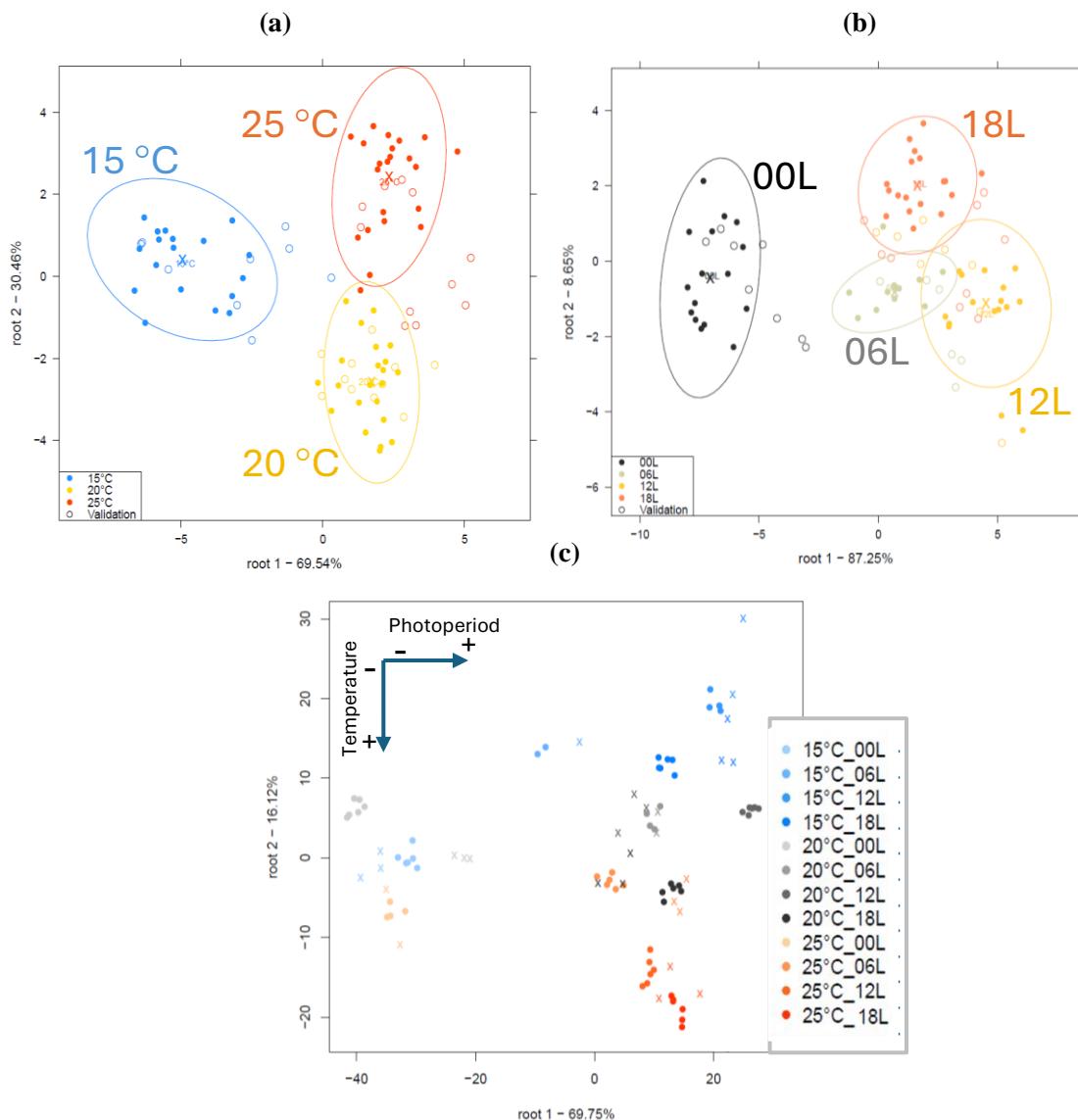
Figure 32. Discriminant analysis (PCA-LDA) of NIRS pea spectra (aqueous microgreens extracts samples) harvested after 11 days under different temperature (15, 20 and 25 °C) and photoperiod (00L, 06L, 12L, 18L) conditions. Clustering by (a) temperature, (b) photoperiod and (c) treatment (temperature-photoperiod). Pretreatments SG 2-45-0 and SNV. Wavelength 1150 to 1850nm. In (a) and (b), 95% confidence intervals of the respective groups are represented by Ellipses, and x-axis represents the group centroids. In (c) dots indicate calibration data, and x marks indicate cross-validation data

When grouped by temperature, a slight overlap is seen among samples from 15 °C, 20 °C, and 25 °C (Figure 32a). The average correct recognition rate reaches 98.98%, and the prediction rate is 85.6% (Appendix-A2_Table 11a), with misclassifications mainly concentrated in the consecutive groups 15 °C-20 °C and 20 °C-25 °C. In the case of photoperiod (Figure 32b), there is greater overlap among the 06L, 12L, and 18L groups, with a correct recognition rate of 94.17% and a prediction rate of 75.83% (Appendix-A2_Table 11b). Misclassifications mainly occurred between the consecutive groups 06L-12L and 12L-18L. For grouping by treatment (Figure 32c), a variable level of overlap is observed among the different groups, with treatments corresponding to lower photoperiod tending to be located near the root 2 axis, while treatments with higher temperatures are closer to the root 1 axis. The correct recognition rate is 100%, and the prediction rate is 75.01% (Appendix-A2_Table 11c).

The PCA-LDA analysis reveals that the discrimination of aqueous microgreens extracts samples from day 11 generally yields higher recognition and prediction accuracies compared to microgreens fresh-cut samples. Similar results were found when analysis was performed in other days. Grouping by temperature demonstrates relatively good separation with some overlap, while grouping by photoperiod shows more considerable overlap, particularly in consecutive groups. The treatment groupings highlight a consistent pattern where the photoperiod and temperature significantly influence the positioning of the samples along the root axes. Overall, aqueous microgreens extracts samples exhibit better discrimination performance, suggesting they provide more informative spectral features for distinguishing between groups.

Table 14. presents a summary of the discriminant analysis for pea microgreens, comparing fresh-cut samples and aqueous extracts samples preparations.

Table 14. Discriminant analysis-summary table for pea microgreens (fresh-cut and aqueous microgreens extracts samples) harvested after 7, 11, 14, 18 days under different temperature (15, 20 and 25 °C) and photoperiod (00L, 06L, 12L, 18L) conditions. Analysis according to various datasets and clustering type selection. Clustering by day, temperature, photoperiod or treatment (temperature-photoperiod). NIRS pretreatments SG 2-45-0 and SNV. Wavelength 1150-1850nm

Data	Clustering by	Microgreens fresh-cut samples						Aqueous microgreens extracts samples					
		n	g	%C	%CV	LV	LV max.	n	g	%C	%CV	LV	LV max.
15C_00L	Day	24	3	100	95.86	4	7	27	3	88.89	88.89	2	8
15C_06L	Day	-	-	-	-	-	-	18	3	100	100	5	5
15C_12L	Day	-	-	-	-	-	-	24	3	98.17	88.89	3	7
15C_18L	Day	24	3	100	75.03	7	7	24	3	100	100	3	7
20C_00L	Day	24	3	97.25	80.07	3	7	27	3	96.33	66.67	4	8
20C_06L	Day	24	3	100	65.29	7	7	21	3	74.32	70.39	2	6
20C_12L	Day	27	3	98.17	63	4	8	24	3	97.46	82.26	3	7
20C_18L	Day	27	3	79.61	55.56	2	8	27	3	78.22	68.96	2	8
25C_00L	Day	21	3	100	94.5	6	6	21	3	100	88.89	4	6
25C_06L	Day	27	3	100	74.11	7	8	27	3	100	81.45	5	8
25C_12L	Day	27	3	88.89	69.97	2	8	24	3	100	100	5	7
25C_18L	Day	27	3	100	100	6	8	24	3	100	89.71	4	7
Day 7	Treatment	69	8	100	56.41	20	20	57	8	100	87.72	16	16
Day 11	Treatment	99	12	100	48.39	22	29	93	12	100	74.57	27	27
Day 14	Treatment	93	12	100	59.72	20	27	102	12	98.15	56.47	18	30
Day 18	Treatment	33	4	95.81	53.18	6	10	36	4	100	63.56	9	11
Day 11	Temperature	99	3	100	81.79	22	32	93	3	98.98	85.58	20	30
Day 14	Temperature	93	3	100	75.76	28	30	102	3	96.76	77.78	21	33
Day 7	Photoperiod	69	4	100	65.49	18	22	57	4	100	85.45	17	18
Day 11	Photoperiod	99	4	86.66	52.4	13	32	93	4	94.17	75.83	16	30
Day 14	Photoperiod	93	4	87.48	67.83	11	30	102	4	95.9	64.6	25	33
Day 18	Photoperiod	33	4	95.81	53.18	6	10	36	4	100	63.56	9	11
All	Day	294	4	75.85	66.95	38	97	288	4	96.58	95.59	20	95
All	Treatment	294	12	90.41	58.54	27	94	288	12	90.2	68.34	27	92
All	Temperature	294	3	93.68	75.74	43	97	288	3	93.08	88.87	24	95
All	Photoperiod	294	4	89.5	71.05	35	97	288	4	81.28	66.89	26	95

LV is the number of latent variables regarding each PCA-LDA model. Calculated LV max. = (n-g/3) which surpassing may cause overfitting (Defernez and Kemsley, 1997).

Classification by day: In the first part of Table 14, samples from each treatment were classified based on the day of harvesting. The results indicate that aqueous microgreens extracts samples achieved higher classification accuracy, with cross-validation percentages ranging from

66.67% to 100%. In contrast, microgreens fresh-cut samples showed lower accuracies, ranging from 55.56% to 100%. Notably, the classification models for aqueous microgreens extracts samples consistently outperformed those for microgreens fresh-cut samples for almost all treatments, except for 15C_00L, 20C_00L, and 25C_00L.

Clustering by treatment, temperature, or photoperiod: In the second part of the Table 14, samples collected on a specific day were grouped by treatment, temperature, or photoperiod. For clustering by treatment, microgreens fresh-cut samples showed cross-validation (CV) classification accuracies between 48.39% and 59.72%, while aqueous microgreens extracts ranged from 56.47% to 87.72%. For temperature clustering at day 11 and day 14, microgreens fresh-cut samples achieved CV classification accuracies of 81.79% and 75.76%, respectively. For aqueous microgreens extracts samples, the accuracy was slightly higher, at 85.58% and 77.78%. Photoperiod clustering yielded CV classification accuracies between 52.4% and 67.83% for microgreens fresh-cut samples, and between 63.56% and 85.45% for aqueous microgreens extracts samples.

Global sample selection: In the final section of Table 14, the complete dataset, encompassing all pea microgreen samples, is presented. Under this "global" sample selection, for microgreens fresh-cut samples, CV classification accuracies were 66.95%, 58.54%, 75.74%, and 71.05% for clustering based on day, treatment, temperature, and photoperiod, respectively. For aqueous microgreens extracts samples, the corresponding accuracies were 95.59%, 68.34%, 88.87%, and 66.89%, respectively.

Overall, these findings highlight that aqueous microgreens extracts samples generally achieve significantly higher classification accuracy compared to microgreens fresh-cut samples, especially when categorized by treatment or temperature. This suggests that the characteristics captured in the liquid phase, such as differences in absorbance patterns related to soluble compounds, water content, or overall matrix homogeneity, are more distinctive, making it easier to differentiate among treatments, temperatures, and other variables. The consistency in better performance of aqueous microgreens extracts samples, except in a few cases, demonstrates their robustness and potential suitability for discriminant analysis in assessing the impact of different growing conditions on pea microgreens. This superior performance might be due to better homogenization or greater sensitivity to compositional changes that occur under different treatments.

Although some models appear promising, in certain cases there is a noticeable gap between calibration and cross-validation results, which may indicate overfitting. The various classification models presented in Table 14 show CV values ranging from 48.39% to 100% for microgreens fresh-cut samples, and from 56.47% to 100% for aqueous microgreens extracts samples.

In comparison, when performing the analysis using simulated data composed of random numbers (Appendix-A2_Table 12), the CV values range from 9.5% to 50%. This suggests that the models are capturing meaningful patterns from the real data, which contain relevant information for classification.

5.3.4. PLSR prediction of agronomic and phytochemical parameters

In Table 15, the PLSR summary table for microgreens fresh-cut samples and aqueous microgreens extracts samples includes the results of 13 analyzed variables, which relate to different characteristics: physical characteristics (height and weight), optical properties (Lab color components), pigments (chlorophyll A, B, and total carotene), chemical characteristics (°Brix, pH, and conductivity), and bioactive compounds (TAC and TPC).

Table 15. Partial least square regression -summary table of NIRS pea microgreens spectra (fresh-cut and aqueous microgreens extracts samples) harvested after 7, 11, 14, 18 days under different temperature (15, 20 and 25 °C) and photoperiod (00L, 06L, 12L, 18L) conditions. Pretreatments SG 2-45-0 and SNV. Wavelength 1150 to 1850nm.

Regression variable	Sample	n	LV	RMSEC	R^2C	RMSECV	R^2CV	RMSEP	R^2pr
Weight	**fresh-cut**	291	8	0.076	0.84	0.10	0.74	0.08	**0.78**
Weight	extract	288	9	0.08	0.81	0.11	0.70	0.10	0.65
Height	**fresh-cut**	291	9	1.63	0.84	1.84	0.79	2.01	**0.70**
Height	extract	279	9	2.05	0.78	2.88	0.56	2.19	0.64
L*	**fresh-cut**	294	10	5.26	0.81	7.13	0.64	6.48	**0.73**
L*	extract	282	8	5.22	0.83	5.75	0.79	5.99	0.71
a*	fresh-cut	294	1	2.30	0.13	2.35	0.091	3.01	0.02
a*	**extract**	288	7	2.02	0.47	2.43	0.23	2.44	**0.23**
b*	**fresh-cut**	285	10	4.91	0.80	6.11	0.69	6.89	**0.70**
b*	extract	279	7	5.72	0.77	6.60	0.70	6.69	0.65
Chlorophyll A	**fresh-cut**	291	8	18.53	0.76	21.36	0.69	20.77	**0.71**
Chlorophyll A	extract	288	8	17.63	0.78	21.00	0.69	21.52	0.68
Chlorophyll B	fresh-cut	291	8	7.55	0.76	8.56	0.69	9.66	0.62
Chlorophyll B	**extract**	288	8	7.75	0.74	9.36	0.63	9.25	**0.65**
Total Carotene	**fresh-cut**	294	8	4.62	0.76	5.65	0.64	4.83	**0.73**
Total Carotene	extract	288	8	4.21	0.80	5.61	0.65	5.12	0.69
Brix	**fresh-cut**	294	10	0.13	0.78	0.17	0.63	0.15	**0.70**
Brix	extract	288	4	0.15	0.72	0.17	0.63	0.17	0.68
pH	fresh-cut	294	2	0.49	0.12	0.51	0.03	0.55	−0.01
pH	**extract**	288	6	0.41	0.31	0.44	0.19	0.47	**0.19**
Conductivity	fresh-cut	294	2	0.45	0.29	0.48	0.19	0.53	−0.02
Conductivity	**extract**	282	5	0.34	0.58	0.38	0.48	0.40	**0.39**
TAC	fresh-cut	105	5	0.08	0.44	0.09	0.35	-	-
TAC	**extract**	99	10	0.04	0.85	0.05	**0.73**	-	-
TPC	fresh-cut	105	5	0.15	0.62	0.16	0.56	-	-
TPC	**extract**	108	10	0.10	0.82	0.13	**0.71**	-	-

*For all parameters was performed Three-fold cross-validation (by repeat), except for TAC (Total antioxidant capacity) and TPC (Total water-soluble phenolic compounds) by Leave-One-Out cross-validation.

Physical characteristics models corresponding to microgreens fresh-cut samples achieved a prediction coefficient of determination (R^2pr) of 0.78 and 0.70 for height and weight, respectively. In comparison, aqueous microgreens extracts samples prediction values were a bit lower with (R^2pr) of 0.64 and 0.65 for height and weight, respectively.

Regarding color components, L* and b* models have higher prediction compared to a* which shows poor performance in both microgreens fresh-cut samples and aqueous microgreens extracts samples. Fresh-cut samples showing a R^2pr of 0.73 for L* and 0.70 for b* had a little better performance compared to aqueous microgreens extracts samples with 0.71 and 0.65, respectively. Proportional findings have been reported, where optical properties like L* and b* tend to be more predictable due to their stronger association with chlorophyll and carotenoid levels (Li *et al.*, 2017, 2019).

Pigments models were consistent with prediction values slightly higher for chlorophyl A and total carotene, compared to chlorophyl B. The R^2pr values for chlorophyl A, B and total carotene were 0.71, 0.62, 0.73 for microgreens fresh-cut samples. Meanwhile, for aqueous microgreens extracts samples R^2pr values corresponded to 0.68, 0.65, and 0.69, respectively.

PLSR models for °Brix showed close predictive values for microgreens fresh-cut samples and aqueous microgreens extracts samples with R^2pr of 0.70 and 0.68, respectively. In the case of pH and conductivity, the models have poor performance for both fresh-cut and aqueous microgreens extracts samples.

For TAC and TPC, the models were much more accurate for aqueous microgreens extracts samples than microgreens fresh-cut samples. For aqueous microgreens extracts samples, the R^2CV for TAC was 0.73 and for TPC was 0.71, conversely, for microgreens fresh-cut samples it was 0.35 and 0.56 for TAC and TPC, respectively.

García-García et al. (2022) predicted different parameters in pea pods using NIRS reflectance (400 to 2500 nm) achieving coefficients of determination between 0.50 to 0.88, specifically reporting R^2CV for °Brix (0.68), TPC (0.86), and color parameters (chroma = 0.81 and hue angle=0.71), more over pH having the lowest prediction capacity compared with other parameters, these tendencies where also found in this study.

The poor predictive performance for pH and conductivity may be explained by the absence of clear or consistent trends in these variables across the different light and temperature treatments. Unlike other parameters such as pigments or bioactive compounds, which exhibited structured variations in response to the experimental conditions and were more effectively captured by NIRS, pH and conductivity showed erratic or minimal variation. This limitation may also be due to the narrow range or lack of structured variation in pH and conductivity values. When the target variable does not exhibit sufficient variability or a defined trend, the PLSR model lacks the

necessary information to establish meaningful correlations with the spectral data, resulting in low predictive performance (Wold, Sjöström and Eriksson, 2001; Shi *et al.*, 2008; de Araújo Gomes *et al.*, 2023).

Techniques like VIS-NIR reflectance spectroscopy, paired with chemometric analysis, are frequently employed for assessing the chemical composition of plant leaves (Li *et al.*, 2017; Prananto, Minasny and Weaver, 2020; Zahir *et al.*, 2022). However, there has been less research on utilizing NIR spectroscopy only. Moreover, information on the use of NIRS in microgreens is limited, partly because their research is more recent compared to other traditional crops. Most studies focus on mature plant leaves, leaving a gap in research on microgreens, which include both leaves and stems. This diversity in composition and size can complicate analyses. As microgreens gain popularity, it is likely that more research will emerge in the future.

In addition to Table 15, Figure 33 shows some representative regressions where certain trends are noticeable. The figure displays the plots belonging to aqueous microgreens extracts samples: weight, L* color component and total carotene. However, the tendency is relatable with microgreens fresh-cut samples as well (not shown). The graphs on the left display calibration and cross-validation, while the graphs on the right show independent prediction.
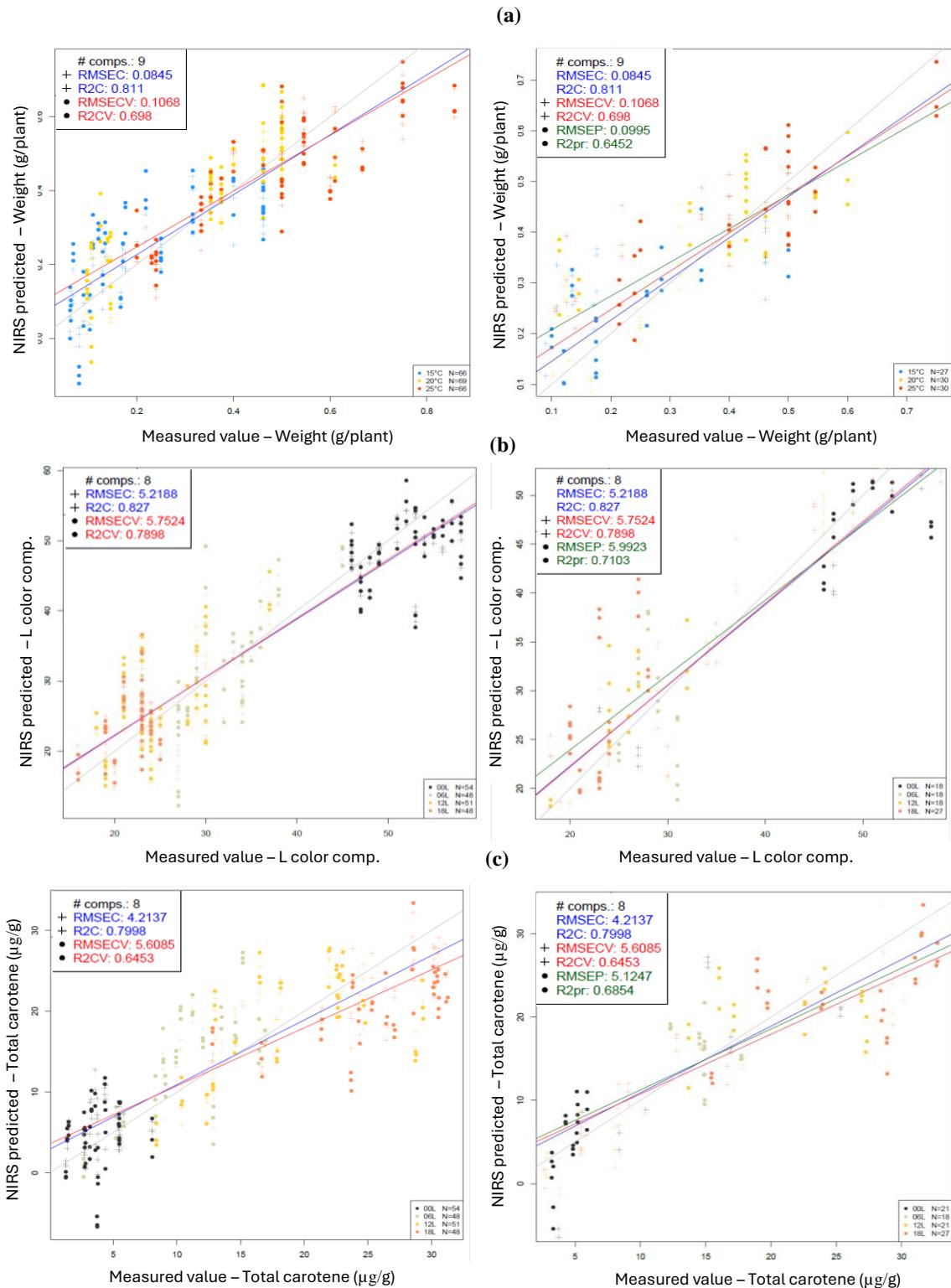
Figure 33. PLSR for (a) weight, (b) L* color component, and (c) total carotene content of NIRS pea spectra (aqueous microgreens extracts samples) harvested after 7, 11, 14, 18 days under different temperature (15, 20 and 25 °C) and photoperiod (00L, 06L, 12L, 18L) conditions. Pretreatments SG 2-45-0 and SNV. Wavelength 1150 to 1850nm. (left) Calibration and cross-validation. (right) Independent prediction

For weight, the trends are more clearly visualized when color-coded by temperature level (Figure 33a). It can be observed that at lower temperatures, the samples are distributed closer to

the axis (with values near zero), whereas at higher temperatures, they are farther from the axis, with values reaching around 0.8 g/plant. Similar trends were found for height and pH.

For the L* color component, trends are better visualized when color-coded by photoperiod level (Figure 33b). At higher photoperiods, the samples are distributed closer to the axis (with values near 20), while at lower photoperiods, they are farther from the axis, with values around 60. Similar trends in distribution by photoperiod were found for a* and b* components.

For variables such as chlorophyll A, chlorophyll B, °Brix, conductivity, TAC, and TPC, the trend visualized in Figure 33c is opposite than it was for color components (Figure 33b). At lower photoperiods, the samples are closer to the axis, whereas at higher photoperiods, they are farther from the axis.

5.3.5.   Most important wavelengths for PLSR

The analyses of the height of pea plants for the microgreens fresh-cut samples revealed important wavelengths around 1196, 1286, 1392, 1417, 1446, 1480, 1508, 1543, 1600, 1704, 1838 nm (Figure 34a1). For aqueous microgreens extracts samples, the most prominent wavelengths are 1337, 1368, 1396, 1409, 1433, 1460, 1484, 1530, 1590, 1640, 1685, 1706, 1746, 1793 nm (Figure 34a2). Some relevant wavelengths have been previously reported in foliar analysis (Appendix-A2_Table 13). The peaks found are associated with O-H, C-H and N-H bounds which are present in common organic compounds like carbohydrates, lipids proteins, commonly found in plant tissues (Curran, 1989; Slavchev *et al.*, 2015).
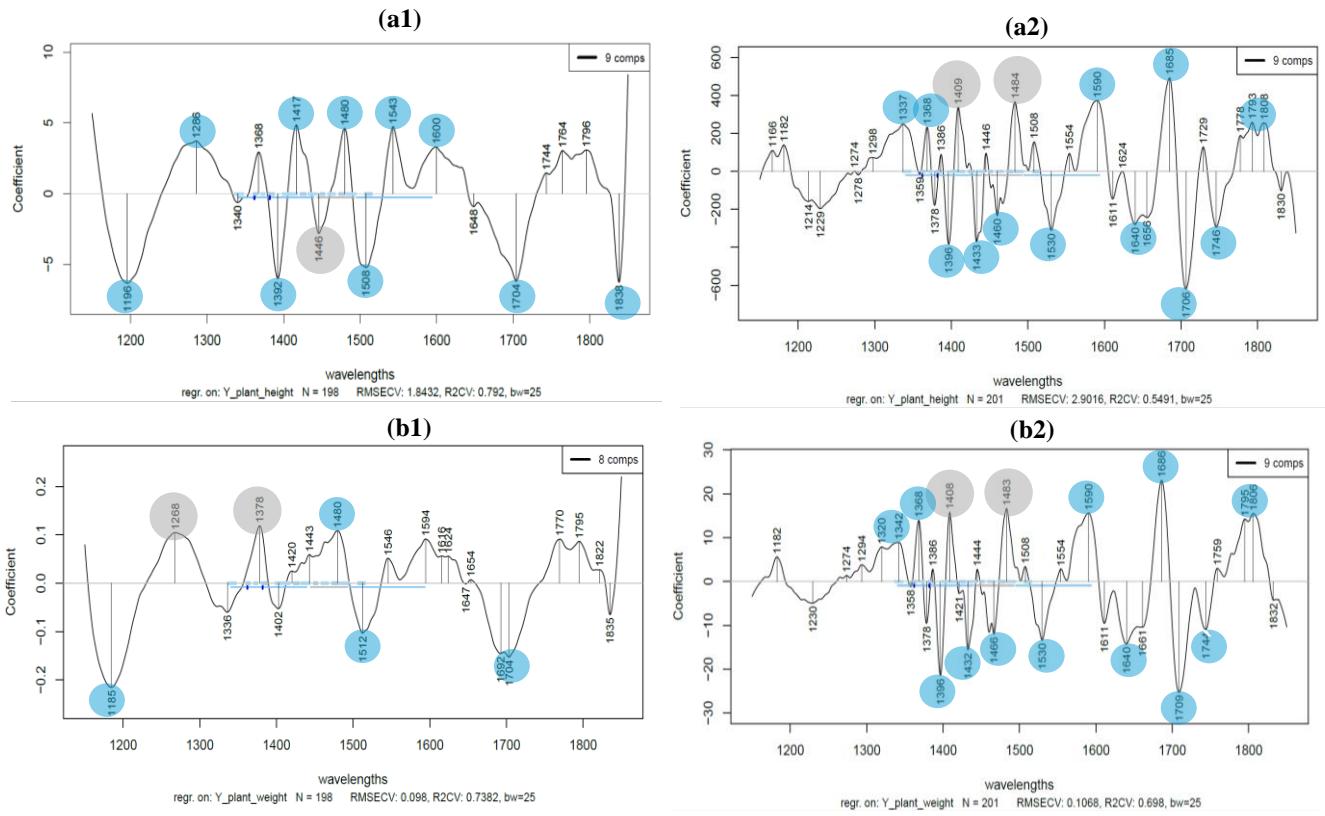
Figure 34. PLSR calibration coefficients highlighting the most important wavelengths for predicting physical parameters. Microgreens fresh-cut samples: (a1) height (b1) weight. Aqueous microgreens extracts samples: (a2) height (b2) weight. Pretreatments SG 2-45-0 and SNV. Wavelength 1150 to 1850nm.

The most prominent wavelengths for weight of the microgreens fresh-cut samples are found around 1185, 1268, 1378, 1480, 1512, 1704 nm (Figure 34b1). For aqueous microgreens extracts samples, the most prominent wavelengths are 1342, 1368, 1396, 1408, 1432, 1466, 1484, 1530, 1590, 1640, 1686, 1709, 1746, 1795 nm (Figure 34b2). The similar wavelength profile between height and weight of pea microgreens can be explained by the fact that both height and weight are closely related to the same physiological and biochemical characteristics of the plants. These characteristics, such as water content, carbohydrate composition, and protein levels, contribute to the growth and biomass accumulation of microgreens (Curran, 1989; Slavchev *et al.*, 2015; Liu *et al.*, 2022).

Important wavelengths related to pigments: chlorophyll A, B and total carotene are shown in Figure 35, where major similarities in their profile are found between the three pigments. For simplification, only the peaks related to chlorophyll A are mentioned (Figure 35a). However, they are easily reflected in chlorophyll B (Figure 35b) and total carotene (Figure 35c), although small variations may be found.
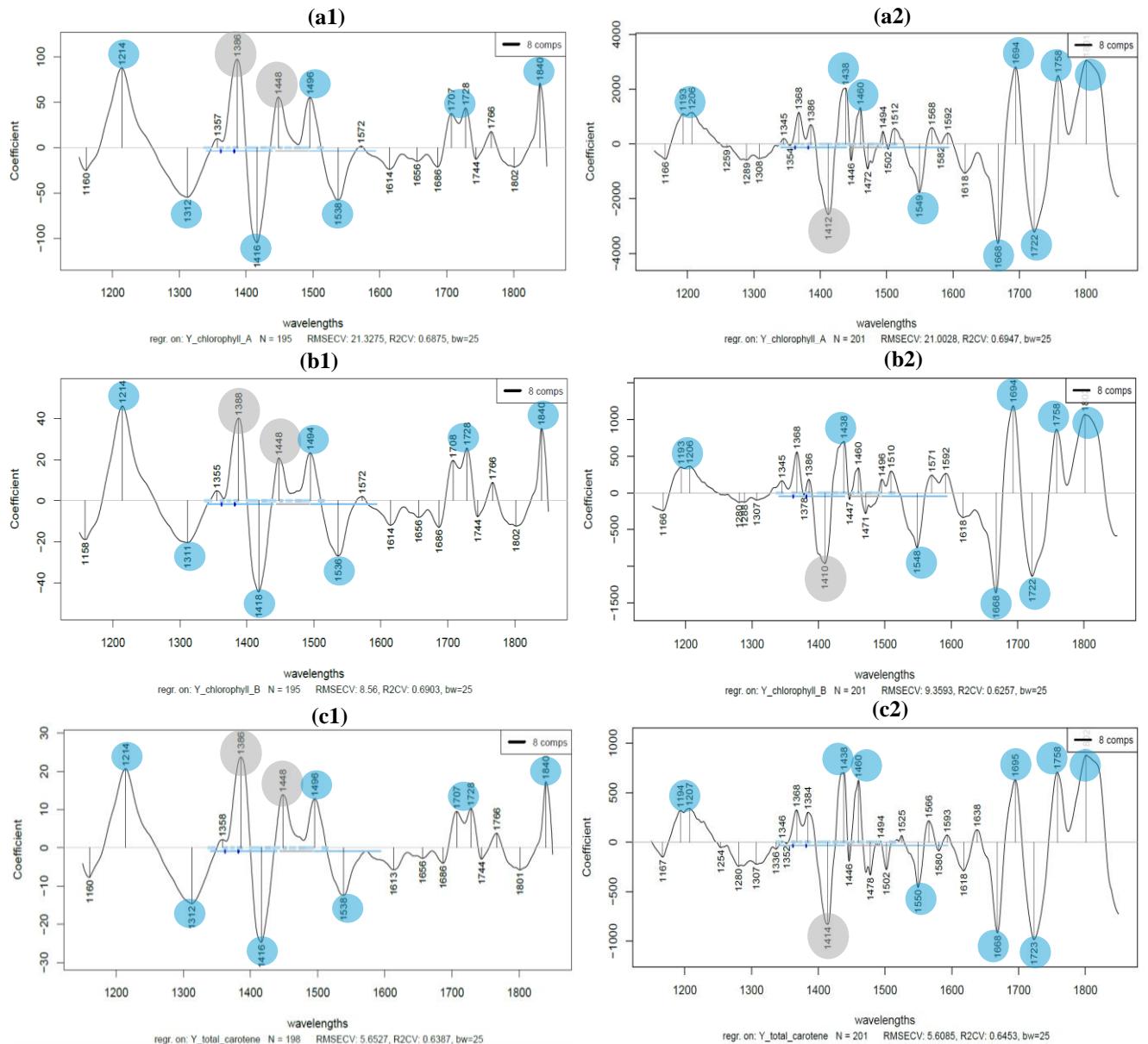
Figure 35. PLSR calibration coefficients highlighting the most important wavelengths for predicting pigments. Microgreens fresh-cut samples(a1) chlorophyll A, (b1) chlorophyll B, (c1) total carotene. Aqueous microgreens extracts samples: (a2) chlorophyll A, (b2) chlorophyll B, (c2) total carotene. Pretreatments SG 2-45-0 and SNV. Wavelength 1150 to 1850nm

For microgreens fresh-cut samples (Figure 35a1), the most prominent wavelengths were 1214, 1312, 1366, 1416, 1448, 1496, 1538, 1728, 1840 nm. Regarding aqueous microgreens extracts samples (Figure 35a2), the most important wavelengths for pigments were around 1206, 1412, 1438, 1460, 1549, 1668, 1694, 1722, 1758, 1801 nm. Some relevant wavelengths have been previously reported in foliar analysis (Appendix-A2_Table 14) The prominent wavelengths associated with chlorophyll A, B, and total carotene show a similar spectral profile due to the shared molecular features of these pigments. C-H and O-H bonds play a significant role in their absorption patterns, as these bonds are integral to the pigments' hydrocarbon chains and hydroxyl groups (Curran, 1989; Slavchev *et al.*, 2015). Interestingly, some wavelengths were also shared

93

between these pigments and the parameters of height and weight, though in fewer instances. This overlap could be attributed to the fact that pigments, like chlorophyll and carotene, are closely linked to plant growth and biomass accumulation. As these compounds are involved in photosynthesis and overall plant health, their molecular bonds may influence both the pigmentation and growth-related traits of microgreens.

Important wavelengths related to color components are shown in Figure 36, where major similitudes in their profile are found between L* and b*. However, major difference is attributed to the a* component which showed a very low prediction capacity. For simplification, only the peaks related to L* are mentioned (Figure 36a). However, they are easily exhibited in b* as well (Figure 36c), although minor differences may be found.
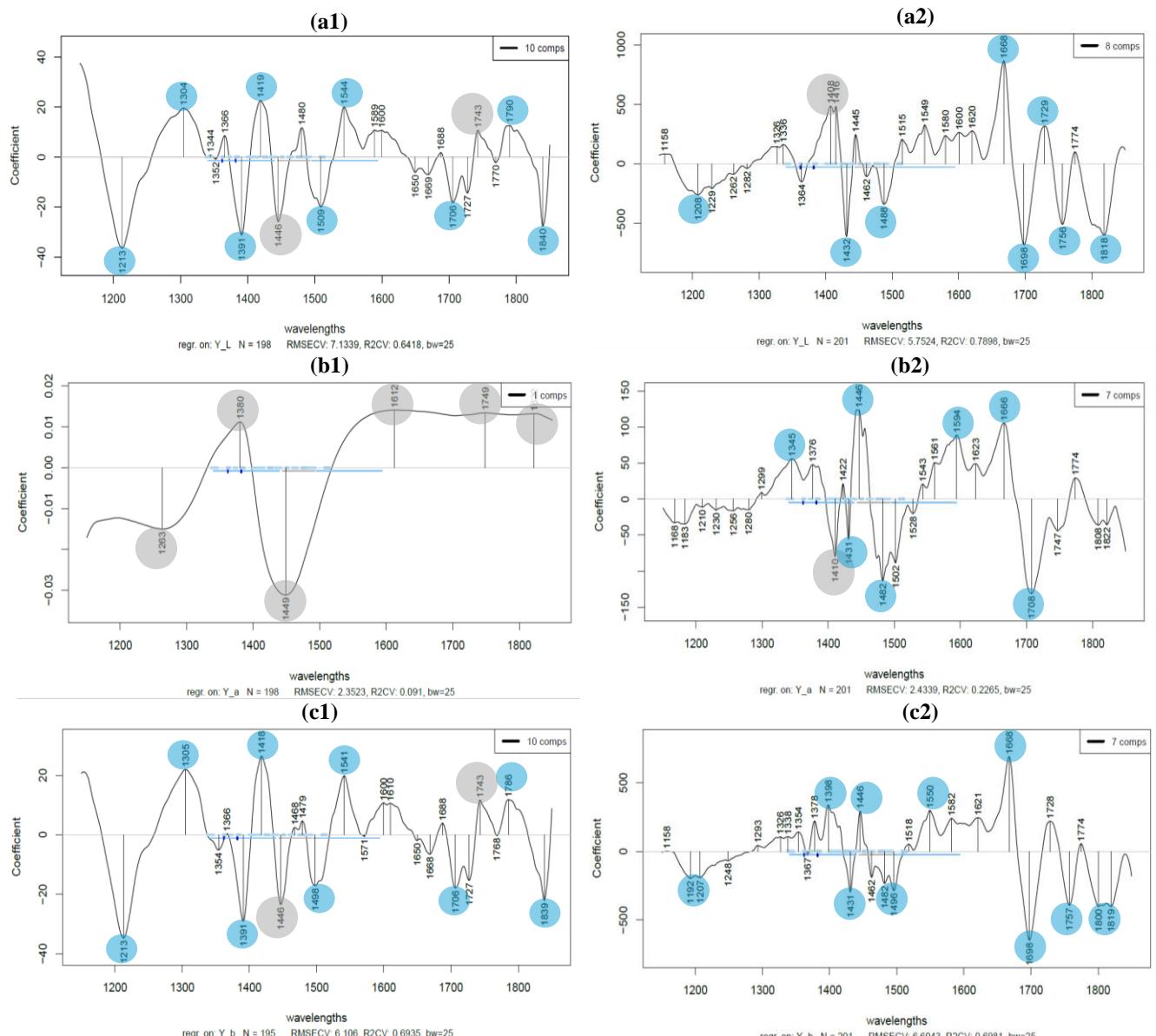

Figure 36. PLSR calibration coefficients highlighting the most important wavelengths for predicting color components. Microgreens fresh-cut samples: (a1) L*, (b1) a*, (c1) b*. Aqueous

microgreens extracts samples: (a2) L*, (b2) a*, (c2) b*. Pretreatments SG 2-45-0 and SNV. Wavelength 1150 to 1850nm

For microgreens fresh-cut samples (Figure 36a1), the most prominent wavelengths related to L* color component were 1213, 1304, 1391, 1419, 1509, 1544, 1706, 1743, 1790, 1840 nm. For aqueous microgreens extracts samples (Figure 36a2), the most prominent wavelengths are 1208, 1410, 1432, 1488, 1668, 1698, 1729, 1756, 1818 nm. Some relevant wavelengths have been previously reported in foliar analysis (Appendix-A2_Table 15)

The analyses of the PLSR most contributing wavelengths of chemical properties will be made by separate for each parameter since they have low similitudes between them, which can be seen in Figure 37.
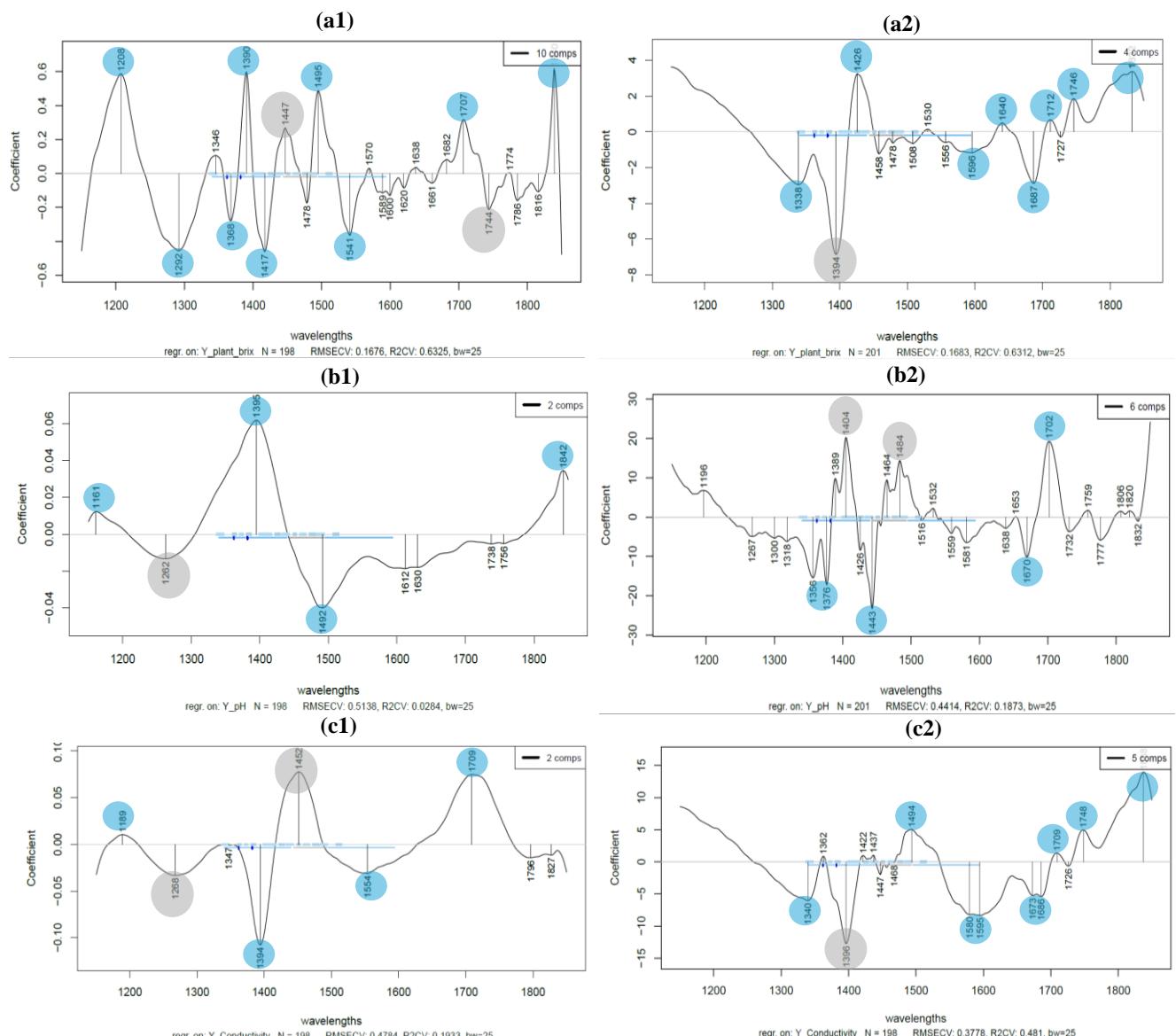

Figure 37. PLSR calibration coefficients highlighting the most important wavelengths for predicting chemical properties. Microgreens fresh-cut samples: (a1) °Brix, (b1) pH, (c1) Conductivity. Aqueous microgreens extracts samples: (a2) °Brix, (b2) pH, (c2) Conductivity. Pretreatments SG 2-45-0 and SNV. Wavelength 1150 to 1850nm.

°Brix of the microgreens fresh-cut samples revealed important wavelengths around 1208, 1292, 1368, 1390, 1417, 1447, 1495, 1541, 1707, 1744, 1840 nm (Figure 37a1). For aqueous microgreens extracts samples, the most prominent wavelengths are 1338, 1394, 1426, 1596, 1640, 1687, 1712, 1746, 1832 nm (Figure 37b1). Some relevant wavelengths have been previously reported in foliar analysis (Appendix-A2_Table 16). The results of the °Brix analysis for microgreens show a notable similarity with the models for height, weight, and chlorophyll. The wavelengths associated with the vibrations of O-H, C-H, and N-H bonds, present in all the models, suggest that the compounds involved in sugar content (°Brix), such as carbohydrates and water, also influence plant growth and photosynthesis (Curran, 1989; Liu *et al.*, 2022). This may explain the shared spectral profile between °Brix, height, weight, and chlorophyll, as these factors are interrelated in the development and metabolism of the plants.

pH and conductivity which showed low prediction capacity present very different wavelength profile (Figure 37b Figure 37c). This suggests that the models do not effectively capture the variance in pH and conductivity, potentially due to insufficient data correlation.

The analyses of TPC of the microgreens fresh-cut samples revealed important wavelengths around 1176, 1284, 1428, 1504, 1555, 1651, 1713 nm (Figure 38a1). For aqueous microgreens extracts samples, the most prominent wavelengths are 1328, 1406, 1418, 1436, 1451, 1510, 1528, 1640, 1685, 1709, 1754, 1778, 1824 nm (Figure 38a2). Some relevant wavelengths have been previously reported in foliar analysis (Appendix-A2_Table 17)
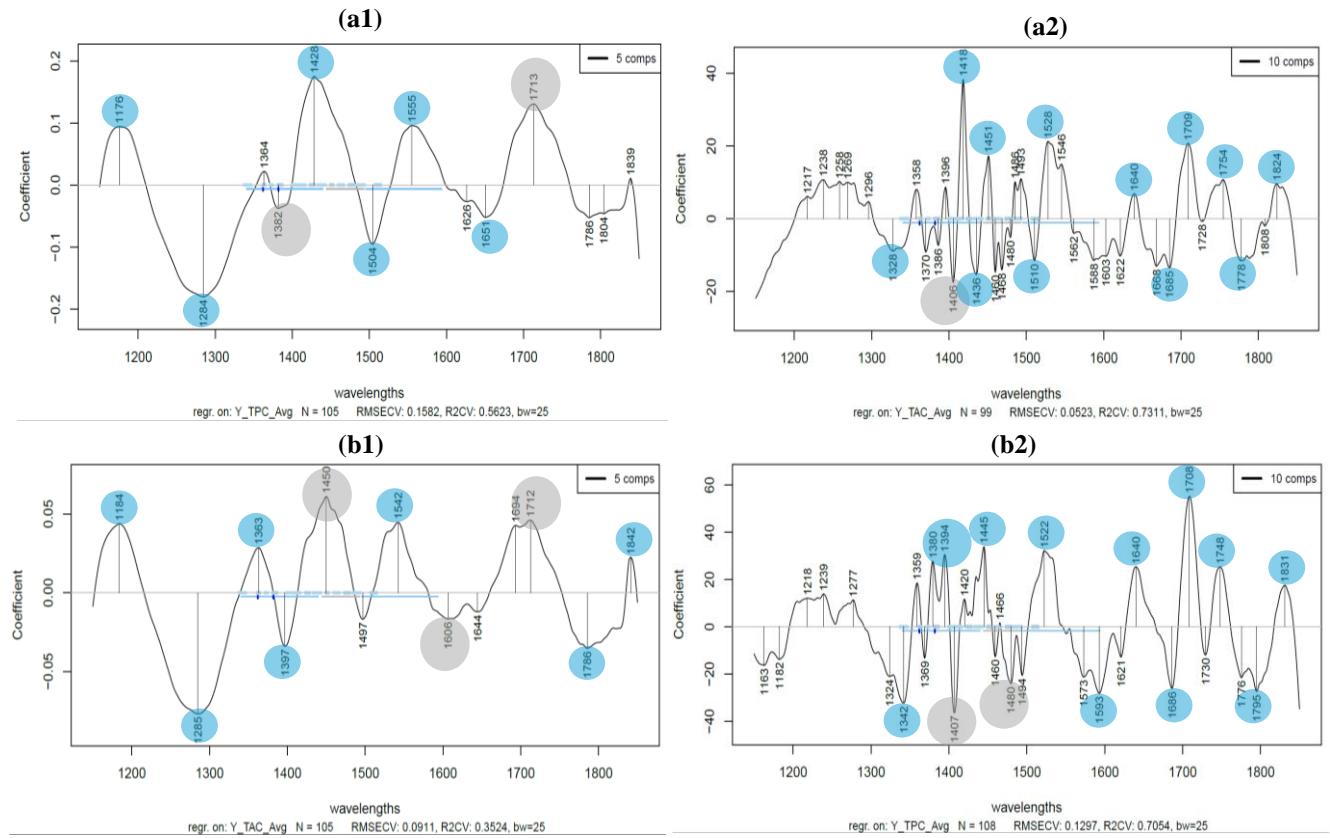
Figure 38. PLSR calibration coefficients highlighting the most important wavelengths for predicting bioactive compounds. Microgreens fresh-cut samples: (a1) TPC, (b1) TAC. Aqueous microgreens extracts samples: (a2) TPC, (b2) TAC. Pretreatments SG 2-45-0 and SNV. Wavelength 1150 to 1850nm

The most contributing wavelengths PLSR plot for TAC, although visually has certain similitude with TPC, however, it has a different wavelengths profile in some extent. The microgreens fresh-cut samples revealed important wavelengths around 1184, 1285, 1363, 1397, 1450, 1542, 1712, 1786, 1842 nm (Figure 38b1). For aqueous microgreens extracts samples, the most prominent wavelengths are 1328, 1342, 1394, 1407, 1445, 1480, 1593, 1640, 1686, 1708, 1748, 1795, 1831 nm (Figure 38b2). For TAC, some relevant wavelengths have been previously reported in foliar analysis (Appendix-A2_Table 18).

As can be seen in Table 16, for microgreens fresh-cut samples, some wavelengths were found in common between parameters, meanwhile others were specific. Height shared several wavelengths with weight including (1480, 1704 nm) °Brix (1417, 1446 nm), and TAC (1397), but differed due to its unique presence at 1286, 1508, and 1600 nm, not found in other parameters. Weight showed key bands at 1480 and 1704 which were also present in height, while 1378 and 1512 nm were more exclusive to weight, differentiating it from pigment or bioactive predictions. Pigments (chlorophyll A, B and total carotene) showed specific wavelengths like 1496, 1538, and 1728 nm, especially distinct from height or weight. L* and b* color components shared prominent bands (1840 nm) with pigments, but differed through 1391, 1509, 1544 and 1743 nm, not present in other

parameters, making it spectrally distinguishable. °Brix featured showed similar wavelengths with pigments (1447 ~1448 nm, 1495 ~1496 nm), and L* and b* (1840 nm), but stood out with 1292 and 1541 nm, which were not shared with others. TPC showed the least overlap with others; 1428, 1504, and especially 1555 and 1651 nm were unique, setting it apart. TAC showed unique wavelengths at 1842, 1450 and 1786, which could highlight TAC specific features.

Table 16. Spectral relationships among microgreens fresh-cut samples parameters

Parameter	Key Wavelengths (nm)	Notable Shared / Unique Features - Wavelengths (nm)
Height	1196, 1286, 1392, 1417, 1446, 1480, 1508, 1543, 1600, 1704, 1838	Shared: Weight (1480, 1704), Brix (1417, 1446), TAC (1397); Unique: 1286, 1508, 1600
Weight	1185, 1268, 1378, 1480, 1512, 1704	Shared: Height (1480, 1704); Unique: 1378, 1512
Chlorophyll A, Chlorophyll B, Total Carotene	1214, 1312, 1366, 1416, 1448, 1496, 1538, 1728, 1840	Shared: L* (1840); Unique: 1496, 1538, 1728
L*, b*	1213, 1304, 1391, 1419, 1509, 1544, 1706, 1743, 1790, 1840	Shared: Chlorophyll A (1840); Unique: 1391, 1509, 1544, 1743
Brix	1208, 1292, 1368, 1390, 1417, 1447, 1495, 1541, 1707, 1744, 1840	Shared: Chlorophyll A (~1447), L* (1840); Unique: 1292, 1541
TPC	1176, 1284, 1428, 1504, 1555, 1651, 1713	Minimal spectral overlap with other variables; Unique: 1428, 1504, 1555, 1651
TAC	1184, 1285, 1363, 1397, 1450, 1542, 1712, 1786, 1842	Shared: Height (1397); Unique: 1450, 1786, 1842

Table 17, present common and specific peaks (wavelengths) between parameters in aqueous microgreens extracts samples. Height had several peaks in common with weight, including 1368, 1396, 1484, 1530, and 1746 nm. Unique wavelengths include 1337 and 1433 nm. Weight included exclusive peaks at 1342, 1466, and 1709 nm. Chlorophyll A, B and total carotene presented common wavelengths with height and weight, at 1460 and 1706–1709 nm. The presence of 1549, 1694, and 1758 were unique to pigment analysis. In the case of L* and b* color components peaks in common were found at 1432 nm (for weight), and 1668 nm (for pigments), meanwhile wavelengths like 1488, 1729, and 1818 nm were more specific to color than agronomic traits. °Brix shared common wavelengths at 1640 and 1746 nm with height and weight, but featured unique wavelengths like 1596 and 1832, absent in other traits. TPC and °Brix presented common wavelength at 1640 nm, but unique phenolic-sensitive bands (for TPC) were found at 436, 1528, 1754, 1778, and 1824 nm. TAC shared peaks in common, at 1328 nm with TPC, 1342 and 1748 nm with weight, but presented unique peaks at 1445, 1593, and 1831 nm.

Table 17. Spectral relationships among aqueous microgreens extracts samples parameters

Parameter	Key Wavelengths (nm)	Notable Shared / Unique Features
Height	1337, 1368, 1396, 1409, 1433, 1460, 1484, 1530, 1590, 1640, 1685, 1706, 1746, 1793	Shared: Weight (1368, 1396, 1484, 1530, 1746); Unique: 1337, 1433
Weight	1342, 1368, 1396, 1408, 1432, 1466, 1484, 1530, 1590, 1640, 1686, 1709, 1746, 1795	Shared: Height; Unique: 1342, 1466, 1709
Chlorophyll A, Chlorophyll B, Total Carotene	1206, 1412, 1438, 1460, 1549, 1668, 1694, 1722, 1758, 1801	Shared: Height, Weight (1460, 1706–1709); Unique: 1549, 1694, 1758
L*, b*	1208, 1410, 1432, 1488, 1668, 1698, 1729, 1756, 1818	Shared: Weight (1432), Chlorophyll A (1668); Unique: 1488, 1729, 1818
Brix	1338, 1394, 1426, 1596, 1640, 1687, 1712, 1746, 1832	Shared: Height/Weight (1640, 1746); Unique: 1596, 1832
TPC	1328, 1406, 1418, 1436, 1451, 1510, 1528, 1640, 1685, 1709, 1754, 1778, 1824	Shared: Brix (1640); Unique: 1436, 1528, 1754, 1778, 1824
TAC	1328, 1342, 1394, 1407, 1445, 1480, 1593, 1640, 1686, 1708, 1748, 1795, 1831	Shared: TPC (1328), Weight (1342, 1748); Unique: 1445, 1593, 1831

1.5.6. Wavelength selection for number of latent variables reduction in PLSR

Although some PLSR models exhibited some predictive capacity, as evidenced by R^2 values above 0.6 in certain cases, a considerable number of latent variables (LVs) were required to achieve these results when the spectral range from 1150 to 1850 nm was used. This trend, described in the previous section, suggests a potential overfitting risk and reduced model interpretability due to high model complexity. Therefore, for model improvement and reduction of the number of LVs, a complementary analysis was conducted focusing on the variables with R^2 for prediction (R^2pr) greater than 0.6.

By selecting the most influential wavelengths based on the regression coefficients obtained from PLSR models of both liquid and solid samples, it was expected that the predictive ability would be maintained or even enhanced while reducing model complexity. However, this approach did not yield significant improvements in terms of increasing R^2pr or reducing the number of LVs in most cases. Nevertheless, when specific wavelength ranges were selected for the PLSR models built with microgreens fresh-cut samples, a noticeable reduction in the number of LVs was achieved for several variables, including weight, height, L*, b* (color components), chlorophyll A, chlorophyll B, total carotene, and Brix, without substantially compromising the predictive accuracy. The comparison between models using the full 1150-1850 nm range and those using

selected wavelength intervals is summarized in Table 18. Meanwhile, a more detailed performance overview, including RMSE and R² values for calibration, cross-validation, and prediction, is provided in Appendix A2_Table 19.

Table 18. Comparison of R^2pr after LVs number reduction in PLSR models of fresh-cut samples of pea microgreens

Regression variable	Sample	n	Wavelength :1150-1850 nm			Selected wavelengths for LV reduction			
			LV	RMSEP	R^2pr	Wavelengths (nm)	LV	RMSEP	R^2pr
Weight	fresh-cut	291	8	0.08	0.78	1185-1770	4	0.1	0.74
Height	fresh-cut	291	9	2.01	0.7	1196-1508	5	1.93	0.72
L*	fresh-cut	294	10	6.48	0.73	1185-1665	6	7.22	0.62
b*	fresh-cut	285	10	6.89	0.7	1185-1665	6	7.16	0.62
Chlorophyll A	fresh-cut	291	8	20.77	0.71	1185-1572; 1695-1850	7	19.9	0.74
Chlorophyll B	fresh-cut	291	8	9.66	0.62	1185-1572; 1695-1850	7	8.67	0.7
Total Carotene	fresh-cut	294	8	4.83	0.73	1185-1572; 1695-1850	7	4.79	0.74
Brix	fresh-cut	294	10	0.15	0.7	1185-1570	6	0.16	0.68

6. CONCLUSIONS AND RECOMMENDATIONS

This research focused on the study of changes induced by stress factors in food materials using near infrared spectroscopy (NIRS) and other correlative techniques (e-senses). Throughout this work, three distinct approaches were explored to assess how various factors, such as the use of by-products in feed, environmental conditions, and the management of probiotics, influence the quality and characteristics of food. These approaches include evaluating the quality of enriched eggs through sensory analysis and electronic techniques; NIRS evaluation of probiotic supplements under different conditions; and assessing the applicability of NIRS in predicting agronomic and physicochemical properties in microgreens grown under varying photoperiods and temperatures.

6.1. Evaluation of enriched eggs by human sensory analysis, e-tongue and e-nose

In the sensory evaluation of enriched eggs by a human panel, using ANOVA and Tukey Test, compared Control, ZP 2.5%, and ZP 5.0% feeding groups across two batches and three egg presentations (raw, boiled, and fried), most sensory attributes showed no significant differences, and the panel generally characterized the eggs as fresh. The sensory evaluation of eggs using an electronic tongue revealed distinct differences between the feeding regimes. Euclidean distance analysis showed the greatest disparity between the Control and ZP 5.0% groups for both experimental batches indicating significant differences in organoleptic characteristics. Principal component analysis demonstrated minimal separation between the three egg groups, though some differentiation between the Control and ZP groups was observed, especially in PC1. The discriminant analysis for separation of treatment groups had calibration accuracy of 95.92% for batch 1 and 100% for batch 2. Cross-validation accuracy was 64.81% for batch 1 and 56% for batch 2, indicating that while classification was imperfect, differentiation between the Control and ZP 5.0% groups was more effective. In the e-nose sensory evaluation for eggs stored for 0, 30, and 60 days, the models corresponding to fresh eggs (0 days of storage) showed slightly greater ability to discriminate between treatment groups compared to models for longer storage times. Upon preheating the samples to 50 °C and 80 °C, there is clear differentiation between batches 1 and 2. At 50 °C, accuracy in calibration of 98.00% and cross-validation of 68.49%. At 80 °C, the accuracy in calibration is 82.65%, and cross-validation 62.22%, with cross-validation results indicating a tendency towards some separation between feeding groups. The use of the electronic nose successfully identified key volatile compounds associated with both egg storage and different feeding treatments. However, the differentiation between feeding groups was less precise compared to the separation between storage days, which reached complete discrimination between fresh eggs, 30 days and 60 days storage eggs.

6.2. Evaluation of probiotic drinks by NIRS

In the evaluation of probiotic supplements under different conditions, the microbiological analysis of probiotic supplements revealed that the viability of microorganisms is significantly affected by temperature which highlights the importance of controlling the temperature of water to which probiotics are exposed to ensure their effectiveness in probiotic drinks. The PCA-LDA analysis performed on the three probiotics (N, A, and P) at 25°C successfully differentiated the groups, with a 100% correct classification for calibration and 99.18% cross-validation accuracy. The optimal pretreatment was SG 2-17-0. Probiotics A and P were more closely related, while probiotic N showed distinct separation. Discrimination based on concentration showed a clear separation between concentration levels at 90°C, with slight misclassification between consecutive concentrations. The models achieved 100% calibration accuracy and over 90% cross-validation accuracy, with probiotic A (95.06%) having the highest cross-validation accuracy, followed by probiotic P (93.52%) and probiotic N (90.12%). The optimal pretreatments were DeTr + MSC (for probiotic N), SG 2-21-0 + DeTr (for probiotic A), and SG 2-17-0 + SG 2-17-2 (for probiotic P). At lower temperatures, discrimination is more probiotic dependent. NIR spectroscopy combined with PCA-LDA seems promising for classification of probiotic concentration in solutions. Temperature-based discrimination of probiotic samples also provided high classification accuracy. Probiotic A showed the most robust performance, achieving 100% classification and cross-validation accuracy. Similarly, probiotics P and N demonstrated high classification over 90%, with slight misclassifications between consecutive temperatures. The optimal pretreatments were de 2-13-0 + SG 2-21-1 (for probiotic N), SG 2-17-0 + MSC (for probiotic A), and de Tr (for probiotic P). NIR spectroscopy shows effective for temperature-based differentiation of probiotic solutions. The best predictive model for CFU counts was achieved using SG 2-21-0 and SG 2-13-2 pretreatments, with a R^2Pr of 0.82 and RMSEP of 0.64 Log CFU/g.

6.3. Evaluation of pea microgreens by NIRS

Pea microgreens were grown under specific conditions of temperature (15, 20 and 25 °C) and photoperiod (0, 6, 12, 18 hours). Microgreens at 15 °C were grown for 18 days, meanwhile, at 20 and 25 °C were cultivated for 14 days, establishing the time for harvesting at 7, 11, 14, and 18 days. An agronomic overview of the relationship between plant height and weight in pea microgreens growth shows that in general when the microgreens increase their height also the weight increases, due to greater biomass accumulation from enhanced photosynthesis and cellular growth. Higher temperatures promote faster growth and weight gain, this is related to the fact that under these conditions, biochemical processes like photosynthesis and respiration are accelerated. Optimal temperature conditions (25 °C, 20 °C, 15 °C) result in significant growth, with the tallest

and heaviest plants observed at 25 °C. Photoperiod also affects growth, were plants in complete darkness exhibit etiolation, and directing to exaggerated height. In some cases, extended light photoperiods at lower temperatures enhance growth; however, at 25 °C, shorter photoperiods may reduce thermal stress, which as consequence can improve growth efficiency.

The °Brix analysis revealed that at lower temperature (15 °C), sugar content, in specific sucrose, increased between days 11 and 14 but decreased by day 18, probably due to sucrose utilization for structural growth. At 20 °C and 25 °C, °Brix values generally declined over the cultivation period, which can be attributed to faster sucrose consumption due to higher metabolic demands at elevated temperatures. Microgreens exposed to 18 hours of light consistently had higher °Brix values, which reflects its importance for photosynthetic activity and sucrose production, while microgreens grown in darkness exhibited lower values. Temperature and light duration are important factors that determine sucrose levels in plants. Increased photoperiod and optimal temperature promote higher sucrose accumulation and microgreens growth.

pH exhibited a more stable behavior, especially on days 11 and 14. The differences for most of treatments are minimal, with consistent values between 5 and 6. This stability may be attributed to the plant's homeostatic mechanisms, which tightly regulate internal pH to maintain the proper functioning of vital metabolic processes. Although there is some variation in the case of some specific conditions, there is no clear pattern with regard to influence of photoperiod and temperature.

Electrical conductivity exhibited significant variability among treatments, that ranged between 1.5 and 2.75 mS/cm. The data in general does not reveal a consistent pattern that can be directly attributed to harvest day, light exposure, or temperature. The results display considerable variability, making it difficult to determine whether any of these factors are significantly affecting conductivity changes. However, at temperatures of 20 °C and 25 °C, the treatments demonstrated certain similar behavior in some cases, with conductivity increasing between days 7 and 11 and then decreasing on day 14. Conversely, the treatments at 15 °C were the most variable, which may be attributed to delayed emergency and growth. In the case of pH and electrical conductivity, the potential trends associated with photoperiod and temperature were less evident compared to other analyzed variables.

The study of pigments in pea microgreens demonstrates the significant influence of photoperiod and temperature on the production of chlorophyll A, B, and total carotene. Treatments with longer photoperiods, such as 18L, favor chlorophyll synthesis, resulting in a vibrant green color characteristic of healthy plants that maximize their photosynthetic capacity. Furthermore, increased temperatures within an optimal range stimulate pigment production, contributing to

greater photosynthetic efficiency. Moreover, the concentration of pigments increases during the growth phase. However, it is crucial to consider that extreme temperatures and photoperiods can adversely affect this production, highlighting the need for a balance in cultivation conditions.

Microgreens respond notably to photoperiod in terms of color and development. Treatments with longer photoperiods, such as 20C_18L and 25C_18L, favor a greater accumulation of chlorophyll, resulting in darker green plants, indicators of better plant health. These microgreens absorb blue and red light more effectively and predominantly reflect green, leading to lower values in the color components L* (luminosity) and b* (blue-yellow). In contrast, treatments without light, such as 15C_00L and 25C_00L, exhibit lighter and yellower colors due to reduced photosynthetic activity. The lack of light limits chlorophyll production, allowing other pigments, such as carotene (yellow) and anthocyanins (red), to dominate the color profile, increasing the a* (green-red) values. In summary, microgreens exposed to more hours of light enhance their photosynthetic capacity and reduce the presence of reddish and yellow tones, reinforcing their green and healthy appearance.

The analysis of bioactive compounds in pea microgreens reveals that both photoperiod and temperature significantly influence the accumulation of total water-soluble phenolic compounds (TPC) and total antioxidant capacity (TAC), with the effect of temperature being more pronounced. Lower temperatures, such as 15 °C, favor the accumulation of these compounds through stress-activated defense mechanisms. Additionally, treatments with longer photoperiods stimulate the production of phenolic compounds and increased antioxidant capacity, reflecting an adaptive response to light and oxidative stress. The treatment 15C_18L stands out among the others, especially on day 14, reaching 2.23 mg GAE/g for total water-soluble phenolic compounds and 5.73 µmol TE/g for antioxidant capacity. Moreover, there is a complex relationship between plant growth and the synthesis of these compounds, where environmental conditions impact the balance between the production and degradation of phenolics throughout the development stages.

As can be noted, the analysis of microgreens' growth is dynamic and multifactorial, with marked effects arising from the interaction of temperature, photoperiod, and growth stage. Finding a balance between these factors is crucial to produce microgreens that meet production standards and quality requirements for consumers. This balance is essential not only for maximizing yield but also for ensuring that microgreens provide the desired nutritional and sensory qualities.

The spectral analysis of pea microgreens was conducted using fresh-cut samples in reflectance mode and aqueous microgreens extracts samples in transmittance mode, covering growth periods of 7, 11, 14, and 18 days. The analysis utilized SG 2-45-0 pretreatment and SNV in the wavelength

range of 1150 to 1850 nm. A prominent feature in both types of samples was the first overtone of water, peaking around 1450 nm, which is critical in biological systems.

PCA analysis revealed a certain tendency for differentiation between groups according to harvesting days, temperature and photoperiod. It was more evident according to photoperiod, although major overlapping existed.

In general, PCA-DA classification models belonging to aqueous microgreens extracts samples showed better performance than from microgreens fresh-cut samples.

In the classification by harvesting days, the PCA-LDA models for each individual treatment (consisting of a specific temperature-photoperiod, in total 12 models for microgreens fresh-cut samples and 12 models for aqueous microgreens extracts samples) revealed that aqueous microgreens extracts samples achieved higher accuracy, with cross-validation percentages between 66.67% and 100%, while microgreens fresh-cut samples ranged from 55.56% to 100%. More explicitly, aqueous microgreens extracts samples classification models outperformed microgreens fresh-cut samples in nearly all treatments, reporting CV between 81.45% to 100% for treatments from 15 ºC and 25 ºC, meanwhile for 20 ºC, it was between 66.67% and 82.26%.

In the classification of microgreens on a specific day according to photoperiod-temperature treatment, microgreens fresh-cut samples showed CV classification accuracies between 48.39% and 59.72%, while aqueous microgreens extracts samples was between 56.47% to 87.72%. The classification according to temperature showed the higher accuracy at day 11 with CV of 81.79% and 85.58%, for microgreens fresh-cut samples and aqueous microgreens extracts samples respectively. Moreover, the best classification according to photoperiod was CV of 67.83% at day 14 for microgreens fresh-cut samples, and CV of 85.45% at day 7 for aqueous microgreens extracts samples.

In a global classification, comprising all pea microgreen samples, once again, models from aqueous microgreens extracts samples showed better performance compared to those from microgreens fresh-cut samples, showing CV classification for clustering according to harvesting day, treatment, temperature and photoperiod of 95.59, 68.34, 88.87 and 66.89%.

The PLSR results for microgreens fresh-cut samples and aqueous microgreens extracts samples include 13 analyzed variables related to physical characteristics, optical properties, pigments, chemical characteristics, and bioactive compounds.

Optical and pigment variables in microgreens fresh-cut samples showed slightly better results, followed by physical and bioactive characteristics, while pH and conductivity were the least precise. Moreover, microgreens fresh-cut samples performed slightly better in physical, optical, and pigment-related variables, while aqueous microgreens extracts samples had superior performance in TAC and TPC parameters.

Physical characteristics in microgreens fresh-cut samples had R²pr values of 0.78 for height and 0.70 for weight, while aqueous microgreens extracts samples showed 0.64 and 0.65, respectively.

Regarding color components, microgreens fresh-cut samples showed R²pr values of 0.73 for L* and 0.70 for b*, comparable to 0.71 and 0.65 in aqueous microgreens extracts samples.

Pigment models showed consistent values, with R²pr of 0.71, 0.62, and 0.73 for chlorophyll A, B, and carotene in microgreens fresh-cut samples, and 0.68, 0.65, and 0.69 in aqueous microgreens extracts samples.

°Brix had similar values in microgreens fresh-cut samples with R²pr of 0.70 and aqueous microgreens extracts samples R²pr of 0.68, but pH and conductivity showed low predictive values.

The models for TAC and TPC were more accurate in aqueous microgreens extracts samples, with R²pr values of 0.73 and 0.71, compared to microgreens fresh-cut samples which showed low predictive capacity.

Although PLSR models using the full spectral range (1150–1850 nm) showed acceptable predictive performance (R² > 0.6), they required in some cases many latent variables, which may cause risk of overfitting. Selecting significant wavelengths ranges reduced model complexity by decreasing the number of latent variables, especially for fresh-cut microgreens, without notably affecting predictive accuracy.

Several PLSR models-most important wavelengths presented similar profiles, especially observed between height, weight, pigments (chlorophyll A, B, and total carotene) and °Brix in pea microgreens. The close association can be derived by their close association with the same physiological and biochemical characteristics, such as water content, carbohydrates, and proteins. These factors contribute to plant growth and biomass accumulation, which are essential for both height and weight. Pigments like chlorophyll and carotene, involved in photosynthesis, share absorption patterns due to common C-H and O-H bonds. The overlap of wavelengths between pigments and growth parameters suggests that the same molecular bonds influencing pigmentation also affect growth. Additionally, the °Brix analysis showed similarities with height, weight, and chlorophyll models, as the shared vibrations of O-H, C-H, and N-H bonds indicate that sucrose content (°Brix), carbohydrates, and water are interconnected with plant growth and photosynthesis, leading to a unified spectral profile. Weight and height of pea microgreens which had the most compatible profile revealed important wavelengths around 1196, 1286, 1392, 1417, 1446, 1480, 1508, 1543, 1600, 1704, 1838 nm. Meanwhile, for aqueous microgreens extracts samples, the most prominent wavelengths were found at 1337, 1368, 1396, 1409, 1433, 1460, 1484, 1530, 1590, 1640, 1685, 1706, 1746, 1793 nm.

In this research, valuable results were found; however, some limitations were encountered. In some cases, there was a large gap between calibration and cross-validation accuracies during the classification of samples, which may indicate a risk of overfitting. Additionally, in the microgreens experiment, a high number of latent variables (LV) was observed in some cases. To determine whether, despite these limitations, the models had any classification capacity and were not merely the result of overfitting, additional models were performed using simulated data. These models performed poorly compared to those using real data, thus suggesting that the models based on real data contained important information for classification.

Similarly, some models from the PLSR analysis showed a high number of LV. In these cases, the number was reduced by selecting specific wavelength ranges, especially in the fresh-cut microgreens models, thereby reducing the LV without significantly affecting accuracy. Although different approaches were applied to find the best possible models for classification and prediction, several models presented modest results. Therefore, for future investigations, it would be interesting to consider the use of other chemometric approaches such as PLS-DA, ANN, k-NN, SVM, among others, which might be able to achieve higher classification and parameter prediction performance in eggs and pea microgreen samples.

Additionally, exploring the applicability of these correlative methods on a larger scale or refining the models with a larger number of samples would be valuable, considering that in this research the models were established by analyzing a limited number of samples. Moreover, it would be interesting to test these correlative techniques by including, in the case of the egg-related experiments, other types of microelements for egg enrichment that could affect their sensory characteristics; for probiotics-related experiments to evaluate how temperature and concentration conditioning factors can affect the viability of other probiotic strains besides LAB; and in the case of microgreens, by including other species or considering additional environmental stressing factors.

7. NEW SCIENTIFIC RESULTS

For the purpose of these new scientific findings, the term benchtop MetriNIR spectrophotometer refers to the MetriNIR (MetriNIR, Research Development and Service Co., Budapest, Hungary), whereas the term benchtop NIR XDS spectrophotometer refers to the NIR XDS spectrometer (Metrohm, Herisau, Switzerland), with two separate attachable modules: Rapid Solid Analyzer (RCA) and Rapid Liquid Analyzer (RLA). The term e-tongue refers to the Alpha Astree potentiometric electronic tongue (Alpha MOS, Toulouse, France) equipped with seven sensors specifically developed for food application (called by the manufacturer: BB, HA, ZZ, GA CA, JE, JB), an Ag/AgCl in 3M KCl reference electrode and a 16-position autosampler. E-nose refers to the Alpha MOS Heracles NEO electronic nose (e-nose), which functions as an ultrafast gas chromatograph analyzer featuring dual columns (MXT-5 and MXT-1701) and performs evaluation of odor intensity associated with volatile substances through the Kovats index.

❖ **New scientific findings focusing on eggs evaluation**

> **Sensory attributes of enriched eggs produced by hens fed with feed with added brewer's yeast and wet yeast biomass enriched with organic zinc, polyphenols, and vitamins (ZP) at concentrations of ZP 0% (Control), ZP 2.5%, and ZP 5.0% as feeding regimes were analyzed. Batch 1 and batch 2 correspond to the eggs collected for evaluation on day 30 and day 60 of the experimental period, respectively.**

Human sensory analysis

1) This study shows that eggs enriched with Zincopyeast (ZP) at 2.5% and 5.0% did not consistently differ in sensory attributes from non-supplemented eggs (control group) across two production batches in case of boiled (albumin color, yolk color, egg odor, unusual odor, albumin flavor, unusual taste, albumin flexibility, and yolk creaminess) and fried eggs (yolk color, egg odor, sweet aroma, strange odor, egg taste, sweet taste, strange taste, and texture). While some statistically significant differences were observed between feeding groups in certain sensory characteristics, these differences were not consistently replicated between the two batches. Therefore, ZP supplementation at the tested levels does not appear to alter the overall sensory profile of boiled or fried eggs.

Characterization of eggs by e-tongue

2) The ability of an electronic tongue (e-tongue) to effectively distinguish egg samples based on feeding regimes with different levels of Zincoppyeast (ZP) supplementation was proven. ZP 2.5%, and ZP 5% were correctly distinguished from the Control showing a 64.81% accuracy in cross-validation for fresh eggs collected at day 30 of the laying period. The largest differences were observed between the groups Control and ZP 5.0% samples.

Characterization of eggs by e-nose

3) The effectiveness of electronic nose (e-nose) to classify enriched eggs according to storage time was proven. Eggs from 0, 30, and 60 days of storage were correctly classified with 100% accuracy in cross-validation. Moreover, the use of e-nose prove to be valuable distinguishing fresh eggs samples based on different feeding-(ZP) supplementation regimens. ZP 2.5%, and ZP 5% were correctly distinguished from the Control with 76.5% accuracy in cross-validation.

4) The e-nose analysis revealed that specific volatile compounds played a critical role in distinguishing storage durations. Among these, methyl acetate and 2-methylpropanal (sensor 528.86), acetaldehyde (469.52 and 430.57), 2,4,5-trimethyl-3-oxazoline and 2-butanone, 3-mercapto (818.98), as well as 2-hexanol and hexanal (803.41) were the primary contributors to the observed separations of eggs stored at 0, 30 and 60 days. Moreover, the major volatile compounds responsible for the separation of the feeding regimes in fresh eggs included, 2-butanol and n-butanol (602.94), homofuraneol and methyl 3-pyridinecarboxylate (1140.88), methyl acetate and 2-methylpropanal (528.86), as well as 2-propanone and propanal (494.47).

❖ **New scientific findings focusing on probiotics evaluation**

Commercial probiotics N, A, and P liquids with 3.0 g/125 mL, 2.5 g/125 mL and 2.0 g/125 mL concentrations and 25 °C, 60 °C, and 90 °C water temperature after cooling down were scanned in the 950–1630 nm range in transflectance mode. PLSR models to predict probiotic viability (log CFU/g).

Prediction of probiotics viability by NIRS (using Benchtop MetriNIR spectrophotometer)

5) It was proven that viability of the probiotic samples, influenced by concentration and temperature stress factors, can be predicted through NIR spectrophotometry coupled with PLSR modeling. The models achieved a R^2Pr of 0.82 and RMSEP of 0.64 Log CFU/g.

❖ **New scientific findings focusing on microgreens evaluation**

Pea microgreens grown under different environment stress conditions of temperature (15, 20, 25 ºC), and photoperiod (0, 6, 12, 18 hours of light) and harvested at 7, 11 and 14 and 18 days were scanned in two modes: diffuse reflectance for microgreens fresh-cut samples and in transmission for aqueous microgreens extracts samples (1:5 plant - distilled water) and analyzed in the 1150–1850 nm range and applied spectral pretreatment SG (p=2, n=45, m=0) + SNV. Classification PCA-LDA models and partial least squares regression (PLSR) models were developed to test prediction capacity for 13 agronomical and physicochemical variables.

Classification of pea microgreens by NIRS (using Benchtop NIR XDS spectrophotometer)

6) The near-infrared spectroscopy (NIRS), combined with PCA-LDA analysis, enabled effective classification of pea microgreens according to harvesting day, temperature, photoperiod, and combined treatment in both fresh-cut and aqueous extract samples. In fresh-cut samples, cross-validation accuracy corresponded to 66.95% for harvesting day, 75.74% for temperature, 71.05% for photoperiod, and 58.54% for treatment. In contrast, aqueous extract samples yielded higher classification rates of 95.59%, 88.87%, 66.89%, and 68.34% for the same parameters, respectively. These results indicate better class separability in aqueous extracts, likely due to the homogenized nature of the samples and enhanced spectral response under transmission mode, reflecting the compositional changes induced by these environmental stressors.

Prediction of pea microgreens for physical characteristics, pigments and bioactive compounds by NIRS (using Benchtop NIR XDS spectrophotometer)

7) The temperature and photoperiod combinations successfully reproduced known growth patterns in pea microgreens. Under these combined stress conditions, NIRS predicted height and weight in fresh-cut samples with R^2 values of 0.78 and 0.70, respectively. Aqueous extract samples yielded lower values of 0.64 and 0.65, despite the theoretically more favorable optical properties of homogeneous solutions in transmission mode, there might be some structural and morphological characteristics retained in fresh-cut samples measured in diffuse reflectance mode such as tissue density, stem thickness, and leaf arrangement that better correlate with physical traits like height and weight. NIRS shows potential as a non-destructive method for estimating biomass traits under environmental stress.

8) It was proven that pea microgreens pigments are influenced by temperature and photoperiod. 20C_18L and 25C_18L treatments showed higher pigments accumulation, denoting that photoperiod is the most limiting factor in this regard when 0L treatments presented chlorophyll values close to 0. The PLSR pigments prediction models had R^2pr of 0.71 for chlorophyll A, 0.62 for chlorophyll B and 0.73 for total carotenes in microgreens fresh-cut samples, comparable to 0.68, 0.65, and 0.69, respectively for aqueous microgreens extracts samples. These results proves the moderate potential of NIRS to measure pigments (chlorophyl A, B, total carotenes) of pea microgreens, subjected to temperature-photoperiod stress factors, in both fresh-cut microgreens samples and

aqueous microgreens extracts samples.

9) °Brix evaluation showed that lower temperatures (15 °C) favor sucrose accumulation compared to higher temperatures (20 °C and 25 °C); furthermore, microgreens with 18 hours of light had higher °Brix values compared to other treatments. The results indicate that the lower temperature and higher photoperiods in this study promotes °Brix accumulation in pea microgreens. The PLSR prediction of °Brix for microgreens fresh-cut samples showed R^2pr of 0.70 and for aqueous microgreens extracts samples R^2pr of 0.68, but pH and conductivity had low predictive accuracy (below 0.34) for both (aqueous microgreens extracts samples and microgreens fresh-cut samples). It is proven that NIRS provides modest accuracy for prediction of chemical properties of pea microgreens subjected to temperature-photoperiod stress factors, however it is capable of measuring °Brix in some extent, in both microgreens fresh-cut samples and aqueous microgreens extracts samples.

10) In the bioactive compound analysis in pea microgreens, it was proven that lower temperatures (15 °C) and longer photoperiods enhance phenolic compounds accumulation and antioxidant capacity, with 15C_18L being the most effective (particularly on day 14). Moreover, the results show proof of the moderate potential of NIRS for measuring TAC and TPC of pea microgreens subjected to temperature-photoperiod stress factors, especially for aqueous microgreens extracts samples. the PLS regression for TAC and TPC for aqueous microgreens extracts samples achieved R^2CV of 0.73 and 0.71 in aqueous microgreens extracts samples, compared to 0.35 and 0.56 in microgreens fresh-cut samples, respectively.

11) The study proves the effectiveness of Near Infrared Spectroscopy (NIRS) for simultaneous prediction of correlated agronomic and physicochemical variables in pea microgreens. Height, weight, pigments (chlorophyll A, B, and total carotene), and °Brix PLSR models for pea microgreens showed similar spectral profiles. The notable wavelengths for weight and height, which had a broad spectral profile and can be compared with the other variables, included important wavelengths at 1196, 1286, 1392, 1417, 1446, 1480, 1508, 1543, 1600, 1704, and 1838 nm in microgreens fresh-cut samples, while the prominent wavelengths for aqueous microgreens extracts samples were 1337, 1368, 1396, 1409, 1433, 1460, 1484, 1530, 1590, 1640, 1685, 1706, and 1746 nm. These wavelengths, pinpointed through PLSR models, underline the capability of NIRS to detect shared spectral markers across diverse variables, advancing its application in quality assessment and predictive modeling of plant characteristics.

8. SUMMARY

The quality characteristics of food can be affected by various factors, agronomical conditions, storage, processing, and consumption habits, which influence important parameters such as freshness, flavor, texture, and nutritional value of food products. In this context, the aim of this thesis was to assess the potential of rapid techniques based on correlative methods for detecting changes in food quality induced by stress factors, such as near infrared spectroscopy (NIRS), electronic tongue (e-tongue), and electronic nose (e-nose), which offer advantages over conventional quality evaluation methods. The first aim was to analyze the applicability of the e-tongue and e-nose to detect potential alterations in the organoleptic properties of eggs produced by hens fed diets enriched with organic zinc by-product. Furthermore, the capacity of NIRS to characterize and predict the viability of probiotics drinks subjected to different concentrations and temperatures conditions will be assessed. Finally, the study analyses the ability of NIRS to characterize pea microgreens growth under various temperature and photoperiod conditions and to predict their agronomic and physicochemical properties.

The sensory evaluation of enriched eggs using both human panels and electronic systems (e-tongue and e-nose) revealed key insights into the effects of different feeding treatments and storage conditions. Human panel assessments, using ANOVA and Tukey's test, showed minimal differences in most sensory attributes across the Control, ZP 2.5%, and ZP 5.0% feeding groups. The e-tongue analysis highlighted higher differentiation, particularly between the Control and ZP 5.0% groups, in Euclidean distance analysis and LDA analysis, with classification accuracy reaching 95.92% in batch 1 and 100% in batch 2, while cross-validation accuracy was lower at 64.81% and 56%, respectively. The e-nose analysis allowed for the identification of specific aroma compounds and their associated sensory descriptors, highlighting variations across different egg groups in terms of batch, storage duration, and feeding treatments. Models demonstrated high classification accuracy, with values of 98.00% at 50 °C and 82.65% at 80 °C, though cross-validation accuracy was more limited at 68.49% and 62.22%, respectively. When analyzing samples stored for 0, 30, and 60 days, clear distinctions between fresh and stored samples were observed, although there was an overlap among treatment groups. Despite lower cross-validation accuracy due to misclassification, especially between consecutive groups. However, greater differentiation was observed between the Control and ZP 5.0% feeding groups. Although the supplementation of the hens' feed with the industrial by-product did not produce noticeable alterations in egg quality detectable by traditional sensory methods, advanced analytical techniques like e-tongue and e-nose were sensitive enough to detect these subtle variations. This suggests that while the by-product can be used in the hens' diet without significantly impacting

sensory attributes, its effects on the eggs can be effectively monitored using precise and advanced technology such as e-tongue and e-nose.

The microbiological analysis revealed that microorganism viability is significantly impacted by high temperatures (60 °C and 90 °C) of water at the moment of the preparation of the probiotic drinks. The PCA-LDA analysis successfully classified probiotics N, A, and P at 25 °C with 100% classification and 99.18% cross-validation accuracy. Probiotics A and P were more closely related, while probiotic N showed distinct separation, likely due to differences in strain composition and matrix structure. Important wavelengths (1376, 1388–1396, and 1576–1590 nm) linked to water, proteins, lipids, and sugars absorption were identified, demonstrating NIR spectroscopy's efficacy in qualitative probiotic analysis. For concentration-based discrimination, the highest cross-validation accuracy was found at higher temperature 90 °C, showing 95.06%, 93.52% and 90.12% correct classification for probiotic A, probiotic P and probiotic N, respectively. Temperature-based discrimination also showed high classification accuracy, with probiotic A achieving 100% classification and cross-validation accuracy, while probiotics P and N exceeded 90%, with minor misclassification between consecutive temperatures. The best predictive model for CFU counts resulted in an R^2Pr of 0.82 and RMSEP of 0.64 log CFU/g. Key wavelengths, particularly between 1300–1600 nm, were critical for predicting probiotic viability, with significant molecular interactions related to water and organic compounds, such as OH and NH stretching, especially at 1458 nm, 1484 nm, and 1140 nm.

The growth of pea microgreens is strongly influenced by temperature and photoperiod, as demonstrated across the analyzed parameters. Microgreens grown at 15 °C, 20 °C, and 25 °C, under varying light exposure (0, 6, 12, and 18 hours per day), exhibited distinct patterns in height, weight, pigment concentration, and bioactive compounds. Higher temperatures, particularly at 25 °C, promoted more rapid growth and greater biomass accumulation, while extended photoperiods were predominantly relevant enhancing photosynthesis, chlorophyll synthesis, and overall plant health. Conversely, shorter photoperiods and lower temperatures slowed growth, but favored the accumulation of bioactive compounds, such as phenolics and antioxidants. In particular, the absence of light caused pale coloration, low pigmentation levels and extreme growth in microgreens, a result of the etiolation process, where plants tend to elongate excessively as they search for a light source. The results indicate a complex interplay between environmental conditions and microgreen development. The NIRS analysis of pea microgreens was performed using fresh-cut samples in reflectance mode and aqueous extracts samples in transmittance mode. The analysis incorporated SG2-45-0 and SNV pretreatments across a wavelength range of 1150 to 1850 nm. A significant aspect identified in the spectra of both sample types was the first overtone of water, which reached a peak around 1450 nm, highlighting its importance in biological systems.

The PCA-LDA analysis yielded better results for aqueous microgreens extracts samples compared to microgreens fresh-cut samples. The cross-validation accuracies for classification according to harvesting day was 95.59%, temperature was 88.87%, photoperiod was 66.89%, and treatment was 68.34%. Additionally, microgreens classified by specific photoperiod-temperature treatments also showed higher cross-validation accuracies for aqueous microgreens extracts samples ranging from 56.47% to 87.72%. In the same manner, temperature-based classification models (CV between 77.78% and 85.58%) and photoperiod-based classification models (CV between 63.56% and 85.45%) demonstrated better accuracy for aqueous microgreens extracts samples than microgreens fresh-cut samples.

On the other hand, the majority of PLSR models showed slightly better accuracy for microgreens fresh-cut samples measured in reflectance mode than for aqueous microgreens extracts samples measured in transmittance mode, with some exceptions. Across the pea microgreens variables (encompassing physical traits, optical properties, pigments, chemical characteristics, and bioactive compounds), microgreens fresh-cut samples related analysis was slightly better predicting physical, optical, and pigment variables, while aqueous microgreens extracts samples were superior in total antioxidant capacity (TAC) and total water-soluble phenolic compounds (TPC). Analysis in microgreens fresh-cut samples recorded R^2pr values of 0.78 for height, 0.70 for weight, 0.73 for L*, 0.70 for b*, 0.71 for chlorophyll A, 0.62 for chlorophyll B, 0.73 for total carotene, °Brix of 0.70. Meanwhile, analysis in aqueous microgreens extracts samples better predicted TAC and TPC with R^2CV values of 0.73 and 0.71, respectively. pH, conductivity and a* color component had poor performance in both microgreens fresh-cut samples and aqueous microgreens extracts samples analysis. The spectral profiles of various PLSR models for pea microgreens were aligned particularly between weight, height, °Brix and pigments (chlorophyll A, B, and total carotene), showing how these variables are interconnected and contribute to the growth of microgreens.

9. LIST OF PUBLICATIONS IN THE FIELD OF STUDIES

➢ David Tjandra Nugraha, John-Lewis Zinia Zaukuu, **Juan Pablo Aguinaga Bósquez**, Zsanett Bodor, Flora Vitalis and Zoltan Kovacs. Near-Infrared Spectroscopy and Aquaphotomics for Monitoring Mung Bean (Vigna radiata) Sprout Growth and Validation of Ascorbic Acid Content. SENSORS (1424-8220): 21 (2) Paper 611. 20 p. (2021). **Q1. IF (3.576).** https://doi.org/10.3390/s21020611.

➢ Flora Vitalis, David Tjandra Nugraha, Balkis Aouadi, **Juan Pablo Aguinaga Bósquez**, Zsanett Bodor, John-Lewis Zinia Zaukuu, Tamás Kocsis, Viktória Zsom-Muha, Zoltan Gillay and Zoltan Kovacs. Detection of Monilia Contamination in Plum and Plum Juice with NIR Spectroscopy and Electronic Tongue. CHEMOSENSORS (2227-9040): 9 (12) Paper 355. (2021). **Q2. IF (3.398).** https://doi.org/10.3390/chemosensors9120355

➢ **Juan Pablo Aguinaga Bósquez**, Zoltan Kovacs, Zoltán Gillay, György Bázár, Csaba Palkó, Hajnalka Hingyi, Éva Csavajda, Márta Üveges, Zsuzsanna Jókainé Szatura, Iuliana Diana Barbulescu, Mihaela Begea and Tamás Tóth. Evaluating the Effect of a Brewery By-Product as Feed Supplementation on the Quality of Eggs by Means of a Human Panel and E-Tongue and E-Nose Analysis. CHEMOSENSORS (2227-9040): 9 (8) Paper 213. 20 p. (2021). **Q2. IF (3.398).** https://doi.org/10.3390/chemosensors9080213

➢ **Juan Pablo Aguinaga Bósquez,** Esma Oguz, Aybike Cebeci, Mariem Majadi, Gabriella Kiskó, Zoltan Gillay and Zoltan Kovacs. Characterization and Viability Prediction of Commercial Probiotic Supplements under Temperature and Concentration Conditioning Factors by NIR Spectroscopy. FERMENTATION (2311-5637): 8 (2) Paper 66. (2022). **Q2. IF (3.975).** https://doi.org/10.3390/fermentation8020066

➢ Gergo Szabo, Flora Vitalis, Zsuzsanna Horvath-Mezofi, Monika Gob, **Juan Pablo Aguinaga Bosquez**, Zoltan Gillay, Tamás Zsom, Lien Le Phuong Nguyen, Geza Hitka, Zoltan Kovacs and Laszlo Friedrich. Application of Near Infrared Spectroscopy to Monitor the Quality Change of Sour Cherry Stored under Modified Atmosphere Conditions. Sensors 2023, 23(1), 479. **Q1. IF (4.35).** https://doi.org/10.3390/s23010479.

➢ Balkis Aouadi, Damian Laryea, **Juan Pablo Aguinaga Bósquez**, Mariem Majadi, István Kertész, Zsanett Bodor, John-Lewis Zinia Zaukuu, Zoltan Kovacs. Aquaphotomics based screening of tomato powder extracts reveals susceptibility to bulking and coloring agents. FOOD CONTROL. **Q1. IF (6).** https://doi.org/10.1016/j.foodcont.2023.11016.

10. APPENDICES

10.1.   A1: Bibliography

Adamiec, J. *et al.* (2002) 'Changes in egg volatiles during storage', *Food Sci.*, 20, pp. 79–82.

Aguinaga Bósquez, J. P. *et al.* (2021) 'Evaluating the effect of a brewery by-product as feed supplementation on the quality of eggs by means of a human panel and e-tongue and e-nose analysis', *Chemosensors*, 9(8), pp. 1–20. doi: 10.3390/chemosensors9080213.

Aguinaga Bósquez, J. P. *et al.* (2022) 'Characterization and Viability Prediction of Commercial Probiotic Supplements under Temperature and Concentration Conditioning Factors by NIR Spectroscopy', *Fermentation*, 8(2), pp. 1–14. doi: 10.3390/fermentation8020066.

Ajdanian, L., Babaei, M. and Aroiee, H. (2019) 'The growth and development of cress (Lepidium sativum) affected by blue and red light', *Heliyon*, 5(7), p. e02109. doi: 10.1016/j.heliyon.2019.e02109.

AlphaM.O.S. (2018) 'Heracles Manual', pp. 1–163.

AlphaM.O.S. (2021) *Electronic Tongue*. Available at: https://www.alpha-mos.com/electronic-tongue.

AOAC (2006) *Official Methods of Analytical methods of Analysis*. Edited by AOAC International. Washington, DC.

Aouadi, B. *et al.* (2020) 'Historical evolution and food control achievements of near infrared spectroscopy, electronic nose, and electronic tongue—critical overview', *Sensors (Switzerland)*, 20(19), pp. 1–42. doi: 10.3390/s20195479.

Apak, R. *et al.* (2004) 'Novel Total Antioxidant Capacity Index for Dietary Polyphenols and Vitamins C and E, Using Their Cupric Ion Reducing Capability in the Presence of Neocuproine: CUPRAC Method', *J. Agric. Food Chem.*, 52(26), pp. 7970–7981. doi: https://doi.org/10.1021/jf048741x.

Araméndiz, C. T., Cardona-Ayala, C. and Alzate, K. R. (2017) 'Electrical conductivity test in the evaluation of physiological quality in seeds of eggplant (Solanum melongena L.)', *Scientia Agropecuaria*. doi: http://dx.doi.org/10.17268/sci.agropecu.2017.03.05.

de Araújo Gomes, A. *et al.* (2023) 'Pattern recognition techniques in food quality and authenticity: A guide on how to process multivariate data in food analysis', *TrAC - Trends in Analytical Chemistry*, 164. doi: 10.1016/j.trac.2023.117105.

Asgari, S. *et al.* (2020) 'Polymeric carriers for enhanced delivery of probiotics', *Advanced Drug Delivery Reviews*, 161–162, pp. 1–21. doi: 10.1016/j.addr.2020.07.014.

Aurand, L. W., Woods, A. E. and Wells, M. R. (1987) 'Sampling and Proximate Analysis', in *Food Composition and Analysis*. Springer, Dordrecht, pp. 19–34. doi: 10.1007/978-94-015-7398-6_2.

Babushok, V. I. (2015) 'Chromatographic retention indices in identification of chemical compounds', *TrAC - Trends in Analytical Chemistry*, 69, pp. 98–104. doi: 10.1016/j.trac.2015.04.001.

Balázs, L. *et al.* (2023) 'Quantifying the Effect of Light Intensity Uniformity on the Crop Yield by Pea Microgreens Growth Experiments', *Horticulturae*, 9(11). doi: 10.3390/horticulturae9111187.

Baldwin, E. A. *et al.* (2011) 'Electronic Noses and Tongues: Applications for the Food and Pharmaceutical Industries', *Sensors*, pp. 4744–4766. doi: 10.3390/s110504744.

Baral, K. C. *et al.* (2021) 'Advancements in the pharmaceutical applications of probiotics: Dosage forms and formulation technology', *International Journal of Nanomedicine*, 16, pp. 7535–7556. doi: 10.2147/IJN.S337427.

Barnes, R. J., Dhanoa, M. S. and Lister, S. J. (1989) 'Standard Normal Variate Transformation and De-trending of Near-Infrared Diffuse Reflectance Spectra', *Applied Spectroscopy*, 43(5), pp. 772–777. doi: 10.1366/0003702894202201.

Di Bella, M. C. *et al.* (2020) 'Morphometric characteristics, polyphenols and ascorbic acid variation in Brassica oleracea L. novel foods: Sprouts, microgreens and baby leaves', *Agronomy*, 10(6), pp. 1–17. doi: 10.3390/agronomy10060782.

Berkhoff, J. *et al.* (2020) 'Consumer preferences and sensory characteristics of eggs from family farms', *Poultry Science*, 99(11), pp. 6239–6246. doi: 10.1016/j.psj.2020.06.064.

Betancourt, L. and Díaz, G. (2009) 'Enriquecimiento de huevos con ácidos grasos omega-3 mediante la suplementación con semilla de lino (Linum usitatissimum) en la dieta', *MVZ*, 14(1), pp. 1602–1610.

Bianchi, F. *et al.* (2007) 'Retention indices in the analysis of food aroma volatile compounds in temperature-programmed gas chromatography: Database creation and evaluation of precision and robustness', *Journal of Separation Science*, 30(4), pp. 563–572. doi: 10.1002/jssc.200600393.

Blesso, C. N. and Fernandez, M. L. (2018) 'Dietary cholesterol, serum lipids, and heart disease: Are eggs working for or against you?', *Nutrients*, 10(4). doi: 10.3390/nu10040426.

Bove, P. *et al.* (2013) 'Lactobacillus plantarum passage through an oro-gastro-intestinal tract simulator : Carrier matrix effect and transcriptional analysis of genes associated to stress and probiosis', *Microbiological Research*, 168(6), pp. 351–359. doi: 10.1016/j.micres.2013.01.004.

Brazaitytė, A. *et al.* (2018) 'Changes in mineral element content of microgreens cultivated under different lighting conditions in a greenhouse', *Acta Horticulturae*, 1227, pp. 507–515. doi: 10.17660/ActaHortic.2018.1227.64.

Brelaz, K. C. B. T. R. *et al.* (2019) 'Fish waste oil in laying hens* Diets', *Revista Brasileira de Ciencia Avicola / Brazilian Journal of Poultry Science*, 21(4). doi: 10.1590/1806-9061-2019-1069.

Büning-Pfaue, H. (2003) 'Analysis of water in food by near infrared spectroscopy', *Food Chemistry*, 82(1), pp. 107–115. doi: 10.1016/S0308-8146(02)00583-6.

Burko, Y. *et al.* (2022) 'PIF7 is a master regulator of thermomorphogenesis in shade', *Nature Communications*, 13(1). doi: 10.1038/s41467-022-32585-6.

Burns, D. and Ciurczak, E. (2008) *Handbook of Near-Infrared Analysis*. 3rd edn. Edited by D. Burns and E. Ciurczak. Taylor & Francis Group.

Calderon Flores, P. *et al.* (2021) 'Effect of chilling acclimation on germination and seedlings response to cold in different seed coat colored wheat (Triticum aestivum L.)', *BMC Plant Biology*, 21(1), pp. 1–13. doi: 10.1186/s12870-021-03036-z.

Cartea, M. E. *et al.* (2011) 'Phenolic compounds in Brassica vegetables', *Molecules*, 16(1), pp. 251–280. doi: 10.3390/molecules16010251.

de Castro, L. A. *et al.* (2020) 'From orange juice by-product in the food industry to a functional ingredient: Application in the circular economy', *Foods*, 9(5). doi: 10.3390/foods9050593.

Chakraborty, K. *et al.* (2014) 'Differential response of plant and soil processes under climate change: A mini-review on recent understandings', *Proceedings of the National Academy of Sciences India Section B - Biological Sciences*, 84(2), pp. 201–214. doi: 10.1007/s40011-013-0221-7.

Chasapis, C. T. *et al.* (2020) 'Recent aspects of the effects of zinc on human health', *Archives of Toxicology*, 94(5), pp. 1443–1460. doi: 10.1007/s00204-020-02702-9.

Chauhan, A. and Jindal, T. (2020) 'Microbiological Methods for Food Analysis', in *Microbiological Methods for Environment, Food and Pharmaceutical Analysis*. Springer, Cham, p. pp.197-302. doi: DOI:10.1007/978-3-030-52024-3_8.

Cherian, G., Goeger, M. P. and Ahn, D. U. (2002) 'Dietary Conjugated Linoleic Acid with Fish Oil Alters Yolk n-3 and Trans Fatty Acid Content and Volatile Compounds in Raw, Cooked, and Irradiated Eggs', *Poultry Science*. doi: 10.1093/ps/81.10.1571.

Cho, S. and Moazzem, S. (2022) 'Recent Applications of Potentiometric Electronic Tongue and Electronic Nose in Sensory Evaluation', *Preventive Nutrition and Food Science*, 27(4), pp. 354–364. doi: 10.3746/pnf.2022.27.4.354.

Choe, U., Yu, L. L. and Wang, T. T. Y. (2018) 'The Science behind Microgreens as an Exciting New Food for the 21st Century', *Journal of Agricultural and Food Chemistry*, 66(44), pp. 11519–11530. doi: 10.1021/acs.jafc.8b03096.

Choudhary, P. *et al.* (2023) 'Probiotics- its functions and influence on the ageing process: A comprehensive review', *Food Bioscience*, 52(October 2022), p. 102389. doi: 10.1016/j.fbio.2023.102389.

Corcoran, B. M. *et al.* (2008) 'Life Under Stress: The Probiotic Stress Response and How it may be Manipulated', *Current Pharmaceutical Design*, 14, pp. 1382–1399. doi: 10.2174/138161208784480225.

da Costa Filho, P. A. (2009) 'Rapid determination of sucrose in chocolate mass using near infrared spectroscopy', *Analytica Chimica Acta*, 631(2), pp. 206–211. doi: 10.1016/j.aca.2008.10.049.

COUNCIL OF THE EUROPEAN COMMUNITIES (1986) *Council Directive 86/609/EEC*. Available at: https://eur-lex.europa.eu/legal-content/EN/TXT/?uri=CELEX%3A31986L0609.

Curran, P. J. (1989) 'Remote sensing of foliar chemistry', *Remote Sensing of Environment*, 30(3), pp. 271–278. doi: 10.1016/0034-4257(89)90069-2.

Dai, J. and Mumper, R. J. (2010) 'Plant phenolics: Extraction, analysis and their antioxidant and anticancer properties', *Molecules*, 15(10), pp. 7313–7352. doi: 10.3390/molecules15107313.

Defernez, M. and Kemsley, E. K. (1997) 'The use and misuse of chemometrics for treating classification problems', *TrAC - Trends in Analytical Chemistry*, 16(4), pp. 216–221. doi: 10.1016/S0165-9936(97)00015-0.

Dere, Ş., Güneş, T. and Sivaci, R. (1998) 'Spectrophotometric determination of chlorophyll - A, B and total caretenoid contents of some algae species using different solvents', *Turkish Journal of Botany*, 22, pp. 13–16. Available at: http://journals.tubitak.gov.tr/botany/issues/bot-98-22-1/bot-22-1-3-96040.pdf.

Desmond, C. *et al.* (2004) 'Improved Stress Tolerance of GroESL-Overproducing Lactococcus lactis and Probiotic Lactobacillus paracasei NFBC 338', *Applied and Environmental Microbiology*, 70(10), pp. 5929–5936. doi: 10.1128/AEM.70.10.5929.

Dong, X. *et al.* (2021) 'Comparison of sensory qualities in eggs from three breeds based on electronic sensory evaluations', *Foods*, 10(9). doi: 10.3390/foods10091984.

Driesen, E. *et al.* (2020) 'Influence of environmental factors light, co2, temperature, and relative humidity on stomatal opening and development: A review', *Agronomy*, 10(12). doi: 10.3390/agronomy10121975.

Drouin-Chartier, J. P. *et al.* (2020) 'Egg consumption and risk of cardiovascular disease: Three large prospective US cohort studies, systematic review, and updated meta-analysis', *The BMJ*, 368. doi: 10.1136/bmj.m513.

Dunno, K. *et al.* (2016) 'The effects of transportation hazards on shelf life of packaged potato chips', *Food Packaging and Shelf Life*, 8, pp. 9–13. doi: 10.1016/j.fpsl.2016.02.003.

Ebert, A. W. (2022) 'Sprouts and Microgreens—Novel Food Sources forHealthy diets', *Plants*, 11(571). doi: https://doi.org/10.3390/plants11040571.

Eslami, M. *et al.* (2019) 'Importance of probiotics in the prevention and treatment of colorectal cancer', *Journal of Cellular Physiology*, 234(10), pp. 17127–17143. doi: 10.1002/jcp.28473.

Evans, J. D. (1995) *Straightforward Statistics for the Behavioral Sciences*. 1st Ed. Pacific Grove, CA: Brooks Cole Publishing Company.

FAO/WHO (2002) *Report of a Joint FAO/WHO Working Group on Drafting Guidelines for the Evaluation of Probiotics in Food*. Ontario, Canada.

Faraloni, C., Di Lorenzo, T. and Bonetti, A. (2021) 'Impact of light stress on the synthesis of both antioxidants polyphenols and carotenoids, as fast photoprotective response in chlamydomonas reinhardtii: New prospective for biotechnological potential of this microalga', *Symmetry*, 13(11). doi: 10.3390/sym13112220.

Fatogoma, S. *et al.* (2023) 'Effects of Cashew Kernels Cake on the Nutritional and Sensory Quality of Hen Eggs', *Journal of Food and Nutrition Sciences*, (June). doi: 10.11648/j.jfns.20231102.11.

Fenster, K. *et al.* (2019) 'The Production and Delivery of Probiotics : A Review of a Practical Approach', *Microorganisms*, 7(83), pp. 1–17. doi: 10.3390/microorganisms7030083.

Fiorentini, Â. M. *et al.* (2011) 'The influence of different combinations of probiotic bacteria and fermentation temperatures on the microbiological and physicochemical characteristics of fermented lactic beverages containing soybean hydrosoluble extract during refrigerated storage', *Ciência e Tecnologia de Alimentos*, 31(3), pp. 597–607. doi: 10.1590/s0101-20612011000300008.

Fischer, M. and Tran, C. D. (1999) 'Investigation of Solid-Phase Peptide Synthesis by the Near-Infrared Multispectral Imaging Technique : A Detection Method for Combinatorial Chemistry', *Analytical Chemistry*, 71(13), pp. 2255–2261. doi: 10.1021/ac990207e.

Fontinele, G. S. P. *et al.* (2017) 'Glycerin from biodiesel in the feeding of red-egg layers', *Semina:Ciencias Agrarias*, 38(2), pp. 1009–1016. doi: 10.5433/1679-0359.2017v38n2p1009.

Franz, C. M. A. P. and Holy, A. Von (1996) 'Thermotolerance of meat spoilage lactic acid bacteria and their inactivation in vacuum-packaged Vienna sausages', *International Journal of Food Microbiology*, 1605(95), pp. 59–73. doi: https://doi.org/10.1016/0168-1605(95)00022-4.

Furuyama, S., Okamoto, H. and Jishi, T. (2023) 'Effect of Cold Exposure on Brix Value of Borecole Leaves Grown in an Unheated Greenhouse in Hokkaido, Subarctic Region', *Horticulture Journal*, 92(2), pp. 171–177. doi: 10.2503/hortj.QH-003.

Gao, L. B. *et al.* (2022) 'A Comparison between the Egg Yolk Flavor of Indigenous 2 Breeds and Commercial Laying Hens Based on Sensory Evaluation, Artificial Sensors, and GC-MS', *Foods*, 11(24), pp. 1–17. doi: 10.3390/foods11244027.

García-García, M. D. C. *et al.* (2022) 'Determination of Quality Parameters in Mangetout (Pisum sativum L. ssp. arvense) by Using Vis/Near-Infrared Reflectance Spectroscopy', *Sensors*, 22(11). doi: 10.3390/s22114113.

Gemperline, P. (2006) *Practical Guide to Chemometrics*. 2nd ed, *Technometrics*. 2nd ed. Edited by P. Gemperline. CRC. Taylor and Francis Group.

Di Gioia, F., Renna, M. and Santamaria, P. (2017) 'Sprouts, Microgreens and "Baby Leaf" Vegetables', in Yildiz, F. and Wiley, R. (eds) *Minimally Processed Refrigerated Fruits and Vegetables*. Boston: Springer, pp. 403–432. doi: 10.1007/978-1-4939-7018-6.

Gómez-Gaete, C. *et al.* (2024) 'Revolutionizing fruit juice : exploring encapsulation techniques for bioactive compounds and their impact on nutrition , flavour and shelf life', *Food Production, Processing and Nutrition*. doi: 10.1186/s43014-023-00190-9.

Goto, T. *et al.* (2019) 'Metabolomics approach reveals the effects of breed and feed on the composition of chicken eggs', *Metabolites*, 9(10). doi: 10.3390/metabo9100224.

Granato, D. *et al.* (2018) 'Trends in Chemometrics: Food Authentication, Microbiology, and Effects of Processing', *Comprehensive Reviews in Food Science and Food Safety*, 17(3), pp. 663–677. doi: 10.1111/1541-4337.12341.

Gunjal, M. *et al.* (2024) 'Microgreens: Cultivation practices, bioactive potential, health benefits, and opportunities for its utilization as value-added food', *Food Bioscience*, 62(July). doi: 10.1016/j.fbio.2024.105133.

Guo, Z. *et al.* (2016) 'Color compensation and comparison of shortwave near infrared and long wave near infrared spectroscopy for determination of soluble solids content of "Fuji" apple', *Postharvest Biology and Technology*, 115, pp. 81–90. doi: 10.1016/j.postharvbio.2015.12.027.

Hailemariam, A. *et al.* (2022) 'Sensory Characteristics, Nutritional Composition, and Quality of Eggs from Different Chickens', *Open Journal of Animal Sciences*, 12(04), pp. 591–615. doi: 10.4236/ojas.2022.124043.

Hammershøj, M. and Johansen, N. F. (2016) 'Review: The effect of grass and herbs in organic egg production on egg fatty acid composition, egg yolk colour and sensory properties', *Livestock Science*, 194(October), pp. 37–43. doi: 10.1016/j.livsci.2016.11.001.

Hao, F. *et al.* (2021) 'Thermotolerance, Survival, and Stability of Lactic Acid Bacteria After Spray Drying as Affected by the Increase of Growth Temperature', *Food and Bioprocess Technology*, 14(1), pp. 120–132. doi: 10.1007/s11947-020-02571-1.

Hara, T. *et al.* (2017) 'Physiological roles of zinc transporters: molecular and genetic importance in zinc homeostasis', *Journal of Physiological Sciences*, 67(2), pp. 283–301. doi: 10.1007/s12576-017-0521-4.

Hărmănescu, M. *et al.* (2008) 'Total Polyphenols Content Determination in Complex Matrix of Medicinal Plants From Romania By Nir Spectroscopy', *Bulletin UASVM, Agriculture*, 65(1), pp. 123–128. doi: https://doi.org/10.15835/buasvmcn-agr:638.

Hayat, Z. *et al.* (2010) 'Sensory evaluation and consumer acceptance of eggs from hens fed flax seed and 2 different antioxidants', *Poultry Science*, 89(10), pp. 2293–2298. doi: 10.3382/ps.2009-00575.

Hejdysz, M. *et al.* (2024) 'Influence of the genotype of the hen (Gallus gallus domesticus) on main parameters of egg quality, chemical composition of the eggs under uniform environmental conditions', *Poultry Science*, 103(1). doi: 10.1016/j.psj.2023.103165.

Hernández-Adasme, C., Palma-Dias, R. and Escalona, V. H. (2023) 'The Effect of Light Intensity and Photoperiod on the Yield and Antioxidant Activity of Beet Microgreens Produced in an Indoor System', *Horticulturae*, 9(4). doi: 10.3390/horticulturae9040493.

Hill, C. *et al.* (2014) 'Expert consensus document: The international scientific association for probiotics and prebiotics consensus statement on the scope and appropriate use of the term probiotic', *Nature Reviews Gastroenterology and Hepatology*, 11(8), pp. 506–514. doi: 10.1038/nrgastro.2014.66.

Huynh, J. (2023) *EVALUATION OF BRASSICA CARINATA UNDER ABIOTIC STRESS AND USING NEAR INFRARED SPECTROSCOPY FOR PHENOMIC SELECTION AND PREDICTION TECHNOLOGIES*.

IEH (2009) *El gran libro del huevo*. 1a edición. Edited by S. A. Editorial Everest. Madrid.

Inal, F. *et al.* (2001) 'The effects of withdrawal of vitamin and trace mineral supplements from layer diets on egg yield and trace mineral composition', *British Poultry Science*, 42(1), pp. 77–80. doi: 10.1080/713655024.

Izutsu, K. *et al.* (2006) 'Near-Infrared Analysis of Protein Secondary Structure in Aqueous Solutions and Freeze-Dried Solids', *J Pharm Sc*, 95(4), pp. 781–789. doi: DOI 10.1002/jps.20580.

Johnson, M. A., Kumar, M. and Thakur, S. (2024) 'Effect of Variation in Temperature and Light Duration on Morpho-physiology and Phytochemical Content in Sprouts and Microgreens of Common Buckwheat (Fagopyrum esculentum Moench)', *Plant Foods for Human Nutrition*, 79(4), pp. 875–885. doi: 10.1007/s11130-024-01221-7.

Kaewsutas, M., Nararatwanchai, T. and Sittiprapaporn, P. (2016) 'The effects of dietary microalgae (Schizochytrium spp .) and fish oil in layers on docosahexaenoic acid omega-3 enrichment of the eggs', *Journal of Applied Animal Nutrition*, 4(e7), pp. 1–6. doi: 10.1017/jan.2016.4.

Kalus, K. *et al.* (2020) 'Laying hens biochar diet supplementation—effect on performance, excreta N content, NH3 and VOCs emissions, egg traits and egg consumers acceptance', *Agriculture (Switzerland)*, 10(237), pp. 1–15. doi: 10.3390/agriculture10060237.

Kay, R. and Phinney, B. (1956) 'The control of plasmid pigment formation by a virescent gene, pale-yellow-1, of maize', *Plant Physiology*, 31(6), pp. 415–420.

Kim, M. *et al.* (2022) 'Low-Temperature Effects on the Growth and Phytochemical Properties of Wheat Sprouts', *Agriculture (Switzerland)*, 12(6). doi: 10.3390/agriculture12060745.

Kong, Y. and Zheng, Y. (2019) 'Variation of phenotypic responses to lighting using a combination of red and blue light-emitting diodes versus darkness in seedlings of 18 vegetable genotypes', *Canadian Journal of Plant Science*, 99(2), pp. 159–172. doi: 10.1139/cjps-2018-0181.

Kovacs, Z. *et al.* (2020) 'Factors Influencing the Long-Term Stability of Electronic Tongue and Application of Improved Drift Correction Methods', *biosensors*, 10(74). doi: 10.3390/bios10070074.

Kovacs, Z. and Pollner, B. (2016) *aquap2 - Multivariate Data Analysis Tools for R including Aquaphotomics Methods*. Available at: https://github.com/bpollner/aquap2.

Krzywinski, M. (2025) 'Image Color Summarizer'. Available at: https://mkweb.bcgsc.ca/colorsummarizer/.

Kwoji, I. D. *et al.* (2021) 'Multi-strain probiotics: Synergy among isolates enhances biological activities', *Biology*, 10(4), pp. 1–20. doi: 10.3390/biology10040322.

Kyriacou, M. C. *et al.* (2019) 'Functional quality in novel food sources: Genotypic variation in the nutritive and phytochemical composition of thirteen microgreens species', *Food Chemistry*, 277(October 2018), pp. 107–118. doi: 10.1016/j.foodchem.2018.10.098.

Kyriacou, M. C. *et al.* (2020) 'Phenolic constitution, phytochemical and macronutrient content in three species of microgreens as modulated by natural fiber and synthetic substrates', *Antioxidants*, 9(3), pp. 1–23. doi: 10.3390/antiox9030252.

Leeson, S., Caston, L. and Maclaurin, T. (1998) 'Organoleptic Evaluation of Eggs Produced by Laying Hens Fed Diets Containing Graded Levels of Flaxseed and Vitamin E', *Poultry Science*, 77(9), pp. 1436–1440. doi: 10.1093/ps/77.9.1436.

Lenzi, A. *et al.* (2019) 'Antioxidant and mineral composition of three wild leafy species: A comparison between microgreens and baby greens', *Foods*, 8(10). doi: 10.3390/foods8100487.

Li, J. and Yang, Y. (2023) 'How do plants maintain pH and ion homeostasis under saline-alkali stress?', *Frontiers in Plant Science*, 14(October), pp. 1–11. doi: 10.3389/fpls.2023.1217193.

Li, M. *et al.* (2017) 'Non-destructive assessment of quality parameters in "Friar" plums during low temperature storage using visible/near infrared spectroscopy', *Food Control*, 73, pp. 1334–1341. doi: 10.1016/j.foodcont.2016.10.054.

Li, T., Lalk, G. T. and Bi, G. (2021) 'Fertilization and pre-sowing seed soaking affect yield and mineral nutrients of ten microgreen species', *Horticulturae*, 7(2), pp. 1–16. doi: 10.3390/horticulturae7020014.

Li, Y. *et al.* (2019) 'Spectroscopic determination of leaf chlorophyll content and color for genetic selection on Sassafras tzumu', *Plant Methods*, 15(1), pp. 1–11. doi: 10.1186/s13007-019-0458-0.

Liaghat, S. *et al.* (2014) 'Early detection of basal stem rot disease (Ganoderma) in oil palms based on hyperspectral reflectance data using pattern recognition algorithms', *International Journal of Remote Sensing*, 35(10), pp. 3427–3439. doi: 10.1080/01431161.2014.903353.

Lima, H. J. . and Souza, L. A. . (2018) 'Vitamin A in the diet of laying hens : enrichment of table eggs to prevent nutritional deficiencies in humans', *World's Poultry Science Journal*, 74(December), pp. 1–8. doi: 10.1017/S004393391800065X.

Liu, K. *et al.* (2022) 'Light Intensity and Photoperiod Affect Growth and Nutritional Quality of Brassica Microgreens', *Molecules*, 27(3). doi: 10.3390/molecules27030883.

Liu, X. *et al.* (2014) 'Thermostability of Probiotics and Their í µí»¼-Galactosidases and the Potential for Bean Products'. doi: 10.1155/2014/472723.

Liu, Yi *et al.* (2019) 'The Influence of Spectral Pretreatment on the Selection of Representative Calibration Samples for Soil Organic Matter Estimation Using Vis-NIR Reflectance Spectroscopy', *Remote Sensing*, 11, pp. 2–16. doi: 10.3390/rs11040450.

Lone, J. K., Pandey, R. and Gayacharan (2024) 'Microgreens on the rise: Expanding our horizons from farm to fork', *Heliyon*, 10(4). doi: 10.1016/j.heliyon.2024.e25870.

Lowe, N. M. *et al.* (2024) 'Preventing and Controlling Zinc Deficiency Across the Life Course: A Call to Action', *Advances in Nutrition*. doi: 10.1016/j.advnut.2024.100181.

Macleod, A. J. and Cavea, S. J. (1975) 'Volatile Flavour Components of Eggs', *Sci. Fd Agric*, pp. 351–360.

Madsen, B. S. (2011) *Statistics for Non-Statisticians*. Edited by Springer. Heidelberg. doi: 10.1007/978-3--642-17656-2.

Maeda, H. and Ozaki, Y. (1995) 'Near infrared spectroscopy and chemometrics studies of temperature- dependent spectral variations of water : relationship between spectral changes and hydrogen bonds', *J. Near Infrared Spectrosc.*, 3, pp. 191–201. doi: 10.1255/jnirs.69.

Marchioni, I. *et al.* (2021) 'Small functional foods: Comparative phytochemical and nutritional analyses of five microgreens of the brassicaceae family', *Foods*, 10(2), pp. 1–15. doi: 10.3390/foods10020427.

Margeta, P. *et al.* (2019) 'Importance of sensory evaluation in assessment of egg quality', *Poljoprivreda*, 25(1), pp. 56–63. doi: 10.18047/poljo.25.1.8.

Marín-Ortiz, J. C. *et al.* (2020) 'Linking physiological parameters with visible/near-infrared leaf reflectance in the incubation period of vascular wilt disease', *Saudi Journal of Biological Sciences*, 27(1), pp. 88–99. doi: 10.1016/j.sjbs.2019.05.007.

Matiella, J. and Hsieh, T. (1991) 'Volatile Compounds in Scrambled Eggs', *Journal of Food Science*, 56(2), pp. 387–390. doi: 10.1111/j.1365-2621.1991.tb05286.x.

Menezes, A. *et al.* (2018) 'Combination of probiotic yeast and lactic acid bacteria as starter culture to produce maize-based beverages', *Food Research International*, 111, pp. 187–197. doi: 10.1016/j.foodres.2018.04.065.

Mian K., S. *et al.* (2017) 'Sensory Evaluation and Consumer Acceptability', in *Handbook of Food Science and Technology*, pp. 362–386. Available at: https://www.researchgate.net/publication/320466080_Sensory_Evaluation_and_Consumer_Acceptability.

Miranda, J. M. *et al.* (2015) 'Egg and egg-derived foods: Effects on human health and use as functional foods', *Nutrients*, 7(1), pp. 706–729. doi: 10.3390/nu7010706.

Mizuse, K. and Fujii, A. (2012) 'Tuning of the Internal Energy and Isomer Distribution in Small Protonated Water Clusters H + (H 2 O) 4 − 8 : An Application of the Inert Gas Messenger Technique', *The Jornal of Physical Chemistry A*, 116, pp. 4868–4877. doi: DOI: 10.1021/jp302030d.

Młodzińska, E. (2009) 'Survey of plant pigments: molecular and environmental determinations of plant colors', *Acta Biologica Cracoviensia Series Botanica*, 51(1), pp. 7–16.

Modesti, M. *et al.* (2022) 'E-Senses, Panel Tests and Wearable Sensors: A Teamwork for Food Quality Assessment and Prediction of Consumer's Choices', *Chemosensors*, 10(7). doi: 10.3390/chemosensors10070244.

Moliner, A. M. and Masaguer, A. (1996) 'CALIDAD DEL AGUA PARA USO AGRARIO', in *Prácticas agrarias compatibles con el medio natural. EL AGUA*. Madrid: Ministerio de Agricultura. Pescay Alimentación. Available at: https://www.researchgate.net/publication/276266542%0ACalidad.

Moon, Y.-H. and Jung, I.-C. (2010) 'Effect of Citrus Byproduct on Quality and Fatty Acid Composition of Chicken Eggs', *Journal of Life Science*, 20(9), pp. 1358–1364. doi: 10.5352/jls.2010.20.9.1358.

MSZT (2003) *Sensory examination. Methodology. General instructions. MSZ ISO 6658: 2018, MSZ ISO 6658: 2018*. Budapest: Hungarin Standards Institution (MSZT). Available at:

http://www.mszt.hu/web/guest/webaruhaz;jsessionid=462C2609C0779DA1BF777CD92FCE6E5F?p_p_id=msztwebshop_WAR_MsztWAportlet&p_p_lifecycle=1&p_p_state=normal&p_p_mode=view&p_p_col_id=column-1&p_p_col_pos=1&p_p_col_count=2&_msztwebshop_WAR_MsztWAportlet_ref=168.

Mukherjee, P., Chakraborty, A. and Chakraborty, M. (2020) 'Recent Advances of Zinc in Human Health: a Review', *International Research Journal Of Pharmacy*, 11(8), pp. 12–15. doi: 10.7897/2230-8407.110873.

Muncan, J. *et al.* (2022) 'Aquaphotomics Research of Cold Stress in Soybean Cultivars with Different Stress Tolerance Ability: Early Detection of Cold Stress Response', *Molecules*, 27(3). doi: 10.3390/molecules27030744.

Muncan, J. and Tsenkova, R. (2019) 'Aquaphotomics — From Innovative Knowledge to Integrative Platform in Science and Technology', *Molecules*, 24(2742), pp. 2–26.

Nagashima, A. I. *et al.* (2013) 'Development of effervescent products , in powder and tablet form , supplemented with probiotics Lactobacillus acidophilus and Saccharomyces boulardii', *Food Science and Technology*, 33(4), pp. 605–611. doi: 10.1590/S0101-20612013000400002.

National Research Council (1994) *Nutrient Requirements of Poultry*. Ninth Revi, *Poultry Science*. Ninth Revi. Edited by N. A. Press. Washington, D.C. doi: 10.17226/2114.

Niroula, A. *et al.* (2019) 'Profile of chlorophylls and carotenoids of wheat (Triticum aestivum L.) and barley (Hordeum vulgare L.) microgreens', *Journal of Food Science and Technology*, 56(5), pp. 2758–2763. doi: 10.1007/s13197-019-03768-9.

Nunes, P. S. O. *et al.* (2024) 'Microbial consortia of biological products: Do they have a future?', *Biological Control*, 188(January). doi: 10.1016/j.biocontrol.2024.105439.

Nwamo, A. C. *et al.* (2021) 'Egg quality and sensory evaluation as affected by temperature and storage days of fertile and non-fertile eggs', *Nigerian Journal of Animal Production*, 48(3), pp. 23–32. doi: 10.51791/njap.v48i3.2961.

Oniszczuk, A. *et al.* (2021) 'Role of gut microbiota, probiotics and prebiotics in the cardiovascular diseases', *Molecules*, 26(4), pp. 1–15. doi: 10.3390/molecules26041172.

Ozaki, Y., Genkawa, T. and Futami, Y. (2017) 'Near-infrared spectroscopy', in *Encyclopedia of Spectroscopy and Spectrometry*. 3rd edn. Elsevier Ltd., pp. 40–49. doi: 10.1016/B978-0-12-409547-2.12164-X.

Paraschivu, M. *et al.* (2022) 'Microgreens: Global Market Trends And Microgreens, Current Status, Global Market Trends', *Scientific Papers Series Management, Economic Engineering in Agriculture and Rural Development*, 21(January).

Parker, E. A. . *et al.* (2018) 'Probiotics and gastrointestinal conditions : An overview of evidence from the Cochrane Collaboration', *Nutrition*, 45, pp. 125–134. doi: 10.1016/j.nut.2017.06.024.

Pasulka, A. L. *et al.* (2021) 'Visualization of probiotics via epifluorescence microscopy and fluorescence in situ hybridization (FISH)', *Journal of Microbiological Methods*, 182(February), p. 106151. doi: 10.1016/j.mimet.2021.106151.

Peng, M. *et al.* (2020) 'Effectiveness of probiotics, prebiotics, and prebiotic-like components in common functional foods', *Comprehensive Reviews in Food Science and Food Safety*, 19(4), pp. 1908–1933. doi: 10.1111/1541-4337.12565.

Perrella, G. *et al.* (2020) 'The impact of light and temperature on chromatin organization and plant adaptation', *Journal of Experimental Botany*, 71(17), pp. 5247–5255. doi: 10.1093/jxb/eraa154.

Petrescu, D. C., Vermeir, I. and Petrescu-Mag, R. M. (2020) 'Consumer understanding of food quality, healthiness, and environmental impact: A cross-national perspective', *International Journal of Environmental Research and Public Health*, 17(1). doi: 10.3390/ijerph17010169.

Pinto, E. *et al.* (2015) 'Comparison between the mineral profile and nitrate content of microgreens and mature lettuces', *Journal of Food Composition and Analysis*, 37(3), pp. 38–43. doi: 10.1016/j.jfca.2014.06.018.

Pokharel, B. (2023) 'Advancements in Food Processing Technologies: Enhancing Safety, Quality, and Sustainability', *Interantional Journal of Scientific Research in Engineering and Management*, 07(06). doi: 10.55041/ijsrem23682.

Prananto, J. A., Minasny, B. and Weaver, T. (2020) *Near infrared (NIR) spectroscopy as a rapid and cost-effective method for nutrient analysis of plant leaf tissues*. 1st edn, *Advances in Agronomy*. 1st edn. Elsevier Inc. doi: 10.1016/bs.agron.2020.06.001.

Prasad, J., Mcjarrow, P. and Gopal, P. (2003) 'Heat and Osmotic Stress Responses of Probiotic Lactobacillus rhamnosus HN001 (DR20) in Relation to Viability after Drying', *Applied and Environmental Microbiology*, 69(2), pp. 917–925. doi: 10.1128/AEM.69.2.917.

Pupa, P. *et al.* (2021) 'The efficacy of three double - microencapsulation methods for preservation of probiotic bacteria', *Nature*, 11(0123456789), pp. 1–9. doi: 10.1038/s41598-021-93263-z.

Qu, L. and Pei, Y. (2024) 'A Comprehensive Review on Discriminant Analysis for Addressing Challenges of Class-Level Limitations, Small Sample Size, and Robustness', *Processes*, 12(7), pp. 1–32. doi: 10.3390/pr12071382.

Ramadan, N. A. *et al.* (2010) 'Effect of using different levels of iron with Zinc and Copper in layer's diet on egg iron enrichment', *International Journal of Poultry Science*, 9(9), pp. 842–850. doi: 10.3923/ijps.2010.842.850.

Ramos, L. (2012) 'Basics and Advances in Sampling and Sample Preparation', *Chemical Analysis of Food: Techniques and Applications*, pp. 3–24. doi: 10.1016/B978-0-12-384862-8.00001-7.

Réhault-Godbert, S., Guyot, N. and Nys, Y. (2019) 'The golden egg: Nutritional value, bioactivities, and emerging benefits for human health', *Nutrients*, 11(3), pp. 1–26. doi: 10.3390/nu11030684.

Rinnan, A., Berg, F. and Engelsen, S. B. (2009) 'Review of the most common pre-processing techniques for near-infrared spectra', *Trends in Analytical Chemistry*, 28(10), pp. 1201–1222. doi: 10.1016/j.trac.2009.07.007.

Rodriguez-Amaya, D. B. (2015) 'Carotenes and xanthophylls as antioxidants', in *Handbook of Antioxidants for Food Preservation*. Elsevier Ltd, pp. 17–50. doi: 10.1016/B978-1-78242-089-7.00002-6.

Rolland, F., Baena-Gonzalez, E. and Sheen, J. (2006) 'Sugar sensing and signaling in plants: Conserved and novel mechanisms', *Annual Review of Plant Biology*, 57, pp. 675–709. doi: 10.1146/annurev.arplant.57.032905.105441.

Roussel, S. *et al.* (2014) 'Multivariate Data Analysis.', in *Process Analytical Technology for the Food Industry*, pp. 7–59. doi: https://doi.org/10.1007/978-1-4939-0311-5_2.

Sanders, M. E. *et al.* (2018) 'Probiotics for human use', *Nutrition Bulletin*, 43(3), pp. 212–225. doi: 10.1111/nbu.12334.

Sati, N. *et al.* (2020) 'Effect of storage days and temperature on the sensory evaluation of fertile and non-fertile chicken eggs in Jos Plateau State', in *Psroceedings of the 45th Annual Conference of the Nigerian Society for Animal Production (NSAP), Bauchi 2020*. Bauchi, Nigeria: Nigerian Society for Animal Production, pp. 720–723.

Savitzky, A. and Golay, M. J. E. (1964) 'Smoothing and Differentiation of Data by Simplified Least Squares Procedures', *Analytical Chemistry*, 36(8), pp. 1627–1639. doi: doi.org/10.1021/ac60214a047.

Schmolze, D. B. *et al.* (2011) 'Advances in microscopy techniques', *Archives of Pathology and Laboratory Medicine*, 135(2), pp. 255–263. doi: 10.5858/135.2.255.

Şekeroğlu, A. *et al.* (2024) 'The Impact of Laying Hen Age, Egg-Laying Time, Cage Tier, and Cage Direction on Egg Quality Traits in Hens in an Enriched Cage System', *Revista Brasileira de Ciencia Avicola / Brazilian Journal of Poultry Science*, 26(2). doi: 10.1590/1806-9061-2024-1902.

Seluzicki, A., Burko, Y. and Chory, J. (2017) 'Dancing in the dark: darkness as a signal in plants', *Plant Cell and Environment*, 40(11), pp. 2487–2501. doi: 10.1111/pce.12900.

Senevirathne, G. I., Gama-Arachchige, N. S. and Karunaratne, A. M. (2019) 'Germination, harvesting stage, antioxidant activity and consumer acceptance of ten microgreens', *Ceylon Journal of Science*, 48(1), pp. 91–96. doi: 10.4038/cjs.v48i1.7593.

Sharma, H. C. *et al.* (2016) 'Elevated CO2 influences host plant defense response in chickpea against Helicoverpa armigera', *Arthropod-Plant Interactions*, 10(2), pp. 171–181. doi: 10.1007/s11829-016-9422-3.

Shi, Z. *et al.* (2008) 'Process characterization of powder blending by near-infrared spectroscopy: Blend end-points and beyond', *Journal of Pharmaceutical and Biomedical Analysis*, 47(4–5), pp. 738–745. doi: 10.1016/j.jpba.2008.03.013.

Siesler, H. W. *et al.* (2002) *Near-infrared spectroscopy. Principles, instruments, applications.* 1rst edn, *Journal of Chemometrics*. 1rst edn. Weinheim: WILEY-VCH Verlag GmbH.

Singh, A. *et al.* (2024) 'Emergence of microgreens as a valuable food, current understanding of their market and consumer perception: A review', *Food Chemistry: X*, 23(June), p. 101527. doi: 10.1016/j.fochx.2024.101527.

Singleton, V. L. and Rossi, J. A. (1965) 'Colorimetry of Total Phenolics with Phosphomolybdic-Phosphotungstic Acid Reagents', *Am. J. Enol. Vitic.*, (16), pp. 144–158. doi: 10.5344/ajev.1965.16.3.144.

Singleton, V., Orthofer, R. and Lamuela-Raventós, R. (1999) 'Analysis of total phenols and other oxidation substrates and antioxidants by means of Folin–Ciocalteu reagent', *Methods in Enzymology*, 299, pp. 152–178. doi: https://doi.org/10.1016/S0076-6879(99)99017-1.

Skrajnowska, D. and Bobrowska-Korczak, B. (2019) 'Role of zinc in immune system and anti-cancer defense mechanisms', *Nutrients*, 11(10). doi: 10.3390/nu11102273.

Slavchev, A. of W. S. P. R. D. in P. G. W. U. for R. B. S. *et al.* (2015) 'Monitoring of Water Spectral Pattern Reveals Differences in Probiotics Growth When Used for Rapid Bacteria Selection', *PLOS ONE*, 10(7), pp. 1–18. doi: https://doi.org/10.1371/journal.pone.0130698.

Sousa Gallagher, M. J., Mahajan, P. V. and Yan, Z. (2011) *Modelling chemical and physical deterioration of foods and beverages*, *Food and Beverage Stability and Shelf Life*. Woodhead Publishing Limited. doi: 10.1533/9780857092540.2.459.

Sun, J. *et al.* (2013) 'Profiling polyphenols in five brassica species microgreens by UHPLC-PDA-ESI/HRMSn', *Journal of Agricultural and Food Chemistry*, 61(46), pp. 10960–10970. doi: 10.1021/jf401802n.

Suokko, A. *et al.* (2005) 'Characterization of a Mobile clpL Gene from Lactobacillus rhamnosus', *Applied and Environmental Microbiology*, 71(4), pp. 2061–2069. doi: 10.1128/AEM.71.4.2061.

Świątkiewicz, S. and Koreleski, J. (2008) 'The use of distillers dried grains with solubles (DDGS) in poultry nutrition', *World's Poultry Science Journal*, 64(2), pp. 257–265. doi: 10.1017/S0043933908000044.

Tadesse, K. T. (2024) 'The Role of Post-Harvest Management in Ensuring Food Security in a Changing World : Review Article', *J Clin Res Case Stud*, 2(3), pp. 1–14. doi: doi.org/10.61440/JCRCS.2024.v2.41.

Teoh, P. L. *et al.* (2011) 'Tolerance of free and encapsulated probiotics towards heat treatment and high sodium concentration Tolerance of free and encapsulated probiotics towards heat treatment and high sodium concentration', *Journal of Food, Agriculture & Environment*, 9(1), pp. 69–73. doi: https://doi.org/10.1234/4.2011.1910.

Thakulla, D., Dunn, B. and Hu, B. (2021) 'Nutrient Solution Temperature Affects Growth and ∘Brix Parameters of Seventeen Lettuce Cultivars Grown in an NFT Hydroponic System Dharti', *Horticulturae*, 7(321). doi: doi.org/10.3390/horticulturae7090321.

The Parliament (2021) *Act XXVIII of 1998 on the protection and sparing of animals*. Hungary: FAOLEX database. Available at: http://www.fao.org/faolex/results/details/en/c/LEX-FAOC015674.

Trumbo et al., P. (2001) 'Dietary ReferenceIntakes for Vitamin A, Vitamin K, Arsenic, Boron, Chromium, Copper, Iodine, Iron,.pdf', *Journal of the American Dietetic Association*, pp. 294–301.

Tsenkova, R. (2009) 'Introduction aquaphotomics: Dynamic spectroscopy of aqueous and biological systems describes peculiarities of water', *Journal of Near Infrared Spectroscopy*, 17(6), pp. 303–314. doi: 10.1255/jnirs.869.

Tsenkova, R. *et al.* (2018) 'Essentials of Aquaphotomics and Its Chemometrics Approaches', *Frontiers in Chemistry*, 6(August), pp. 1–25. doi: 10.3389/fchem.2018.00363.

Tsenkova, R., Kovacs, Z. and Kubota, Y. (2015) 'Aquaphotomics: Near infrared spectroscopy and water states in biological systems', *Sub-Cellular Biochemistry*, 71, pp. 189–211. doi: 10.1007/978-3-319-19060-0_8.

Turan, B. (2019) 'A Brief Overview from the Physiological and Detrimental Roles of Zinc Homeostasis via Zinc Transporters in the Heart', *Biological Trace Element Research*, 188(1), pp. 160–176. doi: 10.1007/s12011-018-1464-1.

Umano, K. *et al.* (1990) 'Volatile Compounds Formed from Cooked Whole Egg, Egg Yolk, and Egg White', *Journal of Agricultural and Food Chemistry*, 38(2), pp. 461–464. doi: 10.1021/jf00092a028.

De Vos, W. M. and De Vos, E. A. J. (2012) 'Role of the intestinal microbiome in health and disease : from correlation to causation', *Nutrition Reviews*, 70, pp. S45–S56. doi: 10.1111/j.1753-4887.2012.00505.x.

Wang, G. *et al.* (2022) 'Characteristics of Probiotic Preparations and Their Applications', *Foods*, 11(16). doi: 10.3390/foods11162472.

Wang, H. P. *et al.* (2022) 'Recent advances of chemometric calibration methods in modern spectroscopy: Algorithms, strategy, and related issues', *TrAC - Trends in Analytical Chemistry*, 153, p. 116648. doi: 10.1016/j.trac.2022.116648.

Wang, Q. *et al.* (2014) 'Discriminating eggs from different poultry species by fatty acids and volatiles profiling: Comparison of SPME-GC/MS, electronic nose, and principal component analysis method', *European Journal of Lipid Science and Technology*, 116(8), pp. 1044–1053. doi: 10.1002/ejlt.201400016.

Wang, Y. J. *et al.* (2020) 'Onsite nutritional diagnosis of tea plants using micro near-infrared spectrometer coupled with chemometrics', *Computers and Electronics in Agriculture*, 175(March), p. 105538. doi: 10.1016/j.compag.2020.105538.

Weenk, G. H. (2003) 'Microbiological assessment of culture media: Comparison and statistical evaluation of methods', in Corry, J., Curtsi, G., and Baird, R. (eds) *Handbook of Culture Media for Food Microbiology*. 1st editio, pp. 1–23. doi: 10.1016/S0079-6352(03)80004-8.

Wei, D. and Salahub, D. R. (1997) 'Hydrated proton clusters : Ab initio molecular dynamics simulation and simulated annealing', *The Journal of Chemical Physics*, (106), pp. 6086–694. doi: 10.1063/1.473607.

Wheeler, T. R. *et al.* (2000) 'Temperature variability and the yield of annual crops', *Agriculture, Ecosystems and Environment*, 82(1–3), pp. 159–167. doi: 10.1016/S0167-8809(00)00224-3.

Wold, S., Sjöström, M. and Eriksson, L. (2001) 'PLS-regression: A basic tool of chemometrics', *Chemometrics and Intelligent Laboratory Systems*, 58(2), pp. 109–130. doi: 10.1016/S0169-7439(01)00155-1.

Workman, J. J. (2000) *The Handbook of Organic Compounds, Three-Volume Set*. 1st editio. San Diego, United States: Academic Press Inc.

Workman, J. J. and Weyer, L. (2012) *Practical Guide and Spectral Atlas for Interpretive Near-Infrared Spectroscopy*. 2nd edn. Boca Raton: Taylor & Francis Group.

Xiang, X. le *et al.* (2019) 'Non-destructive characterization of egg odor and fertilization status by SPME/GC-MS coupled with electronic nose', *Journal of the Science of Food and Agriculture*, 99(7), pp. 3264–3275. doi: 10.1002/jsfa.9539.

Xiao, Z. *et al.* (2012) 'Assessment of vitamin and carotenoid concentrations of emerging food products: Edible microgreens', *Journal of Agricultural and Food Chemistry*, 60(31), pp. 7644–7651. doi: 10.1021/jf300459b.

Xiao, Z. *et al.* (2016) 'Microgreens of Brassicaceae: Mineral composition and content of 30 varieties', *Journal of Food Composition and Analysis*, 49(June), pp. 87–93. doi: 10.1016/j.jfca.2016.04.006.

Xie, A. *et al.* (2023) 'Polysaccharides, proteins, and their complex as microencapsulation carriers for delivery of probiotics: A review on carrier types and encapsulation techniques', *International Journal of Biological Macromolecules*, 242(P1), p. 124784. doi: 10.1016/j.ijbiomac.2023.124784.

Xie, T. *et al.* (2019) 'Effects of Lonicera confusa and Astragali Radix extracts supplementation on egg production performance, egg quality, sensory evaluation, and antioxidative parameters of laying hens during the late laying period', *Poultry Science*, 98(10), pp. 4838–4847. doi: 10.3382/ps/pez219.

Yadav, L. P. *et al.* (2019) 'Antioxidant Potentiality and Mineral Content of Summer Season Leafy Greens: Comparison at Mature and Microgreen Stages Using Chemometric', *Agricultural Research*, 8(2), pp. 165–175. doi: 10.1007/s40003-018-0378-7.

Yang, J. *et al.* (2024) 'Comparative Analysis of the Effect of Dietary Supplementation with Fermented and Water-Extracted Leaf Extracts of Eucommia ulmoides on Egg Production and Egg Nutrition', *Foods*, 13(10), pp. 1–19. doi: 10.3390/foods13101521.

Yimenu, S. M., Kim, J. Y. and Kim, B. S. (2017) 'Prediction of egg freshness during storage using electronic nose', *Poultry Science*, 96(10), pp. 3733–3746. doi: 10.3382/ps/pex193.

Yu, Q. *et al.* (2020) 'Effect of the level and source of supplementary dietary zinc on egg production, quality, and zinc content and on serum antioxidant parameters and zinc concentration in laying hens', *Poultry Science*, 99(11), pp. 6233–6238. doi: 10.1016/j.psj.2020.06.029.

Zahir, S. A. D. M. *et al.* (2022) 'A review of visible and near-infrared (Vis-NIR) spectroscopy application in plant stress detection', *Sensors and Actuators A: Physical*, 338(February), p. 113468. doi: 10.1016/j.sna.2022.113468.

Zawistowska-Rojek, A., Zaręba, T. and Tyski, S. (2022) 'Microbiological Testing of Probiotic Preparations', *International Journal of Environmental Research and Public Health*, 19(9). doi: 10.3390/ijerph19095701.

Zhang, Y. *et al.* (2021) 'Nutritional quality and health benefits of microgreens, a crop of modern agriculture', *Journal of Future Foods*, 1(1), pp. 58–66. doi: 10.1016/j.jfutfo.2021.07.001.

Zhou, J. Y., Hao, D. L. and Yang, G. Z. (2021) 'Regulation of cytosolic pH: The contributions of plant plasma membrane H+-atpases and multiple transporters', *International Journal of Molecular Sciences*, 22(23), pp. 14–16. doi: 10.3390/ijms222312998.

Zugarramurdi, A. *et al.* (2004) 'The effect of improving raw material quality on product quality and operating costs: A comparative study for lean and fatty fish', *Food Control*, 15(7), pp. 503–509. doi: 10.1016/j.foodcont.2003.08.001.

A2: Supplementary tables

A2_Table 1. Ingredients used in the formulation of experimental diets for laying hens

Ingredient (%)	Control	ZP 2.5%	ZP 5.0%
Corn	37.00	36.80	35.60
Extracted soybean meal (46% CP)	13.00	10.60	8.30
Corn–DDGS	11.00	11.00	11.00
Wheat	10.00	10.00	10.00
Extracted sunflower meal	7.70	8.00	8.00
Limestone grit	5.00	5.00	5.00
Corn germ meal	5.00	5.00	5.00
Corn feed flour	5.04	4.84	5.85
Limestone	4.32	4.35	4.40
Zincoppyeast [1]	-	2.50	5.00
MCP	0.55	0.50	0.44
Soybean oil	0.45	0.48	0.49
Salt	0.32	0.32	0.32
Premix [2] (%)	0.30	0.30	0.30
L-lysine-HCL	0.15	0.14	0.13
DL-methionine	0.07	0.07	0.07
Lupro-Cid [3]	0.05	0.05	0.05
Vitafix Plus [4]	0.05	0.05	0.05

Control = 0% Zincoppyeast, ZP 2.5% = 2.5% Zincoppyeast, ZP 5.0% = 5.0% Zincoppyeast. CP = crude protein, DDGS = distiller's dried grains with solubles, MCP = monocalcium phosphate. [1] SC AGSIRA SRL (Romania). [2] Vitamin A 13,333,330 IU/kg; vitamin D 2500 IU/kg; vitamin E 1000,000 mg/kg; vitamin K 11,333 mg/kg; vitamin B1 866.7 mg/kg; vitamin B2 1070 mg/kg; vitamin B6 1733 mg/kg; folic acid 440 mg/kg; vitamin B12 9.7 mg/kg; biotin 43.3 mg/kg; calcium iodate 1333 mg/kg; sodium selenite 100 mg/kg; zinc oxide 33,333 mg/kg; iron carbonate 6666 mg/kg; manganese-oxide 33,333 mg/kg; copper sulphate 5333 mg/kg (producer: Agrifirm Magyarország Zrt., Környe, Hungary). [3] BASF Hungária Kft. (Budapest, Hungary). [4] Agrifirm Magyarország Zrt. (Környe, Hungary).

A2_Table 2. Nutrient composition and energy values of the experimental diets for laying hens

Chemical Composition (%)	Control	ZP 2.5%	ZP 5.0%
Dry matter	89.00	89.00	89.00
Crude protein	17.00	17.00	17.00
Crude fat	4.20	4.20	4.00
Crude fiber	4.80	4.80	4.80
Crude ash	12.90	12.90	12.90
Starch	34.50	34.50	34.50
Sugar (total)	3.00	3.00	3.00
Total calcium	3.70	3.70	3.70
Total phosphorus	0.52	0.53	0.53
Sodium	0.17	0.17	0.17
SID Lys	0.67	0.67	0.67
SID M + C	0.57	0.57	0.57
SID Thr	0.50	0.50	0.50
SID Trp	0.14	0.14	0.14
SID Val	0.68	0.68	0.68
AMEn (MJ/kg)	11.07	11.07	11.07

Control = 0% Zincoppyeast, ZP 2.5% = 2.5% Zincoppyeast, ZP 5.0% = 5.0% Zincoppyeast. SID Lys = standardized ileal digestible lysine, SID Met + Cys = Standardized ileal digestible methionine + cysteine, SID Thr = Standardized ileal digestible threonine, SID Trp = Standardized ileal digestible tryptophan, SID Val = Standardized ileal digestible valine, AMEn = apparent metabolizable energy corrected to zero nitrogen balance.

A2_Table 3. Microbiological characteristics of eggs across the three dietary feeding groups

Microbiological parameter	Control Batch 1	Control Batch 2	ZP 2.5% Batch 1	ZP 2.5% Batch 2	ZP 5.0% Batch 1	ZP 5.0% Batch 2
Mesophilic microorganism count, CFU g^{-1}	<100	10	<100	20	<100	10
Enterobacteriaceae, CFU g^{-1}	<10	<10	<10	<10	<10	<10
Escherichia coli, CFU g^{-1}	<1	<10	<1	<10	<1	<10
Enterococcus spp., CFU g^{-1}	<10	<10	<10	<10	<10	<10
Salmonella spp., CFU/25 g	Negative	Negative	Negative	Negative	Negative	Negative
Listeria monocytogenes, CFU/25 g	Negative	Negative	Negative	Negative	Negative	Negative
Coagulase-positive *Staphylococcus* spp., CFU g^{-1}	<10	<10	<10	<10	<10	<10

Control = 0% Zincoppyeast, ZP 2.5% = 2.5% Zincoppyeast, ZP 5.0% = 5.0% Zincoppyeast. Batch 1: day 30 (n = 30); batch 2: day 60 (n = 30).

A2_Table 4. Lipid and protein levels of eggs in the three different dietary feeding groups

	Group	Average	S. dev	Stat. diff.*
Lipid content (%)	Control	9.48	0.04	A
	ZP 2.5%	9.42	0.06	AB
	ZP 5.0%	9.30	0.13	B
Protein content (%)	Control	12.67	0.22	A
	ZP 2.5%	13.49	0.34	B
	ZP 5.0%	13.35	0.38	B

* Significant difference between means at $p < 0.05$. Letters denote significant differences among the groups based on the one-way analysis of variance and Tukey HSD post hoc test analysis at $p < 0.05$.

A2_Table 5. Confusion table of Random numbers test classification for e-tongue analysis. Groups according to feeding regime: Control, ZP 2.5%, ZP 5.0%

		Random numbers test		
Average Accuracies	%	Control	ZP 2.5%	ZP 5.0%
Calibration 80.07%	Control	**77.20**	12.79	10.01
	ZP 2.5%	10.59	**79.28**	6.25
	ZP 5.0%	12.21	7.92	**83.74**
	%	Control	ZP 2.5%	ZP 5.0%
Cross-validation 29.95%	Control	**19.73**	16.97	45.41
	ZP 2.5%	26.84	**47.63**	32.09
	ZP 5.0%	53.43	35.40	**22.50**

A2_Table 6. Confusion table of Random numbers test classification for e-nose analysis. Groups according to feeding regime: Control, ZP 2.5%, ZP 5.0%

		Random numbers test		
Average Accuracies	%	Control	ZP 2.5%	ZP 5.0%
Calibration 98.77%	Control	**100**	3.67	0
	ZP 2.5%	0	**96.33**	0
	ZP 5.0%	0	0	**100**
	%	Control	ZP 2.5%	ZP 5.0%
Cross-validation 39.64%	Control	**27.83**	33.33	20
	ZP 2.5%	33.33	**44.5**	33.4
	ZP 5.0%	38.83	22.17	**46.6**

A2_Table 7. Labels specifications of probiotic powders

Probiotic Product	CFU (per dose)*	Bacterial Strains*
P	7.5×10^9 (3 g)	*Bifidobacterium bifidus* W23, *Bifidobacterium lactis* W51, *Bifidobacterium lactis* W52, *Lactobacillus acidophilus* W22, *Lacticaseibacillus casei* W56, *Lacticaseibacillus paracasei* W20, *Lactiplantibacillus plantarum* W62, *Ligilactobacillus salivarius* W24, *Lactococcus lactis* W19
A	3×10^9 (3 g)	*Bifidobacterium lactis* W51, *Enterococcus faecium* W54, *Lactobacillus acidophilus* W55, *Lacticaseibacillus casei* W56, *Ligilactobacillus salivarius* W57, *Lactococcus lactis* W58
N	2.5×10^9 (2 g)	*Lactobacillus acidophilus*, *Lacticaseibacillus rhamnosus*, *Enterococcus faecium*, *Bifidobacterium bifidum*, *Bifidobacterium longum*

A2_Table 8. List of NIR spectral pretreatments_Probiotics experiment

N0.	Spectral pretreatment	N0.	Spectral pretreatment
1	SG(2-13-0)	22	SG(2-17-0) + DeTr + MSC
2	SG(2-17-0)	23	SG(2-21-0) + DeTr + MSC
3	SG(2-21-0)	24	SG(2-21-0) + SG(2-21-1)
4	SNV	25	SG(2-21-0) + SG(2-21-2)
5	MSC	26	SG(2-21-0) + SG(2-13-1)
6	DeTr	27	SG(2-21-0) + SG(2-13-2)
7	DeTr + SNV	28	SG(2-21-0) + SG(2-17-1)
8	DeTr + MSC	29	SG(2-21-0) + SG(2-17-2)
9	SG(2-13-0) + SNV	30	SG(2-13-0) + SG(2-21-1)
10	SG(2-17-0) + SNV	31	SG(2-13-0) + SG(2-21-2)
11	SG(2-21-0) + SNV	32	SG(2-13-0) + SG(2-13-1)
12	SG(2-13-0) + MSC	33	SG(2-13-0) + SG(2-13-2)
13	SG(2-17-0) + MSC	34	SG(2-13-0) + SG(2-17-1)
14	SG(2-21-0) + MSC	35	SG(2-13-0) + SG(2-17-2)
15	SG(2-13-0) + DeTr	36	SG(2-17-0) + SG(2-21-1)
16	SG(2-17-0) + DeTr	37	SG(2-17-0) + SG(2-21-2)
17	SG(2-21-0) + DeTr	38	SG(2-17-0) + SG(2-17-1)
18	SG(2-13-0) + DeTr + SNV	39	SG(2-17-0) + SG(2-17-2)
19	SG(2-17-0) + DeTr + SNV	40	SG(2-17-0) + SG(2-13-1)
20	SG(2-21-0) + DeTr + SNV	41	SG(2-17-0) + SG(2-13-2)
21	SG(2-13-0) + DeTr + MSC		

Note: SG(x–y–z) refers to the Savitzky-Golay (SG) smoothing and derivative algorithm, where x indicates the order of the polynomial used (e.g., 2 = 2nd-order polynomial), y is the window size in points (e.g., 13, 17, or 21), and z corresponds to the derivative applied (0 = none, 1 = first derivative, 2 = second derivative).
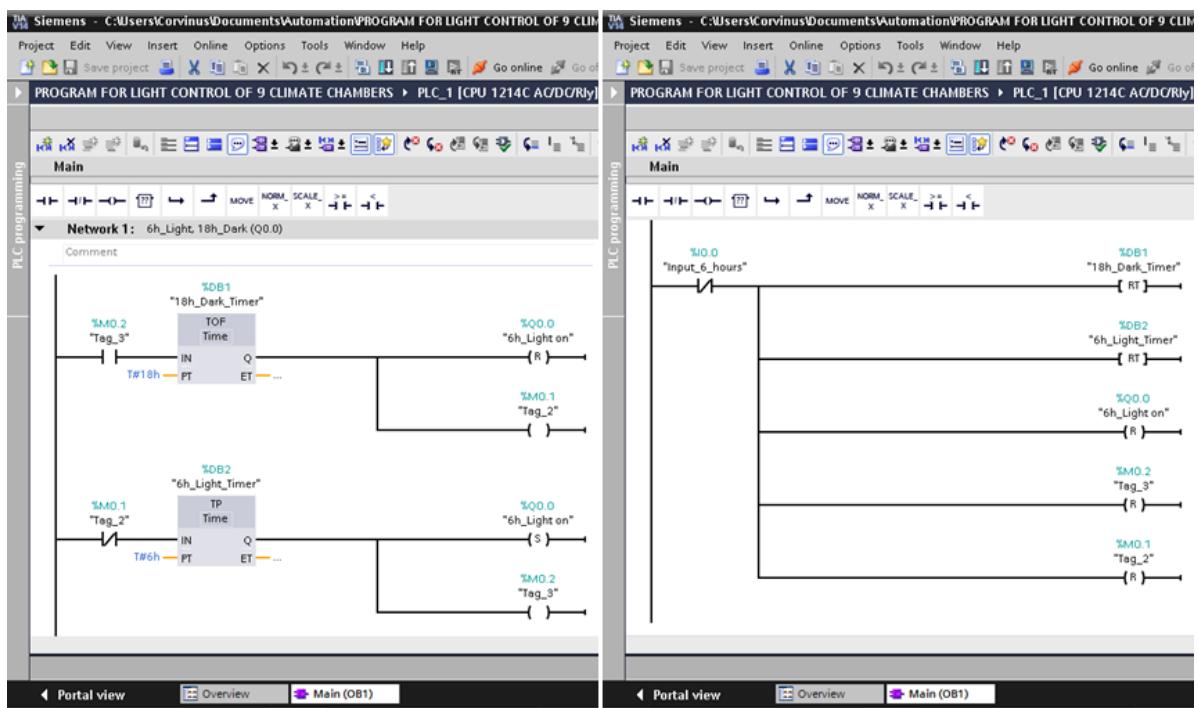
A2_Figure 1. Program fragment for photoperiod control developed in TIA portal software V14
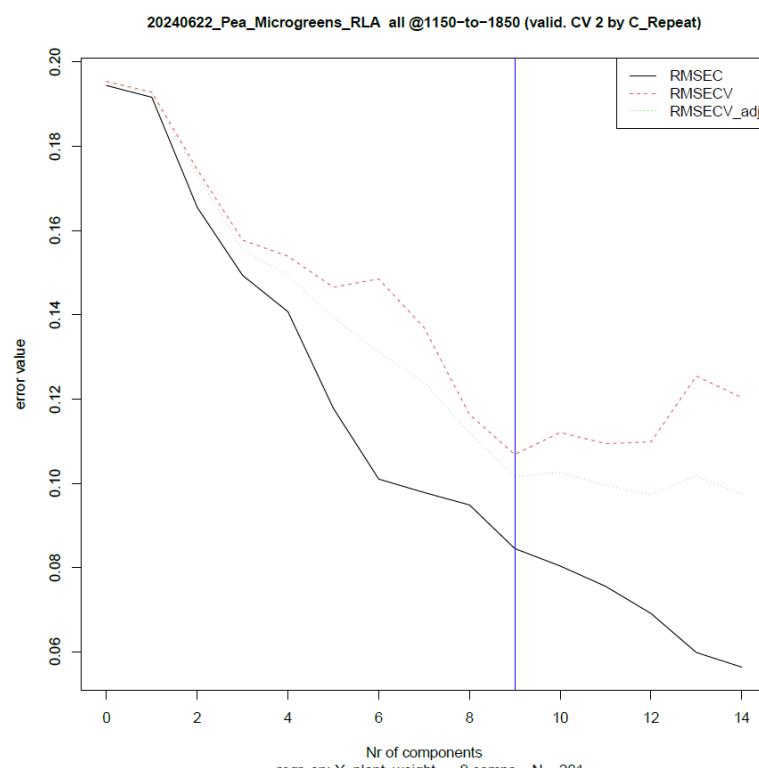
A2_Figure 2. Determination of optimal latent variables in PCA-DA model for pea microgreens classification

A2_Table 9. Summary of the sensory contribution from the discriminant analysis of egg samples on the e-nose data belonging to the MXT-5 column

MXT-5	C-S	Volatile compounds	Sensory description	Discrimination tendency
429.90	428	Acetaldehyde	Ethereal, fresh, fruity, pungent	Figure 5: (b) B/G–50 °C; (d) B–80 °C; Figure 6: (b,d) D*–50 °C; Figure 7: (b,d) D*–80 °C
430.57	425	Methanol	Pungent	
441.88	448	Ethanol	Alcoholic, ethanol, pungent, sweet	Figure 6: (b) D*–50 °C
	448	Methanethiol	Alcoholic, ethanol, pungent, sweet	
469.52		Not found		
493.72	498	2-propanone (or acetone)	Fruity, glue, solvent	Figure 5: (b) G–50 °C; (d) G–80 °C; Figure 6: (b) D*–50 °C; Figure 7: (b,d) D*–80 °C
494.47	499	Propanal	Etherwal, plastic, pungent, solvent	
528.17	527	Methyl acetate	Blackcurrant, ethereal, fruity	Figure 5: (b) G–50 °C; (d) B–80 °C; Figure 6: (b,d) D*–50 °C; Figure 7: (b,d) D*–80 °C
528.86	522	2-methylpropanal	Burnt, fruity, green, malty, pungent, spicy, toasted	
602.58	603	2-butanol	Fusel-alcoholic, oily, winey	Figure 5: (b) G–50 °C; (d) G–80 °C; Figure 6: (b,d) D*–50 °C; Figure 7: (b,d) D*–80 °C
602.94	600	Hexane	Alkane, ethereal, kerosene	
614.28	614	2-methyl-3-buten-2-ol	Earthy, fruity, herbaceous, oily, sweet	Figure 6: (b) D*–50 °C; Figure 7: (b) D*–80 °C
613.86	614	Ethyl acetate	Acidic, butter, caramelized, ethereal, fruity, orange, pineapple	
632.11	636	1-butamine	Alcoholic, bitter, chemical, glue, licorice, solvent, winey	Figure 5: (b) B/G
	627	Propyl formate	Berry, ethereal, green, sweet	
660.89	662	2-methylbutanal	Almond, cocoa, green, malty, strong burnt	Figure 5: (b) B/G–50 °C; Figure 6: (b) D*–50 °C; Figure 7: (b,d) D*–80 °C
665.16	664	n-butanol	Cheese, fermented, fruity	
680.81	681	1- penten-3-one	Fishy, fruity, leather, plastic, pungent, rotten, sewer, spicy	Figure 7: (b) D*–80°
	684	Pent-1-en-3-ol	Butter, green, milky, pungent	
803.41	801	2-hexanol	Fatty, fruity, winey	Figure 6: (b,d) D*–50 °C; Figure 7: (b,d) D*–80 °C
803.46	801	Hexanal	Acorn, fatty, fishy, grassy, green, herbaceous, leafy, tallowy	
818.81	819	2,4,5-trimethyl-3-oxazoline	Musty	Figure 5: (b) B/G–50 °C; Figure 6: (b) D*–50 °C; Figure 7: (b) D*–80 °C
818.98	817	2- butanone, 3-mercapto-	Onion, sulfurous	
985.82	986	3-octanone	Butter, herbaceous, resinous	Figure 5: (b,) B–50 °C; Figure 6: (b,) D*–50 °C
986.50	986	6-methyl-5-hepten-2-one	Blackcurrant, boiled fruit, citrus, earthy, mushroom, rubber	
1000.93	1000	2-octanol	Fatty, mushroom, oily	Figure 7: (b) D*–80 °C
	1001	Propyl pentanoate	Ethereal	
1140.68	1140	Homofuraneol	Caramelized	Figure 5: (b) G–50 °C
1140.88	1140	Methyl 3-pyridinecarboxylate	Herbaceous, sweet, tobacco	
1286.33	1286	Isoborneol, acetate	Balsamic	Figure 5: (b) G–50 °C; Figure 6: (b) D*–50 °C; Figure 7: (d) D*–80 °C
1286.41	1287	Pentyl hexanoate	Fruity	
1312.65	1313	1-ethylnapththalene	Earthy, green, musty, naphthyl	Figure 5: (b,) B/G–50 °C
1312.50	1312	Cinamyl alcohol	Oily	
1399.81	1400	Tetradecane	Alkane, fusel, mild herbaceous, sweet	Figure 5: (b) B/G–50 °C; Figure 6: (b) D*–50 °C
1400.26	1400	Diphenyl ether	Green	
1414.33	1414	Linalyl butanoate	Floral, Pear, sweet	Figure 5: (d) B–80 °C; Figure 7: (b) D*–80 °C
	1415	(e)-beta-damascone	Apple	
1532.40	1532	Cadina-1,4-diene	Fruity, mango, spicy, wood	Figure 5: (b) B–50 °C; Figure 7: (b) D*–80 °C
1533.21	1532	Methyldodecanoate	Coconut, creamy, fatty, fruity, sweet, waxy, weak waxy	
1691.60	1695	Beta-Sinensal	Sweet	Figure 7: (b) *D–80 °C
	1695	Tetradecanenitrile	Fresh	
1807.03	1808	Nootkatone	Banana, citrus, grape, sour fruit, spicy, woody	Figure 5: (b) B–50 °C; (d) B–80 °C; Figure 6: (b) D*–50 °C; Figure 7: (b,d) D*–80 °C
1807.30	1804	2-hexadecanone	Fruity	

A2_Table 10. Discriminant analysis-confusion table of NIRS pea microgreens spectra (microgreens fresh-cut samples) harvested after 11 days under different temperature (15, 20 and 25 °C) and photoperiod (00L, 06L, 12L, 18L) conditions. Clustering by (a) temperature, (b) photoperiod and (c) treatment (temperature-photoperiod). Pretreatments SG 2-45-0 and SNV. Wavelength 1150 to 1850nm

(a)

Temperature

Average recognition (100%)

%	15 °C	20 °C	25 °C
15 °C	100	0	0
20 °C	0	100	0
25 °C	0	0	100

Average prediction (81.8%)

%	15 °C	20 °C	25 °C
15 °C	15°C	20°C	25°C
20 °C	82.73	8.33	3
25 °C	17.27	77.75	12.1

(b)

Photoperiod

Average recognition (86.66%)

	00L	06L	12L	18L
00L	97.98	7.14	0	0
06L	0	85.71	3.72	5.56
12L	0	4.79	83.33	14.83
18L	2.02	2.36	12.94	79.61

Average prediction (52.4%)

	00L	06L	12L	18L
00L	78.33	14.29	3.67	0
06L	13.05	57.14	22.22	11.11
12L	4.31	23.86	22.22	37
18L	4.31	4.71	51.89	51.89

(c)

Treatment

Average recognition (100%)

	15 °C_00L	15 °C_06L	15 °C_12L	15 °C_18L	20 °C_00L	20 °C_06L	20 °C_12L	20 °C_18L	25 °C_00L	25 °C_06L	25 °C_12L	25 °C_18L
15 °C_00L	100	0	0	0	0	0	0	0	0	0	0	0
15 °C_06L	0	100	0	0	0	0	0	0	0	0	0	0
15 °C_12L	0	0	100	0	0	0	0	0	0	0	0	0
15 °C_18L	0	0	0	100	0	0	0	0	0	0	0	0
20 °C_00L	0	0	0	0	100	0	0	0	0	0	0	0
20 °C_06L	0	0	0	0	0	100	0	0	0	0	0	0
20 °C_12L	0	0	0	0	0	0	100	0	0	0	0	0
20 °C_18L	0	0	0	0	0	0	0	100	0	0	0	0
25 °C_00L	0	0	0	0	0	0	0	0	100	0	0	0
25 °C_06L	0	0	0	0	0	0	0	0	0	100	0	0
25 °C_12L	0	0	0	0	0	0	0	0	0	0	100	0
25 °C_18L	0	0	0	0	0	0	0	0	0	0	0	100

Average prediction (48.39%)

	15 °C_00L	15 °C_06L	15 °C_12L	15 °C_18L	20 °C_00L	20 °C_06L	20 °C_12L	20 °C_18L	25 °C_00L	25 °C_06L	25 °C_12L	25 °C_18L
15°C _00L	25.09	0	0	0	0	0	0	0	0	0	0	0
15 °C_06L	37.45	100	22.26	0	0	0	0	0	0	0	0	0
15 °C_12L	0	0	22.26	33.33	0	0	0	0	0	0	0	0
15 °C_18L	0	0	55.48	44.33	22.33	0	0	0	0	0	0	0
20 °C_00L	0	0	0	22.33	44.33	0	0	0	0	11	0	0
20 °C_06L	0	0	0	0	0	100	44.33	0	0	11	33.33	0
20 °C_12L	0	0	0	0	0	0	22.33	33.33	0	0	33.33	0
20 °C_18L	0	0	0	0	0	0	33.33	33.33	0	0	0	66.67
25 °C_00L	37.45	0	0	0	0	0	0	0	100	0	0	0
25 °C_06L	0	0	0	0	33.33	0	0	0	0	22.33	0	0
25 °C_12L	0	0	0	0	0	0	0	0	0	55.67	33.33	0
25 °C_18L	0	0	0	0	0	0	0	33.33	0	0	0	33.33

A2_Table 11. Discriminant analysis-confusion table of NIRS pea spectra (aqueous microgreens extracts samples) harvested after 11 days under different temperature (15, 20 and 25°C) and photoperiod (00L, 06L, 12L, 18L) conditions. Clustering by (a) temperature, (b) photoperiod and (c) treatment (temperature-photoperiod). Pretreatments SG 2-45-0 and SNV. Wavelength 1150 to 1850nm

(a)

Temperature			
Average recognition (98.98%)			
%	15 °C	20 °C	25 °C
15 °C	100	0	0
20 °C	0	100	3.05
25 °C	0	0	96.95
Average prediction (85.6%)			
%	15 °C	20 °C	25 °C
15 °C	96.19	9.09	9.09
20 °C	3.81	84.82	15.18
25 °C	0	6.09	75.73

(b)

Photoperiod			
Average recognition (94.17%)			
	00L	06L	12L	18L
00L	100	0	0	0
06L	0	100	2.06	0
12L	0	0	89.62	12.94
18L	0	0	8.32	87.06
Average prediction (75.83%)			
	00L	06L	12L	18L
00L	100	5.5	0	0
06L	0	77.83	16.62	11.11
12L	0	16.67	62.5	25.89
18L	0	0	20.88	63

(c)

Treatment												
Average recognition (100%)												
	15 °C_00L	15 °C_06L	15 °C_12L	15 °C_18L	20 °C_00L	20 °C_06L	20 °C_12L	20 °C_18L	25 °C_00L	25 °C_06L	25 °C_12L	25 °C_18L
15 °C_00L	100	0	0	0	0	0	0	0	0	0	0	0
15 °C_06L	0	100	0	0	0	0	0	0	0	0	0	0
15 °C_12L	0	0	100	0	0	0	0	0	0	0	0	0
15 °C_18L	0	0	0	100	0	0	0	0	0	0	0	0
20 °C_00L	0	0	0	0	100	0	0	0	0	0	0	0
20 °C_06L	0	0	0	0	0	100	0	0	0	0	0	0
20 °C_12L	0	0	0	0	0	0	100	0	0	0	0	0
20 °C_18L	0	0	0	0	0	0	0	100	0	0	0	0
25 °C_00L	0	0	0	0	0	0	0	0	100	0	0	0
25 °C_06L	0	0	0	0	0	0	0	0	0	100	0	0
25 °C_12L	0	0	0	0	0	0	0	0	0	0	100	0
25 °C_18L	0	0	0	0	0	0	0	0	0	0	0	100
Average prediction (75.01%)												
	15 °C_00L	15 °C_06L	15 °C_12L	15 °C_18L	20 °C_00L	20 °C_06L	20 °C_12L	20 °C_18L	25 °C_00L	25 °C_06L	25 °C_12L	25 °C_18L
15 °C_00L	100	0	0	0	0	0	0	0	0	0	0	0
15 °C_06L	0	100	0	0	0	0	0	0	0	0	0	0
15 °C_12L	0	0	100	0	0	0	0	0	0	0	0	0
15 °C_18L	0	0	0	55.67	0	0	0	0	0	0	0	0
20 °C_00L	0	0	0	0	44.33	0	0	0	0	0	0	0
20 °C_06L	0	0	0	0	0	100	33.33	44.48	0	0	0	11
20 °C_12L	0	0	0	44.33	0	0	66.67	0	0	0	0	0
20 °C_18L	0	0	0	0	0	0	0	44.48	0	33.33	0	0
25 °C_00L	0	0	0	0	55.67	0	0	0	100	0	0	0
25 °C_06L	0	0	0	0	0	0	0	11.04	0	33.33	11	22.33
25 °C_12L	0	0	0	0	0	0	0	0	0	33.33	89	0
25 °C_18L	0	0	0	0	0	0	0	0	0	0	0	66.67

A2_Table 12. Summary PCA-DA analysis for simulated data in pea microgreens experiment

Data	Clustering by	Simulated Data Modeling (Random numbers 0-1)					
		n	g	%C	%CV	LV	max. LV=(n-g/3)
15C_00L	Day	24	3	44.3	27.31	2	7
15C_06L	Day	-	-	-	-	-	-
15C_12L	Day	-	-	-	-	-	-
15C_18L	Day	24	3	50.68	46.84	2	7
20C_00L	Day	24	3	77.27	49.47	5	7
20C_06L	Day	24	3	79.11	50	5	7
20C_12L	Day	27	3	81.75	49.15	7	8
20C_18L	Day	27	3	43.48	31.09	2	8
25C_00L	Day	21	3	57.33	31.93	3	6
25C_06L	Day	-	-	-	-	-	-
25C_12L	Day	27	3	78.22	45.41	7	8
25C_18L	Day	27	3	76.38	47.24	8	8
Day 7	Treatment	69	8	59.62	27.53	11	20
Day 11	Treatment	99	12	34.12	9.5	6	29
Day 14	Treatment	93	12	25.15	10.68	2	27
Day 18	Treatment	33	4	79.51	43.38	7	10
Day 11	Temperature	99	3	66.35	47.5	22	32
Day 14	Temperature	93	3	54.47	35.27	6	30
Day 7	Photoperiod	69	4	64.16	38.15	17	22
Day 11	Photoperiod	99	4	70.81	34.15	20	32
Day 14	Photoperiod	93	4	47.91	36.88	6	30
Day 18	Photoperiod	33	4	79.51	43.38	7	10
All	Day	294	4	49.78	28.85	33	97
All	Treatment	294	12	36.74	12.88	20	94
All	Temperature	294	3	79.39	40.69	84	97
All	Photoperiod	294	4	56.95	28.68	41	97

A2_Table 13. NIR absorption features related to height: Foliar bands reported in literature and detected in pea microgreens fresh-cut samples and aqueous microgreens extracts samples

Microgreens fresh-cut samples			Aqueous microgreens extracts samples		
Wavelength (nm)	Feature	Reference	Wavelength (nm)	Feature	Reference
1196	O-H bend (1st overtone)	Curran (1989)	1368	O-H stretch (1st overtone)	Slavchev et al. (2015)
1392	O-H (1st overtone), C-H stretching	Slavchev et al. (2015)	1396	O-H bend (1st overtone) associated with water	Curran (1989)
1417	C-H stretch and deformation	Curran (1989)	1409	O-H bend (1st overtone) associated with water	Curran (1989)
1446	O-H stretch (1st overtone), C-H stretch	Curran (1989)	1484	O-H stretch (1st overtone)	Curran (1989)
1480	O-H (1st overtone), N-H (1st overtone)	Slavchev et al. (2015)	1530	O-H stretch (1st overtone)	Curran (1989)
1508	N-H stretch (1st overtone)	Curran (1989)	1685	C-H stretch (1st overtone)	Curran (1989)
1543	O-H stretch (1st overtone)	Curran (1989)			
1704	C-H stretch (1st overtone)	Curran (1989)			
1838	O-H stretch, C-H stretch (2nd overtone)	Curran (1989)			

Only wavelengths reported in the literature (Curran, 1989; Slavchev *et al.*, 2015) for foliar spectra are included. Bands found in the present study but not previously described are not listed.

A2_Table 14. NIR absorption features related to chlorophyll A: foliar bands reported in literature and detected in pea microgreens fresh-cut samples and aqueous microgreens extracts samples

Microgreens fresh-cut samples			Aqueous microgreens extracts samples		
Wavelength (nm)	Feature	Reference	Wavelength (nm)	Feature	Reference
1366	O-H (1st overtone)	Slavchev et al. (2015)	1206	O-H bend (1st overtone)	Curran (1989)
1417	C-H stretch and deformation	Curran (1989)	1412	C-H stretch and deformation	Curran (1989)
1446	O-H stretch (1st overtone), C-H stretch	Curran (1989)	1549	O-H stretch (1st overtone)	Curran (1989)
1496	O-H stretch (1st overtone)	Curran (1989)	1694	C-H stretch (1st overtone)	Curran (1989)
1538	O-H stretch (1st overtone)	Curran (1989)			
1838	O-H stretch, C-H stretch (2nd overtone)	Curran (1989)			

Only wavelengths reported in the literature (Curran, 1989; Slavchev *et al.*, 2015) for foliar spectra are included. Bands found in the present study but not previously described are not listed.

A2_Table 15. NIR absorption features related to L* color component: foliar bands reported in literature and pea microgreens fresh-cut samples and aqueous microgreens extracts samples

Microgreens fresh-cut samples			Aqueous microgreens extracts samples		
Wavelength (nm)	Feature	Reference	Wavelength (nm)	Feature	Reference
1391	O-H (1st overtone), C-H stretching	Slavchev et al. (2015)	1208	O-H bend (1st overtone)	Curran (1989)
1419	C-H stretch and deformation	Curran (1989)	1410	O-H bend (1st overtone)	Curran (1989)
1509	N-H stretch (1st overtone)	Curran (1989)	1488	O-H stretch (1st overtone)	Curran (1989)
1544	O-H stretch (1st overtone)	Curran (1989)	1698	C-H stretch (1st overtone)	Curran (1989)
1706	C-H stretch (1st overtone)	Curran (1989)	1818	O-H stretch, C-O stretch (2nd overtone)	Curran (1989)
1840	O-H stretch, C-H stretch (2nd overtone)	Curran (1989)			

Only wavelengths reported in the literature (Curran, 1989; Slavchev *et al.*, 2015) for foliar spectra are included. Bands found in the present study but not previously described are not listed.

A2_Table 16. NIR absorption features related to °Brix: foliar bands reported in literature and pea microgreens fresh-cut samples and aqueous microgreens extracts samples

Microgreens fresh-cut samples			Aqueous microgreens extracts samples		
Wavelength (nm)	Feature	Reference	Wavelength (nm)	Feature	Reference
1208	O-H bend (1st overtone)	Curran (1989)	1394	O-H bend (1st overtone)	Curran (1989)
1417	C-H stretch and deformation	Curran (1989)	1426	C-H stretch, C-H deformation	Curran (1989)
1447	O-H stretch (1st overtone), C-H stretch	Curran (1989)	1687	C-H stretch (1st overtone)	Curran (1989)
1495	N-H stretch (1st overtone)	Curran (1989)			
1541	O-H stretch (1st overtone)	Curran (1989)			
1707	C-H stretch (1st overtone)	Curran (1989)			
1840	O-H stretch, C-H stretch (2nd overtone)	Curran (1989)			
1390	O-H (1st overtone), C-H stretching	Slavchev et al. (2015)			

Only wavelengths reported in the literature (Curran, 1989; Slavchev *et al.*, 2015) for foliar spectra are included. Bands found in the present study but not previously described are not listed.

A2_Table 17. NIR absorption features related to TPC: foliar bands reported in literature and detected in pea microgreens fresh-cut samples and aqueous microgreens extracts samples

Microgreens fresh-cut samples			Aqueous microgreens extracts samples		
Wavelength (nm)	Feature	Reference	Wavelength (nm)	Feature	Reference
1428	C-H stretch, C-H deformation	Curran (1989)	1406	O-H bend (1st overtone)	Curran (1989)
1504	N-H stretch (1st overtone)	Curran (1989)	1418	C-H stretch, C-H deformation	Curran (1989)
			1451	O-H stretch (1st overtone)	Curran (1989)
			1510	N-H stretch (1st overtone)	Curran (1989)
			1528	O-H stretch (1st overtone)	Curran (1989)
			1685	C-H stretch (1st overtone)	Curran (1989)
			1824	1st overtone IHB stretch	Slavchev et al. (2015)

Only wavelengths reported in the literature (Curran, 1989; Slavchev *et al.*, 2015) for foliar spectra are included. Bands found in the present study but not previously described are not listed.

A2_Table 18. NIR absorption features related to TAC: foliar bands reported in literature and detected in pea microgreens fresh-cut samples and aqueous microgreens extracts samples

Microgreens fresh-cut samples			Aqueous microgreens extracts samples		
Wavelength (nm)	Feature	Reference	Wavelength (nm)	Feature	Reference
1397	O-H bend (1st overtone)	Curran (1989)	1394	O-H bend (1st overtone)	Curran (1989)
1451	O-H stretch (1st overtone), C-H stretch	Curran (1989)	1407	O-H bend (1st overtone)	Curran (1989)
1542	O-H stretch (1st overtone)	Curran (1989)	1445	O-H stretch (1st overtone)	Curran (1989)
1786	C-H stretch (1st overtone), O-H stretch	Curran (1989)	1685	C-H stretch (1st overtone)	Curran (1989)

Only wavelengths reported in the literature (Curran, 1989; Slavchev *et al.*, 2015) for foliar spectra are included. Bands found in the present study but not previously described are not listed.

A2_Table 19. LVs number reduction in PLSR models of fresh-cut samples of pea microgreens

Regression variable	Sample	Wavelenghts (nm)	n	LV	RMSEC	R^2C	RMSECV	R^2CV	RMSEP	R^2pr
Weight	fresh-cut	1185-1770	291	4	0.08	0.79	0.10	0.72	0.10	0.74
Height	fresh-cut	1196-1508	291	5	2.10	0.73	2.27	0.68	1.93	0.72
L*	fresh-cut	1150-1850	294	6	6.05	0.76	7.60	0.62	7.22	0.62
b*	fresh-cut	1185-1665	285	6	5.81	0.74	6.73	0.66	7.16	0.62
Chlorophyll A	fresh-cut	1185-1572; 1695-1850	291	7	19.48	0.74	21.19	0.69	19.90	0.74
Chlorophyll B	fresh-cut	1185-1572; 1695-1850	291	7	8.31	0.71	9.28	0.64	8.67	0.70
Total Carotene	fresh-cut	1185-1572; 1695-1850	294	7	4.74	0.75	5.41	0.67	4.79	0.74
Brix	fresh-cut	1185-1570	294	6	0.15	0.72	0.17	0.64	0.16	0.68

11. ACKNOWLEDGEMENT

I would like to express my heartfelt gratitude to all those who supported and guided me throughout this academic journey.

A special acknowledgment to my supervisors Dr. Zoltán Kovacs and Dr. Zoltán Gillay for your support and guidance throughout the research process. Your expertise and insightful advice have been essential elements in shaping this work.

I am very grateful to Dr. Gabriella Kiskó (MATE University), Dr. György Bázár (Adexgo Ltd.), Dr. Csilla Benedek (Semmelweis University), and Dr. Balázs László (MATE University) for their valuable support and collaboration, particularly in facilitating key measurements and analyses that significantly contributed to the completion of my PhD dissertation.

My sincere appreciation goes to all the professors and colleagues at the Department of Food Measurements and Process Control, Hungarian University of Agriculture and Life Sciences (MATE), for the valuable contribution in this work. I am particularly grateful to my fellow PhD students and colleagues—Dr. Szanett Bodor, Dr. Lewis Zinia, Dr. Balkis Aouadi, Dr. Flóra Vitalis, Mariem Majadi, Lueji Regatieri Santos, Mátyás Lukács, and Péter Erdélyi, for their camaraderie, insightful discussions, and continuous support.

To my family and dear friends, thank you for your unwavering support, encouragement, and positivity. I am deeply grateful for the community that stood by me through every challenge and triumph, always offering help when needed.

On a personal note, I wish to express my heartfelt gratitude to my wife, Cristina, for her unwavering support, patience, and encouragement throughout this journey, especially during its most challenging moments.